

DISSECTING THE PEROXISOMAL AND MITOCHONDRIAL DIVISION MACHINERIES
IN ARABIDOPSIS

By

Kyaw Aung

A DISSERTATION

Submitted to
Michigan State University
in partial fulfillment of requirements
for the degree of

DOCTOR OF PHILOSOPHY

Plant Biology

2011

ABSTRACT

DISSECTING THE PEROXISOMAL AND MITOCHONDRIAL DIVISION MACHINERIES IN ARABIDOPSIS

By

Kyaw Aung

In eukaryotic cells, peroxisomes and mitochondria are ubiquitous organelles playing essential roles in development. Peroxisomes and mitochondria not only house a number of organelle-specific biochemical reactions, but also function together in accomplishing several intracellular metabolic pathways. As multifunctional organelles, they are highly dynamic and plastic, in which the conserved fission proteins, Dynamin-related protein (DRP) and Fission1 (FIS1), govern the division of both organelles. In addition, several lineage-specific factors also exist to mediate the division of peroxisomes and mitochondria. To further dissect the division machinery of peroxisomes and mitochondria in Arabidopsis, I explored novel division factors and examined the regulation of known division factors. First, I identified and characterized two novel plant-specific proteins, Peroxisomal And Mitochondrial Division Factor1 (PMD1) and its homologue PMD2. We demonstrated that PMD1 is a C-terminal tail-anchored (C-TA) protein of peroxisomes and mitochondria and involved in the division and morphogenesis of these organelles. PMD2, on the other hand, is targeted only to mitochondria and involved specifically in mitochondrial division/morphogenesis. As there is no detectable physical interaction between PMD1 and the known division proteins DRP3 and FIS1, PMD1 is suggested to be involved in peroxisomal and mitochondrial division in a DRP3/FIS1-independent manner. DRPs are large GTPases, functioning as molecular scissors during vesicle fission. In Arabidopsis, DRP3A and

DRP3B play critical roles in peroxisomal and mitochondrial division, whereas DRP5B mediates the division of chloroplasts and peroxisomes. In this study, I further characterized these three DRP proteins for their roles in organelle division. Our results showed that DRP5B is not physically associated with mitochondria, but its mutants exhibit an elongated mitochondrial phenotype similar to that of the *drp3* mutants, suggesting that DRP5B is indirectly involved in the division or morphogenesis of mitochondria. Genetic and biochemical analyses showed that DRP5B may function in a manner that is independent from DRP3A and DRP3B, as DRP5B is not crucial for forming the DRP3 protein complexes. Furthermore, I studied post-translational regulation of DRP3, the major division factor of peroxisomes and mitochondria. I showed that the function of DRP3 is regulated by protein phosphorylation at DRP3A^{Ser575} and DRP3B^{Ser560}. Overexpression of phospho-mimic DRP3s fails to rescue the *drp3* mutants and causes peroxisomal and mitochondrial division deficiencies in wild-type Col-0, suggesting that DRP3 phosphorylated at these serine residues is inactive. Lastly, I discovered that the absence of the mitochondrial and peroxisomal adenine nucleotide transporter, AAC1, or the peroxisomal NAD⁺ carrier PXN, alters the morphologies and abundance of the organelles. These findings suggest that metabolic homeostasis within peroxisomes and mitochondria is also involved in the morphogenesis and proliferation of these organelles. In summary, my work has provided significant insights into the molecular control of the morphogenesis and proliferation of peroxisomes and mitochondria in Arabidopsis.

ACKNOWLEDGEMENTS

First of all, I would like to express my special appreciation to Dr. Tzyy-Jen Chiou (Academia Sinica, Taiwan). Working with Tzyy-Jen has not only strengthened my ability but also ignited my passion for sciences. What I have learned from her has set a foundation for my future path. Since then, Tzyy-Jen has always be a role model to me.

To be where I am today, I would like thanks to my mentor Jianping Hu for providing the opportunity to work in her lab and giving me a great deal of freedom to explore and experience. She has taught me, both consciously and unconsciously, to be a better scientist. What I have learned from her has had a tremendous impact on my work. I am also thankful for the support and guidance from my committee members Dr. Brad Day, Dr. Kathy Osteryoung, and Dr. Rob Last.

I would like to acknowledge all the past and present Hu lab members, especially Navneet Kaur and Dr. Gaëlle Cassin for many great discussions about science and the friendship we've all shared.

I also would like to thanks all my colleagues and friends from MSU, especially Jeongwoon Kim, Christine Shyu, Chin-mei Lee, and Joyce Liu.

Last but not least, a special thanks to Ya-ni Chen and my family for their love and support.

TABLE OF CONTENTS

LIST OF TABLES	vii
LIST OF FIGURES	viii
ABBREVIATIONS	xi
CHAPTER 1: Literature review	
1.1 Introduction.....	2
1.2 Origin and function of peroxisomes.....	2
1.3 Origin and function of mitochondria.....	5
1.4 Maintaining peroxisomal and mitochondrial populations in cells.....	7
1.4.1 The initial step in peroxisome division.....	8
1.4.2 The fission complex of peroxisomes and mitochondria.....	13
1.4.3 Recruitment of DRP to the division sites of the organelles.....	16
1.4.4 Post-translational regulation of DRP.....	21
1.5 Aims of the thesis research.....	25
CHAPTER 2: The <i>Arabidopsis</i> tail-anchored protein PEROXISOMAL AND MITOCHONDRIAL DIVISION FACTOR1 is involved in the morphogenesis and proliferation of peroxisomes and mitochondria	
Abstract.....	31
Introduction.....	32
Results.....	36
Discussion.....	49
Methods.....	91
Acknowledgements.....	101
CHAPTER 3: <i>Arabidopsis</i> DYNAMIN-RELATED PROTEIN5B is also involved in mitochondrial morphogenesis and division	
Abstract.....	104
Introduction.....	105
Results and Discussion.....	107
Methods.....	123
Acknowledgements.....	126
CHAPTER 4: Phosphorylation of DRP3A and DRP3B in regulating peroxisomal and mitochondrial division	
Abstract.....	129
Introduction.....	130
Results and Discussion.....	134
Methods.....	154
CHAPTER 5: Metabolic Regulation of Peroxisomal and Mitochondrial Morphogenesis in <i>Arabidopsis</i>	

Abstract.....	157
Introduction.....	158
Results and Discussion.....	163
Methods.....	179
Acknowledgements.....	182
CHAPTER 6: Conclusion and Future Perspectives.....	183
APPENDICES	
Appendix A: The Arabidopsis peroxisome division mutant <i>pdd2</i> is defective in the <i>DYNAMIN-RELATED PROTEIN3A (DRP3A)</i> gene.....	193
Appendix B: Dissecting the functional domain of PMD1 in peroxisomal and mitochondrial division.....	200
REFERENCES.....	211

LIST OF TABLES

Table 2.1. In silico identification of peroxisomal membrane proteins containing long coiled-coil domains.....	87
Table 2.2. DNA primers used in this study.....	89
Table 2.3. Vectors used in this study.....	90
Table 4.1. DNA primers used in this study.....	153

LIST OF FIGURES

Figure 1.1. A model for peroxisomal and mitochondrial divisions in Arabidopsis.....	27
Figure 1.2. Comparative models for the recruitment of DRP to the organelle division sites.....	28
Figure 2.1. Structural and sequence analysis of PMD1.....	58
Figure 2.2. Subcellular localization of YFP-PMD1 and YFP-PMD2.....	60
Figure 2.3. Transient expression of C-terminal YFP fusion of PMD1 in Tobacco epidermal cells.....	62
Figure 2.4. PMD1 is anchored to the organelle membranes by the C-terminus.....	63
Figure 2.5. <i>pmd1</i> mutants exhibit abnormal peroxisomal and mitochondrial morphologies.....	66
Figure 2.6. Plant morphologies of the <i>pmd1</i> loss- and gain-of-function lines and localization of YFP-PMD1 in transgenic plants.....	69
Figure 2.7. Quantification of organelle size and number.....	71
Figure 2.8. PMD1 self-interacts but does not interact with the known peroxisomal and mitochondrial division factors.....	73
Figure 2.9. Localization of DRP3 proteins in the <i>pmd1</i> mutant.....	75
Figure 2.10. Proteins pulled down from <i>35S_{pro}:YFP-PMD1</i> or <i>PMD1_{pro}:BIO-PMD1</i> plants and the gene structure of <i>PMD2</i>	77
Figure 2.11. PMD1 and PMD2 are able to form homo- and heterocomplexes.....	79
Figure 2.12. PMD2 is involved in mitochondrial morphogenesis.....	81
Figure 2.13 Organelle targeting signals reside in the C-terminus of PMD1 and PMD2.....	83
Figure 3.1. YFP-DRP5B is not targeted to mitochondria in Arabidopsis.....	116
Figure 3.2. The <i>drp5B</i> mutants also exhibit defects in mitochondrial division.....	117
Figure 3.3. PCR genotyping of the <i>drp</i> mutants.....	118
Figure 3.4. Phenotypes of the <i>drp</i> double and triple mutants.....	119

Figure 3.5. Yeast two-hybrid analysis to test interaction between DRP5B and DRP3 proteins.....	120
Figure 3.6. Expression of endogenous DRP3A and DRP3B in Arabidopsis.....	121
Figure 3.7. Detection of endogenous DRP3A- and DRP3B-containing protein complex in Arabidopsis.....	122
Figure 4.1. Protein structure of DRP3A and DRP3B.....	142
Figure 4.2. Complementation of <i>drp3</i> mutants using wild-type DRP3 and phospho-mutants of DRP3.....	143
Figure 4.3. Immunoblot analysis of overexpressed DRP3 variants in Arabidopsis	145
Figure 4.4. Peroxisomal and mitochondrial morphology in DRP3-overexpressors.....	146
Figure 4.5. Peroxisomal and mitochondrial targeting of YFP-DRP3 variants.....	147
Figure 4.6. Yeast two-hybrid analyses for interactions between the wild-type and mutant DRP3A or DRP3B.....	149
Figure 4.7. Immunoblot analysis to detect the formation of the DRP3 protein complex in transgenic plants expressing HA-DRP3.....	151
Figure 5.1. Subcellular localization of AAC1-YFP.....	170
Figure 5.2. Peroxisomal and mitochondrial morphology in <i>aac1</i> mutants.....	171
Figure 5.3. Plant morphology of <i>aac1</i> mutants.....	173
Figure 5.4. Expression level of <i>AtAACs</i> in Arabidopsis.....	174
Figure 5.5. Assessment of β -oxidation in the <i>aac1</i> mutants.....	175
Figure 5.6. Peroxisomal and mitochondrial morphology in <i>pxn-3</i>	177
Figure 5.7. Peroxisomal and mitochondrial size in <i>aac1</i> and <i>pxn-3</i> mutants.....	178
Figure A.1. Phenotypic analyses of <i>pdd2</i>	198
Figure A.2. Identification of the PDD2 gene.....	199
Figure B.1. Schematic drawings of PMD1 variants for mapping the functional domain.....	205

Figure B.2. Induction of peroxisomal and mitochondrial proliferation by overexpression of HA-PMD1.....206

Figure B.3. Expression of the HA-fusion proteins in Tobacco leaves..... 209

Figure B.4. Mapping the self-interacting domain of PMD1 by yeast two-hybrid analysis.....210

ABBREVIATIONS

β-gal	Beta-galactosidase
Δ	Deletion
35S	Cauliflower Mosaic Virus 35S promoter
AA	Amino acid
ABRC	Arabidopsis Biological Resource Center
AD	Activation domain
ARC	Accumulation and Replication of Chloroplasts
ATP	Adenosin-5'-Triphosphate
Bar	BASTA resistant
BD	DNA binding domain
BLAST	Basic Local Alignment Search Tool
C	Celsius
CaMKIα	Ca ²⁺ /calmodulin-dependent protein kinase Iα
CC	Coiled-coil domain
CFP	Cyan fluorescent protein
Co-IP	Co-Immunoprecipitation
C-TA	C-terminal tailed-anchored protein
DRP	Dynamin-related protein
ER	Endoplasmic reticulum
EMPTY	Empty vector
EMS	Ethane methyl sulfonate

FIS1	Fission1
Fts	Filamentation temperature sensitive
GDP	Guanosine-5'-diphosphate
GFP	Green fluorescent protein
GST	Glutathione-S-transferase
GTP	Guanosine-5'-triphosphate
GTPase	Guanosine triphosphatase
IBA	Indole 3-butyric acid
LEA	Late embryogenesis abundant LEA domain-containing protein
Ler	Landsberg <i>erecta</i>
LNG1	LONGIFOLIA1
MARCH-V	Membrane associated RING-CH-V
Mff	Mitochondrial fission factor
MFP	MAR-binding filament like protein 1
MiD	Mitochondrial dynamics protein
MIEF	Mitochondrial elongation factor
MITOL	Mitochondrial ubiquitin ligase
MAPL	Mitochondrial-anchored protein ligase
NADPH	Nicotinamide adenine dinucleotide phosphate (reduced)
PEX	Peroxin
PTS1	Peroxisomal targeting signal 1
PTS2	Peroxisomal targeting signal 2
RALA	The small Ras-GTPase protein

RALBP1	Effector protein of RALA
SD	Synthetic dropout
SD/-HUT	SD media lacking histidine, uracil, and tryptophan
SD/-HUTL	SD media lacking histidine, uracil, tryptophan, and leucine
SENP5	SUMO1/sentrin-specific peptidase 5
TBST	Tris-buffered saline with Tween 20
TMD	Transmembrane domain
Ubc9	SUMO-conjugating enzyme
UBQ	Ubiquitin
YFP	Yellow fluorescent protein

CHAPTER 1

LITERATURE REVIEW

The division of peroxisomes and mitochondria

1.1 Introduction

In eukaryotic cells, organelles are delimited by their own lipid bilayers, providing membrane-bound compartments for specific biochemical reactions. Although each type of organelle carries a unique set of biochemical functions, several intracellular metabolic pathways span across multiple organelles. In plants for example, the recycling of phosphoglycolate during photorespiration is executed by the sequential action of chloroplasts, peroxisomes, and mitochondria (Peterhansel et al., 2010). The conversion of fatty acids to sucrose is required for successful establishment of oilseeds, in which lipid bodies, peroxisomes, mitochondria, and the cytosol function cooperatively (Baker et al., 2006; Penfield et al., 2006). Given their cooperative relationship in several metabolic processes, different organelles have been found to utilize shared fission factors in maintaining the population of the organelles. Among them, peroxisomes and mitochondria share a set of evolutionarily conserved division factors, i.e., dynamin-related protein (DRP) and Fission1 (Fis1), across diverse kingdoms. In this chapter, division of peroxisomes and mitochondria in eukaryotic cells will be mainly discussed.

1.2 Origin and function of peroxisomes

Peroxisomes are often found as roughly spherical organelles, 0.1-1 μm in diameter, and are encircled by single membranes (Purdue and Lazarow, 2001). Peroxisomes are present in almost all eukaryotic cells and are indispensable in humans (Steinberg et al., 2006) and plants (Lin et al., 1999; Hu et al., 2002; Wanders, 2004; Fan et al., 2005). Peroxisome disorders in humans are caused by impaired biogenesis or function of peroxisomes, which leads to death during infancy or early childhood

(Fidaleo, 2010). In *Arabidopsis*, mutations within core proteins required for peroxisome biogenesis result in embryonic lethality, indicating the essential role of peroxisomes during plant growth and development (Sparkes et al., 2003; Fan et al., 2005; Kaur et al., 2009). Unlike peroxisomes in plants and mammals, yeast peroxisomes are dispensable and peroxisome-deficient yeast cells are viable in YPD rich medium. However, peroxisomes become essential when yeasts are grown on limited growth substrates (e.g., methanol and oleic acid), under which conditions peroxisomal β -oxidation activity is required to metabolize the fatty acids into usable carbon sources (van der Klei and Veenhuis, 2006). In general, peroxisomes perform diverse and crucial metabolic functions, including fatty acid metabolism through β -oxidation and degradation of reactive oxygen species such as H_2O_2 (Schrader and Fahimi, 2008). Moreover, other pathways and functions demonstrated or indicated to be mediated by plant peroxisomes include photorespiration, the glyoxylate cycle, jasmonic acid biosynthesis, indole-3-butyric acid (IBA) metabolism, signaling, photomorphogenesis, and plant-pathogen interaction (Hu et al., 2002; Nyathi and Baker, 2006; Reumann and Weber, 2006; Kaur et al., 2009).

The peroxisome is believed to be an endoplasmic reticulum (ER)-derived member of the endomembrane system, which can bud out of the ER upon a total absence of peroxisomes in yeast (Hoepfner et al., 2005; Gabaldon et al., 2006; Schluter et al., 2006; Titorenko and Mullen, 2006). In addition, new peroxisomes can also proliferate from pre-existing peroxisomes through growth and division (Purdue and Lazarow, 2001; Fagarasanu et al., 2007; Kaur and Hu, 2009). Unlike endosymbiotic organelles, peroxisomes lack their own genome. Hence, most of the peroxisomal

proteins, except the few that are pre-packed or pre-assembled in the ER, are imported into the organelle post-translationally. Peroxisomal matrix proteins are translated and folded in the cytosol and imported into peroxisomes with the assistance of at least 20 peroxin (PEX) proteins localized in the cytosol or on the peroxisomal membrane (Ma et al., 2011). In brief, PEX5 and PEX7 function as receptors for peroxisomal matrix proteins, which recognize the cargo proteins in the cytosol and shuttle them across peroxisomal membrane with the assistance of peroxisomal membrane proteins, PEX13, PEX14, and PEX17, which provide docking sites for the cargo-bound receptors (Platta and Erdmann, 2007; Kaur et al., 2009). Because peroxisomes are believed to originate from the ER, the membrane-bound peroxisomal protein import machinery resembles that of ER-associated protein degradation (ERAD) (Schliebs et al., 2010). In particular, a ubiquitin-conjugating-enzyme (PEX4), ubiquitin-protein ligases (PEX2, PEX10, and PEX12), and AAA ATPases (PEX1 and PEX6) are believed to function in concert to recycle the receptor protein PEX5 to the cytosol or degrade obsolete matrix proteins of peroxisomes (Platta and Erdmann, 2007; Kaur et al., 2009). Peroxisomal membrane proteins, on the other hand, are recognized by PEX19 in the cytosol and recruited to the membrane by a membrane-bound receptor PEX3. Although the peroxisomal protein import machinery is not yet well established, yeast, mammals, and plants seem to utilize the similar apparatus in recruiting the peroxisomal proteins (Platta and Erdmann, 2007; Kaur et al., 2009).

Recent proteome analyses of peroxisomes identified 85 and 61 peroxisomal genes in human and yeast *Saccharomyces cerevisiae*, respectively (Schrader and Fahimi, 2008). In contrast, *Arabidopsis* contains over 130 genes validated to date to

encode peroxisomal proteins (<http://www.peroxisome.msu.edu/>). This difference in peroxisomal proteome size suggests that plant peroxisomes may house more pathways and perform more complex functions compared with peroxisomes from yeast and mammals.

1.3 Origin and function of mitochondria

Mitochondria are enclosed by double membranes and are often found as rod-shaped organelles (Shaw and Nunnari, 2002; Millar et al., 2008). In yeast and mammalian cells, elongated mitochondria to elaborate tubular mitochondrial networks are also observed (Shaw and Nunnari, 2002). Mitochondria are ubiquitously found in almost all eukaryotic cells and serve as the powerhouse of cells by performing functions such as ATP synthesis, respiration, and the tricarboxylic acid (TCA) cycle (Millar et al., 2008). In addition to their pivotal roles in energy production, mitochondria also house several anabolic reactions, such as synthesis of a number of substances (e.g., nucleotides, amino acids, lipids, vitamins and other metabolites) as well as ionic homeostasis in cells (Bereiter-Hahn, 1990; Millar et al., 2008). Furthermore, mitochondria also play critical roles in signaling, cellular differentiation, and program cell death (Chan, 2006). Given their fundamental roles in cell metabolism, several neurodegenerative diseases (e.g., Parkinson's and Alzheimer's disease) and aging (Schapira, 2006) are linked to mitochondrial disorders in human. Recently, critical roles of mitochondria in biotic and abiotic stresses have been reported in *Arabidopsis* (Gleason et al., 2011; Jacoby et al., 2011).

The mitochondrion is believed to be a direct descendent of α -proteobacteria after

ancient endosymbiosis (Gray et al., 1999). Although mitochondria contain their own transcriptional and translational machinery (Gray et al., 2001), the vast majority of mitochondrial proteins are encoded in the nucleus and imported into mitochondria post-translationally (Unsold et al., 1997). The general mitochondrial protein import mechanism is fairly well-characterized in different organisms and is suggested to utilize a partially conserved apparatus (Millar et al., 2008; Schmidt et al., 2010). In short, nuclear-encoded mitochondrial proteins are imported into mitochondria through a translocase on the outer mitochondrial membrane (TOM). The imported proteins are then sorted to their destination membranes or matrixes. The matrix proteins carrying N-terminal cleavable targeting signals are subsequently imported into the matrix through the inner membrane complex (TIM) together with the presequence translocase-associated motor (PAM). In addition, targeting of the mitochondrial outer membrane proteins and inner membrane proteins is accomplished by the sorting and assembly machinery of outer membrane protein (SAM) and the mitochondrial intermembrane space assembly (MIA) respectively (Millar et al., 2008; Schmidt et al., 2010). The outer mitochondrial membrane proteins contain a relatively short transmembrane domain followed by positively charged residues (Rapaport, 2003). In plants, some of the inner mitochondrial membrane proteins contain a cleavable N-terminal signal peptide (Murcha et al., 2005). To date, a total number of 1098 (Pagliarini et al., 2008) and 749 (Reinders et al., 2006) mitochondrial proteins were identified in mammals and yeast respectively. In *Arabidopsis*, 2,585 proteins are predicted to compose the mitochondrial proteome (Millar et al., 2008; Cui et al., 2011), suggesting that plant mitochondria might have evolved novel functions.

1.4 Maintaining peroxisomal and mitochondrial populations in cells

Given their critical roles in plant growth and development, peroxisomal and mitochondrial morphology, abundance and positioning are highly regulated in cells to maintain cellular homeostasis (Miyagishima et al., 2003; Osteryoung and Nunnari, 2003). During eukaryotic cell division, populations of organelles need to be replicated and distributed equally to two daughter cells. In unicellular red alga *Cyanidioschyzon merolae*, mitochondrion and chloroplast undergo duplication process followed by the mitotic cycle (Suzuki et al., 1994). Recently, cell-cycle-dependent proliferation of peroxisomes were observed in *Arabidopsis* synchronized cell cultures, in which expression of genes encoding the core division complex, such as Peroxin11 (PEX11), is regulated by the cell cycle (Lingard et al., 2008). In addition, peroxisomes are capable of changing their morphology, abundance, and content in response to developmental, metabolic, and environmental changes (Fagarasanu et al., 2007; Kaur and Hu, 2009). The peroxisomal population is believed to maintain by division/proliferation and degradation of the organelles. Mitochondria, on the other hand, undergo frequent fusion in addition to the fission and degradation (Chan, 2006; Hoppins et al., 2007).

New peroxisomes can derive *de novo* from subdomains of the endoplasmic reticulum (ER) or by fission from pre-existing peroxisomes (Fagarasanu et al., 2007). In contrast, being descendents of ancient endosymbionts with bacterial origins, mitochondria divide exclusively by binary fission from pre-existing organelles (Osteryoung and Nunnari, 2003). Despite having distinct evolutionary histories and ultrastructures, peroxisomes and mitochondria share at least two families of proteins,

DRP and FIS1, in the fission process across animal, fungal, and plant kingdoms (Fagarasanu et al., 2007; Kaur and Hu, 2009). The major difference in division process between mitochondria and peroxisomes is that peroxisomes require an elongation step before membrane constriction and final fission while mitochondria lack this significant step.

1.4.1 The initial step in peroxisome division

1.4.1.1 Identification of PEX11 proteins in peroxisome elongation

Peroxin11 (PEX11) is specifically involved in the early elongation of peroxisomes (Figure 1.1) (Fagarasanu et al., 2007; Kaur and Hu, 2009). Among the peroxisome division factors, *S. cerevisiae* Pex11p protein was first identified from purified peroxisomal membrane proteins (Erdmann and Blobel, 1995; Marshall et al., 1995). Pex11p null mutant cells contain enlarged peroxisomes and reduced number of these organelles (Erdmann and Blobel, 1995; Sakai et al., 1995). On the other hand, overexpression of Pex11p leads to tubulated peroxisomes and increased peroxisome populations, suggesting that Pex11p is involved in the early elongation step of the peroxisome division (Marshall et al., 1995; Yan et al., 2005). Two additional *S. cerevisiae* Pex11p-related proteins, Pex25p and Pex27p, are involved in the same step, but seem to be functionally distinct from Pex11p (Erdmann and Blobel, 1995; Marshall et al., 1995; Smith et al., 2002; Rottensteiner et al., 2003; Tam et al., 2003). Since Pex25p and Pex27p lack obvious homologs in other species, both proteins are considered to be specific to yeast (Rottensteiner et al., 2003; Tam et al., 2003). In mammals, PEX11 α , - β , and - γ are three PEX11 homologs contributing to peroxisome

elongation at various degrees (Fidaleo, 2010). The functional role of mammalian PEX11 in peroxisomal elongation was suggested by the appearance of elongated peroxisomes in cells overexpressing PEX11- β (Schrader et al., 1998), which also suggests that PEX11 is involved in early elongation of peroxisomes.

Homology-based searches using the *C. boidnni* Pex11p led to the discovery of five Arabidopsis PEX11s, namely AtPEX11a-e (Mullen, 2002; Lingard and Trelease, 2006). Phylogenetic analysis of PEX11 sequences from various species has classified five members of AtPEX11 into three subfamilies, PEX11a, PEX11b, and PEX11c-e (Orth et al., 2007). Online database information and RT-PCR analyses using various Arabidopsis tissues verified that the five AtPEX11 genes are differentially expressed in various plant tissues. All AtPEX11s have been shown to target exclusively to peroxisomes and are integral membrane proteins of peroxisomes (Lingard and Trelease, 2006; Orth et al., 2007). Suppression of AtPEX11c-e significantly reduces peroxisome abundance in Arabidopsis, whereas the single knock-out mutant has no obvious defect in peroxisome division, implying the functional redundancy of AtPEX11s (Orth et al., 2007). Akin to results from other models, ectopic expression of individual five PEX11 members leads to tubulated peroxisomes and subsequently increases in its population in Arabidopsis (Lingard and Trelease, 2006; Orth et al., 2007). Together, PEX11s are positive regulators of peroxisome division, playing a rate-limiting role in the early stage of the division process (Thoms and Erdmann, 2005; Yan et al., 2005; Platta and Erdmann, 2007; Schrader and Fahimi, 2008; Kaur and Hu, 2009). More recently, it was shown that overexpression of mammalian Pex11 induces the formation of pre-peroxisomal membrane structures (Delille et al., 2010) or juxtaposed elongated

peroxisomes (Koch et al., 2010) in addition to inducing peroxisome elongation, suggesting the functional role of Pex11 in the early step of peroxisomal division by remodeling the peroxisomal membrane.

As PEX11s contain amino acid identity within the conserved domains, all of them are believed to be evolved from a common ancestor (Orth et al., 2007). Hence, it is not surprising that most PEX11 proteins maintain similar functions in the division of peroxisomes. This conclusion is based on the fact that *Arabidopsis* PEX11c and PEX11e partially suppress the growth phenotypes of the *S. cerevisiae pex11* mutation (Orth et al., 2007; Koch et al., 2010). In addition, heterogeneous expression of PEX11 from yeast, mammals, and plants in mammalian cells and *Arabidopsis* plants shows that all the tested proteins are recruited exclusively to peroxisomes. Moreover, overexpression of the proteins in heterogeneous system also leads to similar morphological changes of peroxisomes (Koch et al., 2010).

1.4.1.2 Mode of action for PEX11

Although several findings have defined the functional role of PEX11 in the initial step of peroxisome division, the exact molecular mechanism of PEX11 function in the division machinery is still largely unknown. All the studied PEX11 proteins were proven to be integral membrane proteins (Schrader et al., 1998; Lingard and Trelease, 2006; Orth et al., 2007), with an exception of the *S. cerevisiae* Pex11p, which is peripherally associated with the membrane of peroxisomes (Marshall et al., 1995). Due to the presence of ligand-binding domain-liked amino acid sequences on PEX11, Pex11p was suggested to bind phospholipid (Barnett et al., 2000). In addition, some PEX11 proteins

in diverse species contain the dilysine motif (KXKXX), which presumably binds to the COPI coatmer, and the proteins were therefore predicted to perform their function through membrane vesiculation via a coatmer-dependent pathway (Passreiter et al., 1998; Anton et al., 2000). Recently it was shown that *Penicillium chrysogenum* Pex11 contains a conserved amphipathic helix at its N-terminus, which is suggested to be important for the function of Pex11 in binding to the negatively charged lipid and inducing membrane tubulation (Opaliński et al., 2011). In addition to being directly involved in membrane remodeling, the functional role of PEX11s in transporting fatty acids (Voncken et al., 2003) and recruiting downstream factors (Marelli et al., 2004) were also hypothesized.

1.4.1.3 Transcriptional or post-translational regulation of PEX11

To cope with environmental and metabolic changes, peroxisomes are capable of changing their morphology and abundance by multiplying the existing peroxisomes *via* division (Yan et al., 2005; Kaur and Hu, 2009). Among the known peroxisomal division factors, PEX11 are regulated at the transcription level. The peroxisome population in *S. cerevisiae* can be induced by growing the cells on limited growth substrates (e.g. methanol or oleic acid), in which expression of Pex11p is up-regulated by the oleate-activated transcription factor Adr1p, Oaf1p, and Pip2p. The transcription factors coordinately bind to an upstream activation sequence (UAS1) and oleate response elements (ORE) in the promoter of Pex11p (Gurvitz and Rottensteiner, 2006). In mammalian cells, peroxisomal division is induced by fatty acids and hypolipidemic ligands through up-regulation of the PEX11 gene; this transcriptional activation is

controlled by peroxisome proliferator-activated receptor alpha PPAR α . As a target gene of PPAR α , PEX11 α contains the PPAR response element (PPRE), which was shown to be bound by the transcription factor (Desvergne and Wahli, 1999; Kersten et al., 2000).

Although there is no cognate orthologs of the aforementioned transcription factors in Arabidopsis, multiplication of peroxisomes in response to environmental cues is also partly achieved by regulation of *AtPEX11* genes at the transcription level. In Arabidopsis, peroxisome abundance has been shown to be induced by light (Desai and Hu, 2008) and salt stress (Mitsuya et al., 2010). Among the five *AtPEX11* genes, *AtPEX11b* is strongly induced by light. Moreover, the *AtPEX11b* knock-down mutant responds subtly to illumination. Together, these data suggest a pivotal role of the PEX11b isoform in light-induced peroxisome proliferation. Light-dependent induction of *AtPEX11b* is regulated through the far-red light receptor phyA and the bZIP transcription factor, HYH (HY5 Homolog) (Desai and Hu, 2008), suggesting that the increase in peroxisome proliferation during dark-to-light transition in Arabidopsis seedlings is, at least in part, a result of *AtPEX11b* gene activation (Figure 1.1). Similar to light signals, salt stress also up-regulates the expression of PEX11 in Arabidopsis (Mitsuya et al., 2010) and rice (Nayidu et al., 2008), resulting in an increased peroxisome population in Arabidopsis (Mitsuya et al., 2010). In addition, the induction of *AtPEX11e* is regulated through ABA and JA signaling-dependent pathways, in which those hormones act as upstream regulators (Mitsuya et al., 2010).

Post-translational regulation of Pex11p was recently demonstrated in yeast (Knoblach and Rachubinski, 2010). It was shown that Pex11p is phosphorylated in vivo at Ser165 and Ser167. The phosphorylated Pex11p is an active form in peroxisome

division since these phosphorylations are required for the peroxisomal association of the protein (Knoblach and Rachubinski, 2010). According to the Arabidopsis Protein Phosphorylation Site Database (<http://phosphat.mpimp-golm.mpg.de/>), AtPEX11b is phosphorylated at Thr64. It would be interesting to see whether the phosphorylation plays a role in regulating the function of AtPEX11b and consequently regulates peroxisome division.

1.4.2 The fission complex on peroxisomes and mitochondria

1.4.2.1 Identification of dynamin-related proteins (DRPs) in peroxisomal and mitochondrial division

Recent studies of the molecular mechanisms of mitochondrial and peroxisomal division have led to the identification of dynamin-related protein (DRP) as an evolutionarily conserved division factor that executes the final fission of peroxisomes and mitochondria in yeast, mammals and plants (Benard and Karbowski, 2009; Kaur and Hu, 2009). The involvement of DRP in mitochondrial division was first identified in the yeast *S. cerevisiae* (Otsuga et al., 1998). The yeast DRP Dnm1p physically associates with mitochondria at the constriction sites (Bleazard et al., 1999) and forms a spiral-like structure to mediate membrane fission through GTP hydrolysis (Ingerman et al., 2005). In addition to mitochondrial fission, Dnm1p is also involved in the division of peroxisomes (Kuravi et al., 2006). Silencing of the mammalian DRP gene Drp1/DLP1 results in elongated peroxisomes that have already been constricted, causing the “beads-on-a-string” phenotype (Hoepfner et al., 2001; Kuravi et al., 2006). Ectopic expression of *PEX11* in cells lacking a functional Drp1 only results in tubulated

peroxisomes without increasing the peroxisome population. These findings together suggest that DRP is responsible for executing the fission step of peroxisomal and mitochondrial division (Koch et al., 2003; Koch et al., 2005; Schrader, 2006).

The Arabidopsis genome contains 16 DRP proteins, which are categorized into six subfamilies (DRP1-6) based on their sequence and protein structure similarity (Hong et al., 2003). A phylogenetic study of dynamin-related proteins across diverse species showed that Arabidopsis DRP3 proteins DRP3A and DRP3B belong to the same subclade as Dnm1p and Drp1 (Arimura and Tsutsumi, 2002; Miyagishima et al., 2008), suggesting functional conservation among DRP3A, DRP3B and other members of this subgroup. Indeed, DRP3A and DRP3B are involved in the division of peroxisomes and mitochondria based on the observation that *drp3* mutants show impaired division in both organelles (Arimura et al., 2004; Logan et al., 2004; Mano et al., 2004; Aung and Hu, 2009; Fujimoto et al., 2009; Zhang and Hu, 2009). Since *drp3A* mutants show much stronger peroxisomal and mitochondrial phenotypes compared to the *drp3B* mutants, DRP3A is suggested to play a dominant role over DRP3B in organelle division (Mano et al., 2004; Fujimoto et al., 2009; Zhang and Hu, 2009). Moreover, DRP5B, a DRP distantly related to DRP3, was found to be localized, and involved in the division of, peroxisomes and chloroplasts, organelle that are also linked through a number of metabolic pathways (Gao et al., 2003; Zhang and Hu, 2010).

1.4.2.2 Mode of action for DRP

Dynamins and DRPs are large GTPases that mediate membrane fission by forming collar-like oligomeric complexes around the neck of constriction sites and acting

as mechanochemical enzymes through GTP hydrolysis (Osteryoung and Nunnari, 2003). Dynamins are composed of five conserved domains, including the GTPase domain (DYN1, which contains GTPase activity), middle domain (DYN2, which is involved in the assembly of dynamin-dynamin complex through coiled-coil domain), GTPase-effector domain (GED, which is involved in dynamin-dynamin assembly through the coiled-coil domain as well as stimulation of the GTPase activity), pleckstrin-homology domain (PH, which binds to lipid), and a proline- and arginine-rich domain (PRD, which contains a protein-protein interaction domain, SH3-binding domain). DRP contains at least three of the five conserved domains: DYN1, DYN2 and GED. Similar to dynamin, yeast Dnm1p has GTPase activity, can self-assemble to form a spiral-like structure, in which the size of the ring structure matches the size of the mitochondrial constriction sites (Ingerman et al., 2005). The assembled DRP polymers were suggested to act as mechanochemical enzymes in a GTP hydrolysis-dependent manner (Osteryoung and Nunnari, 2003; Praefcke and McMahon, 2004; Fagarasanu et al., 2007). Recently, the three-dimensional (3D) structure of Dnm1p was solved using cryo-electron microscopy, which shows that the Dnm1p spiral-like structure undergoes a large conformational change upon the presence of GTP. This conformational change is suggested to initiate the mitochondrial membrane constriction and fission (Mears et al., 2011). Furthermore, the high-resolution crystal structure of human Dynamin1 was presented in two independent studies (Ford et al., 2011; Faelber et al., 2011). Both groups utilized an assembly-deficient Dynamin1 mutant to solve the protein structure of Drp1 monomers. Crystal structure of the nearly full-length Dynamin1 showed that the higher order assembly of Drp1 is achieved through the criss-cross assembly of the

stalks (Ford et al., 2011; Faelber et al., 2011). These findings provide valuable information not only to the understanding of the molecular mechanism of Dynamin1 in membrane scission, but also to the investigation of the formation of higher order DRP complexes and its molecular function in peroxisomal and mitochondrial division.

1.4.3 Recruitment of DRP to the division sites of the organelles

Since most DRPs lack a putative lipid binding domain (Pleckstrin homology domain; PH domain) or transmembrane domain, they are often found in the cytosol and recruited to the division sites by membrane-bound receptors with or without the assistance of cytosolic adaptors. Biochemical analyses showed that only approximately 3% of the total mammal Drp1 protein was cofractionated with mitochondria (Smirnova et al., 2001), suggesting that the vast majority of Drp1 remains in the cytosol or associates with other organelle like peroxisomes. In general, DRP is often found at the end or the constriction sites of mitochondria. However, the targeting of DRP to peroxisomes is not easily observed; it can be found in juxtaposition to the peroxisome.

1.4.3.1 FIS1 in peroxisomal and mitochondrial division

The last decade has been a prolific period in identification of proteins involved in recruiting DRP to the division sites or regulators of DRP's function. Multiple lines of evidence have suggested that FISSON1 (FIS1), a protein dual-targeted to peroxisomes and mitochondria, functions as a membrane-bound receptor recruiting DRP directly or indirectly to the membranes of organelles (Mozdy et al., 2000; James et al., 2003; Koch et al., 2003; Yoon et al., 2003; Koch et al., 2005; Kobayashi et al., 2007). FIS1 is

tethered to the membranes by its C-terminal tail and contains an N-terminal tetratricopeptide repeat (TPR) domain that is exposed to the cytosol (Mozdy et al., 2000; Koch et al., 2003; Koch et al., 2005; Kobayashi et al., 2007). This topology suggests that the DRP or DRP-containing complex is recruited to the division sites directly or indirectly through FIS1's protein-protein interaction domain (TPR). The functional role of FIS1 in peroxisomal and mitochondrial division was evidenced by a significant defect in the division of the organelles shown in the knock-out or knock-down mutants (Koch et al., 2005; Kobayashi et al., 2007). Suppression of *FIS1* by siRNA phenocopied the *Drp1* siRNA mutant, whereas ectopic expression of the *FIS1* gene caused an increase in the number of peroxisomes and mitochondria, implying the rate-limiting role of Fis1 in peroxisomal/mitochondrial fission (Koch et al., 2005; Kobayashi et al., 2007).

Arabidopsis contains two FIS1 orthologs, FIS1A (BIGYIN) and FIS1B. Both proteins have been identified as peroxisomal and mitochondrial division factors. Loss-of-function mutants contain a reduced number of peroxisomes and mitochondria, whereas plants overexpressing each gene showcase a significant increase in peroxisomal/mitochondrial number (Zhang and Hu, 2009). Although FIS1s have been characterized as positive regulators in organelle division and shown to interact with DRP3/5B (Zhang and Hu, 2010), their ability to directly or indirectly recruit DRPs has yet to be demonstrated in *Arabidopsis*. Since FIS1 is found in almost all species studied, it is believed to be another conserved division factor in peroxisome and mitochondria (Figure 1.2).

1.4.3.2 Yeast *Mdv1p* and *Caf4p* in peroxisomal and mitochondrial division

Even though FIS1 is a conserved membrane-bound receptor in recruiting the DRP protein to the organelle membranes, recent discoveries of lineage-specific adaptor proteins and membrane-bound receptors challenge the prominent role of FIS1 as the major receptor of DRP. In yeast, the membrane-bound receptor Fis1p functions together with two WD40 repeat proteins, Mdv1p and its paralog, Caf4p, which serve as cytosolic adaptor proteins (Tieu and Nunnari, 2000; Tieu et al., 2002; Hoppins et al., 2007; Motley et al., 2008). Mdv1p and Caf4p contain three distinct functional domains; an N-terminal domain that interacts with Fis1p, the middle coiled-coil domain involved in homodimerization, and the C-terminal WD-40 domain that heterodimerizes with Dnm1p (Koirala et al., 2010). The *mdv1p* null mutant phenocopies the *dnm1p* mutant by blocking the fragmentation of mitochondria (Tieu and Nunnari, 2000), whereas disruption of Caf4p has no detectable effect on mitochondrial morphology (Griffin et al., 2005). Mdv1p and Caf4p physically interact with both Fis1p and Dnm1p (Tieu and Nunnari, 2000; Griffin et al., 2005), suggesting their role as molecular adaptors in recruiting Dnm1p to the constriction site. Due to the lack of apparent functional or structural homologs of Mdv1p and Caf4p in other species, those two proteins are currently defined as yeast-specific factors in peroxisomal and mitochondrial division (Figure 1.2A).

1.4.3.3 The mammalian *Mff1* in peroxisomal and mitochondrial division

A screen of the *Drosophila* RNAi library for mutants with abnormal mitochondria has identified a metazoan-specific mitochondrial fission factor, Mff. The mammalian Mff

ortholog was demonstrated for its role in the division of peroxisomes and mitochondria, as mammalian cells lacking Mff contain interconnected mitochondria and elongated peroxisomes (Gandre-Babbe and van der Bliik, 2008). Since Mff is a tail-anchored coiled-coil protein on the mitochondrial outer membrane and peroxisomal membrane, it was postulated to be a membrane-bound receptor for division factors, such as DRP. Consistent with the hypothesis, Otera et al. (2010) showed that Mff1 transiently interacts with Drp1 and recruits Drp1 to the constriction site of mitochondria, suggesting that Mff1 is a membrane-bound receptor of Drp1. Since disrupting the functional Fis1 does not interfere with the recruitment of Drp1 to the constriction sites, the targeting of Drp1 in mammals is mainly dependent on Mff1 (Otera et al., 2010). In addition to recruiting Drp1 to the division site, Mff also has a positive effect in regulating the GTPase activity of Drp1, presumably through stimulating the self-assembly of Drp1 at the fission site (Otera and Mihara, 2011). As Mff is identified only in metazoan, it is considered to be a metazoan-specific division factor (Figure 1.2B).

1.4.3.4 The role of mammalian MIEF1/MiD51 and MiD49 in mitochondrial division

Studies in human from two independent groups have led to the identification of novel Drp1 regulators, mitochondrial elongation factor 1 (MIEF1/MiD51) (Palmer et al., 2011a; Zhao et al., 2011) and its homolog mitochondrial dynamics protein (MiD49) (Palmer et al., 2011a). MIEF is a membrane protein, which anchors to the outer membrane of mitochondria through a transmembrane domain at its N-terminus. It shows similar sub-cellular and sub-organelle localization patterns as Drp1 by targeting to punctate foci on mitochondria. In addition to the same sub-organelle localization,

MIEF1 and MiD49 physically associate with Drp1 and recruit DRP1 to the division site independently from Fis1 or Mff1 (Palmer et al., 2011a; Zhao et al., 2011). Unlike other DRP regulators, MIEF plays a negative role by inhibiting the activity of DRP at the division site. Suppression of MIEF resulted in fragmented mitochondria, which is due to an increased rate of the organelle division (Zhao et al., 2011). Moreover, overexpression of MIEF caused massively tubulated mitochondria, suggesting that MIEF inhibits fission but promotes the fusion of mitochondria (Zhao et al., 2011). This finding adds an additional layer of complexity to the mitochondrial division machinery in mammals (Figure 1.2B). Since MIEF inhibits Drp1 activity in mitochondrial division, it is interesting to investigate whether MIEF has a functional role in peroxisomal division as Drp1 is shared between those two organelles.

1.4.3.5 *Arabidopsis ELM1 in mitochondrial division*

In *Arabidopsis*, Elongated mitochondria1 (ELM1) was identified through a genetic screen of abnormal mitochondrial morphology by showing extensive elongation of mitochondria in the *elm1* null mutant (Arimura et al., 2008). Using fluorescent microscopy, ELM1 was detected on the outer surface of mitochondria (Arimura et al., 2008) and appeared as ring-like structures around mitochondria (Duncan et al., 2011). In addition to the membrane association, ELM1 physically interacts with DRP3A and DRP3B and can re-translocate DRP3A from the cytosol to mitochondria upon transient induction of ELM1 in the *elm1* null mutant harbouring an estradiol-inducible *ELM1* (Arimura et al., 2008). As there is no detectable physical interaction between ELM1 and FIS1, the recruitment of the DRP3A-ELM1 complex seems to be independent from FIS1

(Figure 1.3C, Arimura et al., 2008). In addition, ELM1 seems to function only in mitochondrial division as there is no significant impact on peroxisomal morphology in the mutant (Arimura et al., 2008). Given that the protein has no ortholog in other eukaryotes, it is postulated to be a plant-specific mitochondrial division factor (Arimura et al., 2008).

1.4.4 Post-translational regulation of DRP

Since DRP1 is the major molecular regulator of peroxisomal and mitochondrial division, it is not surprising that multiple post-translational modification mechanisms target Drp1 and regulate its function in the division of mitochondria. To date, phosphorylation, sumoylation, ubiquitination, and *S-Nitrosylation* have been shown to regulate the function of the mammalian Drp1 protein.

1.4.4.1 Phosphorylation

Among the different types of post-translational modifications, phosphorylation plays both positive and negative roles in regulating the activity of Drp1 in mammals. The first line of evidence came from the study of mitochondrial dynamics in mitotic HeLa cells, in which Drp1 was phosphorylated at Ser616 by cyclin B-CDK1 kinase (Taguchi et al., 2007). The phosphorylation results in an induction of mitochondrial fragmentation/fission during mitosis through a yet uncharacterized mechanism. Recently, it was shown that RALA, a small Ras-GTPase, and its effector RALBP1 function together to activate cyclin B-CDK1 kinase, resulting in the phosphorylation of Drp1 at Ser616 (Kashatus et al., 2011). In addition, Drp1 is also phosphorylated at

Ser637 in the GED domain by cyclic AMP-dependent protein kinase (Chang and Blackstone, 2007; Cribbs and Strack, 2007). This phosphorylation attenuates the GTPase activity of Drp1 and as a result, inhibits mitochondrial fission (Chang and Blackstone, 2007; Cribbs and Strack, 2007). The phosphorylation at Ser637 can be reversed by calcineurin, a phosphatase, in which the dephosphorylation promotes association of Drp1 with mitochondria (Cereghetti et al., 2008). Intriguingly, phosphorylation at the same residue, Ser637, by Ca^{2+} /calmodulin-dependent protein kinase I α (CaMKI α), was shown in another study to promote the translocation of Drp1 from the cytosol to mitochondria and hence inducing mitochondrial division (Han et al., 2008). These contradictory results may suggest that temporal or spatial regulation of Drp1 by kinase proteins, which themselves might be differentially regulated in different cell types or by different stimuli, is involved in maintaining the mitochondrial population.

1.4.4.2 Ubiquitination

Ubiquitin is a small protein that regulates the activity of a wide range of target proteins through ubiquitination (Kerscher et al., 2006). Identification and characterization of human membrane associated RING-CH (MARCH)-V revealed the functional role of the mitochondrial membrane-associated E3 ubiquitin ligase (also known as MITOL) in mitochondrial division (Nakamura et al., 2006; Yonashiro et al., 2006). MARCH-V is involved in the fission and fusion of mitochondria by physical interaction with ubiquitinated Drp1, Fis1 (Nakamura et al., 2006; Yonashiro et al., 2006), and mitofusin 2 (MFN2) (Yonashiro et al., 2006). In addition, MARCH-V promotes ubiquitination of Drp1 by functioning as an E3 ubiquitin ligase (Nakamura et al., 2006).

Disruption of the function of MARCH-V results in elongated mitochondria (Karbowski et al., 2007). Although the molecular consequences of DRP1 ubiquitination are not yet well understood, it was suggested that ubiquitination activates Drp1 and therefore promotes mitochondrial fission. Hence, ubiquitination of the mitochondrial fission and fusion factors by MARCH-V plays a critical role in the regulation of mitochondrial dynamics in mammals.

1.4.4.3 Sumoylation

Sumoylation is a type of post-translational modification that is similar to ubiquitination, in which a small ubiquitin-like modifier (SUMO) is conjugated to target proteins by three enzymatic enzymes: SUMO E1, SUMO E2, and SUMO E3 (Geiss-Friedlander, 2007). The SUMO1 protein physically interacts with Drp1 in mammalian cells, and overexpression of SUMO1 results in stabilization of Drp1 and thus induction of mitochondrial fragmentation (Harder et al., 2004), suggesting that sumoylation of Drp1 positively regulates its activity. Similarly, the SUMO-conjugating enzyme Ubc9 also physically associates with Drp1 and can sumoylate the protein (Figuroa-Romero et al., 2009). In addition, the mitochondrial-anchored protein MAPL was identified as a SUMO E3 ligase, which is involved in sumoylation of Drp1 in vivo (Neuspiel et al., 2008; Braschi et al., 2009). Similar to SUMO1, ectopic expression of MAPL induces mitochondrial fragmentation (Neuspiel et al., 2008), providing further evidence that sumoylation of DRP1 plays a positive role in mitochondrial division. Although Drp1 does not contain canonical sumoylation sequences, lysine residues within the B domain were suggested to be sumoylated (Figuroa-Romero et al., 2009).

Sumoylation is a reversible process, in which many SUMO-specific proteases have been identified for their role in removing SUMOs from sumoylated proteins. By screening for suppressors of SUMO1-induced mitochondrial fragmentation in mammalian COS-7 cells, SUMO1/sentrin-specific peptidase 5 (SEN5) was identified as the SUMO protease. Ectopic expression of SEN5 results in elongated mitochondria due to the suppression of SUMO1-induced mitochondrial division. In contrast, inhibition of SEN5 leads to fragmented mitochondria by increasing Drp1-dependent division (Zunino et al., 2007). Together, all data point toward a conclusion that sumoylation of Drp1 induces its function in mitochondrial division, although the exact mechanism has yet to be demonstrated.

1.4.4.4 *S-Nitrosylation*

Nitric oxide (NO) is known as a signaling molecule. In addition, NO confers post-translational modification of target proteins by covalently attaching a nitrogen monoxide group to cysteine, a process termed *S-Nitrosylation* (Hess et al., 2005). Drp1 was found to be *S-Nitrosylated* at Cys644, and the *S-Nitrosylated* Drp1 induces mitochondria fragmentation (Cho et al., 2009). Since *S-Nitrosylation* of dynamin has been shown to promote homodimerization of dynamin and increase its GTPase activity (Wang et al., 2006), it is hypothesized that *S-Nitrosylation* of Drp1 may also promote mitochondrial fission through a similar mechanism.

Taken together, studies of the mammalian Drp1 protein have demonstrated that post-translational modification plays critical roles in regulating the activity and/or sub-cellular localization of Drp1 in mitochondrial division. Although the individual covalent

modifications confer either positive or negative effect on Drp1, it is speculated that one type of modification can influence post-translational modifications at other residues. Given that Drp1 is also the key regulator in the division of peroxisomes, it is tempting to hypothesize that the modifications result in similar effects on peroxisomal division.

1.5 Aims of the thesis research

This thesis is aimed at dissecting the division machinery of peroxisomes and mitochondria in *Arabidopsis* by identifying novel division factors and examining the regulation of the known division factors. In Chapter 2, I identified a plant-specific protein, Peroxisomal And Mitochondrial Division Factor1 (PMD1), which promotes the division of peroxisomes and mitochondria through an unknown mechanism that is independent from DRP3-FIS1. PMD2, a close homolog of PMD1, was identified as PMD1-interacting protein that is targeted exclusively to mitochondria and involved in mitochondrial morphogenesis. In *Arabidopsis*, DRP3A and DRP3B are involved in the division of peroxisomes and mitochondria, and DRP5B (ARC5) is a division factor for chloroplasts (Gao et al., 2003) and peroxisomes (Zhang and Hu, 2010). In Chapter 3, I further characterized these three DRP proteins, revealing a role for DRP5B in mitochondrial division/morphogenesis and showing that DRP3A is the core component of the DRP3 complex. In Chapter 4, I studied post-translational regulation of DRP3 and provided evidence that the function of DRP3A and DRP3B are regulated by protein phosphorylation. In Chapter 5, I characterized the *Arabidopsis* dual-targeted adenine nucleotide transporter (AAC1) and the peroxisomal NAD⁺ carrier (PXN) for their role in organelle morphogenesis. My data suggested a role for peroxisomal and mitochondria

metabolism in regulating the division or morphogenesis of these organelles in Arabidopsis. In appendices, I presented the identification of a new *drp3A* allele, *peroxisome division defective 2 (pdd2)*, and domain analysis of PMD1.

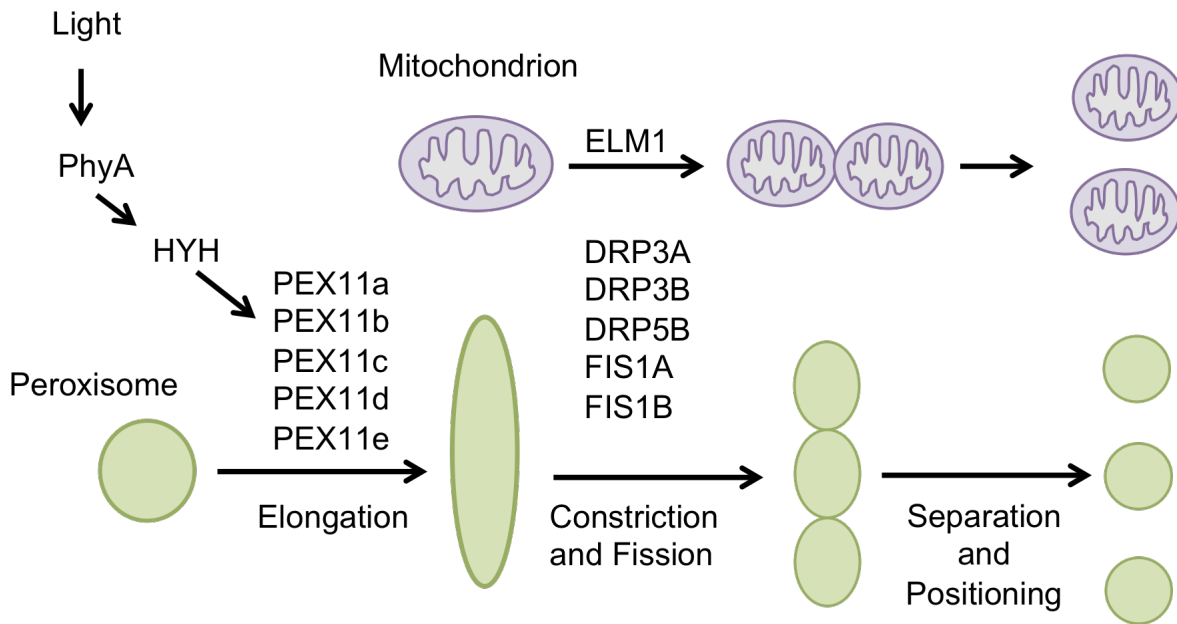
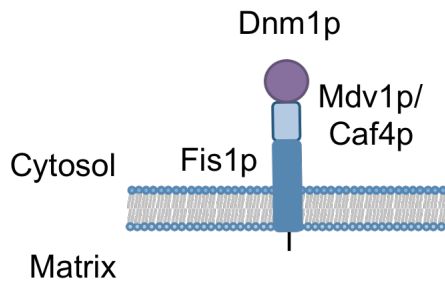


Figure 1.1. A model for peroxisomal and mitochondrial divisions in Arabidopsis.

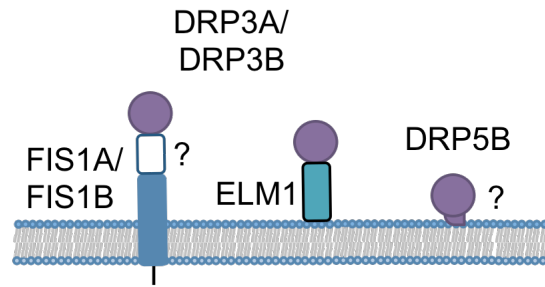
PEROXIN11 (PEX11) is conserved in eukaryotes and specifically involved in promoting peroxisome elongation/tubulation. Dynamin-related proteins (DRPs) are large self-assembling GTPases involved in the fission and fusion of membranes by acting as mechanochemical enzymes. FISSION1 (FIS1) proteins are C-terminal tail-anchored (C-TA) proteins, which mediate peroxisome and mitochondrial fission by recruiting DRP proteins to the organelle membrane. Elongated Mitochondria 1 (ELM1) is specifically involved in mitochondrial division by interacting with DRP3 proteins.

For interpretation of the references to color in this and all other figures, the reader is referred to the electronic version of this dissertation.

A. Yeast



C. Plants



B. Mammals

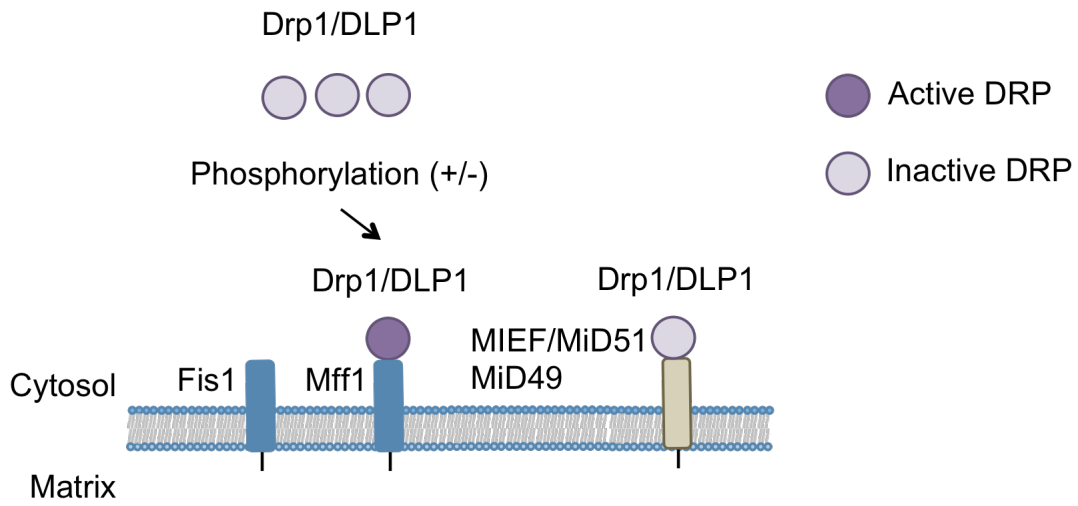


Figure 1.2

Figure 1.2 (cont'd)

Figure 1.2. Comparative models for the recruitment of DRP to the organelle division sites.

Dynamamin-related proteins (Dnm1p in yeast, Drp1/DLP1 in mammals and DRP3 in plants) are mostly found in the cytosol due to the absence of transmembrane domain or lipid binding domain (Arabidopsis DRP5B contains a putative lipid binding domain). Hence the membrane association of most DRPs is achieved through their interaction with cytosolic adaptor proteins and/or membrane-bound receptors.

(A) In yeast, Dnm1p interacts with WD40-domain containing cytosolic adaptor proteins, Mdv1p and Caf4p, and the complex is recruited to the membrane by a membrane-bound receptor, Fis1p.

(B) In mammals, the recruitment of Drp1 is achieved at least partly through its physical interaction with a C-terminal tailed-anchored protein, Mitochondrial fission factor1 (Mff1). In addition, two membrane proteins, mitochondrial elongation factor 1 (MIEF1/MiD51) and its homolog mitochondrial dynamics protein MiD49, also recruit Drp1 to the membrane through physical association; however, the interaction between MiD and Drp1 inhibits the activity of Drp1. Moreover, phosphorylation of Drp1 also affects the membrane association of the protein.

(C) In Arabidopsis, three members of the DRP superfamily have been characterized for their role in organelle division. Although the functional role of FIS1 in recruiting DRP3 to the membrane has not been demonstrated, Elongated Mitochondria1 (ELM1) can tether DRP3 to the membrane. As DRP5B contains a lipid-binding domain (PH), the protein is predicted to bind directly to the membrane.

CHAPTER 2

The *Arabidopsis* tail-anchored protein PEROXISOMAL AND MITOCHONDRIAL DIVISION FACTOR 1 is involved in the morphogenesis and proliferation of peroxisomes and mitochondria

The work presented in this chapter has been accepted:
Kyaw Aung and Jianping Hu (2011)
Plant Cell 10.1105/tpc.111.090142.

ABSTRACT

Peroxisomes and mitochondria are multifunctional eukaryotic organelles that are not only interconnected metabolically but also share proteins in division. Two evolutionarily conserved division factors, dynamin-related protein (DRP) and its organelle anchor FISSION1 (FIS1), mediate the fission of both peroxisomes and mitochondria. Here, we identified and characterized a plant specific protein shared by these two types of organelles. The Arabidopsis PEROXISOMAL and MITOCHONDRIAL DIVISION FACTOR 1 (PMD1) is a coiled-coil protein tethered to the membranes of peroxisomes and mitochondria by its C-terminus. Null mutants of *PMD1* contain enlarged peroxisomes and elongated mitochondria, and plants overexpressing *PMD1* have an increased number of these organelles that are smaller in size and often aggregated. PMD1 lacks physical interaction with the known division proteins DRP3 and FIS1; it is also not required for DRP3's organelle targeting. Affinity purifications pulled down PMD1's homolog, PMD2, which exclusively targets to mitochondria and plays a specific role in mitochondrial morphogenesis. PMD1 and PMD2 can form homo- and heterocomplexes. Organelle targeting signals reside in the C-termini of these proteins. Our results suggest that PMD1 facilitates peroxisomal and mitochondrial proliferation in a FIS1/DRP3-independent manner, and that the homologous proteins PMD1 and PMD2 perform non-redundant functions in organelle morphogenesis.

INTRODUCTION

In eukaryotic cells, organelles are delimited by their own lipid bilayers, providing membrane-bound compartments for specific biochemical reactions to occur. Peroxisomes and mitochondria are ubiquitous and multifunctional organelles with essential roles in development. Surrounded by a single membrane, peroxisomes house a variety of metabolic processes such as fatty acid β -oxidation, scavenging of reactive oxygen species and peroxides, ether phospholipid biosynthesis and fatty acid α -oxidation in mammals, and photorespiration and the glyoxylate cycle in plants (Wanders and Waterham, 2006; Kaur et al., 2009). Mitochondria are enclosed by a double membrane, and serve as the powerhouse of the cell by performing functions such as respiration, ATP synthesis, and tricarboxylic acid (TCA) cycle (Millar et al., 2008). Although each type of organelle carries a unique set of biochemical functions, a number of intracellular metabolic pathways are known to be completed coordinately by multiple organelles including peroxisomes and mitochondria. In plants for example, the recycling of phosphoglycolate during photorespiration is executed by the sequential action of chloroplasts, peroxisomes, and mitochondria (Peterhansel et al., 2010). The conversion of fatty acids to sucrose during oilseed establishment involves the cooperative participation of lipid bodies, peroxisomes, mitochondria, and the cytosol (Baker et al., 2006; Penfield et al., 2006).

In light of these highly coupled functions, it is not that surprising that peroxisomes and mitochondria also share division factors (Delille et al., 2009; Kaur and Hu, 2009). The peroxisome is believed to be an endoplasmic reticulum (ER)-derived member of the endomembrane system and can form out of the ER in cells in which peroxisomes are

lost (Hoepfner et al., 2005; Gabaldon et al., 2006; Schluter et al., 2006; Titorenko and Mullen, 2006). Peroxisomes can also proliferate from pre-existing peroxisomes through growth and division (Purdue and Lazarow, 2001; Fagarasanu et al., 2007; Kaur and Hu, 2009). Mitochondria, like chloroplasts, are descendents of ancient endosymbionts with bacterial origins and thus divide exclusively by binary fission from pre-existing organelles (Osteryoung and Nunnari, 2003). Despite having distinct evolutionary histories and ultrastructures, peroxisomes and mitochondria share at least two proteins in the fission process across animal, fungal, and plant kingdoms (Fagarasanu et al., 2007; Kaur and Hu, 2009). Dynamin-related proteins (DRPs) are key factors in peroxisomal and mitochondrial division, where these large and self-assembling GTPases form a spiral-like structure around the membranous structures to mediate membrane fission through GTP hydrolysis (Praefcke and McMahon, 2004; Kaur and Hu, 2009). Through forward genetic screens followed by homology-based searches, two *Arabidopsis* DRP homologs, DRP3A and DRP3B, have been found to mediate the division of peroxisomes and mitochondria, with DRP3A playing a predominant role (Arimura and Tsutsumi, 2002; Arimura et al., 2004; Aung and Hu, 2009; Fujimoto et al., 2009; Zhang and Hu, 2009). DRP5B, a DRP distantly related to DRP3, was found to be localized to peroxisomes and chloroplasts and mediate the division of these two organelles, which are also linked through a number of metabolic pathways (Gao et al., 2003; Zhang and Hu, 2010). Since most eukaryotic DRPs lack a putative lipid binding domain (Pleckstrin homology domain; PH domain) or transmembrane domain, they are often found in the cytosol and only recruited to the division sites by interacting directly or indirectly with a membrane-bound receptor named FISSION1 (FIS1) (reviewed in Kaur

and Hu, 2009). FIS1 is tethered to the membranes by its C-terminus, exposing its N-terminal tetratricopeptide repeat (TPR) domain to the cytosol (Mozdy et al., 2000; Koch et al., 2003; Koch et al., 2005; Kobayashi et al., 2007). Arabidopsis contains two homologs of FIS1, FIS1A (BIGYIN) and FIS1B. Protein localization and reverse genetic analyses confirmed the role of the Arabidopsis FIS1A and FIS1B in peroxisomal and mitochondrial division, although their role in recruiting DRP3 proteins to the division sites has not been proved yet (Scott et al., 2006; Lingard et al., 2008; Zhang and Hu, 2008; Zhang and Hu, 2009).

In addition to FIS1 and DRP, the yeast peroxisomal and mitochondrial division complex also contains adaptor proteins, Mdv1p and Caf4p, which are WD-40 proteins that interact with both DRP and FIS1 to target DRP to the fission sites (Tieu and Nunnari, 2000; Tieu et al., 2002; Motley et al., 2008; Nagotu et al., 2008). Although homologs of Mdv1p/Caf4p have not been identified in metazoans and plants, Mitochondrial fission factor (Mff) is a metazoan specific and tail-anchored coiled-coil protein that is involved in the division of peroxisomes and mitochondria (Gandre-Babbe and van der Blik, 2008). It interacts directly with Drp1 and recruits it to the mitochondrial fission sites in a Fis1-independent manner (Otera et al., 2010). In Arabidopsis, ELONGATED MITOCHONDRIA1 (ELM1) is a plant specific protein that mediates mitochondrial division by recruiting DRP3A to the mitochondrial division sites; it does not play a role in peroxisomal division. ELM1 lacks putative transmembrane domains and does not interact with FIS1, thus the mechanism by which it recruits DRP3A to the mitochondrial membrane remains to be elucidated (Arimura et al., 2008). In summary, whereas the core peroxisomal and mitochondrial division factors DRP and

FIS1 are conserved in eukaryotes, lineage and organelle specific components of the division machineries also exist.

Efforts to uncover components of the plant peroxisome division apparatus, such as forward genetic screens in Arabidopsis plants expressing a fluorescent protein tagged by the C-terminal Peroxisome Targeting Signal Type 1 (PTS1), repeatedly identified alleles of *DRP3A* (Mano et al., 2004; Aung and Hu, 2009; Zhang and Hu, 2009). To identify additional components, we employed an in silico strategy by searching the Arabidopsis genome for uncharacterized proteins with putative transmembrane domains (TMDs) in addition to a protein-protein interaction domain that is also found in previously identified organelle division proteins. We initially focused on the coiled-coil (CC) domain because several CC proteins have been shown to function in organelle division in diverse species. A CC domain consists of heptad repeats, each of which contains hydrophobic residues in the first and fourth positions and charged/polar residues in the fifth and seventh positions. CC proteins are known to homo- or heterodimerize and involved in diverse cellular functions (Rose et al., 2004; Rose et al., 2005). In addition to the aforementioned mammalian mitochondrial and peroxisome division factor Mff, which is a C-terminal tail-anchored (C-TA) protein with a cytosolic coiled-coil domain (Gandre-Babbe and van der Bliet, 2008; Otera et al., 2010), Arabidopsis homologous proteins PLASTID DIVISION 1 and 2 (PDV1 and PDV2) also contain CC domains. The PDV proteins are anchored to the outer envelope membrane of plastids via the transmembrane domain and use the N-terminal cytosolic CC domain to recruit the large GTPase DRP5B (ARC5) to the division site (Miyagishima et al., 2006; Yang et al., 2008).

Here, we report the identification of a coiled-coil protein, PMD1, from the ARABI-COIL database (<http://136.227.60.226/arabidopsis/main.html>) (Rose et al., 2004). PMD1 is an integral membrane protein localized to both peroxisomes and mitochondria. Genetic analyses of the *pmd1* mutants revealed its role in the morphogenesis and proliferation of peroxisomes and mitochondria. We also identified a PMD1 homolog, PMD2, as a PMD1-interacting protein that functions exclusively in mitochondria. The C-terminus of PMD1 and PMD2 constitute organelle targeting signals. Our results suggest that the plant specific protein PMD1 contributes to peroxisomal and mitochondrial proliferation in a pathway that is independent from the previously defined pathway controlled by the FIS1-DRP3 complex. Furthermore, the homologous proteins PMD1 and PMD2 perform non-redundant functions in organelle morphogenesis.

RESULTS

PMD1 is Dual Localized to Peroxisomes and Mitochondria, whereas its Homolog, PMD2, Exclusively Targets to Mitochondria

To identify additional proteins involved in peroxisome division/proliferation, we used two criteria to search the ARABI-COIL database available at <http://136.227.60.226/arabidopsis/main.html> (Rose et al., 2004). First, the protein has to have at least one putative transmembrane domain (TMD), as predicted by the plant membrane protein database (Aramemnon: <http://aramemnon.uni-koeln.de/>). Second, since it was estimated that ~10% of the total proteins of an organism contain CC motifs (Liu and Rost, 2001), we first focused on proteins that contain long coiled-coil domains,

i.e., those that cover more than 50% of the entire protein sequence. As a result, seven proteins were retrieved. Four of them had been experimentally verified by previous studies to target to the cytosol, nucleus, plasma membrane, or plastid, two were predicted to be mitochondrial, and one was predicted to localize to multiple non-peroxisomal compartments (Table 2.1). We made yellow fluorescent protein (YFP)-fusions of these proteins and co-expressed them transiently with a peroxisomal marker in *Nicotiana tabacum*. Fluorescent microscopy of the infiltrated tobacco leaf epidermal cells was performed to identify those candidate proteins that are associated with peroxisomes. Only one protein, which is encoded by At3g58840, was found to co-localize with peroxisomes. We named this protein PEROXISOMAL AND MITOCHONDRIAL DIVISION FACTOR 1 (PMD1), because it was later found to localize to both peroxisomes and mitochondria (see below).

The *PMD1* gene has a single exon (Figure 2.1A). Its protein product contains four putative coiled-coil domains at the N-terminus and a single segment of TMD near the C-terminal end (Figure 2.B). Therefore, PMD1 qualifies as a C-TA (C-terminal tail anchored) protein, as defined previously for proteins with a single membrane-spanning domain at or near the C-terminus (Abell and Mullen, 2011). Arabidopsis has a homolog of PMD1, which is encoded by At1g06530; this homolog was later named PMD2. PMD2 also has a single exon and was among the seven candidate proteins identified from our *in silico* searches (Table 2.1). PMD1 and PMD2 share an overall 35% amino acid identity and similar domain structures along the length of the proteins (Figure 2.1C). Using protein sequence similarity-based blast searches, we were able to identify

homologous sequences from other plant species but did not find obvious homologs of PMD1 and PMD2 in non-plant genomes.

To confirm the subcellular localization of PMD1, we expressed the *YFP-PMD1* fusion gene under the control of the 995-bp *PMD1* native promoter in Arabidopsis plants containing a peroxisomal marker (Cyan Fluorescent Protein-PTS1, or CFP-PTS1) (Fan et al., 2005) or a mitochondrial marker (*S. cerevisiae* COX4-CFP) (Nelson et al., 2007). Subcellular localization of YFP-PMD1 was examined using confocal laser scanning microscopy in T₂ plants. YFP-PMD1 colocalized with CFP-PTS1 and also formed a ring-like structure on the surface of COX4-CFP-tagged mitochondria (Figure 2.2A). In agreement with the view that most C-TA proteins use the TMD-containing C-terminal region for targeting (Borgese et al., 2007; Abell and Mullen, 2011), the PMD1-YFP fusion protein, in which YFP is located at the C-terminus of PMD1, was found only in the cytosol, possibly due to masking of the C-terminus by YFP, which prevented its organelle targeting (Figure 2.3).

Although PMD2 was not found to be associated with peroxisomes in our initial transient studies, the sequence and structural similarities it shares with PMD1 prompted us to re-analyze its subcellular localization. To this end, YFP-PMD2 was expressed under the control of the 35S promoter in Arabidopsis plants that carry CFP-PTS1 or COX4-CFP. Confocal imaging of T₂ transgenic plants discovered the localization of YFP-PMD2 on the surface of COX4-CFP-labelled mitochondria, as shown by ring-like structures outside mitochondria. However, none of the YFP-PMD2 signals co-localized with the CFP-PTS1-marked peroxisomes, suggesting that the protein is sorted to mitochondria only (Figure 2.2B).

In summary, our data corroborated with results from a recent genome-wide analysis of C-TA proteins in Arabidopsis, which showed the localization of PMD1 to mitochondria (Kriechbaumer et al., 2009). In addition, we uncovered the association of PMD1 with peroxisomes. In contrast, PMD1's homolog, PMD2, localizes exclusively to mitochondria.

PMD1 is C-terminally Anchored to the Membrane of Peroxisomes and Mitochondria

A biochemical approach was employed to verify the presence of PMD1 on peroxisomes and mitochondria. We first isolated peroxisomes and mitochondria from leaves of 4-week-old Arabidopsis transgenic plants expressing $35S_{pro}:YFP-PMD1$, using previously published methods (Kruft et al., 2001; Werhahn and Braun, 2002; Reumann et al., 2009). To determine the purity of the isolated organelles, ~10 μ g of each type of organelle proteins were separated on SDS-PAGE gels (Figure 2.4A), and then subjected to immunoblot analyses using organelle specific antibodies, i.e., α -PEX11d (Peroxin 11d) for peroxisomes and α -VDAC (voltage-dependent anion channel protein) for mitochondria. Our data showed that the peroxisomal and mitochondrial proteins were highly enriched (Figure 2.4B). The peroxisomal and mitochondrial proteins were then treated by TE buffer, a high concentration of sodium chloride (1M NaCl), and strong alkaline solutions (Na_2CO_3 , pH 11.0), respectively, to separate membrane from soluble proteins and integral membrane proteins from those that are peripherally associated with the membrane. Soluble (S) and insoluble (P) fractions were separated through centrifugation. Similar to the peroxisomal membrane protein PEX11d

and the mitochondrial membrane protein VDAC, YFP-PMD1 was detected only in the insoluble fractions of both peroxisomal and mitochondrial proteins after the treatments (Figure 2.4C and 2.4D), suggesting that PMD1 is embedded in the membrane of the organelles. In contrast, the peroxisomal matrix protein CFP-PTS1 and the mitochondrial luminal protein COX4-CFP were mostly detected in the soluble fractions (Figure 2.4C and 2.4D). We concluded that PMD1 is an integral membrane protein of the peroxisome and mitochondrion.

Previously characterized C-TA proteins share a similar membrane topology on the subcellular compartments to which they are tethered; that is, a cytosolic N-terminus that contains the functional domain(s), a TMD at or close to the C-terminus, and a short C-terminal end protruding into the matrix/luminal side of the compartments (Borgese et al., 2007; Abell and Mullen, 2011). To determine the topology of PMD1 on the organelle membranes, we performed protease protection assays, in which we treated the purified peroxisomes and mitochondria with thermolysin, a protease that can only access and degrade the cytosolic part of the outer membrane proteins (Tranel et al., 1995). Since YFP was fused to the N-terminal end of PMD1, a GFP antibody was used to probe the long coiled-coil domain that was hypothesized to be exposed to the cytosolic side of the organelle membranes. Immunoblot analysis with α -GFP demonstrated that, after thermolysin treatments, YFP-PMD1 was barely detected, whereas the amount of the matrix/luminal proteins CFP-PTS1 and COX4-CFP remained largely unchanged (Figure 2.4E and 2.4F). Our data collectively demonstrated that PMD1 is anchored to the membrane of peroxisomes and the outer envelope membrane of mitochondria by its C-terminus, with the N-terminal long CC domain facing the cytosol.

Mutants of *PMD1* Exhibit Abnormal Morphologies and Abundance of Peroxisomes and Mitochondria

The identification of the dual localized plant-specific protein *PMD1* prompted us to determine whether this protein plays a role in regulating the morphology, size, and/or abundance of peroxisomes and mitochondria. To this end, we characterized two T-DNA insertion alleles of *PMD1*: *pmd1-1* (CS84214), which has a T-DNA insertion in the middle of the sole exon, and *pmd1-2* (SALK_139577), which has an insertion 60 bp upstream from the translational start site ATG (Figure 2.1A). Reverse transcription PCR (RT-PCR) analyses of RNA from the T-DNA insertion lines did not detect *PMD1* transcripts in either allele (Figure 2.5A), indicating that, despite their overall indistinguishable appearance from the wild type throughout development (Figure 2.6A), *pmd1-1* and *pmd1-2* are both null mutants. We then transformed the peroxisomal (CFP-PTS1) and the mitochondrial (COX4-YFP) markers into the mutants to examine the organelle morphologies. Confocal images taken from T₂ plants revealed that both *pmd1-1* and *pmd1-2* contain peroxisomes that are larger in diameter than those in the wild type (Figure 2.5B). A quantification of the size and abundance of peroxisomes showed that the average size of a peroxisome in the *pmd1* mutants, as measured by CFP fluorescent area using IMAGE J, is about 2.7 times of that of a peroxisome in the wild type, whereas the total numbers of peroxisomes reduced to 65-70% in the mutant (Figure 2.7A and 2.7B). Mitochondria in *pmd1-1* and *pmd1-2* were markedly elongated (Figure 2.5B). The average size of a mitochondrion increased to ~2.5-2.7 times, and the total number of mitochondria decreased to ~64-72% of that in the wild type plants

(Figure 2.7C and 2.7D online). The organelle phenotypes of the loss-of-function *pmd1* mutants pointed to a role of the PMD1 protein in the morphogenesis and possibly division of peroxisomes and mitochondria.

To further study the function of PMD1 in the organelles, we ectopically expressed *PMD1* in wild-type Columbia (Col-0) *Arabidopsis* plants containing both CFP-PTS1 and COX4-YFP, and confirmed the induction of the genes in the transgenic plants by RT-PCR (Figure 2.5A). Plants expressing *35S_{pro}:PMD1* displayed retarded growth (Figure 6B), and massive proliferation and aggregation of peroxisomes and mitochondria as observed by confocal microscopy (Figure 2.5B). Transmission electron microscopic (TEM) analysis further revealed that the aggregated organelles were composed of over-proliferated peroxisomes and mitochondria, which are smaller than those in the wild type (Figure 2.5C). Within a $2\ \mu\text{m}^2$ area of a leaf mesophyll cell, we normally found one to two peroxisomes or mitochondria in a wild-type plant, yet as many as five peroxisomes and up to 12 mitochondria were present in the *35S_{pro}:PMD1* plants. Likewise, plants expressing *35S_{pro}:YFP-PMD1* also displayed increased proliferation and aggregation of peroxisomes and mitochondria and inhibition of plant growth (Figure 2.6B and 2.6C). The organelle phenotypes in the *PMD1*-overexpressing plants, together with phenotypes observed in the *pmd1* null mutants, suggested a positive role for PMD1 in increasing the abundance of peroxisomes and mitochondria.

PMD1 Interacts with Itself but Lacks Physical Interaction with Known Peroxisomal and Mitochondrial Division Factors in Arabidopsis

Organelle phenotypes of the *PMD1* gain- and loss-of-function mutants are to a large extent reminiscent of those of *FIS1*, which encodes a dual-localized C-TA protein serving as the membrane anchor for DRPs (reviewed in Kaur and Hu, 2009). In light of this, we speculated that *PMD1* may be a plant specific factor with a role similar to *FIS1* in the fission of peroxisomes and mitochondria, possibly by functioning in the same complex as *FIS1* and *DRP3*. In addition, since CC proteins are well known for their ability to interact with themselves or other CC domain-containing proteins (Rose et al., 2004; Rose et al., 2005), we were also interested to determine whether *PMD1* can form homocomplexes through self-interaction. To this end, we conducted co-immunoprecipitation (co-IP) and yeast two-hybrid (Y2H) assays to test whether *PMD1* can interact or form a complex with itself, *FIS1*, and *DRP*.

For the co-IP assay, YFP was fused to the N-terminal end of the full-length coding sequences of *PMD1*, *DRP3A*, *DRP3B*, *DRP5B*, *FIS1A*, and *FIS1B*, respectively, to create bait proteins. We also generated the prey protein biotinylated-*PMD1* (BIO-*PMD1*), by fusing the biotin carboxyl carrier protein domain (BCCP) of the biotinylate subunit of MCCase (MCCA; At1g03090) (Qi and Katagiri, 2009) to the N-terminus of *PMD1*. Each YFP- and BIO-fusion protein pair was then transiently co-expressed in tobacco leaves. Proteins extracted from the infiltrated leaves were subjected to immuno-pull down by agarose-conjugated GFP antibody, followed by immunoblot analysis. As shown in Figure 2.8A, most of the YFP-fusion proteins were expressed at very low levels in the input samples, unable to be detected by α -GFP. However, they were highly enriched by immunoprecipitation, suggesting that they are efficiently pulled down by α -GFP. Consistent with the notion that CC proteins dimerize, BIO-*PMD1* was

pulled down by YFP-PMD1, whereas the control protein YFP-PTS1 was unable to precipitate BIO-PMD1, suggesting that PMD1 interacts with itself. Similar to YFP-PTS1, none of the YFP-DRP and YFP-FIS1 proteins was able to pull down BIO-PMD1 (Figure 2.8A), which is indicative of a lack of physical interaction or close proximity between PMD1 and the Arabidopsis DRP3A, DRP3B, DRP5B and FIS1 proteins.

We used Y2H assays (ProquestTM two-hybrid system) to verify the co-IP results. PMD1 deleted for TMD was cloned into pDestTM32 to generate PMD1^{ΔTMD}-DNA binding domain (BD) fusion. PMD1^{ΔTMD}, DRP3/DRP5B, and FIS1^{ΔTMD} were cloned into pDESTTM22 to create protein fusions with the activation domain (AD). The proteins were then co-expressed in yeast strain Mav203. A robust growth of cells on medium lacking Ura, Trp, and His in the presence of 10 mM of 3-Amino-1,2,4-triazole (3-AT) suggested an interaction between the two proteins expressed. Consistent with our co-IP data, only a strong self-interaction of PMD1 was detected (Figure 2.8B). Taken together, results from the Y2H assays supported our conclusion that PMD1 can interact with itself, yet it has no physical interaction or does not form a complex with the known fission factors DRP3A, DRP3B, DRP5B, or FIS1.

Although physical interactions between PMD1 and DRP3s were not detected by co-IP and Y2H experiments, the membrane anchored PMD1 protein may still be indirectly involved in the recruitment of DRP3s to the division sites of peroxisomes and mitochondria. To test this possibility, we used the FAST technique (Li et al., 2009) to transiently express *35S_{pro}:YFP-DRP3A* or *35S_{pro}:YFP-DRP3B* in wild-type Col-0 or *pmd1-1* seedlings, which are already expressing the peroxisomal marker CFP-PTS1 or

the mitochondrial marker COX4-CFP. Both YFP-DRP3A and YFP-DRP3B were properly targeted to the constriction sites or tips of peroxisomes and mitochondria in *pmd1-1*, just like in the wild-type cells (Figure 2.9), suggesting that PMD1 alone is not critical for recruiting DRP3 proteins to the organelles. Results from the co-IP, Y2H, and protein localization studies collectively led us to the conclusion that PMD1 may mediate peroxisomal and mitochondrial division/proliferation by a mechanism that is independent from the action of the FIS1-DRP3 complex.

PMD1 Interacts with PMD2, which is Specifically Involved in Mitochondrial Morphogenesis

The lack of association of PMD1 with known division factors led us to take alternative approaches to identify PMD1-interacting proteins, with the hope to uncover the functional role of PMD1 in organelle proliferation. For this purpose, we adopted two independent affinity purification methods, biotin-streptavidin purification (Qi and Katagiri, 2009) and GFP purification. To perform biotin-streptavidin purification, *PMD1_{pro}:BIO-PMD1* was expressed in *mcca* (SALK_137966) background to eliminate the purification of endogenous MCCA (Qi and Katagiri, 2009). To pull down proteins interacting with YFP-PMD1, we used plants expressing *35S_{pro}:YFP-PMD1* and CFP-PTS1. Arabidopsis plants expressing the fusion proteins were subjected to biotin-streptavidin purification as described in Qi and Katagiri (2009) or GFP pull-down assays (see Methods), and *mcca* and plants expressing YFP-PTS1 alone were used as negative controls. The purified proteins were separated on SDS-PAGE and visualized by silver staining (Figure 2.10A and 2.10B). Proteins pulled down by each strategy were identified using LC-MS-MS as

previously described (Reumann et al., 2009), with two replicates for each method. PMD2 was the only protein identified in common by both methods, suggesting that PMD2 might be a bona fide PMD1-interacting protein.

We confirmed the interaction between PMD1 and PMD2 using yeast two-hybrid and co-IP assays. Interaction between PMD1 and PMD2, both of which were deleted for the putative TMD, was first tested using the Matchmaker LexA Y2H system. When the protein pairs $PMD1^{\Delta TMD}$ and $PMD1^{\Delta TMD}$, $PMD1^{\Delta TMD}$ and $PMD2^{\Delta TMD}$, and $PMD2^{\Delta TMD}$ and $PMD2^{\Delta TMD}$ were co-expressed in the yeast strain EGY48, yeast cells grew strongly in medium lacking Ura, Trp, His and Leu (SD/Galactose-UTHL) and turned blue in the presence of X-gal. In contrast, yeast cells transformed with the $PMD1^{\Delta TMD}$ or $PMD2^{\Delta TMD}$ fusion protein and an empty vector did not grow on the selection media, indicating specific interactions between the tested PMD protein pairs (Figure 2.11A). We next performed co-IP to confirm the Y2H results, using YFP- and HA-tagged PMD proteins transiently expressed in tobacco leaf epidermal cells. YFP-PMD1 and YFP-PMD2 efficiently pulled down HA-PMD1 and HA-PMD2, respectively, and YFP-PMD2 pulled down HA-PMD1 (Figure 2.11B). Consistent with the lack of interaction between PMD1 and FIS1 (Figure 2.8), YFP-PMD2 also failed to pull down HA-FIS1A (Figure 2.11B). These data demonstrated the ability for PMD1 and PMD2 to form homo- as well as heterocomplexes.

To characterize the functional role of PMD2, it was necessary to observe organelle morphologies in loss-of-function *pmd2* mutants. Since T-DNA insertion mutants for *PMD2* were unavailable, we generated artificial microRNA (amiR) lines (see

Methods and Figure 2.10C) to specifically reduce the expression of *PMD2* in wild-type Col-0 plants, which expressed the peroxisomal marker CFP-PTS1 and the mitochondrial marker COX4-YFP. In addition, we transformed *amiR PMD2* into *pmd1-1* plants, which also co-expressed the peroxisomal and mitochondrial fluorescent markers, to see whether compounded phenotypes can be created in the double mutant. We obtained 16 transgenic *amiR PMD2* lines each in the Col-0 and *pmd1-1* background. RT-PCR analysis showed efficient knock-down of the expression of *PMD2* in 15 lines in the Col-0 background, without affecting the transcript level of *PMD1*, and in 14 lines in the *pmd1-1* background. Results from three lines in each background, all of which were indistinguishable from wild type plants in appearance, are presented in Figure 2.12A.

Plants from the T₃ generation of the *PMD2* knock-down lines were analyzed by confocal microscopy to observe the peroxisomal and mitochondrial morphologies. Consistent with *PMD2*'s specific localization to mitochondria (Figure 2.2B), suppression of the *PMD2* gene rendered morphological changes to mitochondria only (Figure 2.12B). The size and number of mitochondria in the *amiR PMD2* lines were comparable to those in the *pmd1* mutants (Figure 2.7C and 2.7D). On the other hand, no obvious effect on the morphology and abundance of peroxisomes was observed (Figure 2.12B; Figure 2.7A and 2.7B). The double mutant contained peroxisomes with morphology and size similar to those in *pmd1*; its mitochondrial phenotype was also similar to those in *pmd1* or *amiR PMD2* (Figure 2.12B; Figure 2.7). We concluded that *PMD2* has an exclusive role in the morphogenesis and/or proliferation of mitochondria, and the functions of *PMD1* and *PMD2* in mitochondria are non-redundant.

The C-termini of the PMD Proteins Contain Organelle Targeting Signals

Previous studies of C-TA proteins demonstrated that their organelle-specific targeting signals reside in the TMD and its flanking sequences (reviewed in Abell and Mullen, 2011). Despite their sequence similarities along the length of the proteins, PMD1 and PMD2 showed distinct organelle targeting patterns, i.e., PMD1 is dual targeted whereas PMD2 only targets to mitochondria. To determine whether the C-terminus carries targeting signals for PMD1 and PMD2, we made various truncations of the PMD proteins, which were subsequently fused to the C-terminus of YFP. The 35S promoter-driven fusion proteins were transiently expressed in tobacco leaves together with the peroxisomal marker CFP-PTS1 or the mitochondrial marker COX4-CFP (Figure 2.13).

Confocal microscopy of tobacco leaf epidermal cells showed that, like full-length PMD1, the C-terminus of PMD1 (cPMD1²⁶¹⁻³¹⁸ and cPMD1²⁹³⁻³¹⁸) was able to direct the YFP-fusion protein to both peroxisomes and mitochondria, whereas YFP fused to the N-terminus of PMD1 (nPMD1¹⁻²⁶⁰) mis-localized to the cytosol (Figure 2.13C-F). To determine whether the sequence downstream from TMD is required for organelle targeting, we also tested the localization of YFP-cPMD1²⁶¹⁻³¹⁴, in which the last four amino acids were deleted, and found the fusion proteins to be distributed in the cytosol (Figure 2.13G). These data together suggested that the segment covering TMD and the C-terminal end 3' to TMD is necessary and sufficient for PMD1's dual targeting. Furthermore, although ectopically expressed YFP-PMD1 often led to organelle proliferation in tobacco cells (Figure 2.13C) as it did in transgenic Arabidopsis plants

(Figure 2.6C), overexpression of YFP-cPMD1 did not cause such a phenotype (Figure 2.13E-F). This result supports the view that the functional domain of PMD1 is located at its cytoplasmic N-terminus.

Similar to what was found for PMD1, the C-terminus, but not the N-terminus, of PMD2, was critical to direct the YFP to mitochondria (Figure 2.13I-K). In addition, the five amino acids downstream from the TMD at the C-terminal end are also required for PMD2's localization to mitochondria, as YFP-cPMD2²⁸⁰⁻³¹⁸ localized to the cytosol (Figure 2.13L). Thus, like many previously reported C-TA proteins, PMD1 and PMD2 both use the C-terminus, which includes the TMD and the sequences 3' to the TMD, for their organelle targeting. However, unlike YFP-PMD1, overexpression of YFP-PMD2 did not cause mitochondrial overproliferation in tobacco cells (Figure 2.13H) or transgenic Arabidopsis plants (Figure 2.2B). These findings suggest that PMD2's role in mitochondrial morphogenesis may be distinct from that of PMD1. This notion is further supported by the fact that a chimeric protein, in which the N-terminus of PMD1 was fused to the C-terminus of PMD2 (nPMD1+cPMD2; Figure 2.13A), exclusively localized to mitochondria and induced massive mitochondrial proliferation (Figure 2.13M). We concluded that the PMD proteins carry their organelle targeting signals at the C-termini and the functional domains at the N-termini. For PMD1 in particular, its N-terminus is responsible for inducing the proliferation of the organelles.

DISCUSSION

PMD1 is a Plant Specific Protein that Promotes Peroxisomal/Mitochondrial Proliferation Independently from the FIS1-DRP3 Complex

The peroxisomal and mitochondrial division machineries are composed of evolutionarily conserved factors such as DRP and FIS1, as well as lineage specific proteins such as Mdv1p and Caf4p from yeast, Mff1 from metazoans, and the mitochondrial division protein ELM1 from Arabidopsis (see Introduction). In this work, we discovered PMD1 as another plant specific factor involved in the organelle division/proliferation process. Null mutants of *PMD1* have enlarged peroxisomes and elongated mitochondria, whereas overexpression of the gene leads to massive proliferation and aggregation of these organelles (Figure 2.5). These phenotypes are to large degrees similar to what we previously observed in the mutants of Arabidopsis *FIS1*, which encode a C-TA protein that is dual localized to peroxisomes and mitochondria and recruits DRP proteins to the division site. The loss-of-function *fis1A* and *fis1B* mutants contain enlarged peroxisomes and mitochondria, and the *FIS1* overexpressors have an increased number of both organelles, which are often aggregated together (Scott et al., 2006; Zhang and Hu, 2008; Zhang and Hu, 2009). Results from the mutant analyses in this work suggest that PMD1 is involved in the division/proliferation of peroxisomes and mitochondria in Arabidopsis.

Among the lineage specific peroxisomal and mitochondrial division proteins, Mdv1p and Caf4p are part of the FIS1-DRP complex. Mff1 and ELM1 both function independently from FIS1, yet are still required for the recruitment of DRP proteins (reviewed in Kaur and Hu, 2009). By contrast, PMD1 lacks physical interaction with FIS1 or DRP3/DRP5B in both co-IP and Y2H analyses (Figure 2.8). It does not play an

obvious role in the organelle targeting of DRP3A and DRP3B, either (Figure 2.9). Based on these data, we speculate that PMD1 directly or indirectly mediates the division/proliferation of peroxisomes and mitochondria independently from the FIS1 and DRP3/DRP5B proteins.

Loss of function mutants of *PMD1*, *PMD2*, and the *pmd1 pmd2* double mutant do not show obvious defects in growth and development. *PMD1*-overexpressors are slow growing (Figure 2.6A-B), and this growth defect might be a consequence of the gross organelle aggregation. It seems that although PMD1 and PMD2 have obvious functions in organelle morphogenesis, loss of these proteins is not sufficient to severely disturb the physiology of the organelles under general plant growth conditions. The *fis1A fis1B* double mutant is also slightly impaired in growth (Zhang and Hu, 2009). It would be interesting to generate a mutant in which the functions of all four C-TA proteins – PMD1, PMD2, FIS1A, and FIS1B, are knocked out, to determine whether the pathways, in which PMD1/PMD2 and FIS1A/FIS1B respectively exert their functions, are partially redundant. The mutants can also be challenged with various stresses to determine whether one of the pathways operates primarily under some adverse growth conditions.

PMD1 and PMD2 Play Non-redundant Roles

Although PMD1 and PMD2 share 35% amino acid identity and similar domain structures, these two proteins are not redundant in function. First, PMD1 is dual localized and mediates the morphogenesis and proliferation of both peroxisomes and mitochondria. However, PMD2 appears to have an exclusive function in the morphogenesis of mitochondria. In addition, the fact that YFP-PMD2 forms a ring-like

pattern outside mitochondria and that PMD2 and PMD1 share similar domain structures strongly suggests that PMD2 is another C-TA protein that is tethered to the outer envelope membrane of mitochondria. However, the functions of PMD1 and PMD2 in mitochondria do not overlap. The *amiR PMD2* lines, in which the expression of *PMD2* is significantly reduced, phenocopy the elongated mitochondrial phenotype of *pmd1-1*, suggesting that PMD2 possesses a similar molecular function as PMD1 on mitochondria. However, *pmd1-1 amiR PMD2* double mutant displays a mitochondrial phenotype identical to the *pmd1* single mutants, leading us to speculate that the functions of these two proteins in mitochondria are not exchangeable. Third, unlike PMD1, overexpression of PMD2 does not induce mitochondrial proliferation, further supporting the view that these two proteins carry out distinct functions in mitochondria. Based on these findings, we favor the hypothesis that PMD1 and PMD2 form a complex on the membrane of mitochondria and function cooperatively to mediate the morphogenesis and/or proliferation of mitochondria, with PMD1 playing a rate-limiting role.

Mode of Action for the PMD Proteins

Eukaryotic genomes contain a large number of genes encoding C-TA proteins that are involved in various cellular processes, from gene expression to vesicle trafficking (Abell and Mullen, 2011). Bioinformatic screens predicted the presence of over 500 C-TA proteins in Arabidopsis; the functions of the majority of them are unknown (Kriechbaumer et al., 2009; Pedrazzini, 2009). The functional domains in the C-TA proteins often reside in the N-terminus, which occupies the bulk of the protein. For

PMD1, its N-terminal region has a long CC domain that can be separated into four shorter CC domains (Figure 2.1).

CC proteins are ubiquitous eukaryotic proteins with diverse functions. Whereas short CC domains often function as dimerization motifs in transcription factors, other CC domains, including those that are over 100 amino acid long, have been found to be involved in the attachment of proteins or protein complexes to larger subcellular compartments (Gillingham and Munro, 2003; Rose et al., 2005). Given that several membrane-bound CC proteins in organelle division serve as membrane tethers for effector proteins (see Introduction) and the phenotypes of the *pmd1* mutants, the most likely function for PMD1 is to recruit downstream cytosolic effectors for division. The lack of interaction detected between PMD1 and the peroxisomal/mitochondrial division effector DRP3 implies that other yet unidentified effector proteins may be recruited by PMD1 to the organelle membranes.

Our confocal microscopic analysis showed that overexpressing the *PMD1* gene causes massive clustering/aggregation of peroxisomes and mitochondria (Figure 2.5), hinting at a role for PMD1 in organelle positioning and distribution. However, further TEM experiments revealed more and smaller peroxisomes and mitochondria in the overexpressors, suggesting a role of PMD1 in organelle division/proliferation rather than distribution. The clustering phenotype may have been caused by the fact that the division effect of ectopically expressed *PMD1* overwhelmed the machinery responsible for separating the organelles after division. Consistent with this hypothesis, cells overexpressing Arabidopsis *FIS1A* or *FIS1B* also show peroxisomal and mitochondrial aggregations (Zhang and Hu, 2008). Given that PMD1 forms homocomplexes, the

strong organelle aggregations may also have been caused by dimerization of the overly abundant membrane-tethered PMD1 proteins between organelles.

Although we favor a role for PMD1 (and likely PMD2 as well) in inducing the proliferation/division of the organelles, other possibilities also exist. For example, they may be involved in shaping of peroxisomes and mitochondria with a yet-unknown mechanism, which indirectly affects the abundance of these organelles. In addition, although little is known about the fusion of peroxisomes and mitochondria in plants, it is also a formal possibility that PMD proteins function directly as suppressors of organelle fusion. Lastly, given the organelle aggregation phenotype in the *PMD1* overexpressors and the fact that PMD1 and PMD2 form homo- and heterocomplexes, it was tempting to hypothesize that these proteins may function as molecular tethers in maintaining a close proximity/juxtaposition of the metabolically connected peroxisomes and mitochondria. Supporting this hypothesis is the findings that some CC-containing proteins are involved in tethering mitochondria to the ER in mice (de Brito and Scorrano, 2008) or binding the vacuole to mitochondria in *Cyanidoschyzon merolae* (Fujiwara et al., 2010). However, so far we have been unable to observe differences in the distance/association between peroxisomes and mitochondria in the *pmd* single and double mutants and wild-type plants, thus making this hypothesis less favored at present.

Organelle Targeting Mechanism for PMD1 and PMD2

In this work, we have provided evidence to demonstrate PMD1's dual targeting to peroxisomes and mitochondria and PMD2's exclusive localization to mitochondria. At this point we do not have evidence for preferential targeting of PMD1 to a particular

organelle, as almost all CFP-PTS1-labelled peroxisomes and COX4-CFP-labelled mitochondria co-localized with YFP-PMD1. However, in general we do observe fewer peroxisomes than mitochondria in a given cell. In our experience, it is easier to capture high-quality images of mitochondria near the surface of cells, where much fewer peroxisomes are found.

Our biochemical analysis demonstrated that YFP-PMD1 is an integral membrane protein on both organelles. In the membrane association assay, the YFP-PMD1 protein bands detected in the mitochondrial fraction is much weaker than those in the peroxisomal proteins (Figure 2.4C and 2.4D). One possible explanation is that YFP-PMD1 is not as tightly associated with the mitochondrial membrane as it is to the peroxisomal membrane, and therefore was easier to be lost during organelle isolation procedures. Alternatively, given that the proteome of mitochondria is 10 times larger than that of the peroxisome (Reumann et al., 2004; Millar et al., 2008), there is a higher enrichment of peroxisomal proteins than mitochondrial proteins when equal amount of organelle proteins are used in the assays and hence the peroxisome-localized protein shows a stronger band on the immunoblot.

Multiple pathways have been reported on the sorting of C-TA proteins to their destined cellular membranes; various pathways even exist for proteins targeting to the same membrane, such as the ER membrane (Abell and Mullen, 2011). Given the small number of plant C-TA proteins that have been characterized, especially those localized to peroxisomes, and the complex nature of the targeting mechanisms, predicting the targeting destinations of C-TA proteins with high accuracy may not be a simple task (Kriechbaumer et al., 2009). Consistent with the view that the targeting signals for C-TA

proteins are located at the C-termini, we have shown in this study that the C-terminal tail of PMD1 or PMD2, which possesses the putative TMD and the flanking sequences downstream of TMD, is necessary and sufficient to target the proteins to their destined organelles. The peroxisomal targeting of the human C-TA proteins FIS1 (hFis1) and PEX26 requires the cytoplasmic receptor/chaperone protein PEX19; binding sites for PEX19 were also mapped onto the C-terminus of these proteins (Halbach et al., 2006; Delille and Schrader, 2008). The C-terminal sequences of these proteins and PMD1/PMD2 vary greatly, therefore it is hard to predict the role for the Arabidopsis PEX19 homolog in PMD1's peroxisomal targeting without experimental evidence. Taken together, a much more detailed dissection of this region in PMD1 and PMD2 will be needed to pinpoint precisely the residues and structural features required for peroxisomal or mitochondrial targeting and to further identify factors that mediate the targeting.

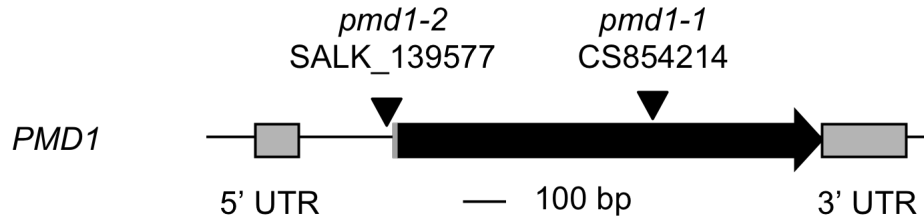
Peroxisomes and Mitochondria are Interconnected in Various Ways

In plants, an ever increasing number of proteins have been found to be dual localized to peroxisomes and mitochondria, raising the interesting possibility that these two organelles are more closely connected than previously known. Our discovery of PMD1 as a dual localized protein that mediates the division/proliferation of both peroxisomes and mitochondria further substantiates this notion.

In addition to the metabolic pathways and division factors that link peroxisomes and mitochondria, other ways of interaction or communication also exist between these two organelles. For instance, in yeast *Saccharomyces cerevisiae*, mitochondrial

dysfunction induces peroxisome biogenesis and increases peroxisomal functions via a retrograde signaling pathway controlled by the transcription factor RTG (Chelstowska and Butow, 1995; Epstein et al., 2001). In addition, a mammalian RIG-I-like receptor (RLR) adaptor protein called MADS, which is also a C-TA protein, was recently found to be anchored to the membrane of peroxisomes and the outer envelope membrane of mitochondria, serving as part of an anti-viral signaling system to induce the expression of defense genes (Seth et al., 2005; Dixit et al., 2010). Furthermore, mammalian mitochondrial derived vesicles carrying specific cargos were found to merge with a population of peroxisomes. Interestingly, the vesicles carry the MAPL protein, a SUMO ligase that can enhance the activity of the mitochondrial/peroxisomal division protein Drp1 (Neuspiel et al., 2008), providing evidence for a new way of communication between mitochondria and peroxisomes (Andrade-Navarro et al., 2009). Our study supports the view that subcellular compartments within a eukaryotic cell are highly interactive. In particular, the regulation of the abundance, morphology, and distribution of the metabolically related peroxisomes and mitochondria may be highly coordinated to maintain cellular homeostasis. Further investigation of the role of the PMD proteins and other dual targeted proteins will be instrumental to a better understanding of the coordination and communication among cellular compartments.

A



B



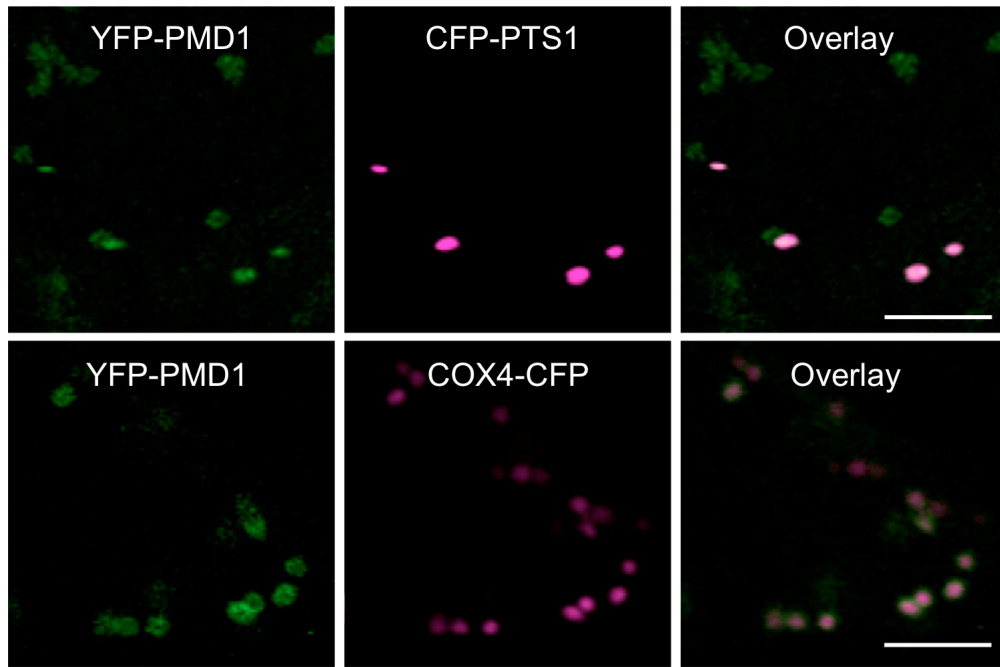
Figure 2.1. Structural and sequence analysis of PMD1.

(A) Genomic structure of *PMD1*. The T-DNA insertion sites in *pmd1-1* and *pmd1-2* are indicated.

(B) Putative protein structure of PMD1. CC, coiled-coiled domain; TMD, transmembrane domain.

(C) Sequence alignment of PMD1 and PMD2. Coiled-coil domains are underlined and the TMD is double underlined. Identical sequences are shaded in black. All domain assignments are based on analysis of PMD1.

A



B

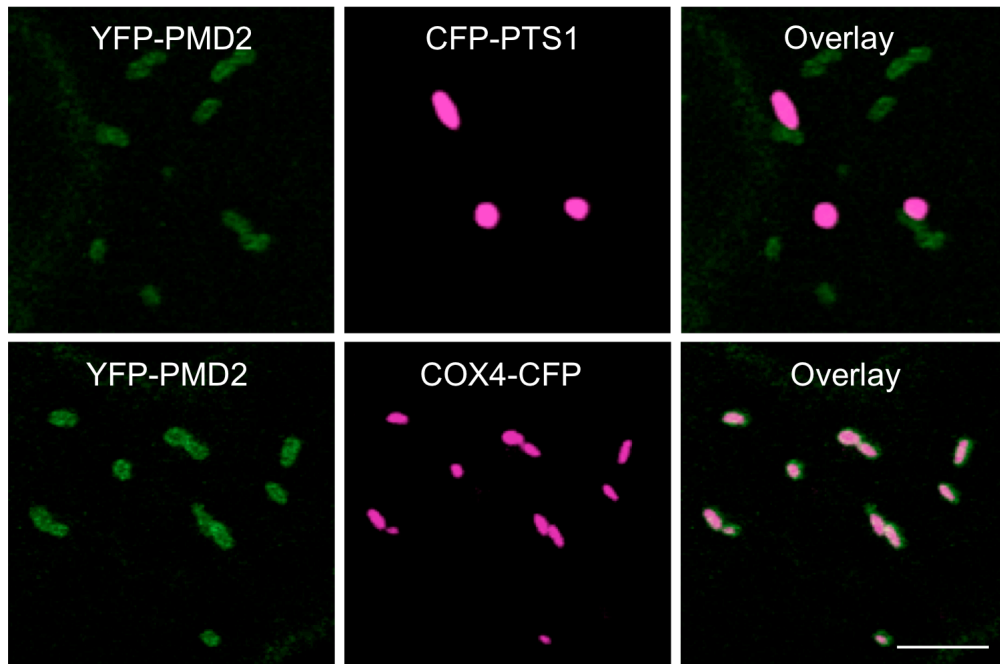


Figure 2.2

Figure 2.2 (cont'd)

Figure 2.2. Subcellular localization of YFP-PMD1 and YFP-PMD2.

Confocal images are from leaf epidermal cells from transgenic plants expressing *PMD1_{pro}:YFP-PMD1* (A) or *35S_{pro}:YFP-PMD2* (B) along with the peroxisomal marker *CFP-PTS1* or the mitochondrial marker *COX4-CFP*. YFP signals are in green and CFP signals are in magenta. Merged images show the colocalization of the YFP fusion protein to peroxisomes or mitochondria. Scale bars = 5 μ m.

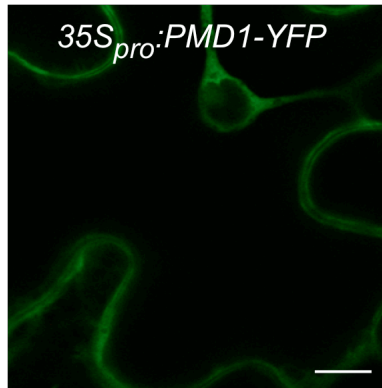
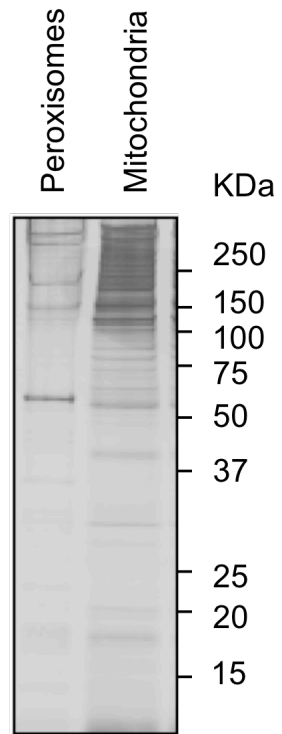


Figure 2.3. Transient expression of C-terminal YFP fusion of PMD1 in Tobacco epidermal cells.

Agrobacterium cells harboring $35S_{pro}:PMD1-YFP$ were infiltrated into tobacco epidermal cells for transient expression of the protein. Scale bar = 10 μm .

A



B

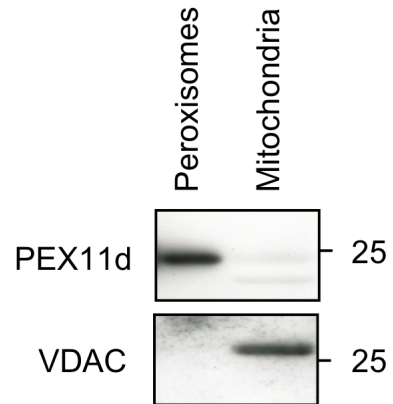
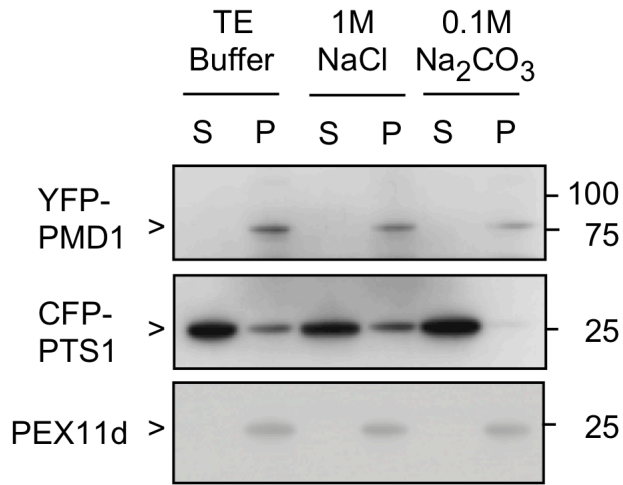


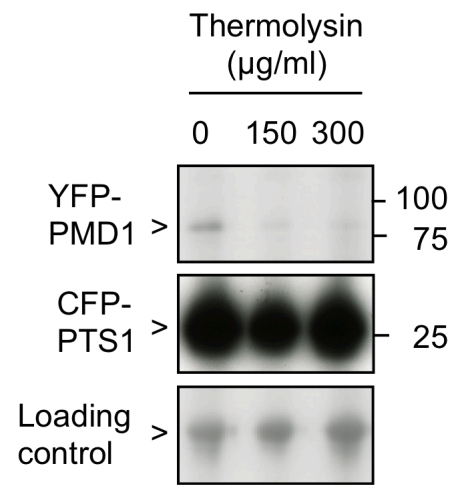
Figure 2.4

Figure 2.4 (cont'd)

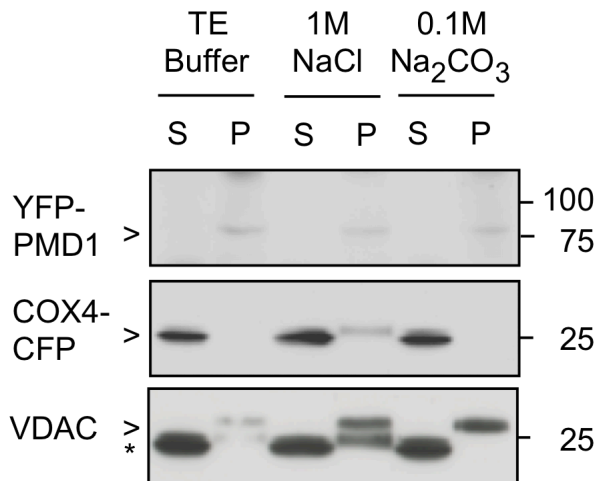
C



E



D



F

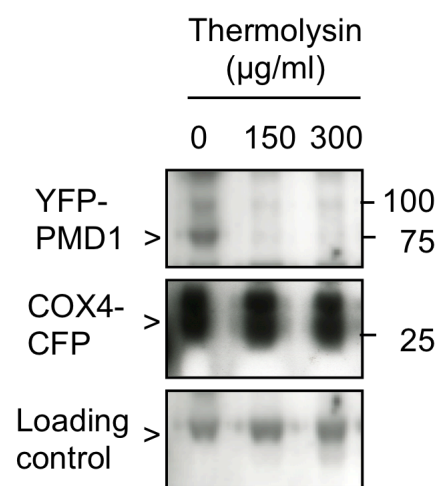


Figure 2.4 (cont'd)

Figure 2.4. PMD1 is anchored to the organelle membranes by the C-terminus.

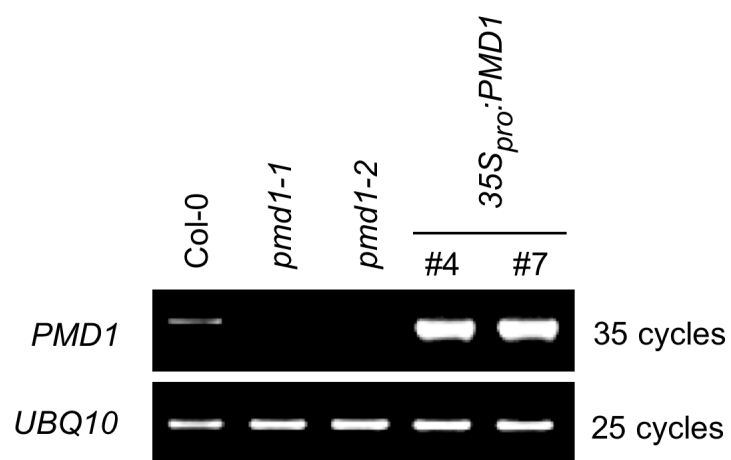
(A) Arabidopsis plants expressing YFP-PMD1 and the peroxisomal marker CFP-PTS1 or the mitochondrial marker COX4-CFP were used to isolate the organelles. Isolated peroxisomes and mitochondria were separated on a 4-12% NuPAGE gel before visualized by silver staining of the gel.

(B) Immunoblotting analysis of peroxisomal and mitochondrial proteins purified from Arabidopsis plants expressing YFP-PMD1, using antibodies against the peroxisomal specific protein PEX11d and the mitochondrial specific protein VDAC.

(C) and (D) Immunoblot analyses of purified Arabidopsis leaf peroxisomes (C) and mitochondria (D) after the proteins were treated with sodium chloride (NaCl) or sodium carbonate (Na₂CO₃) and fractionated into soluble (S) and pellet (P) fractions. The GFP antibody was used to detect the expression of CFP- and YFP-fusion proteins. CFP-PTS1 and COX4-CFP served as controls for matrix proteins, and PEX11d and VDAC were organelle-specific membrane protein controls. Asterisk in (D) marks cross-hybridized signals detected by the GFP antibody.

(E) and (F) Immunoblot analyses of peroxisomes (E) and mitochondria (F) that were treated with various concentrations of thermolysin. The levels of CFP- and YFP-fusion proteins were detected with the GFP antibody. A non-specific band was used as loading control.

A



B

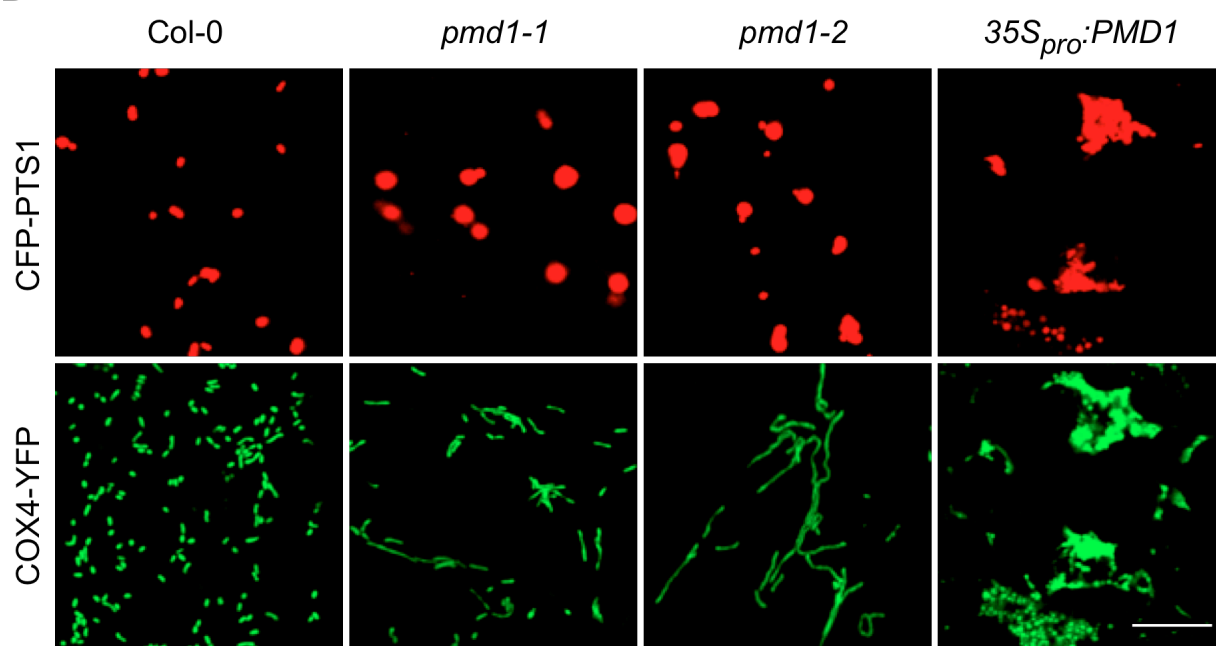


Figure 2.5

Figure 2.5 (cont'd)

C

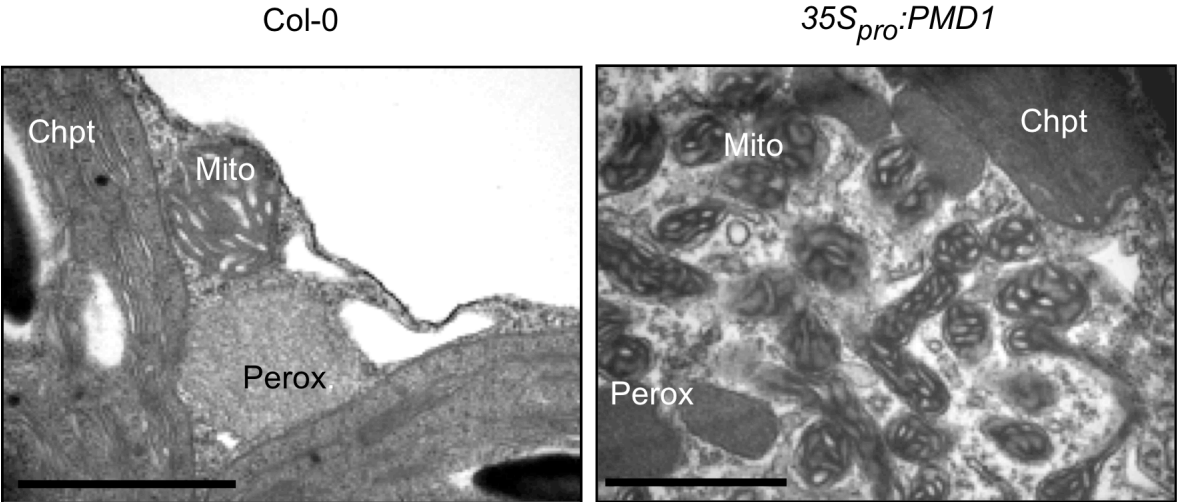


Figure 2.5 (cont'd)

Figure 2.5. *pmd1* mutants exhibit abnormal peroxisomal and mitochondrial morphologies.

(A) RT-PCR analyses showing the levels of *PMD1* mRNA in wild type (Col-0), loss-of-function mutants (*pmd1-1* and *pmd1-2*) and gain-of-function mutants (*35S_{pro}:PMD1* line No.4 and 7). *UBQ10* transcripts are used as loading controls.

(B) Confocal images from leaf epidermal cells of the indicated plants showing morphologies of peroxisomes (labeled by CFP-PTS1) and mitochondria (marked by COX4-YFP). Images were taken at the same magnification; scale bar = 10 μ m.

(C) TEM images from leaf mesophyll cells illustrating the ultrastructure of peroxisomes (Perox), mitochondria (Mito), and chloroplasts (Chpt) in Col-0 and *35S_{pro}:PMD1* plants.

Scale bars = 1 μ m.

A

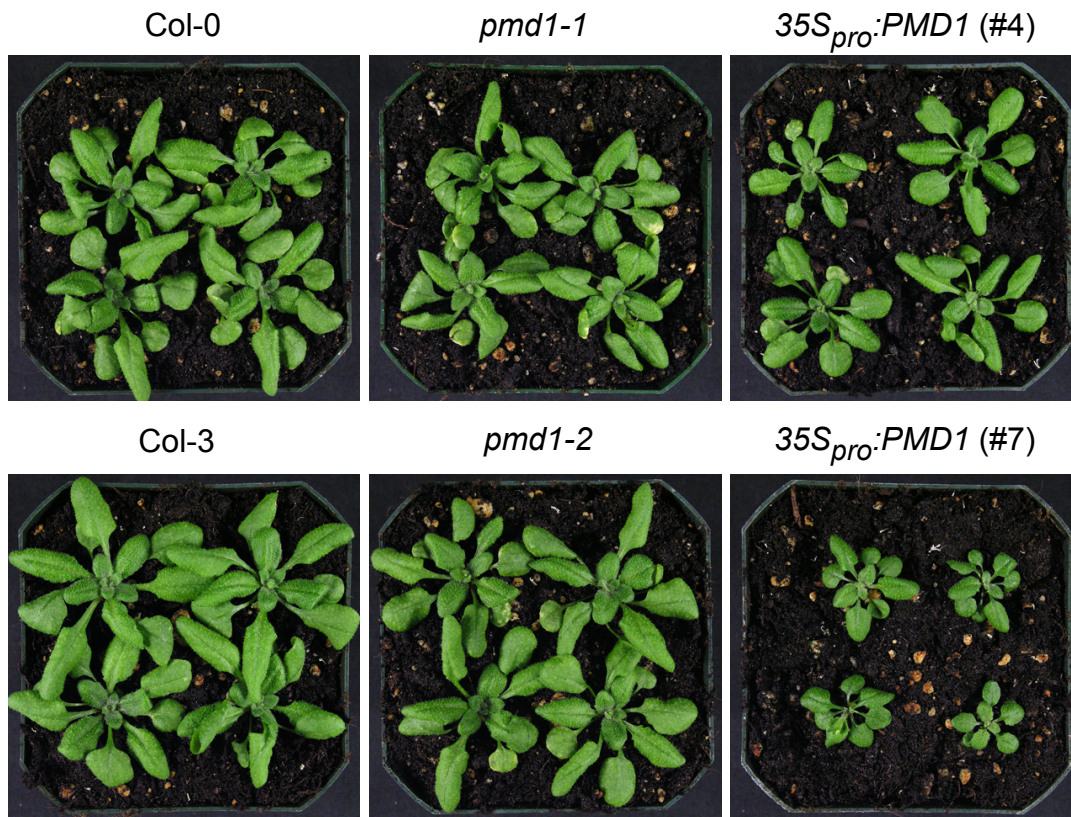


Figure 2.6. Plant morphologies of the *pmd1* loss- and gain-of-function lines and localization of YFP-PMD1 in transgenic plants.

(A) and (B) Plants shown are four weeks old from the T₂ generation.

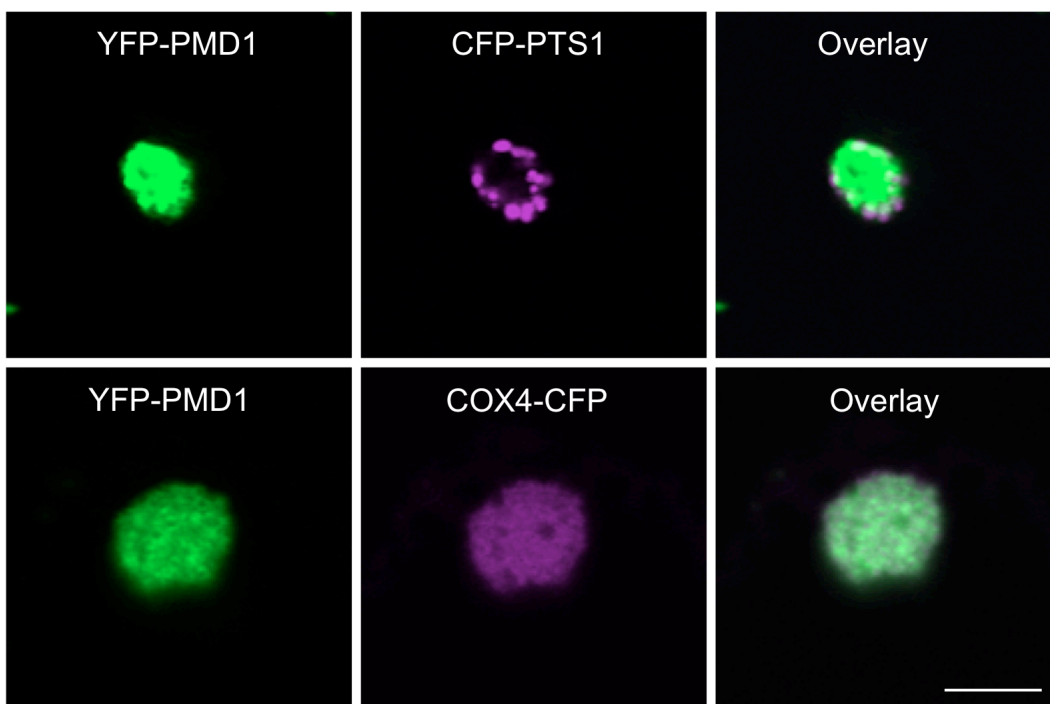
(C) Confocal images from leaf epidermal cells from T₁ transgenic plants expressing $35S_{pro}:YFP-PMD1$ along with the peroxisomal marker *CFP-PTS1* or the mitochondrial marker *COX4-CFP*. YFP signals are in green and CFP signals are in magenta. Merged images show the colocalization of the YFP fusion protein to peroxisomes or mitochondria. Images were taken at the same magnification; scale bar = 10 μ m.

Figure 2.6 (cont'd)

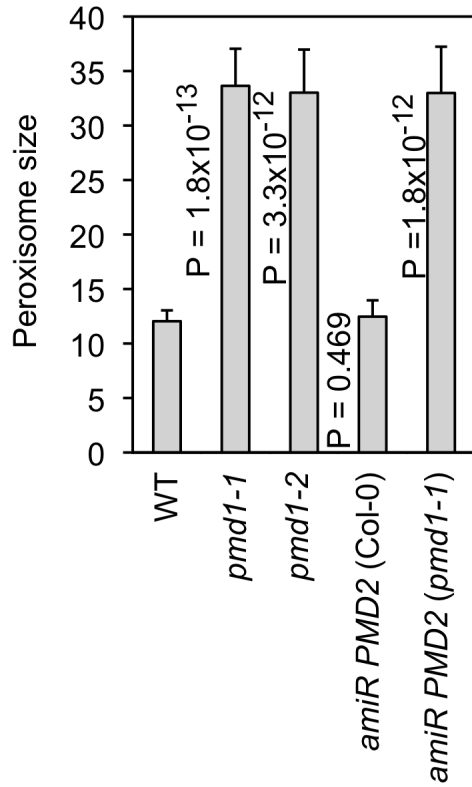
B



C



A



B

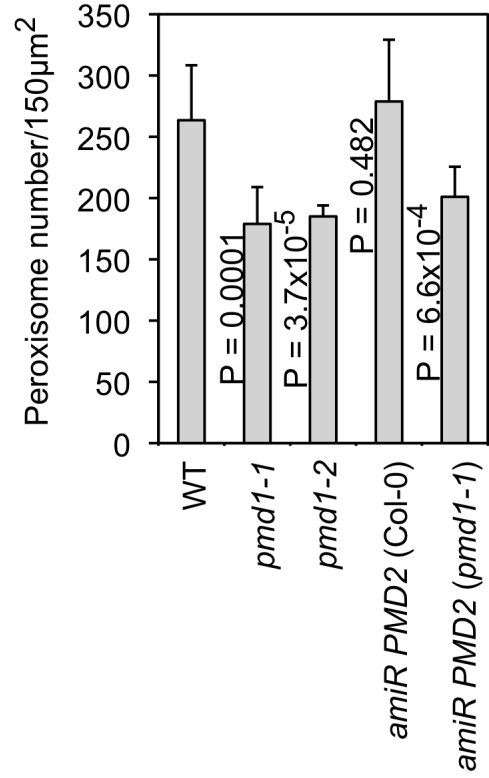
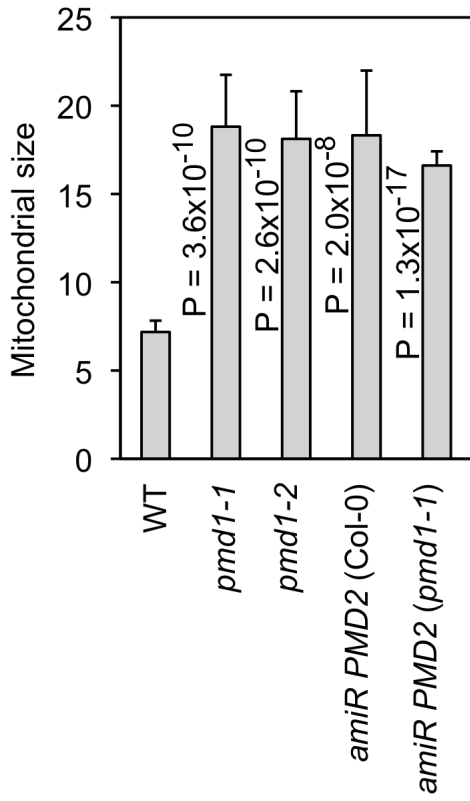


Figure 2.7. Quantification of organelle size and number.

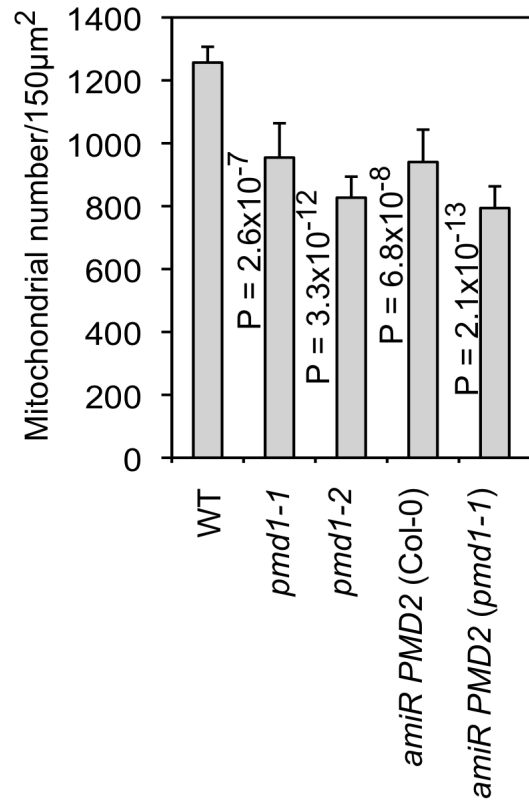
An area of $150 \mu\text{m}^2$ from leaf epidermal cells ($n=10$) was used to quantify the organelle morphologies. Error bars are standard deviations.

Figure 2.7 (cont'd)

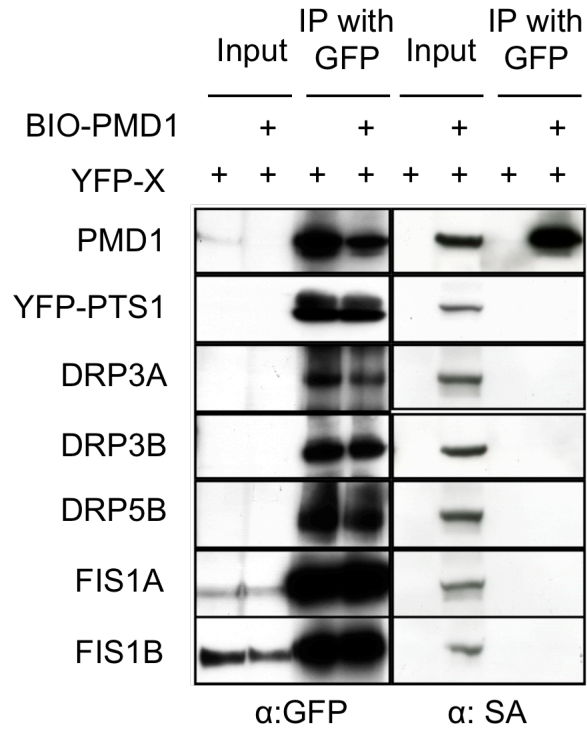
C



D



A



B

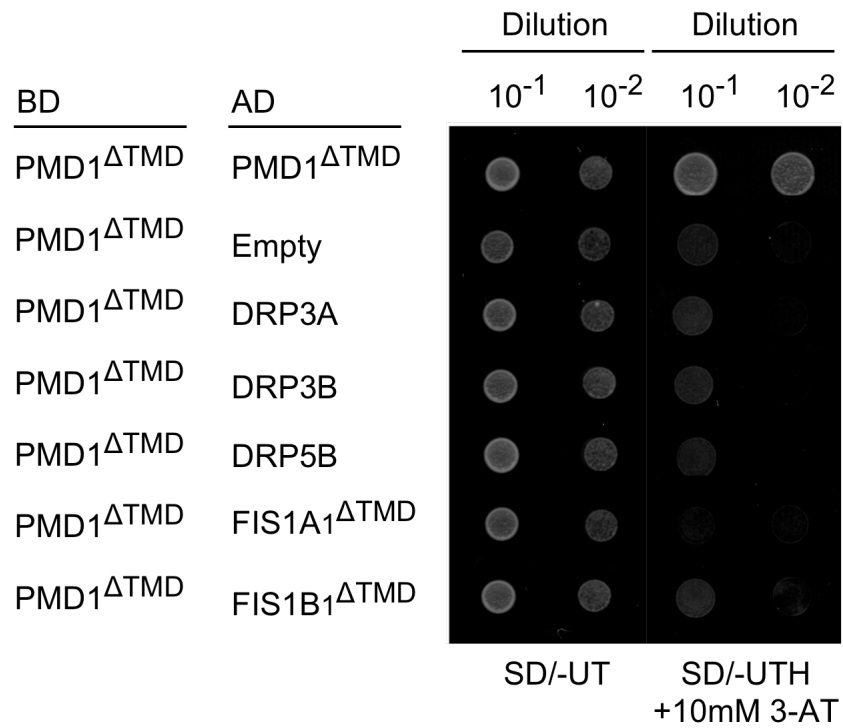


Figure 2.8

Figure 2.8 (cont'd)

Figure 2.8. PMD1 self-interacts but does not interact with the known peroxisomal and mitochondrial division factors.

(A) Co-IP analyses to test for protein-protein interaction. Various combinations of the fusions were transiently expressed in tobacco leaf epidermal cells, followed by immunoprecipitation using the GFP antibody. A GFP antibody or a streptavidin antibody (α -SA) was used to detect the proteins. YFP-PTS1 was used as a negative control.

(B) Yeast two-hybrid analyses. SD/-UT selects for transformants and SD/-UTH + 10 mM 3-AT select for protein-protein interactions. Empty, pDEST22 vector only.

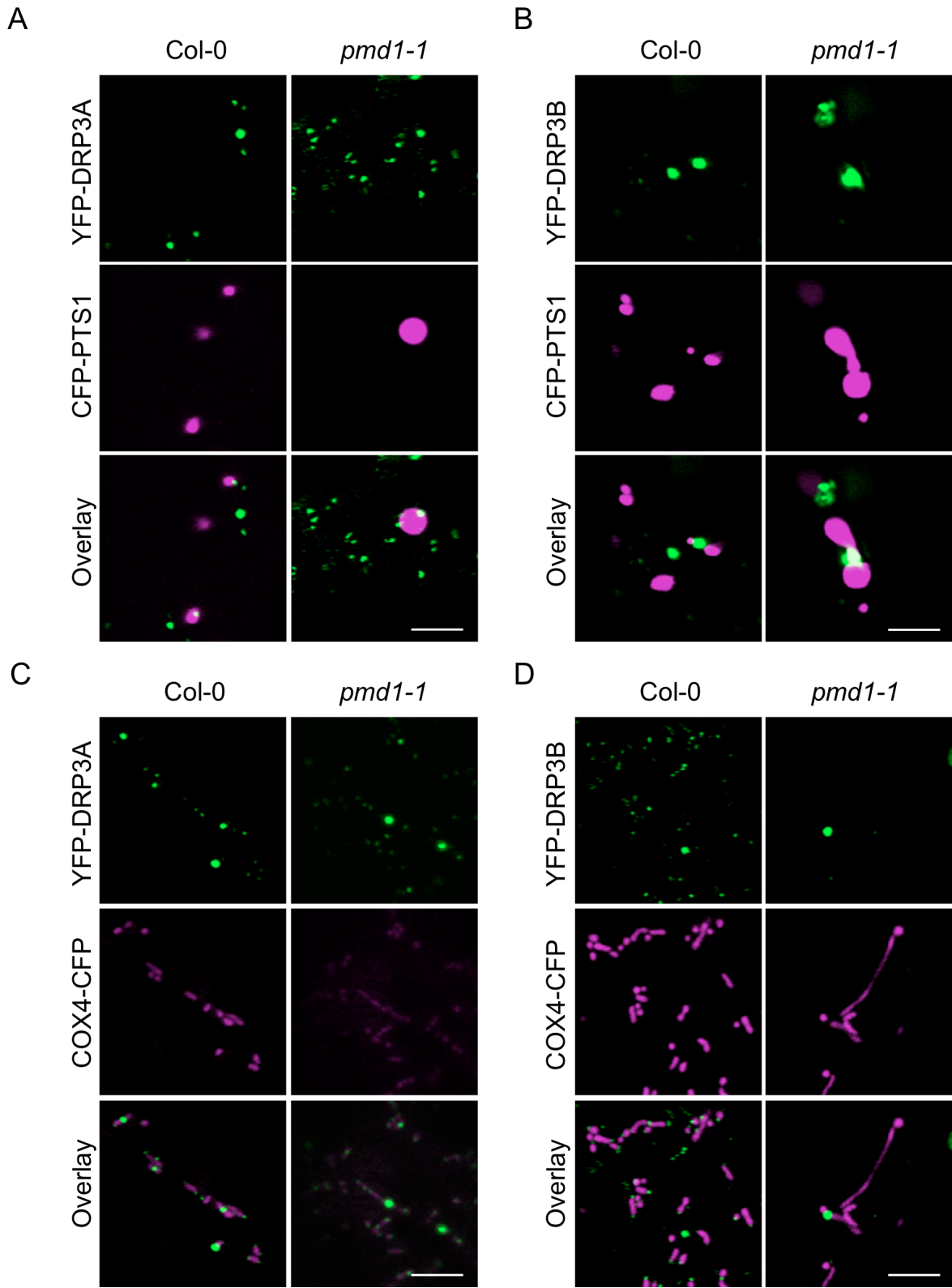


Figure 2.9

Figure 2.9 (cont'd)

Figure 2.9. Localization of DRP3 proteins in the *pmd1* mutant.

Confocal images from cotyledon cells from Arabidopsis seedlings transiently expressing YFP-DRP3A (A and C) or YFP-DRP3B (B and D). The merged images show the association of the YFP-DRP3 proteins (green) with the CFP-PTS1-labeled peroxisomes (magenta) and the COX4-CFP-labeled mitochondria (magenta). Images were taken at the same magnification; scale bars = 5 μ m.

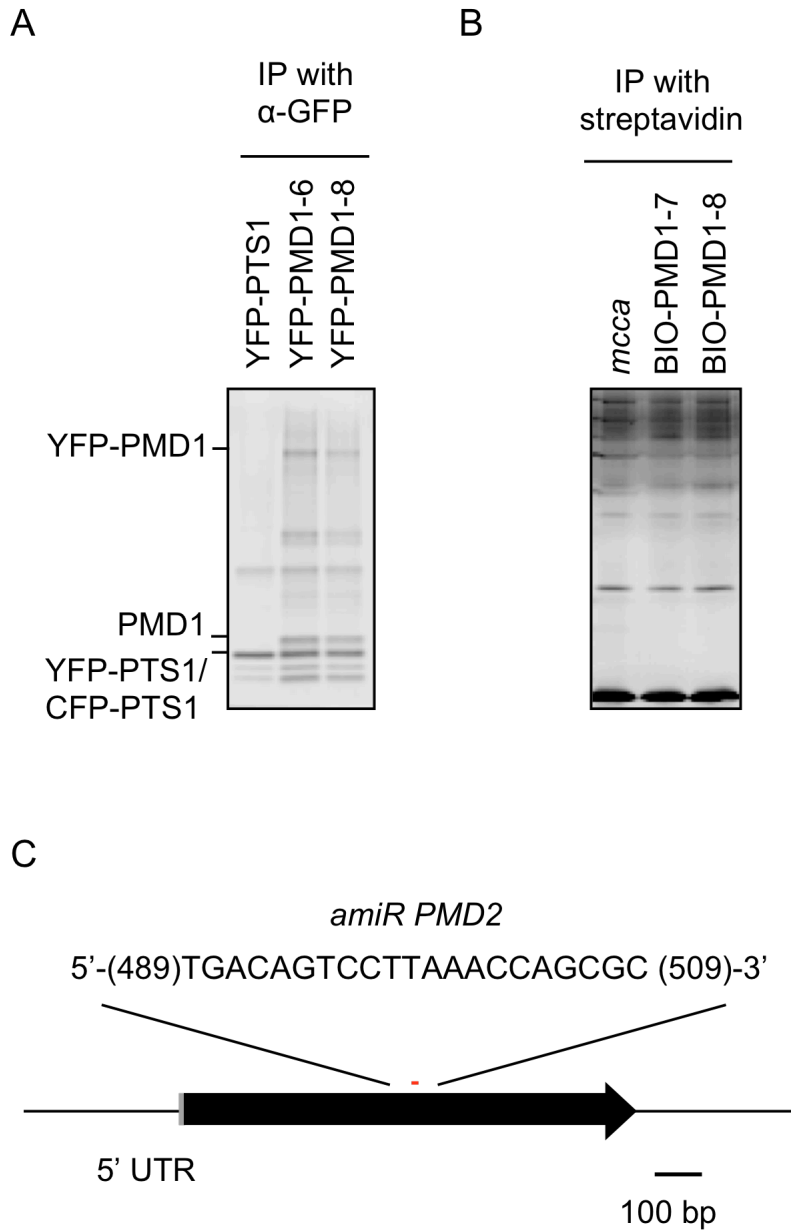


Figure 2.10

Figure 2.10 (cont'd)

Figure 2.10. Proteins pulled down from *35S_{pro}:YFP-PMD1* or *PMD1_{pro}:BIO-PMD1*

plants and the gene structure of *PMD2*.

(A) and (B) Silver-stained gels of proteins pulled down by the GFP antibody (A) or streptavidin (B). Two independent transgenic lines (*35S_{pro}:YFP-PMD1* No. 6 and 8, and *PMD1_{pro}:BIO-PMD1* No. 7 and 8) were subjected to the pull-down assays. Plants only expressing YFP-PTS1 or the *mcca* mutant were used as controls.

(C) Genomic structure of *PMD2*. The targeting site (in red) and the sequence of *amiR_{PMD2}* are shown.

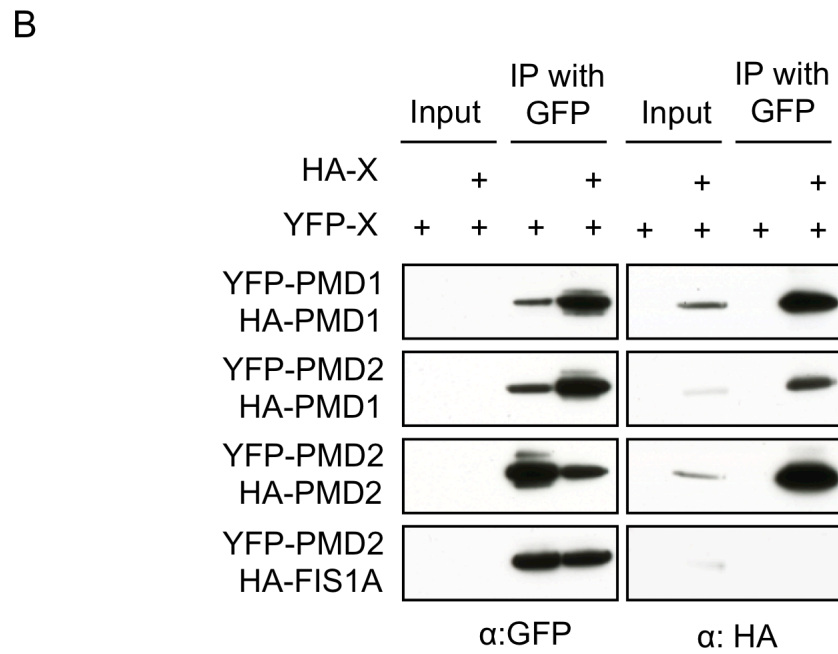
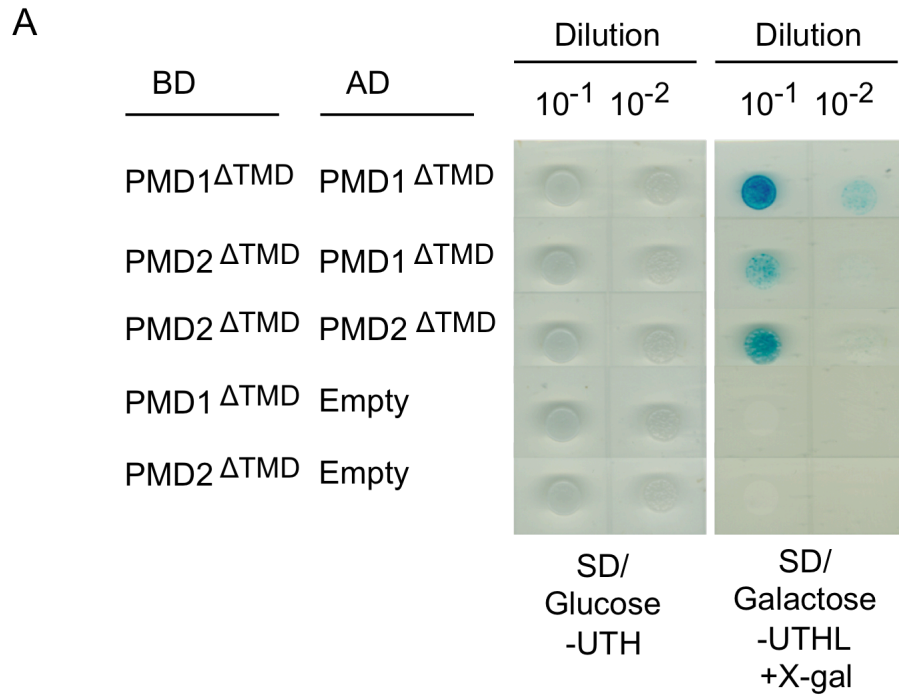


Figure 2.11

Figure 2.11 (cont'd)

Figure 2.11. PMD1 and PMD2 are able to form homo- and heterocomplexes.

(A) Yeast two-hybrid analyses. SD/Glucose-UTH selects for transformants and SD/Galactose-UTHL + X-gal select for protein-protein interactions. Empty, pB42AD-GW vector only.

(B) Co-IP analyses. Various combinations of the fusions as indicated were transiently expressed in tobacco leaf epidermal cells, followed by immuno-precipitation using the GFP antibody. A GFP or HA antibody was used to detect the proteins.

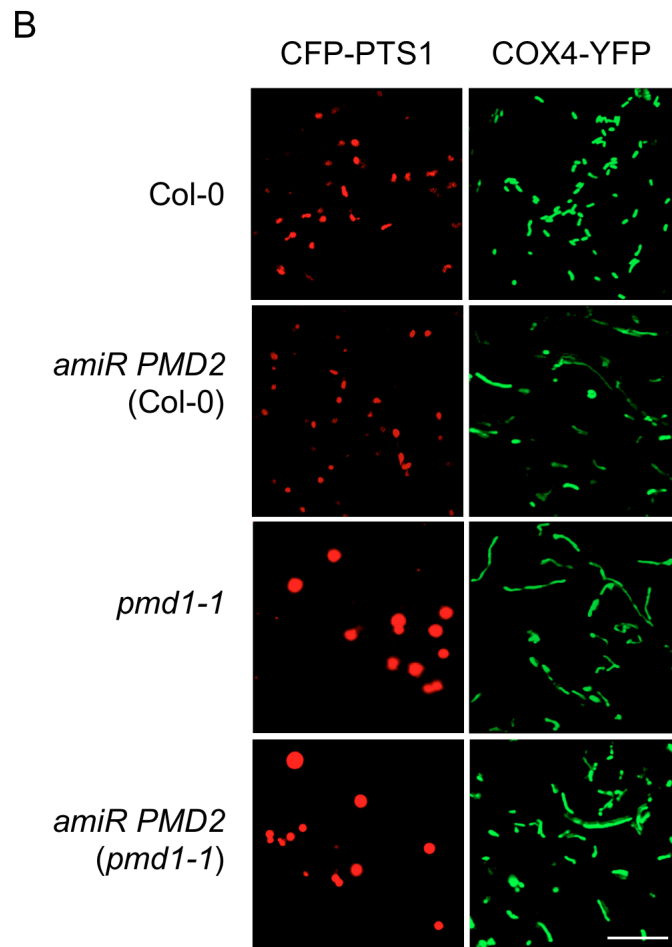
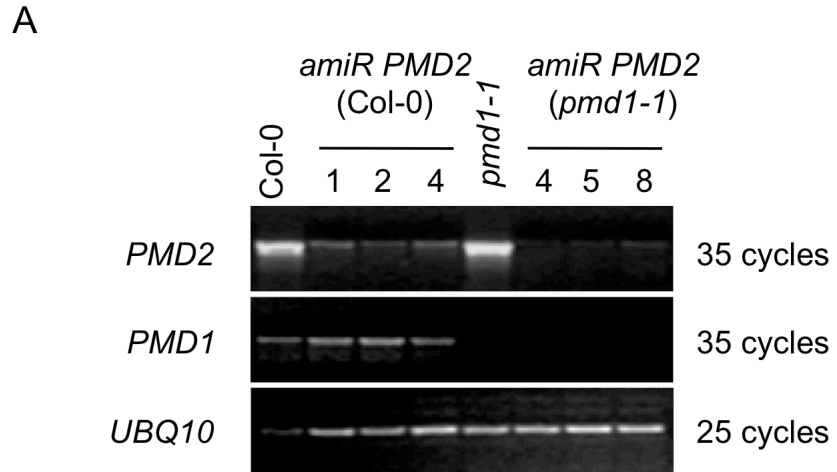


Figure 2.12

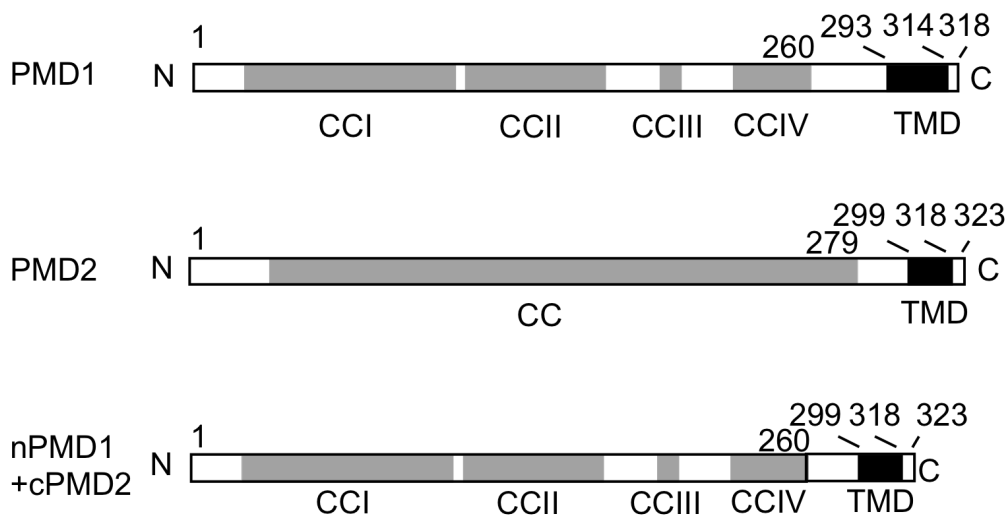
Figure 2.12 (cont'd)

Figure 2.12. PMD2 is involved in mitochondrial morphogenesis.

(A) RT-PCR analyses showing the transcripts of *PMD1*, *PMD2*, and *UBQ10* in Col-0, *amiR PMD2*, *pmd1-1* and *pmd1-1 amiR PMD2* plants. Three independent lines that contain *amiR PMD2* in the Col-0 (lines 1, 2, 4) or *pmd1-1* (lines 4, 5, 8) background are shown.

(B) Confocal images from leaf epidermal cells of plants co-expressing the organelle markers. Peroxisomes were labeled by CFP-PTS1 and mitochondria were marked by COX4-YFP. Images were taken at the same magnification; scale bar = 10 μ m.

A



B

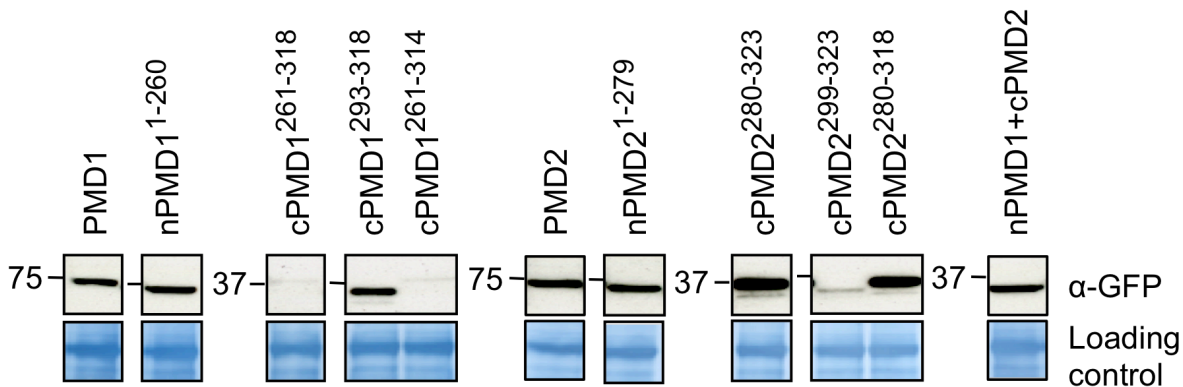


Figure 2.13

Figure 2.13 (cont'd)

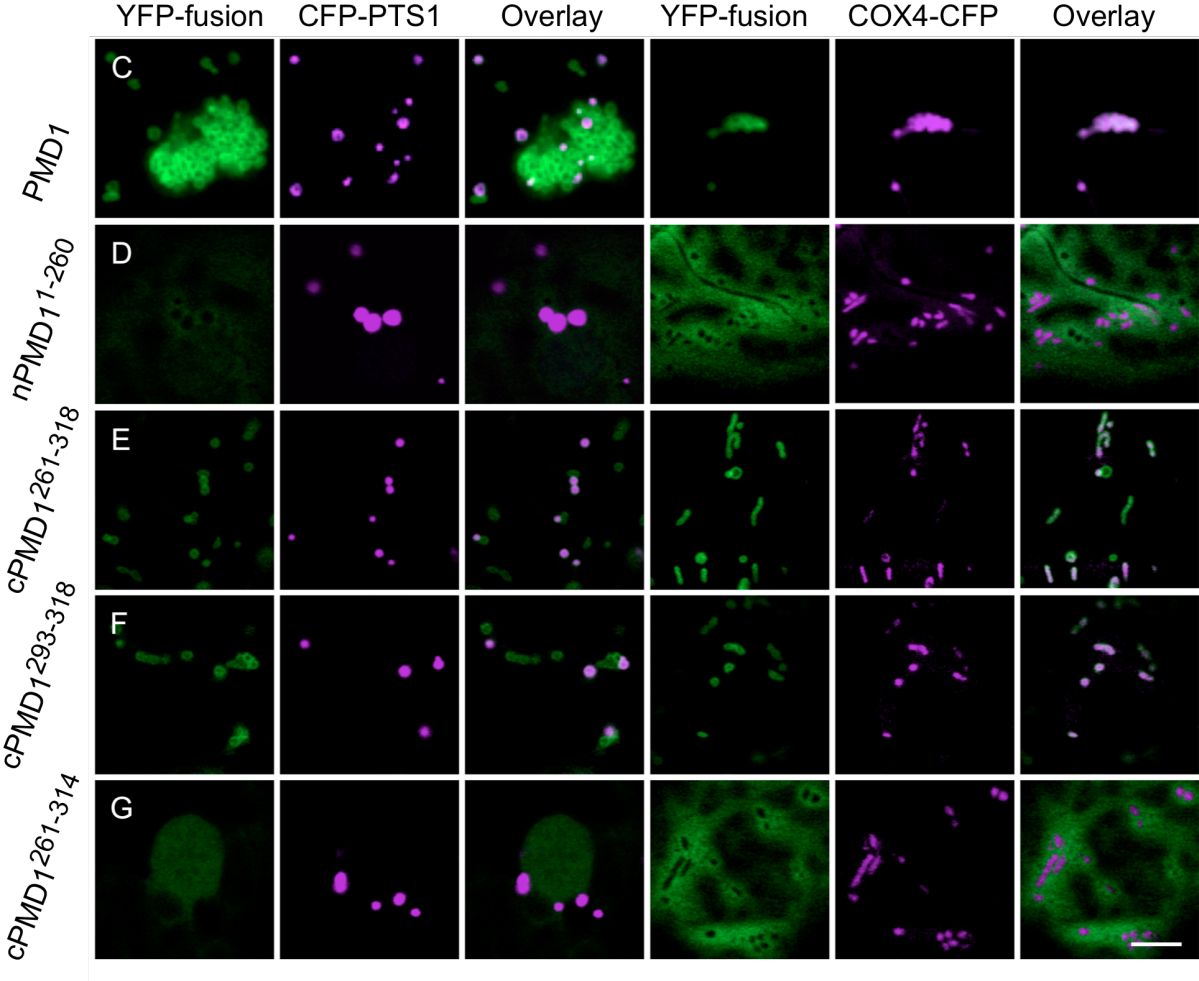


Figure 2.13 (cont'd)

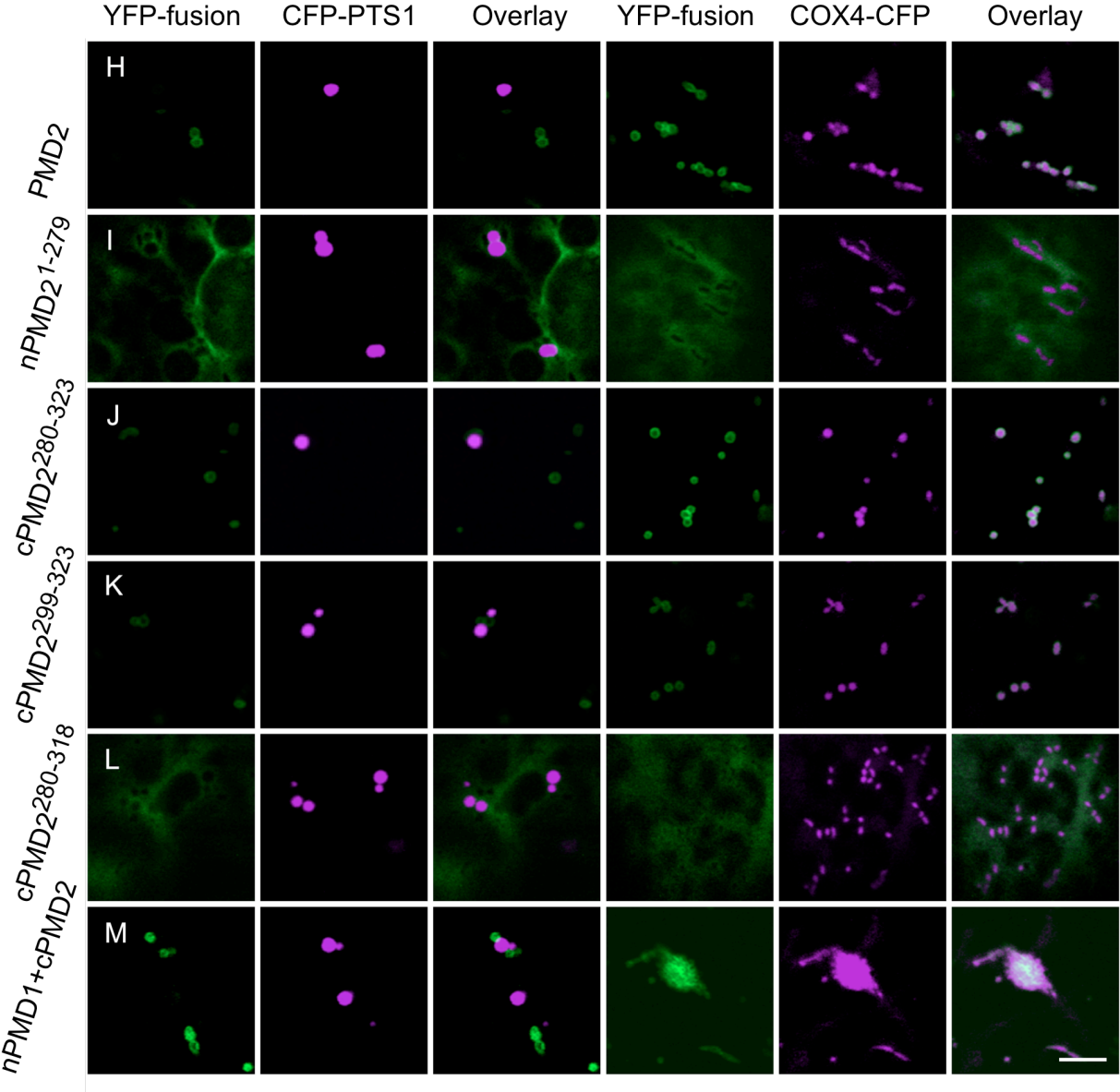


Figure 2.13 (cont'd)

Figure 2.13. Organelle targeting signals reside in the C-terminus of PMD1 and PMD2.

(A) Schematics of PMD1, PMD2, and nPMD1+cPMD2, with the CC domains, TMD, and amino acids indicated. Despite sequence similarities between PMD1 and PMD2, PMD2 was annotated as having a single and long CC domain.

(B) Immunoblot analysis to detect the YFP-PMD variants expressed in tobacco cells. The large subunit of RUBISCO was used as the loading control. Numbers indicate MW in kDa.

(C) to (M) Subcellular targeting of the YFP-PMD1/PMD2 fusions. YFP signals are in green and CFP signals are in magenta. Images were taken at the same magnification; scale bars = 10 μm . To better illustrate colocalization between YFP-fusion and CFP-PTS1, images in (C) were taken from a region where peroxisome proliferation/aggregation was not so strong.

Table 2.1. In silico identification of peroxisomal membrane proteins containing long coiled-coil domains.

AGI	a.a.	CC %	TMD	Annotation	Sub-cellular localization	Note
At1g06530	323	76	1	PMD2	Mt ^a	C-TA
At2g32240	775	85	1	TMD1	PM ^b	C-TA
At5g15880	348	50	1	LNG1	Cyt ^c , Nu ^c	C-TA
At3g58840	318	75	1	PMD1	Mt ^a , Px ^a	C-TA
At1g05320	828	73	1	TMD2	PM ^b	C-TA
At3g16000	724	70	1-3	MFP1	Nu ^d , Pt ^d	
At3g17520	298	51	1	LEA	Other ^e	

a.a.: amino acid

CC: Coiled-Coil

TMD: Transmembrane Domain

PMD1: Peroxisomal and Mitochondrial Division Factor1

PMD2: Peroxisomal and Mitochondrial Division Factor2

LNG1: LONGIFOLIA1 (Lee et al., 2006)

MFP1: MAR-binding filament like protein 1

LEA: Late embryogenesis abundant LEA domain-containing expressed protein

Mt: Mitochondrion

Px: Peroxisome

PM: Plasma membrane

Cyt: Cytosol

Nu: Nucleus

Table 2.1 (cont'd)

a: Confirmed experimentally in this study

b: Confirmed experimentally by Iris Meier's group

c: Confirmed experimentally by Lee et al., (2006)

d: Confirmed experimentally by Samaniego et al., (2005)

e: The protein was predicted to be targeted to cytosol, ER, nucleus, extracellular or plastid according to SUBA (Heazlewood et al., 2007).

Table 2.2. DNA primers used in this study.

Primer	Sequence (5'-3')
PMD1-attB1	ggggacaagttgtacaaaaagcaggcttcatggcggatgtgaagatcg
PMD1-attB2-N	ggggaccactttgtacaagaaagctgggtctcaccttagcttagaatagcagac
PMD1-attB2-C	ggggaccactttgtacaagaaagctgggtcccttagcttagaatagcagac
PMD1pro-attB1	ggggacaagttgtacaaaaagcaggcttctgctgtttagttcgggttca
PMD1pro-YFP-3' YFP-Rev	agctcctcgccttggccattttagcttctactagagaaaattc
PMD1pro-YFP-5' YFP-Rev	ggatcactctcggcatggacgagatggcggatgtgaaga
PMD2-attB1	ggggacaagttgtacaaaaagcaggcttcatggcggaaagagaggagc
PMD2-attB2	ggggaccactttgtacaagaaagctgggtctcaaaccctcctcgagtgg
cMCCA-attB1	ggggacaagttgtacaaaaagcaggcttcatgaccagctccgaaacatc
cMCCA-PMD1-Rev	cttcaacatccgcatccctttagcttctgaatag
cMCCA-PMD1-Fw	ctattcaggatcaaagggatggcggatgtgaag
nPMD1 (1- 260)-attB2	ggggaccactttgtacaagaaagctgggtcttatggccactgatactcagc
cPMD1 (261-318)-attB1	ggggacaagttgtacaaaaagcaggcttcatgtttgctttgaatgagagaac
cPMD1(293-318)-attB1	ggggacaagttgtacaaaaagcaggcttcatgccagtgtgtgctgctg
cPMD1 (261-314)-attB2	ggggaccactttgtacaagaaagctgggtctcaatagcagacgaaaaag
nPMD2 (1- 279)-attB2	ggggaccactttgtacaagaaagctgggtctcatccaccggaaccaacag
cPMD2 (280-323)-attB1	ggggacaagttgtacaaaaagcaggcttcatgccactgaatggcattg
cPMD2 (299-323)-attB1	ggggacaagttgtacaaaaagcaggcttcatggctgtggcagcgggtg
cPMD2 (280-318)-attB2	ggggaccactttgtacaagaaagctgggtctcagtaaatgtagcagacaacagc
DRP3A-attB1	ggggacaagttgtacaaaaagcaggcttcatgactattgaagaagttccg
DRP3A-attB2	ggggaccactttgtacaagaaagctgggtcttagaatccgtatccatttgggtg
DRP3B-attB1	ggggacaagttgtacaaaaagcaggcttcatgtccgtcgacgatctccc
DRP3B-attB2	ggggaccactttgtacaagaaagctgggtcttcatatgaagccgtccgttc
DRP5B-attB1	ggggacaagttgtacaaaaagcaggcttcatggcggaaagtatcagc
DRP5B-attB2	ggggaccactttgtacaagaaagctgggtgtcaatgctgcaccgaagg
FIS1A-attB1	ggggacaagttgtacaaaaagcaggcttcatggatgctaagatcggac
FIS1A-attB2	ggggaccactttgtacaagaaagctgggtctcatttcttgcgagacatcgc
FIS1B-attB1	ggggacaagttgtacaaaaagcaggcttcatggacgcggcgatagggag
FIS1B-attB2	ggggaccactttgtacaagaaagctgggtcttagctgcgtaatatggctg
PMD2-amiR2-I miR-s	gaTGACAGTCCTTAAACCAGCGCtctctctttgtattcc
PMD2-amiR2-II miR-a	gaGCGCTGTTTTAAGGACTGTCAAtcaagagaatcaatga
PMD2-amiR2-III miR*s	gaGCACTGTTTTAAGCACTGTCTTcacaggctcgtgatatg
PMD2-amiR2-IV miR*a	gaAGACAGTGCTTAAACCAGTGCTctacatatatattcct
CS854214-LP	tctgactacgatcaaggtgggtg
CS854214-RP	gcttagaatagcagacgaaaaagg
Wisc LP	aacgtccgcaatgtgtattaagttg
SALK_139577-LP	cagctccttctcgtttttg
SALK_139577-RP	aactctgcaagcaacgatttg
Lb1.3	attttgccgatttcggaac

Table 2.3. Vectors used in this study.

Vector	Description	Reference
pDonor 207	Donor vector	Invitrogen
pDonor/Zeo	Donor vector	Invitrogen
pEarleyGate 101	YFP-GW	(Earley et al., 2006)
pEarleyGate 104	GW-YFP	(Earley et al., 2006)
pEarleyGate 100	35S-GW	(Earley et al., 2006)
pEarleyGate 201	HF-GW	(Earley et al., 2006)
pDest-35S-6xHis-YFP-X	YFP-GW	(Reumann et al., 2009)
pGWB1	pPMD1-YFP-PMD1	(Nakagawa et al., 2007)
pGWB2	35S-GW	(Nakagawa et al., 2007)
pMDC32	35S-GW	(Curtis et al., 2003)
pGilda-gateway	Yeast two-hybrid	Modified from pGilda (Clontech)
pB42-AD-gateway	Yeast two-hybrid	Modified from pB43-AD (Clontech)
pDEST22	Yeast two-hybrid	Invitrogen
pDEST32	Yeast two-hybrid	Invitrogen

METHODS

Plant Material, Growth Conditions, Transformation and Plant Selection

Arabidopsis thaliana plants were grown at 20°C with 70% humidity, irradiated with 70 to 80 $\mu\text{mol m}^{-2} \text{s}^{-2}$ of white light for 14 h per day. T-DNA insertion mutants, *pmd1-1* (CS84214) and *pmd1-2* (SALK_139577), were obtained from the Arabidopsis Biological Recourse Center (ABRC). *pmd1-1* is in Col-3 background and *pmd1-2* is in Col-0 background. The presence of the T-DNAs and the homozygosity of mutants were identified by polymerase chain reaction (PCR) of genomic DNA using the following primers (*pmd1-1*: CS854214-LP, CS854214-RP, Wisc LP; *pmd1-2*: SALK_139577-LP, SALK_139577-RP, LbB1.3). The absence of *PMD1* transcripts was determined by reverse transcription PCR (RT-PCR) using PMD1-attB1 and PMD1-attB2-N as listed in Supplemental Table 2. .

To generate plants with organelle markers, the peroxisomal marker CFP-PTS1 (conferring resistance to gentamycin) and the mitochondrial marker *Saccharomyces cerevisiae* COX4-YFP were co-transformed into the null mutants or wild-type Col-0. The COX4-YFP construct has two versions: one confers resistance to kanamycin and was used for transformation into *pmd1-1* and Col-0, and the other confers resistance to Basta and was used for transformation of *pmd1-2*. T₁ generation was screened with kanamycin or basta for the presence of the mitochondrial marker and with epifluorescence microscope for the presence of CFP signals (peroxisomes) and YFP signals (mitochondria). T₂ or T₃ generation of the transgenic plants was subjected to confocal microscopy to identify plants that contain both markers.

To generate gain-of-function mutants, *35S_{pro}:PMD1* or *35S_{pro}:YFP-PMD1/PMD2* was constructed as described below and transformed into the double marker plants in Col-0 background. Transgenic plants were screened with Basta and the T₃ generations were subjected to confocal imaging. To generate knock-down mutants, *amiR PMD2* was constructed as described below and transformed into the double marker plant in Col-0 or *pmd1-1* background. The transgenic plants were screened with hygromycin and the T₃ generation was used to observe organelle and plant morphologies.

The simplified Arabidopsis transformation method (<http://entomology.wisc.edu/~afb/protocol.html>) was used to perform all Arabidopsis plant transformations using *Agrobacterium tumefaciens* strain GV3101 (pMP90). For selections of transgenic plants, T₁ seeds were plated on 0.5 Linsmaier and Skoog medium with 100 µg/ml of gentamycin, 50 µg/ml of kanamycin, or 50 µg/ml of hygromycin. For Basta screening, T₁ individuals were grown on soil and sprayed at 7 days and 9 days after germination with 0.1% (v/v) of Basta (Finale; Farnam Companies) and 0.025% (v/v) Silwet L-77 to select transgenic plants. The putative transgenic plants were further screened with epifluorescence microscopy, which confirmed that the transgenes fused with a fluorescent protein tag were expressed, or with RT-PCR, which checked the expression levels of the overexpressed genes without a fluorescent protein tag.

Agrobacterium-mediated transient expression in Arabidopsis was performed according to a published method (Li et al., 2009). 4-day-old Arabidopsis Col-0 and *pmd1-1* expressing the peroxisomal marker CFP-PTS1 or the mitochondrial marker

COX4-CFP were inoculated with *A. tumefaciens* cells harboring YFP-DRP3A or YFP-DRP3B to transiently express the fusion genes. Two days later, the transfected plants were subjected to confocal imaging.

Nicotiana tabacum plants were grown at 24°C with 70% humidity, and irradiated with 50 $\mu\text{mol m}^{-2} \text{s}^{-2}$ of white light for 14 h per day. Six to 8-week-old plants were subjected to *Agrobacterium tumefaciens*-mediated infiltration to transiently express the genes of interest. *A. tumefaciens* cells harboring the plasmid(s) of interest were incubated at 28°C with shaking (200 rpm) for approximately 24 h. The cells were then spun down, washed, and resuspended with water to an A_{600} of 0.05. Cells harboring genes of interest were infiltrated into mature leaves, using a syringe. The infiltrated plants were incubated in the same growth condition for 2 days. Then, the infiltrated leaves were subjected to confocal imaging, co-immunoprecipitation, or immunoblot analysis.

Gene Cloning and Plasmid Construction

The genes of interest were amplified with Gateway-compatible primers from the cDNA synthesized from total RNA of wild type (Col-0) seedling or cDNA clones obtained from ABRC, using Phusion High-Fidelity DNA polymerase (New England Biolabs). The PCR fragments were cloned to the donor vector (pDonorTM207 or pDonorTM/Zeo) and different destination vectors using a standard Gateway cloning system (Invitrogen). *PMD1_{pro}:YFP-PMD1* was generated using an overlapping PCR approach (<http://gfp.stanford.edu/protocol/index5.html>) and cloned into a binary vector pGWB1

(Nakagawa et al., 2007). To generate YFP-fusion proteins, the genes of interest were cloned into a binary vector pEarleyGate 104 (Earley et al., 2006) or pDest-35S-6xHis-YFP (kindly provided by Sheng Quan, MSU). To clone overexpressors, the genes were cloned into pEarleyGate 100 (Earley et al., 2006) or pGWB2 (Nakagawa et al., 2007) .

To create the biotinylated PMD1 construct, a biotin tag containing 80 amino acids from the biotin carboxyl carrier protein domain (BCCP) of the Arabidopsis *MCCA* gene (At1g03090) was fused to the N-terminus of *PMD1*, using the overlapping PCR method described above. The overlapped PCR fragment was subcloned into pMDC32 (CD3-738) (Qi and Katagiri, 2009). Later, the 35S promoter was replaced with the *PMD1* native promoter, using restriction sites *KpnI* and *HindIII*.

To create HA-fusion proteins, full-length coding sequence of PMD1, PMD2 and FIS1 was cloned into a binary vector pEarleyGate 201 (Earley et al., 2006).

To clone the artificial microRNA construct, WMD3-Web MicroRNA Designer (<http://wmd3.weigelworld.org/cgi-bin/webapp.cgi>) was used to design *amiRNA PMD2*. One of the recommended amiRNAs, 5'-(489) TGACAGTCCTTAAACCAGCGC (509)-3', was selected and cloned using an overlapping PCR as described in the WMD3-Web MicroRNA Designer (http://wmd3.weigelworld.org/downloads/Cloning_of_artificial_microRNAs.pdf). The precursor miRNA was amplified by Gateway-compatible primers and cloned into pGWB2 (Nakagawa et al., 2007). The primers and vectors used in this study are listed in Supplemental Table 2 and 3.

RT-PCR Analysis

RNA from leaves of 4-week-old *Arabidopsis* plants was purified as previously described (Zhang and Hu, 2009). For RT-PCR analysis, 0.5 µg of total RNA was used to make cDNA using high capacity RNA-to-cDNA master mix (Applied Biosystems). PCR amplification was performed as previously described (Zhang and Hu, 2010) using primers specific for *PMD1* (At3g58840), *PMD2* (At1g06530), and *UBQ10* (At4g05320). The number of cycles used in the RT-PCR was optimized to be in the linear range of amplification. Primers used in this study are listed in Supplemental Table 2.

Immunoblot Analysis

50 mg of fresh tissues were ground with plastic pestles using liquid nitrogen and 500 µl of SDS-containing extraction buffer (60 mM Tris-HCL pH 8.8, 2% SDS, 2.5% glycerol, 0.13 mM EDTA pH 8.0, and 1X protease inhibitor cocktail complete from Roche). The tissue lysates were vortexed for 30 s, heated at 70 °C for 10 minutes, and centrifuged at 13,000 g twice for 5 minutes at room temperature. The supernatants were then transferred to new tubes. For SDS-PAGE analysis, 5 µl of the extract in 1x NuPAGE LDS sample buffer (Invitrogen) was separated on 4-12% NuPage (Invitrogen) before transferred to the PVDF membrane. The membrane was incubated with 3% BSA in 1x TBST (50 mM Tris-base, 150 mM NaCl, 0.05% Tween 20, pH 8.0) over night at 4°C. Then it was probed with the antibody prepared in the blocking buffer at room temperature for 1 h. The antibodies used are as follows: 1:20,000 α-GFP (abcam), 1:20,000 α-horseradish peroxidase conjugated Streptavidin (Millipore), 1:1,000 α-PEX11d (Orth et al., 2007), 1:5,000 α-VDAC (Reumann et al., 2009), and 1:100 α-HA (Cell signaling). The probed membrane was washed three times with 1x TBST for 5 min

before incubated with the secondary antibody at room temperature for 1 h. The secondary antibodies used are: 1:20,000 goat anti-rabbit IgG for α -GFP and α -PEX11d, 1:20,000 goat anti-mouse IgG for α -horseradish peroxidase conjugated Streptavidin (Millipore), α -VDAC, and α -HA. Finally, the membrane was washed four times with 1x TBST for 10 min before the signals were visualized with SuperSignal[®] West Dura Extended Duration Substrate (Pierce Biotechnology).

Purification of Peroxisomal and Mitochondrial Proteins

Rosette leaves from 4-week-old transgenic plants expressing *35S_{pro}:YFP-PMD1* and an organelle marker were used for organelle purification. Peroxisomes were isolated from the peroxisomal marker (CFP-PTS1) background as described previously (Reumann et al., 2009).

Mitochondria were purified from the mitochondrial marker (COX4-CFP) background as described in (Kruft et al., 2001; Werhahn and Braun, 2002) with minor modifications. Leaves were harvested and homogenized on ice with 120 ml of grinding buffer (450 mM Sucrose, 1.5 mM EGTA, 0.2% BSA, 0.6% PVP-40, 10 mM DTT, 0.2 mM PMSF, and 15 mM MOPS/KOH, pH7.4), using a mortar and a pestle. The homogenized solution was filtered with two layers of Miracloth. Chloroplasts and other organelles and particles were sedimented by centrifugation for 10 min at 3,500 g (5 min each time) and 5 min at 6,000 g. The supernatant was then centrifuged for 10 min at 17,000 g to pellet down the fraction enriched in mitochondria. The pellet was washed with 80 ml of washing buffer (0.3 M Sucrose, 10 mM MOPS/KOH, pH 7.2). 10 ml of mitochondria in washing buffer were topped onto a three-step Percoll gradient, which

contains 18%, 29% and 45% Percoll in 0.3 M Sucrose and 10 mM MOPS/KOH, pH 7.2. The Percoll gradients were centrifuged for 40 min at 45,000 g; mitochondria were recovered from the interphase between 29% and 45%. The mitochondrial fractions were pooled together and diluted with washing buffer. After two washes with washing buffer and a 10-min centrifugation at 17,000 g for 10 min, the mitochondria were resuspended with 3 ml of washing buffer containing the protease inhibitor cocktail complete (Roche).

The purity of peroxisomal and mitochondrial proteins was determined using immunoblot analyses as described above. A polyclonal PEX11d antiserum, which was raised against Arabidopsis PEX11d (Orth et al., 2007), was used to detect the expression of the peroxisome-specific protein PEX11d. A monoclonal VDAC antiserum, which was raised against the VDAC protein of maize (*Zea Mays*) and used in our previous study (Reumann et al., 2009), was used to detect the mitochondrion-specific protein VDAC.

Assays for Membrane Association and Topology

Peroxisomal and mitochondrial membrane association of PMD1 was tested as previously described (Orth et al., 2007). The orientation of the coiled-coil domains was tested by protease protection, using thermolysin as described previously (Cline et al., 1984) with minor modifications. 200 μ l of the purified peroxisomal and mitochondrial proteins were treated with 0, 150 or 300 μ g/ml of thermolysin in an incubation buffer containing 50 mM HEPES/NaOH, pH 7.5, 0.33 M sorbitol, and 0.5 mM CaCl₂. The reactions were carried out at 4°C for 1 h, and stopped by adding 5 mM EDTA. 20 μ l of

the treated proteins were subjected to immunoblot analysis using the GFP antibody as described above.

Co-IP Assay

BIO-PMD1, YFP-PMD1/PMD2, and HA-PMD1/PMD2/FIS1A proteins were transiently expressed in tobacco as described above. Approximately 1 g fresh weight of infiltrated leaf was collected 2 days after infiltration. The tissue was homogenized in RIPA buffer (Thermo) with 1x complete protease inhibitor cocktail (Roche) and lysed on a rotator at 4°C for 1 h. The samples were centrifuged at 13,000 g for 10 min to remove cell debris. The supernatants were then incubated with 20 µl of Agarose conjugated anti-GFP (MBL) on a rotator for 1 h to pull down the YFP fusion proteins. The agarose beads were then spun down at 3000 g for 15 sec and washed four times with RIPA buffer. Proteins associated with the YFP-fusion protein were eluted by adding 50 µl of 1x NuPAGE LDS sample buffer (Invitrogen) and heating at 75°C for 10 min. The eluted proteins were analyzed by immunoblot assays as described above.

Yeast Two-Hybrid Assays

The ProQuestTM two-hybrid system was used to test the interaction between PMD1 and peroxisome division factors. PMD1^{ΔTMD} was cloned into pDestTM32 to generate the bait clone. Full-length DRP, FIS1^{ΔTMD}, and PMD1^{ΔTMD} were cloned into the pDestTM22 vector to generate the prey clones. The plasmid DNA was transformed into yeast strain MaV203. The presence of the transformed plasmid DNAs was

screened using Standard Synthetic Dropout medium (SD/-Ura-Trp). SD medium with 10 mM 3-AT and without Ura, Trp, and His was used to test the physical interaction of the tested proteins.

Matchmaker two-hybrid system (Clontech) was also used to test the self-interaction of PMD1, PMD2, and interaction between PMD1 and PMD2. PMD^{ΔTMD} was cloned into a derivative of pGilda or pB42AD containing the gateway cassette (attR1-Cmr-ccdB-arrR2). The plasmid DNA was transformed into the yeast strain EGY48, using Frozen-EZ Yeast Transformation KitTM as recommended by the manufacturer (Zymo). Transformants were screened using Standard Synthetic Dropout medium (SD/Glucose-Ura-Trp-His). SD/Galactose medium with X-gal (5-bromo-4-chloro-3-indolyl-beta-D-galactopyranoside) and minus Ura, Trp, His, and Leu was used to test for protein interaction.

Confocal and TEM Analyses

All the confocal images were taken by a confocal laser scanning microscope (Zeiss LSM 510 META). Before imaging, leaf discs were fixed with a fixation buffer, which contains 2% formaldehyde, 10 mM EGTA, 5 mM MgSO₄, 50 mM PIPES, pH 7.0, for 10 min, to stop the movement of organelles, and then rinsed with water. YFP and CFP signals were detected as previously reported (Reumann et al., 2009). All images, except those shown in Figure 2.5B and 2.12B, were obtained from a single focal plane. For images in Figure 2.5B and 2.12B, Z series of 6 images, each 10 μm in depth, were collected and superimposed into one image.

To observe the ultrastructure of organelles in mesophyll cells, 4-week-old wild-type (Col-0) and *35S_{pro}:PMD1* Arabidopsis plants were subjected to transmission electron microscopy analysis, using methods previously described (Duek and Fankhauser, 2005).

Quantification of Organelles

Peroxisomes and mitochondria were visualized in leaf epidermal cells from wild-type and various *pmd* mutants that express the fluorescent organelle markers, using confocal microscopy. Z series of 10 images, each 18 μ m in depth, were collected and superimposed into one image to quantify peroxisomes. A total of 10 images from wild type and *pmd1-1* were analyzed by IMAGE J (URL: <http://rsb.info.nih.gov/ij>) as previously reported (Desai and Hu, 2008). The size of peroxisomes or mitochondria was measured as average fluorescent area per organelle, using units assigned by IMAGE J. The p values were calculated by Student's two-tailed t-test against the wild type.

Affinity Purification of the PMD1 Protein Complex

To perform the biotin-streptavidin purification, T₃ homozygous plants expressing cMCCA-PMD1 were used to isolate the PMD1-interacting proteins, using methods described before (Qi and Katagiri, 2009). For the GFP pull-down assay, T₃ homozygous plants expressing YFP-PMD1 in the peroxisomal marker (CFP-PTS1) and mitochondrial marker (COX4-CFP) backgrounds were used. 30 g of leaf tissues were homogenized in 50 ml of RIPA buffer (Thermo) containing 1x complete protease inhibitor cocktail

(Roche) and lysed on a rotator at 4°C for 1 h. The samples were subjected to centrifugation at 13,000 g for 10 min to remove cell debris. The supernatants were then incubated with 200 µl of Agarose conjugated anti-GFP (MBL) on a rotator for 1 h to pull-down the YFP fusion proteins. The agarose beads were spun down at 3000 g for 15 sec and washed four times with RIPA buffer. The YFP-interacting proteins were eluted by adding 1x NuPAGE LDS sample buffer (Invitrogen) and heating at 75°C for 10 min. The eluted proteins were subjected to electrophoresis in 4-12% gradient NuPAGE gels (Invitrogen) and silver-staining or liquid chromatography-tandem mass spectrometry (LC-MS-MS) analyses as described before (Reumann et al., 2009).

Accession Numbers

Arabidopsis Genome Initiative locus identifiers for the genes mentioned in this article are as follows: PMD1 (At3g58840), PMD2 (At1g06530), UBQ10 (At4g05320), DRP3A (At4g33650), DRP3B (At2g14120), DRP5B (At3g19720), FIS1A (At3g57090), FIS1B (At5g12390). Germplasm identification number for *pmd1-1* and *pmd1-2* alleles used in this work is as follows: *pmd1-1* (WiscDsLox393-396O15; The Arabidopsis Information Resource stock number CS854214), and *pmd1-2* (SALK_139577).

ACKNOWLEDGEMENTS

We thank the ABRC (Columbus, OH, USA) for providing the T-DNA insertion mutants, Detlef Weigel (Department of Molecular Biology, Max Planck Institute for Developmental Biology, Tübingen, Germany) for providing pRS300 vector for amiRNA cloning, Tsuyoshi Nakagawa (Research Institute of Molecular Genetics, Shimane

University, Matsue, Japan) for the pGWB1 and pGWB2 vectors. We also thank Melinda Frame and Alicia Pastor (Center of Advance Microscopy, MSU) for their help with confocal microscopy and TEM analyses. This work was supported by grants from the National Science Foundation (MCB 0618335) and the Chemical Sciences, Geosciences and Biosciences Division, Office of Basic Energy Sciences, Office of Science, U.S. Department of Energy (DE-FG02-91ER20021) to J.H.

CHAPTER 3

Arabidopsis *DYNAMIN-RELATED PROTEIN5B* is also involved in mitochondrial morphogenesis and division

ABSTRACT

Dynamamin-related protein5B (DRP5B/ARC5) was first identified for its role in the division of chloroplasts and was recently demonstrated to be a peroxisomal division factor. Since peroxisomes and mitochondria share the same set of division components like DRP3A and DRP3B, we tested whether DRP5B is involved in mitochondrial division. In vivo localization of yellow fluorescent protein (YFP) fusion shows that YFP-DRP5B is not targeted to mitochondria. However, *drp5B-1* and *drp5B-2* exhibit elongated mitochondria, suggesting that DRP5B may be involved in regulating mitochondrial morphogenesis and division indirectly. Genetic studies show that the *drp3A-2 drp3B-2 drp5B-2* triple mutant phenocopies the dwarf growth phenotype of *drp3A-2 drp3B-2* but exhibits enhanced organelle morphological phenotypes by having enormously elongated and aggregated mitochondria and dumbbell-shaped chloroplasts. DRP5B does not interact physically with DRP3A or DRP3B in yeast two-hybrid assays and is not a major component of DRP3-containing protein complexes, suggesting that DRP5B functions in mitochondrial division independently from DRP3 complex. In summary, DRP5B may be indirectly involved in the division of mitochondria and its role in peroxisomal and mitochondrial division is independent from DRP3.

INTRODUCTION

DRP belongs to the dynamin superfamily, which plays critical roles in eukaryotic cells by functioning in diverse cellular processes, including vesicle scission, organelle fusion and fission, cytokinesis, and pathogen resistance (Praefcke and McMahon, 2004). Classical dynamin proteins contain five conserved domains: the GTPase domain (DYN1) hydrolyzes guanosine triphosphate (GTP), the middle domain (DYN2) is responsible for self-interaction of dynamins through its coiled-coil region, the GTPase effector domain (GED) is involved in forming protein complex and activates GTPase activity, the pleckstrin-homology domain (PH) binds to negatively charged lipid, and proline- and arginine-rich domain (PRD) provides the binding site for dynamin-binding proteins (Hinshaw, 2000; Heymann and Hinshaw, 2009). In general, DRP is defined by the presence of at least the first three characteristic domains (Heymann and Hinshaw, 2009). However, Arabidopsis DRPs are designated by the presence of the GTP-binding motif (GXXXSGKS/T) and the dynamin signature (L-P-[PK]-G-[STN]-[GN]-[LIVM]-V-T-R) within the DYN1 (Hong et al., 2003).

The Arabidopsis genome contains 16 members of the dynamin-related protein family (DRP), which have been classified into six subgroups (DRP1-6) based on their amino acid sequences similarity, functional domains, and their molecular functions (Hong et al., 2003). The DRP1 subfamily contains five members (DRP1A-E) and plays important roles in cytokinesis and cell expansion. Among the five members, *DRP1A*, *DRP1C*, and *DRP1E* are highly expressed in almost all cell types in Arabidopsis and the proteins are sorted to the cytokinetic cell plates (Hong et al., 2003; Konopka and Bednarek, 2008). Since DRP1A, DRP1C and clathrin light chain (CLC) were found in

the same sub-cellular compartment and showed similar dynamic behaviors, DRP1A and DRP1C are suggested to function in clathrin-mediated membrane endocytosis (Collings et al., 2008; Konopka et al., 2008; Fujimoto et al., 2010). Moreover, DRP1C and DRP1E were identified for their role in mitochondrial division and morphogenesis (Jin et al., 2003). DRP2 contains all five characteristic domains of Dynamin and is composed by two family members (DRP2A-B) (Hong et al., 2003). Although DRP1 and DRP2 are classified into two different families, both DRP2A and DRP2B were found to play a role in clathrin-mediated endocytosis just like DRP1 (Bednarek and Backues, 2010; Fujimoto et al., 2010; Taylor, 2011). The DRP3 subgroup has two members (DRP3A-B) (Hong et al., 2003) and belongs to the same subclade as peroxisomal and mitochondrial division factors of mammals and yeast (Arimura and Tsutsumi, 2002). In line with the phylogenetic analysis, DRP3A and DRP3B play central roles in the division of both peroxisomes and mitochondria (Arimura et al., 2004; Mano et al., 2004; Aung and Hu, 2009; Fujimoto et al., 2009; Zhang and Hu, 2009). Four members of DRP4 (DRP4A-D) are present in the Arabidopsis genome (Hong et al., 2003); however, their molecular functions haven't been characterized yet. The DRP5 subfamily contains two members (DRP5A-B) and is involved in different cellular functions. DRP5A is suggested to function in cytokinesis (Miyagishima et al., 2008), whereas DRP5B (ARC5) is involved in the division of chloroplasts and peroxisomes (Gao et al., 2003; Zhang and Hu, 2010). The DRP6 subfamily only contains one member, whose function hasn't been characterized yet (Hong et al., 2003).

During the division of peroxisomes and mitochondria, DRP acts as the force-generating molecule, which functions in the final fission process of the organelles (see

Chapter 1). As peroxisomes and mitochondria in Arabidopsis share DRP3A and DRP3B in the division processes, we sought to determine whether DRP5B is also a component of the mitochondrial division machinery. Our data showed that YFP-DRP5B is not physically associated with mitochondria. However, DRP5B is believed to involve in mitochondrial morphogenesis as the *drp5B* mutants exhibit tubulated mitochondria. Genetic analyses of the triple mutant showed that *drp3A-2 drp3B-2 drp5B-2* is viable and contains elongated mitochondria and dumbbell-shaped chloroplasts. Our yeast two-hybrid assay and blue native gel electrophoresis suggested that DRP5B does not interact with DRP3 and is not critical for the formation of DRP3-containing protein complexes in vivo. Together, DRP5B is shown to indirectly involve in mitochondrial morphogenesis through a DRP3-independent mechanism.

RESULT AND DISCUSSION

DRP5B is not associated with mitochondria

DRP5B is a plant and algal-specific protein, which is composed of four functional domains, DYN1, DYN2, GED, and PH (Hong et al., 2003). Using fluorescence microscopy, GFP-DRP5B was observed as ring structures at the division sites of the bilobed chloroplasts and co-localized with the entirety of peroxisomes. In addition to their physical association with the organelles, DRP5B is involved in the division of both chloroplasts and peroxisomes (Gao et al., 2003; Zhang and Hu, 2010). As Arabidopsis DRP3A and DRP3B are involved in the division of peroxisomes and mitochondria, we aimed to study the functional role of DRP5B in mitochondrial division. To this end, we determined the mitochondrial association of DRP5B using the yellow fluorescent protein

(YFP) tag. The YFP-DRP5B fusion protein, which was driven by the 35S promoter, was stably expressed in Col-0 that contains the mitochondrial marker (COX4-CFP). T₁ transgenic plants were selected and subjected to confocal imaging to examine the subcellular localization of the fusion protein. Consistent with previous reports (Gao et al., 2003; Zhang and Hu, 2010), we detected the YFP-DRP5B signals as ring-like structures at the constriction sites of the bilobed chloroplasts (Figure 3.1). However, no YFP signals were found on the mitochondria, suggesting that the YFP-DRP5B is not physically associated with mitochondria like DRP3A and DRP3B. To confirm this result, we are currently trying to verify the subcellular localization of *DRP5B_{Pro}:GFP-DRP5B*, which is cloned from the wild-type Landsberg *erecta* (Ler) DRP5B gene and has been shown to function properly in the Ler background (Gao et al., 2003).

DRP5B affects mitochondrial morphogenesis and division

In a parallel study, we introduced the mitochondrial marker (*Saccharomyces cerevisiae* Cytochrome C Oxidase IV-Yellow Fluorescent Protein, or COX4-YFP) into *drp5B* mutants to observe the functional role of DRP5B on mitochondrial morphogenesis and division. The mitochondrial marker was transformed into Ler and *drp5B-1* (*arc5*) using floral dipping method and introduced into *drp5B-2* by genetic crosses. The T₂ generation of the transgenic plants and homozygous *drp5B-2* mutants in the F₂ population of the crosses were subjected to microscopic imaging to examine mitochondrial morphology. As presented in Figure 3.2, the *drp5B* mutants exhibit extended tubular structures instead of the rod-shaped structures as seen in wild-type

plants (Col-0 and Ler). As the mitochondrial phenotype of *drp5B* resembles that of *drp3A-2* and *drp3B-2*, we speculate that DRP5B may be indirectly involved in mitochondrial division. Collectively, our results demonstrate that DRP5B has a role in maintaining the mitochondrial morphogenesis without being physically associated with the organelle. As mitochondria are highly dynamic organelles, the morphology of the organelle can be affected by internal or external cues. In the *drp5B* mutants, the enlarged chloroplasts may drastically change the intracellular architecture of the cells, resulting in changes in mitochondrial morphology. To test this hypothesis, it would be necessary to analyze the mitochondrial morphology in other plastid division mutants such as *arc6* (Robertson et al., 1995; Vitha et al., 2003) and *ftsZ* (Osteryoung et al., 1998; Yoder et al., 2007). Although our previous findings that the localization of YFP-DRP5B on peroxisomes was not affected in the *arc6* mutant seems to contradict to this theory (Zhang and Hu, 2010), we cannot exclude the possibility that the impact of chloroplast division defects is far more dramatic on mitochondria than on peroxisomes.

Analysis of the *drp3A-2 drp3B-2 drp5B-2* triple mutant

As DRP3A, DRP3B, and DRP5B have been demonstrated to play roles in the division or morphogenesis of peroxisomes and mitochondria, we tested the functional redundancy between these proteins. DRP3A and DRP3B have some overlapping functions in the division of peroxisomes and mitochondria. DRP3 single mutants exhibit different degrees of deficiency in peroxisomal and mitochondrial division, whereas *drp3A-2 drp3B-2* double mutants are severely defective in mitochondrial division by showing interconnected mitochondria in cells (Fujimoto et al., 2009). In addition to the

organelle phenotype, the double mutant also shows slow growth and a curly leaf phenotype (Fujimoto et al., 2009). Although the double mutant displays a pleiotropic phenotype, the plants are fertile and the organelles are still present in all cell types. This suggests that additional fission factors (other DRP proteins) or a DRP-independent machinery exist to maintain the basal level of organelle division.

To test the hypothesis that DRP5B is another fission factor in the same division machinery, in which DRP3A and DRP3B are functioning, we generated *drp3A-2 drp3B-2 drp5B-2* triple mutant in Col-0 background expressing the mitochondrial marker COX4-YFP. The triple mutant was generated by genetic crosses between the *drp* single mutant expressing the mitochondrial marker, and homozygous lines were identified by PCR of genomic DNA in the F₂ population of the crosses (Figure 3.3). The plant and mitochondrial morphologies of the triple mutant were compared with the wild-type Col-0 and the double mutants. As shown in Figure 3.4A, the triple mutant resembles the double mutant phenotype by displaying similar growth retardation and curly leaf phenotypes, suggesting that DRP5B does not play a significant role in plant growth and development. In terms of the organelle morphology, the triple mutant exhibits a massive elongation and aggregation of mitochondria as well as dumbbell-shaped chloroplasts (Figure 3.4B). As the double mutant also shows elongated and clumped peroxisomes (Zhang and Hu, 2009), we expect to observe the same peroxisomal phenotype in the triple mutant. To verify our prediction, the peroxisomal marker will be introduced into the triple mutant. Our data suggest that the function of DRP3A and DRP3B in regulating mitochondrial division is predominant compared with that of DRP5B, whereas DRP5B's major role is in the division of chloroplasts. However, the more dramatic organelle

phenotype suggests that DRP5B and DRP3 share certain overlapping function in the division of the organelles.

DRP5B lacks physical interaction with DRP3A and DRP3B in yeast two-hybrid assays

DRP proteins form a collar-like structure around the mitochondria division site via oligomerization of the protein (Ingerman et al., 2005). Consistent with this, DRP3A and DRP3B have been shown to be able to form homo- or heterodimeric complexes (Arimura et al., 2008; Fujimoto et al., 2009), suggesting that the two proteins might cooperatively function in the division of peroxisomes and mitochondria. To test whether DRP5B also functions together with DRP3A and DRP3B, we employed the yeast two-hybrid (Y2H) approach, as described in Chapter 2, to examine the physical interaction between the DRPs. Unlike DRP3A and DRP3B, neither self-interaction of DRP5B nor interaction between DRP5B and DRP3 was detected using the Y2H assays (Figure 3.5). These data are inconsistent with our previous finding, which showed the physical interactions between DRP5B and DRP3 in bimolecular fluorescence complementation BiFC and the ability for these proteins to form a complex using co-immunoprecipitation (Zhang and Hu, 2010). The results in this study can be explained in one or more way: (1) the association between DRP5B and DRP3 is transient or not strong enough to be detected using the Y2H assay, (2) an additional protein is required to bridge the interaction between DRP5B and DRP3, or (3) DRP5B is not targeted to the yeast nucleus, which is required for testing the interaction using the system, as the protein contain a putative lipid binding domain.

The fact that the triple mutant plants are viable and contain mitochondria in all cell types suggests that mitochondria still undergo division and are inherited to the daughter cells in these plants. This implies that there might exist a DRP-independent machinery in regulating organelle division or other DRP members can partially complement for the loss of DRP5B and DRP3. Evidence supporting the latter possibility is that DRP1C and DRP1E have been demonstrated to be involved in the division or morphogenesis of mitochondria (Jin et al., 2003). However, the relationship between the DRP1s, DRP3s, and DRP5B needs to be established. Comprehensive and systematic analyses of organelle morphologies in all the *drp* single and higher order mutants combined with physical interaction analyses between the proteins will provide us with a complete picture of the function of Arabidopsis DRP proteins in organelle fission.

Detection of endogenous DRP3A and DRP3B

To further dissect the peroxisomal and mitochondrial division machinery, it is important to characterize the relationship between DRP3A, DRP3B, and DRP5B. Because the expression of endogenous DRP3A and DRP3B has not been examined, we first analyzed the expression of the proteins in wild type and *drp* mutants. To this end, we generated DRP3A (α -DRP3A) and DRP3B (α -DRP3B) anti-peptide antibodies (Chapter 4, Figure 4.1). The presence of DRP3A and DRP3B in wild-type Col-0 and *drp* mutants was detected by using denatured gel immunoblot analysis with purified antibodies (see Methods). Using the α -DRP3A antibodies, we detected the endogenous DRP3A protein in Col-0, *drp3B-2*, and *drp5B-2* but not in *drp3A-2* (Figure 3.6), showing that the antibody is highly specific. Similarly, the endogenous DRP3B was detected by

α -DRP3B in Col-0, *drp3A-2*, and *drp5B-2*, whereas the corresponding band was missing in *drp3B-2* (Figure 3.6). These immuno blot assays showed that the peptide antibodies specifically recognized the cognate endogenous proteins. In addition, the absence of a functional DRP3 has no effect on the steady-state accumulation of DRP3A or DRP3B in Arabidopsis. Moreover, we also observed that DRP3A is expressed at a much higher level than DRP3B in two-week-old seedlings. Using the same experimental procedures, DRP3A was detected within a short exposure time, whereas DRP3B was detected only after longer exposure of the film (Figure 3.6). As the conclusion is reached based on the results using two different antibodies, which may have different binding efficiency, we used the same antibody (α -DRP3B or α -HA) to detect the overexpressed DRP3 in the transgenic plants. Similar results were obtained, showing that the expression of DRP3A is higher than that of DRP3B.

DRP3A is a major component of the DRP3A-DRP3B protein complex

As DRP3A and DRP3B have been shown to form homo- or heterodimeric complexes (Arimura et al., 2008; Fujimoto et al., 2009), we aimed to detect the presence of DRP3 protein complexes. To this end, we employed the blue native polyacrylamide gel electrophoresis (BN-PAGE) approach. As shown in Figure 3.7, DRP3A and DRP3B protein complexes were detected as ~1,000 KDa smear signals in Arabidopsis Col-0, suggesting that DRP3 forms a higher order protein complex. The lack of a major band might be due to the fact that DRP proteins form different degrees of multimeric structures. We next detected the presence of this protein complex in *drp3A-2*, *drp3B-2* and *drp5B-2* mutants. Using α -DRP3A, the same ~1,000-KDa protein

complex was detected in *drp3B-2* and *drp5B-2*. However, only a faint signal was detected at this size in *drp3A-2*, suggesting that DRP3A is an essential component of the DRP3A supercomplex (Figure 3.7). Akin to DRP3A, DRP3B is also required for forming the DRP3B-containing protein complex as only a weak signal of DRP3B protein complex was detected in *drp3B-2* (Figure 3.7). Interestingly, the level of the DRP3B protein complex is also largely decreased in *drp3A-2*, suggesting that DRP3A is a major component of the DRP3B complex. In *drp5B-2*, no differences in the level of DRP3A- or DRP3B complex compared to that of the wild type was observed (Figure 3.7). Consistent with our Y2H result, there is no change to the formation of DRP3A- and DRP3B-containing protein complexes in the *drp5B-2* mutant (Figure 3.7), suggesting that DRP5B may function through a DRP3A/DRP3B-independent machinery in regulating peroxisomal and mitochondrial division.

Together, we provide the first biochemical evidence showing the presence of DRP3A- and DRP3B-containing high-molecular-mass protein complexes in Arabidopsis (Figure 3.7). In addition, we demonstrated that DRP3A is a major component of the DRP3-containing protein complex, whereas DRP3B has no or minor affect on the formation of the DRP3A protein complex. The result further implies that DRP3A and DRP3B are present in the same protein complex, as *drp3A-2* mutant does not accumulate normal amount of DRP3B-containing protein complex (Figure 3.7). Consistent with the previous genetic evidence, our biochemical analyses further verify a critical role for DRP3A in the peroxisomal and mitochondrial division complex. In summary, genetic and biochemical analyses have demonstrated that DRP5B is also indirectly involved in the mitochondrial division and morphogenesis. As DRP5B does not

interact with DRP3 and is not a major component of the DRP3-containing complexes, we hypothesize that DRP5B acts through a DRP3A/DRP3B-independent machinery.

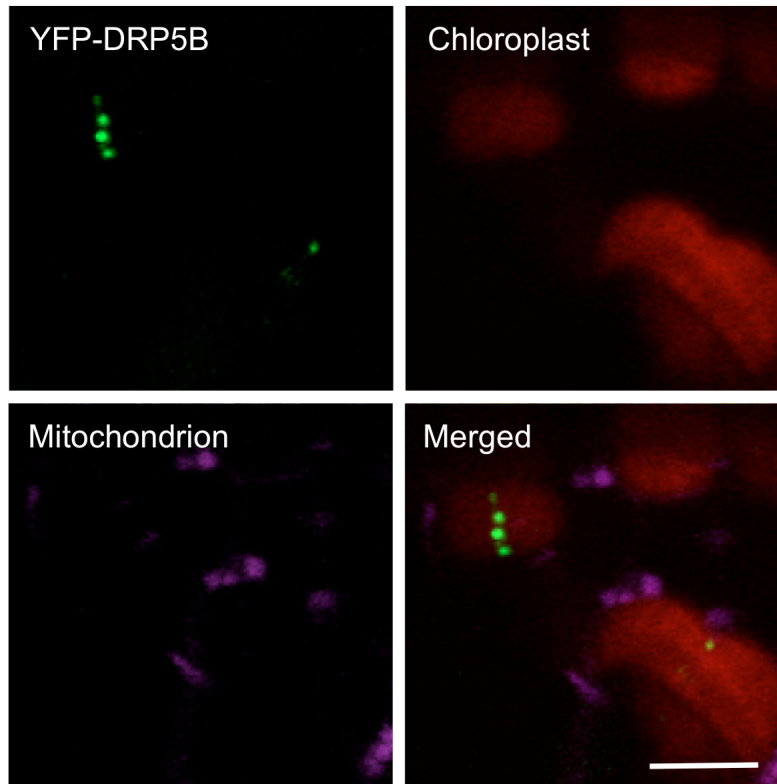


Figure 3.1. YFP-DRP5B is not targeted to mitochondria in Arabidopsis.

Confocal images were taken from leaf epidermal cells of transgenic Col-0 plants expressing $35S_{pro}:YFP-DRP5B$ together with the mitochondrial marker (COX4-CFP). YFP signals are in green, chloroplast signals generated by autofluorescence are in red, and CFP signals are in magenta. The images were taken at the same magnification; scale bar = 5 μm .

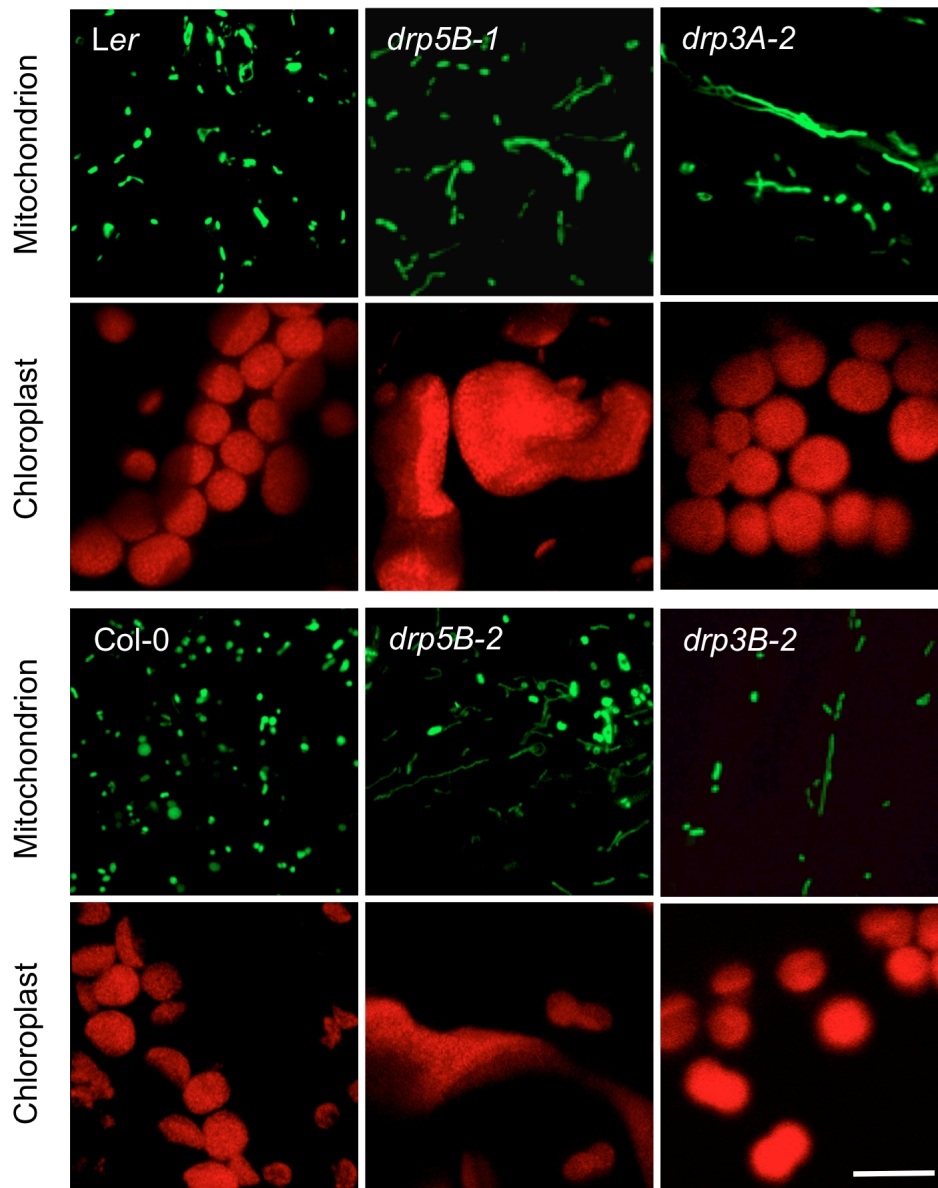


Figure 3.2. The *drp5B* mutants also exhibit defects in mitochondrial division.

Confocal images were taken from Arabidopsis leaf epidermal cells showing morphologies of mitochondria and chloroplasts. Mitochondria are labeled by COX4-YFP and chloroplast signals were generated by autofluorescence. The images were taken at the same magnification; scale bar = 10 μ m.

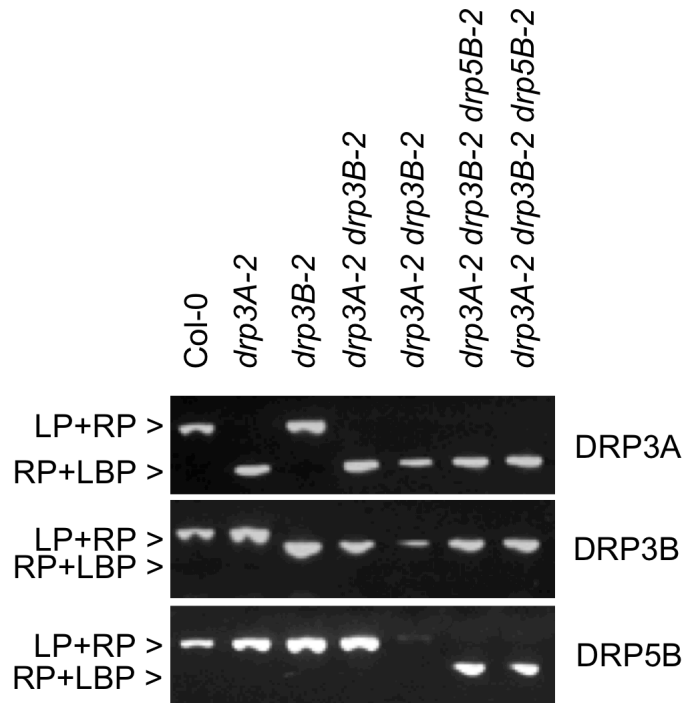


Figure 3.3. PCR genotyping of the *drp* mutants.

PCR reactions were performed using gene-specific primers together with or without a T-DNA specific primer as listed in Table 3.1. Genotype of two individual lines of the double and triple mutants is shown.

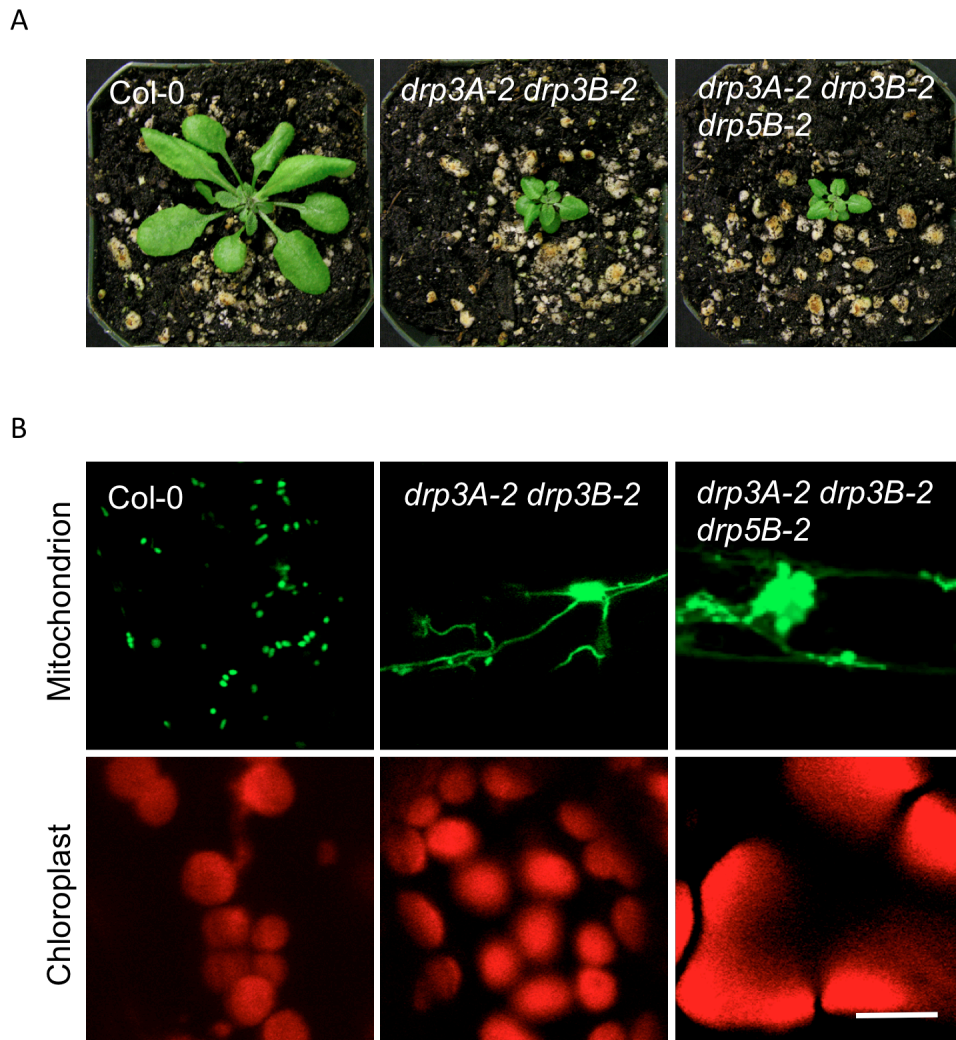


Figure 3.4. Phenotypes of the *drp* double and triple mutants.

(A) Four-week-old plants imaged under the same magnification.

(B) Confocal images from leaf epidermal cells illustrating the organelle morphologies.

Mitochondria are labeled by COX4-YFP and the chloroplast signals were generated by autofluorescence. The images were taken at the same magnification; scale bar = 10 μm .

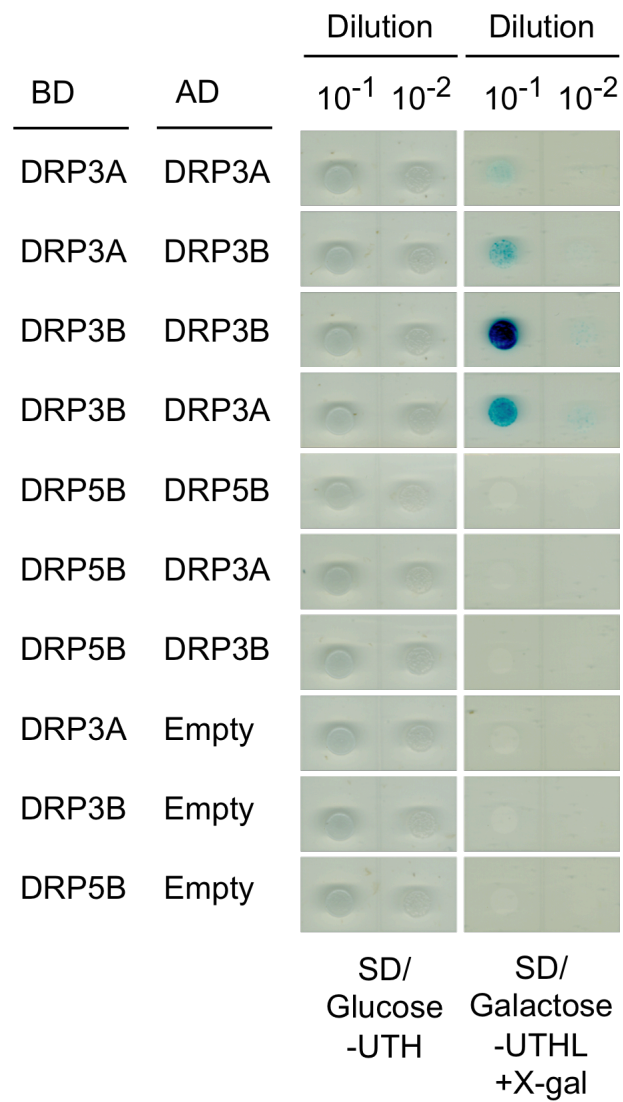


Figure 3.5. Yeast two-hybrid analysis to test interaction between DRP5B and DRP3 proteins.

SD-Glucose (-UTH) selects for transformants, and SD-Galactose (-UTHL) plus X-gal select for protein-protein interactions. Empty means the pB42AD-GW vector.

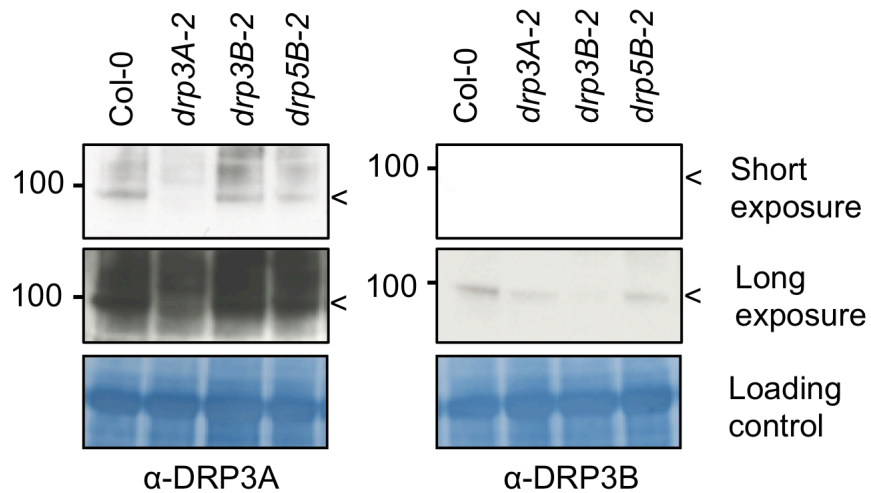


Figure 3.6. Expression of endogenous DRP3A and DRP3B in Arabidopsis.

SDS-PAGE analyses show the steady state expression level of native DRP3A and DRP3B in wild-type Col-0, *drp3A-2*, *drp3B-2*, and *drp5B-2*. α -DRP3A or α -DRP3B peptide antibody was used to detect the presence of the protein in Arabidopsis. The Rubisco large subunit was shown as a loading control. Numbers on the left indicate the molecular weight in kDa. Arrowheads mark the position of the expected DRP3A (89.7 kDa) and DRP3B (89.9 kDa) proteins.

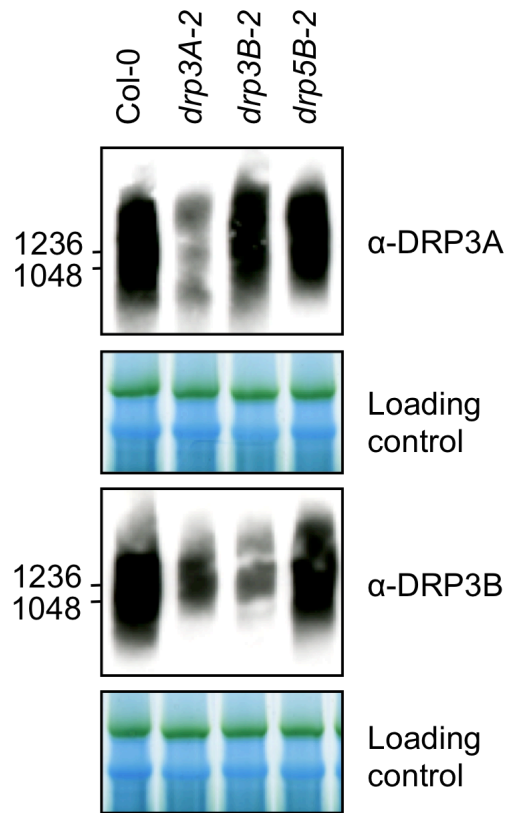


Figure 3.7. Detection of endogenous DRP3A and DRP3B-containing protein complex in Arabidopsis.

BN-PAGE analyses show the presence of DRP3A and DRP3B supercomplexes in wild-type Col-0, *drp3A-2*, *drp3B-2*, and *drp5B-2*. α -DRP3A or α -DRP3B peptide antibody was used to detect the presence of the protein complex. The photosystem I and photosystem II (PS1/PS2) core dimer (green band) was used as the loading control. Numbers indicate the molecular weight in kDa.

METHODS

Plant material, Growth conditions and Transformation

Arabidopsis thaliana plants were grown as described in Chapter 2. T-DNA insertion mutants, *drp3A-2* (SALK_147485), *drp3B-2* (SALK_112233), and *drp5B-2* (SAIL_71D_11), were obtained from the Arabidopsis Biological Recourse Center (ABRC; Columbus, OH, USA). *drp5B-1* (*arc5*) is a gift from Katherine Osteryoung (MSU). The presence of the T-DNAs and the homozygosity of the mutants were verified by the polymerase chain reaction (PCR) using genomic DNA as templates. *drp3A-2* was genotyped with the following primers: SALK_147485-LP (5'-AACCACAGGTTTACCTCCTGG-3') and SALK_147485-RP (5'-ACGCCTCCTTCTTCTTCTACG-3'). *drp3B-2* was genotyped with the following primers: SALK_112233-LP (5'-TAAAATGGCCTTCAGGAAAGG-3') and SALK_112233-RP (5'-TGAGGAGAGAAATAGCACCTTTG-3'). LBb1.3 (5'-ATTTTGCCGATTTTCGGAAC-3') was used to genotype the SALK mutants. *drp5B-2* was genotype with the following primers: SAIL_71D_11-LP (5'- TGTGTTGGATGCCCTTAAGAC-3'), SAIL_71D_11-RP (5'-TGTCACCTGATGAAGGAAAGG-3'), and SAIL_LB3 (5'-GCATCTGAATTCATAACCAATC-3'). All the T-DNA insertion mutants are in Col-0 background; *drp5B-1* is in *Ler* background. The mitochondrial marker COX4-YFP was introduced into *drp5B-2* by genetic crosses. Seedlings of the F₂ generation from the crosses were screened for homozygosity of the mutants using PCR and for presence of COX4-YFP using confocal microscopy. In addition, the mitochondrial marker was transformed into *drp5B-1* and *Ler* through floral dipping method as described previously (Chapter 2). The same floral dip transformation method was used to introduce

35S_{pro}:YFP-DRP5B into Arabidopsis Col-0 expressing the mitochondrial marker. T₁ seeds were grown on soil and screened for transgenic plants as described in Chapter 2. The selected plants were further confirmed for the expression of YFP-fusion proteins using epifluorescence microscopy and the expression of HA-tagged or un-tagged protein using immunoblot analysis as described below.

Gene Cloning and Plasmid Construction

First, full-length open reading frame of *DRP5B* was amplified from cDNA generated from total mRNA of Arabidopsis Col-0 seedling using the following primers, *DRP5B-attB1* (5'-ggggacaagttgtacaaaaaagcaggctcatggcggaagtatcagc-3') and *DRP5B-attB2* (5'-ggggaccactttgtacaagaaagctgggtgtcaatgctgcaccgaagg-3'). The amplified product was cloned using Gateway[®] system according to the manufacturer's instructions (Invitrogen) as described in Chapter 2. The destination vectors include: *pEarleyGate101* (CD3-683) for constructing *35S_{pro}:YFP-DRP5B*, and *pGilda-GW* or *pB42AD-GW* (Chapter 2) for generating bait and prey fusion proteins for yeast two-hybrid assays.

Microscopy analyses

All the confocal images were taken by a confocal laser scanning microscope (Zeiss LSM 510 META) as previously reported (Reumann et al., 2009).

Yeast two-hybrid assay

The Matchmaker two-hybrid system (Clontech) was used to test the homo- and heteromeric interactions between DRP5B and DRP3 as previously described (Chapter 2).

Immunoblot analysis

50 mg of fresh tissues were ground with a plastic pestle using liquid nitrogen with the addition of 500 μ l of SDS-containing extraction buffer (60 mM Tris-HCL pH 8.8, 2% SDS, 2.5% glycerol, 0.13 mM EDTA pH 8.0, and 1X protease inhibitor cocktail complete from Roche). The samples were vortexed for 30 seconds and heated at 70 °C for 10 minutes, followed by centrifugation at 13,000 xg twice (5 minutes each time) at room temperature. The supernatants were then transferred to new tubes. For SDS-PAGE analysis, 10 μ l of samples (5 μ l of the protein extracts and 5 μ l of 2x NuPAGE LDS sample buffer) was separated on 4-12% NuPAGE (Invitrogen) and blot to a PVDF membrane. The membrane was then blocked with 3% BSA in 1x TBST (50 mM Tris-base, 150 mM NaCL, 0.05% Tween 20, pH 8.0) overnight at 4°C, before being probed with the antibody prepared in the blocking buffer. DRP3A antibody (α -DRP3A: 489-RKRMDEVIGDFLREGLEP-506) and DRP3B antibody (α -DRP3B: 535-HPVARPDTVEPER-548) were designed and synthesized by Open Biosystems, Inc (Chapter 4, Figure 4.1). To clean up the sera, they were diluted to 1:400 in the blocking buffer and incubated with the PVDF membrane that contains total proteins transferred from *drp3A-2* or *drp3B-2* at 4°C overnight. The treated antibodies were used to probe the PVDF membrane containing transferred proteins of interest for 1 hour at room temperature. The membrane was rinsed three times (10 min/each time) with 1x TBST.

The rinsed membrane was then detected with a secondary antibody 1:20,000 goat anti-rabbit IgG and HRP-conjugate (Millipore) in 1x TBST. Signals were detected with 4x-diluted SuperSignal[®] West Dura Extended Duration Substrate (Pierce Biotechnology).

The membrane was exposed to a film to visualize the signals.

To perform blue-native polyacrylamide gel electrophoresis (BN-PAGE), 50 mg fresh weight of 2-week-old *Arabidopsis* seedlings was homogenized with pestle and liquid nitrogen. Total native proteins were isolated using NativePAGE[™] Sample Prep Kit according to instructions by the manufacturer (Invitrogen). Specifically, 100 μ l of 1x loading buffer containing 2% detergent (DDM) was added to the homogenized samples and the mixtures were incubated on ice for 30 minutes. The incubated samples were centrifuged at 17,000 xg two times (15 min/each time) at 4°C and the supernatants were transferred to new tubes. 2 μ l of 5% G-250 sample additive was added to 20 μ l of sample solution and the samples were separated on 4-12% NativePAGE[™] using 1x NativePAGE[™] Running Buffer and Cathode Buffer Additive. The gel was incubated with 2x NuPAGE[™] transfer buffer for 10 minutes before being transferred to the PVDF membrane, which was later subjected to immuno blot analysis as mentioned above.

ACKNOWLEDGEMENTS

We thank the ABRC (Columbus, OH, USA) for providing the T-DNA insertion mutants (*drp3A-2*, *drp3B-2*, and *drp5B-2*) and Kathy Osteryoung (MSU) for kindly providing *drpB5-1* (*arc5*) seeds and *DRP5B_{pro}:GFP-DRP5B* construct. We also thank

Melinda Frame (Center of Advance Microscopy, MSU) for the help with confocal microscope. This work was supported by grants from the National Science Foundation (MCB 0618335) and the Chemical Sciences, Geosciences and Biosciences Division, Office of Basic Energy Sciences, Office of Science, U.S. Department of Energy (DE-FG02-91ER20021) to J.H.

CHAPTER 4

Phosphorylation of DRP3A and DRP3B in regulating peroxisomal and mitochondrial division

ABSTRACT

A subset of Dynamin-Related Proteins (DRPs) function in the final fission process of organelle division and their functions are evolutionarily conserved across kingdoms. In Arabidopsis, DRP3A and DRP3B have been identified for their role in the division of peroxisomes and mitochondria, in which DRP3A is suggested to play the prominent role. DRP3A and DRP3B are phosphorylated at Ser575 and Ser560 according to the Arabidopsis Protein Phosphorylation Site Database. Genetic complementation assays showed that phospho-null DRP3A functions like the wild-type protein, whereas phospho-mimic DRP3A results in peroxisomal and mitochondrial division defects when ectopically expressed. In contrast, overexpression of DRP3B causes peroxisomal and mitochondrial division deficiencies in wild type and fails to complement the *drp3B-2* mutant phenotype. Our preliminary results also suggest that phosphorylation on DRP3A and DRP3B may alter their protein activity rather than subcellular targeting or formation of the protein complex. In summary, the function of DRP3 in peroxisomal and mitochondrial division is regulated by phosphorylation.

INTRODUCTION

Mitochondria and peroxisomes are ubiquitous organelles and play essential roles in almost all eukaryotic cells. Mitochondria are surrounded by a double membrane and believed to be a descendent of α -proteobacteria (Gray et al., 1999). In addition to the fundamental roles in eukaryotic cells as the primary source of energy, mitochondria are also important in intracellular signaling, cellular differentiation, program cell death, and several biotic and abiotic stresses (Chan, 2006; Millar et al., 2008; Palmer et al., 2011b). Peroxisomes, on the other hand, are delimited by a single membrane (Purdue and Lazarow, 2001), and believed to be originated from the Endoplasmic Reticulum (Hoepfner et al., 2005). Peroxisomes are well-known for their ability to degrade reactive oxygen species and metabolize fatty acid through β -oxidation (Schrader and Fahimi, 2008). In addition, plant peroxisomes have evolved several functions unique to plants (see Chapter 1). Peroxisome deficiencies have been demonstrated to cause plant growth and developmental defects (Fan et al., 2005; Kaur and Hu, 2009) and several human diseases (Fidaleo, 2010). Although peroxisomes and mitochondria are separated by their own membrane and house several organelle-specific biochemical reactions, the two organelles are cooperatively involved in a number of metabolic reactions in plants, such as photorespiration and fatty acid catabolism (Penfield et al., 2005; Baker et al., 2006; Peterhansel and Maurino, 2011).

Given their critical roles in eukaryotic organisms, peroxisomes and mitochondria are highly dynamic in response to both internal and external stimuli. Mitochondria undergo frequent fission and fusion (Benard and Karbowski, 2009), whereas peroxisomes are believed to regulate their population mainly through

division/proliferation process to maintain the cellular homeostasis (Fagarasanu et al., 2007). In addition, morphological changes of peroxisomes in response to environmental cues have been reported in Arabidopsis (Sinclair et al., 2009). Recent studies from yeast, mammals, and plants have uncovered that the division of peroxisomes and mitochondria is governed through the same set of conserved division complex, which is composed of Dynamin-Related Protein (DRP) and Fission1 (FIS1) (Fagarasanu et al., 2007; Kaur and Hu, 2009). DRP and FIS1 function together in the final fission process of the organelle division, with DRP as a molecular scissor and FIS1 as a membrane-bound receptor of DRP (see Chapter 1).

In Arabidopsis, several forward genetic screens for mutants containing abnormal peroxisomal morphologies have led to the identification of DRP3A as a major division factor of peroxisomes (Mano et al., 2004; Aung and Hu, 2009; Zhang and Hu, 2009) and mitochondria (Mano et al., 2004). In addition, reverse genetic studies also demonstrated the functional role of DRP3B, a close homolog of DRP3A, in the division of peroxisomes and mitochondria (Fujimoto et al., 2009; Zhang and Hu, 2009). As null mutants of *DRP3B* show only slightly elongated peroxisomal phenotypes, DRP3B is demonstrated to play a minor role in peroxisomal division (Fujimoto et al., 2009; Zhang and Hu, 2009). Although the single mutant of *DRP3A* or *DRP3B* has no major defects in plant growth and development, the *drp3A drp3B* double mutant exhibits pleiotropic phenotypes including retarded growth and curly leaves (Fujimoto et al., 2009). Despite showing several defects in plant growth and development, the double mutant is viable and all cell types in the mutant contain peroxisomes and mitochondria, suggesting that other DRP proteins might play a role in the division of the organelles. Consistent with

this, DRP5B (ARC5), which was previously characterized for its role in the division of chloroplasts (Gao et al., 2003), was shown to be an additional component of the peroxisomal division machinery (Zhang and Hu, 2010). In Chapter 3, we demonstrated that DRP5B is indirectly involved in maintaining mitochondrial division and morphogenesis through a DRP3-independent mechanism. Moreover, DRP1C and DRP1E have been implicated to be involved in the division or morphogenesis of mitochondria (Jin et al., 2003).

As a membrane constriction/scission protein, DRP should function on the outer surface of the organelles. However, only 3% of mammalian Drp1 is physically associated with mitochondria, as demonstrated by biochemical assays (Smirnova et al., 2001). Since most eukaryotic DRPs, including Drp1, DRP3A and DRP3B, do not contain a transmembrane domain (TMD) or lipid-binding domain, the peroxisomal or mitochondrial association of DRP is believed to be achieved through the assistance of membrane-bound receptors or cytosolic adaptor proteins. Among the DRP recruiters, FIS1 is postulated to function as a membrane bound receptor of DRP and present in almost all eukaryotic organisms. FIS1 is a C-terminal tailed-anchored protein (C-TA) with a tetratricopeptide repeat (TPR)-like protein-protein interacting domain at the N-terminus (Fagarasanu et al., 2007; Kaur and Hu, 2009). In yeast, Fis1p functions together with two WD-40 containing adaptor proteins, Mdv1p and Caf4p, in recruiting Dnm1p to the peroxisomal and mitochondrial division sites (Tieu and Nunnari, 2000; Motley et al., 2008; Nagotu et al., 2008). Although FIS1 was initially identified as the evolutionarily conserved factor in recruiting DRP to the organelle membrane, several FIS1-independent and lineage specific mechanisms have been recently revealed. In

mammals, mitochondrial fission factor 1 (Mff1) is a C-TA protein involved in peroxisomal and mitochondrial division (Gandre-Babbe and van der Bliet, 2008), in which Mff1 functions as membrane-bound receptor of Drp1 by directly recruiting the protein through physical interaction (Otera et al., 2010). In Arabidopsis, Elongated Mitochondria1 (ELM1) physically associates with DRP3s and is able to recruit DRP3A to the constriction sites of mitochondria in a FIS1 independent manner (Arimura et al., 2008). In addition to the recruiter proteins, the physical association and functions of mammalian Drp1 to the mitochondrial division sites is also modulated by post-translational modification such as phosphorylation (see Chapter 1).

Arabidopsis utilizes at least two DRP proteins, DRP3A and DRP3B, in peroxisomal and mitochondrial division. In this work, we aimed to further explore the regulatory mechanism that governs the function of these key components of the organelle division machinery. Here, we addressed the impact of post-translational modification, i.e., phosphorylation, on DRP3A and DRP3B. Our data showed that overexpression of phospho-mimic DRP3A (presumably DRP3B also) inhibits the division of peroxisomes and mitochondria, suggesting that de-phosphorylated DRP3A is the functional component of the division machinery. Unlike DRP3A, ectopic expression of DRP3B fails to rescue the *drp3B-2* phenotype and results in peroxisomal and mitochondrial division deficiencies in wild type Col-0. Phosphorylation of DRP3 does not affect the targeting of DRP3 to mitochondrial constriction sites, their ability to form homo- or hetero-dimers, or the formation of the DRP3A- and DRP3B-containing protein complex; thus, it may affect the activity of DRP3.

RESULT AND DISCUSSION

DRP3A and DRP3B might be post-translationally regulated by phosphorylation

Most organisms, such as yeast and mammals, utilize only one major DRP in regulating the division of both peroxisomes and mitochondria. In Arabidopsis, at least five members of the DRP superfamily (DRP1C, DRP1E, DRP3A, DRP3B, and DRP5B) have been suggested to play a role in maintaining the number and morphogenesis of mitochondria and/or peroxisomes; of them, DRP3A is suggested to play a major role (Mano et al., 2004; Aung and Hu, 2009; Zhang and Hu, 2009). The *drp3A* single mutants exhibit severe defects in peroxisomal and mitochondrial division (Mano et al., 2004; Aung and Hu, 2009; Zhang and Hu, 2009), and overexpression of DRP3A can rescue the *drp3A drp3B* double mutant phenotypes (Fujimoto et al., 2009). Given the central role of DRP3A in the division of peroxisomes and mitochondria, we were interested in understanding the regulation of DRP3A. We first focused on post-translational modification, as mammalian Drp1 was shown to be regulated by different post-translational modifications (Chang and Blackstone, 2010; Otera and Mihara, 2011). According to the Arabidopsis Protein Phosphorylation Site Database (<http://phosphat.mpimp-golm.mpg.de/>), DRP3A and DRP3B were experimentally identified to be phosphorylated between the DYN2 and GED domains at Ser575 and Ser560, respectively (Figure 4.1). To study the putative roles of these phosphorylation events in the division of peroxisomes and mitochondria, we introduced point mutations to DRP3A^{Ser575} and DRP3B^{Ser560}. The phosphorylation site, Serine residue (S), was mutated into Alanine residue (A) to abolish the phosphorylation and create a phospho-null mutant. In addition, Aspartic acid (D) or Glutamine acid (E) was used to replace the

Serine residue to confer constitutive phosphorylation and create a phospho-mimic mutant.

Phosphorylated DRP3s are unable to complement the mutant phenotype

To understand the functional role of the phosphorylation at DRP3A^{Ser575} and DRP3B^{Ser560}, we performed genetic complementation assays in *drp3A-2* or *drp3B-2*. Because the absence of functional DRP3A and DRP3B results in elongated mitochondria in Arabidopsis (Fujimoto et al., 2009), we used the mitochondrial phenotype as a marker to evaluate the complementation efficiency. For this purpose, wild type, phospho-null mutants, and phospho-mimic mutants, which were driven by the 35S promoter, were introduced into the *drp3* mutants expressing the mitochondrial marker COX4-YFP. Transgenic plants were first screened with the selection marker Basta, and then confirmed for the induction of the proteins by immunoblot assays using α -DRP3A or α -DRP3B. As shown in Figure 4.2A and Figure 4.2B, DRP3A and DRP3B are overexpressed in the transgenic plants. The overexpressors were then subjected to confocal imaging to observe the mitochondrial morphology. Similar to what was reported previously (Fujimoto et al., 2009), we observed full complementation of the *drp3A-2* mutant by ectopic expression of DRP3A, in which small and punctate forms of mitochondria are formed in the mutant (Figure 4.2C). In addition, overexpression of the phospho-null mutant (DRP3A^{S575A}) also efficiently rescued the *drp3A-2* mutant phenotype (Figure 4.2C), suggesting that the de-phosphorylated DRP3A is a functional protein. In contrast, ectopic expression of the phospho-mimic mutant proteins

(DRP3A^{S575E} and DRP3A^{S575D}) fails to complement the *drp3A-2* mutant phenotype, implying that these phospho-mimic DRP3A proteins are not functional (Figure 4.2C).

Similar to DRP3A, overexpression of phosphomimic DRP3B (DRP3B^{S560E} and DRP3B^{S560D}) cannot rescue the *drp3B-2* phenotype, either (Figure 4.2D). In contrast to DRP3A, wild-type DRP3B and phospho-null mutant (DRP3B^{S560A}) fail to complement the mitochondrial phenotype of *drp3B-2* (Figure 4.2D). This finding is consistent with the previous report that overexpression of DRP3B fails to complement the peroxisomal phenotype of the *drp3A drp3B* double mutant, but instead induces peroxisomal elongation in the double mutant (Fujimoto et al., 2009).

Overexpression of DRP3B results in incomplete fission of peroxisomes and mitochondria

As DRP3B was unable to complement the *drp3B-2* phenotype, we overexpressed DRP3A and 3B in wild-type Col-0 expressing the peroxisomal marker CFP-PTS1 and the mitochondrial marker COX4-YFP to observe the effect on peroxisomal and mitochondrial morphologies. Immunoblot analysis with α -DRP3B, which cross-reacts with the overexpressed DRP3A in Arabidopsis, showed the overexpression of the proteins (Figure 4.3). Although both DRP3A and DRP3B are highly expressed in the transgenic plants compared to that of wild type, DRP3A accumulated at a much higher level than that of DRP3B (Figure 4.3). At least five independent transgenic plants per genotype were examined using confocal microscopy. As shown in Figure 4.4, overexpression of DRP3A has no major impact on peroxisomal

and mitochondrial morphologies (Figure 4.4), whereas plants expressing $35S_{pro}:DRP3B$ showed deficiency in peroxisomal and mitochondrial division (Figure 4.4). Our genetic evidence in this study together with the finding in Fujimoto et al., (2009) suggest that overexpression of DRP3B negatively affect the division of peroxisomes and mitochondria.

As DRP3B has been demonstrated to be a minor component of DRP3A-protein complex *in vivo* (Chapter 3, Figure 3.7), we speculate that DRP3B functions in the same complex with DRP3A in regulating the division of peroxisomes and mitochondria. When the minor component DRP3B is overexpressed, the DRP3-containing complex is disrupted, thus inhibiting the division process. Hence, we hypothesize that overexpression of DRP3B disrupts the proper ratio between DRP3A and DRP3B, resulting in inhibition of peroxisomal and mitochondrial division. Consistent with this hypothesis, manipulating the expression level of the chloroplast division proteins, FtsZ1 and FtsZ2, disrupted the functional chloroplast division complex (Schmitz et al., 2009). To test this hypothesis, *in vitro* assembly of DRP3A and DRP3B on artificial liposomes may be necessary. Careful manipulation of DRP3B levels in Arabidopsis would also be necessary to observe organelle morphological changes resulting from variations of the DRP3B/DRP3A ratio.

Overexpression of phospho-mimic DRP3A and DRP3B results in incomplete fission of peroxisomes and mitochondria

To study the functional role of DRP3 phosphorylation in organelle division, we overexpressed DRP3 variants in wild type Col-0 containing the peroxisomal marker

(CFP-PTS1) and the mitochondrial marker (COX4-YFP). Similar to results from the genetic complementation assays, ectopic expression of wild-type DRP3A or phospho-null DRP3A (DRP3A^{S575A}) has no or minor effect on the morphology of peroxisomes and mitochondria. However, overexpression of phospho-mimic DRP3 (DRP3A^{S575E} and DRP3A^{S575D}) caused an incomplete fission of both organelles (Figure 4.4), suggesting that expression of the phospho-mimic DRP3A inhibits the division of the organelles. Similar to *35S_{pro}:DRP3B*, overexpression of the DRP3B phospho-null or phospho-mimic mutants also showed defects in the division of peroxisomes and mitochondria (Figure 4.4). Although we speculate that the overexpression of DRP3B phospho-mimic mutants causes dominant negative effects, it is difficult to draw a conclusion as overexpression of wild-type DRP3B already exhibits the peroxisomal and mitochondrial division deficiencies. Together, our data pointed toward the conclusion that phosphorylated DRP3A, and probably DRP3B as well, is an inactive form, and overexpression of the inactive form results in a dominant negative effect on the division of peroxisomes and mitochondria.

Together, our genetic complementation assay and ectopic expression of DRP3 suggest that de-phosphorylated DRP3A is the functional molecule. The effects on organelle morphologies upon overexpression of point-mutated proteins should be the consequences of changes in the phosphorylation of the amino acid rather than disruption of the protein structure. This hypothesis is supported by the fact that phospho-null mutant of DRP3A functions like wild type, and two independent phospho-mimic mutants give rise to the same effect on peroxisomal and mitochondrial

morphology.

Phosphorylation site mutations do not affect proper targeting of the YFP-DRP3 fusion proteins to the constriction sites of peroxisomes or mitochondria

In mammalian cells, sub-organeller targeting of Drp1 has been shown to be controlled by phosphorylation/de-phosphorylation of the protein (Cereghetti et al., 2008; Han et al., 2008). We thus sought to study whether phosphorylation on DRP3A and DRP3B influences the sub-organeller targeting of the proteins. To this end, yellow fluorescent protein (YFP) was fused to the N-terminus of DRP3 to create the fusion proteins, which were driven by the 35S promoter. The fusion proteins were expressed in Arabidopsis plants expressing the mitochondrial marker COX4-CFP to test the mitochondrial association. Epidermal cells of T₃ transgenic Arabidopsis were subjected to confocal imaging. As shown in Figure 4.5, all the tested YFP-fusion proteins (shown in green) were associated at the ends or the constriction sites of mitochondria (shown in magenta). Similar to the mitochondrial association, all the tested fusion proteins are also targeted to the peroxisomal division sites (Figure 4.5). Collectively, our data demonstrated that the peroxisomal and mitochondrial targeting of DRP3A and DRP3B is not affected by the phosphorylation at Ser575 on DRP3A or Ser560 on DRP3B.

Phosphorylation site mutations do not affect the protein-protein interactions between DRP3A and DRP3B

DRP3A and DRP3B contain the middle domain (DYN2), which is suggested to induce self-oligomerization of DRP. In line with this, the homo- and hetero-dimerization

of DRP3A and DRP3B have been demonstrated (Arimura et al., 2008; Fujimoto et al., 2009). Although the phosphorylation sites of DRP3A and DRP3B do not reside within DYN2, we tested whether the phosphorylation affects the protein-protein interaction between DRP3s using the yeast two-hybrid approach as mentioned in Chapter 2 (Y2H; Matchmaker LexA). As reported previously, we were able to verify the homo- or hetero-dimerization between DRP3A and DRP3B, shown as the robust growth of blue colonies on the induction medium (-HULT+ β -gal) (Figure 4.6). Similar to the wild type DRP3, all the tested DRP3 variants were able to interact with DRP3A or DRP3B (Figure 4.6), indicating that the phosphorylation has no effect on the formation of DRP3-containing protein complexes.

We further tested whether the phosphorylation impacts the formation of DRP3-containing protein complexes. To detect the protein complex, we first generated Arabidopsis transgenic plants overexpressing haemagglutinin (HA)-DRP3 fusion proteins in Col-0 background. Proteins from T₃ plants were subjected to immunoblots using the HA antibody to detect the expression of the transgenes. As shown in Figure 4.7A, the proteins are highly accumulated in the transgenic plants. We next employed the blue native gel electrophoresis method (BN-PAGE) as described in Chapter 3 to detect the DRP3 protein complexes using HA antibody. Similar to wild-type DRP3A and DRP3B, all the phospho-null and -mimic mutants are able to form the supercomplexes (Figure 4.7B). The presence of Peroxin11d (PEX11d) protein complex was used as an internal control (Figure 4.7C). Our yeast two-hybrid assays and protein complex analysis together demonstrated that phosphorylation at DRP3A^{S575} or DRP3B^{S560} has

no discernible effect on homo- or heterodimerization between the proteins and the assembly of the DRP3-containing protein complexes.

In summary, we propose that phosphorylation on DRP3A^{Ser575}, probably also DRP3B^{Ser560}, negatively regulates the function or activity of the proteins in organelle division. Although our studies have established that phosphorylation of DRP3A or DRP3B at Ser575 or Ser560 plays a significant role in regulating the function of DRP3, the molecular consequence of this modification hasn't been identified yet. To date, our data have suggested that this phosphorylation event (1) does not affect the organelle targeting of DRP3A and DRP3B, (2) does not interrupt the formation of homo- or heterodimerization between DRP3A and DRP3B, and (3) does not disrupt the formation of the DRP3-containing protein complex.

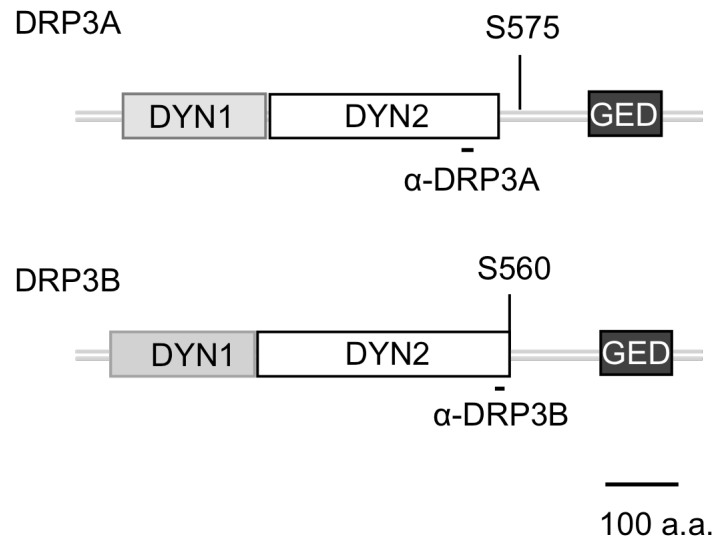


Figure 4.1. Protein structure of DRP3A and DRP3B.

Phosphorylation sites on DRP3A (Ser575) and DRP3B (Ser560) are marked. The region utilized to generate the peptide antibodies was indicated (α -DRP3A and α -DRP3B). DNY1: dynamin 1 (dynamin GTPase domain). DYN2: dynamin 2 (dynamin central region). GED: dynamin GTPase effector domain.

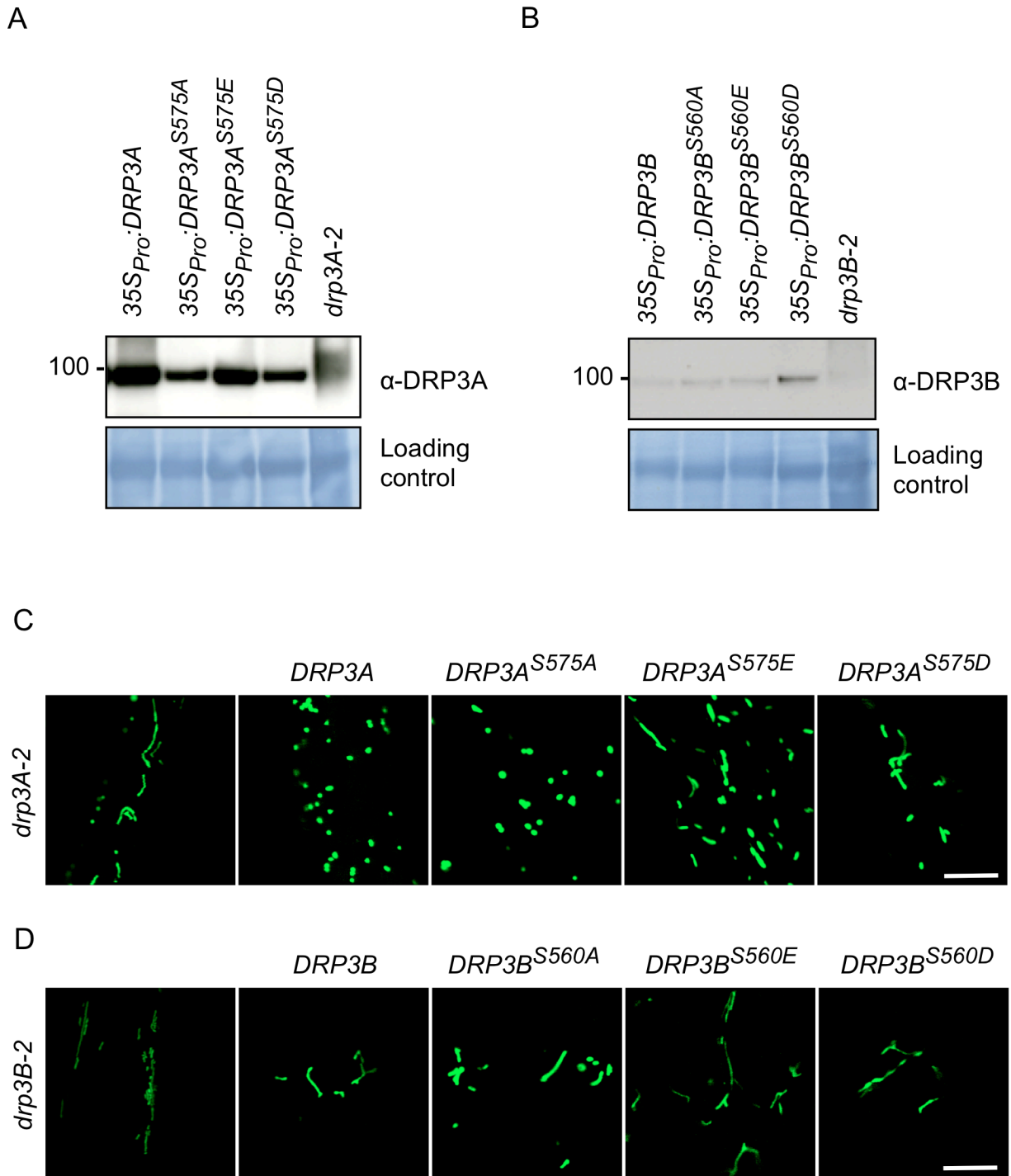


Figure 4.2.

Figure 4.2 (cont'd)

Figure 4.2. Complementation of *drp3* mutants using wild-type DRP3 and phospho-mutants of DRP3.

(A) and (B) Immunoblot analysis was employed to detect the expression of DRP3A and DRP3B using α -DRP3A or α -DRP3B antibody. The Rubisco large subunit was shown as a loading control. Numbers indicate the molecular weight in kDa.

(C) and (D) Confocal images showed the mitochondrial morphology in the transgenic plants overexpressing DRP3A and DRP3B. Mitochondria were labeled with COX4-YFP. Images were taken at the same magnification; scale bar = 10 μ m.

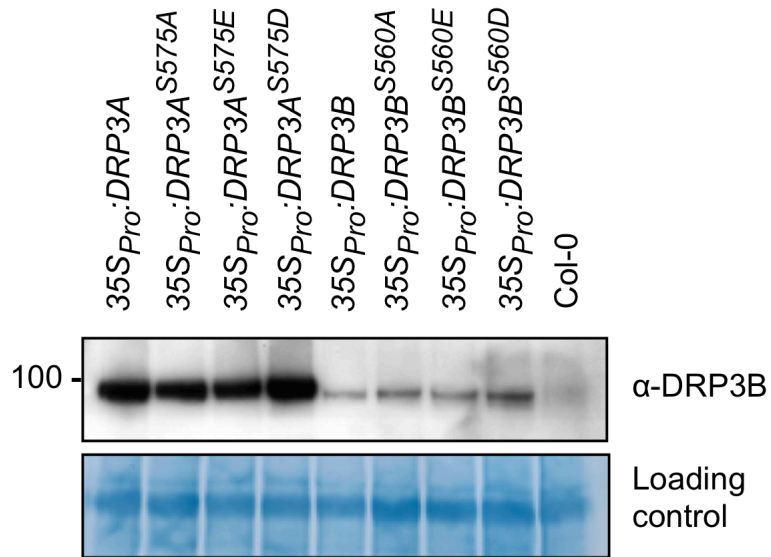


Figure 4.3. Immunoblot analysis of overexpressed DRP3 variants in Arabidopsis.

The overexpressed DRP3 and their variants are detected by α -DRP3B. The Rubisco large subunit is shown as a loading control. 100 indicates the molecular weight in kDa.

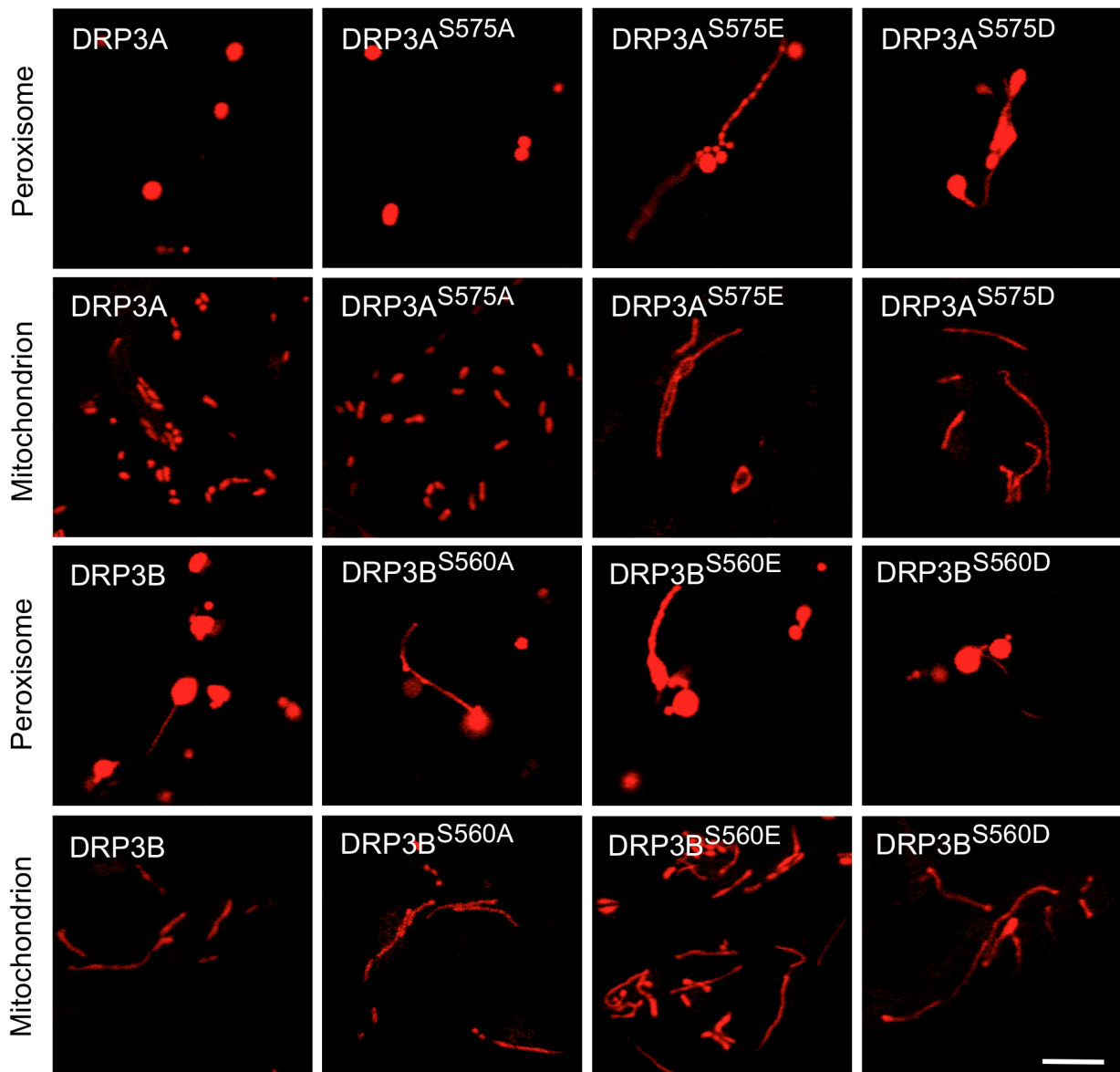


Figure 4.4. Peroxisomal and mitochondrial morphology in DRP3-overexpressors.

Confocal images were taken from epidermal cells of transgenic plants overexpressing DRP3 variants in *Arabidopsis* expressing the organelle markers. Peroxisomes were labeled with CFP-PTS1 and mitochondria were marked with COX4-CFP. Images were taken at the same magnification; scale bar = 5 μm .

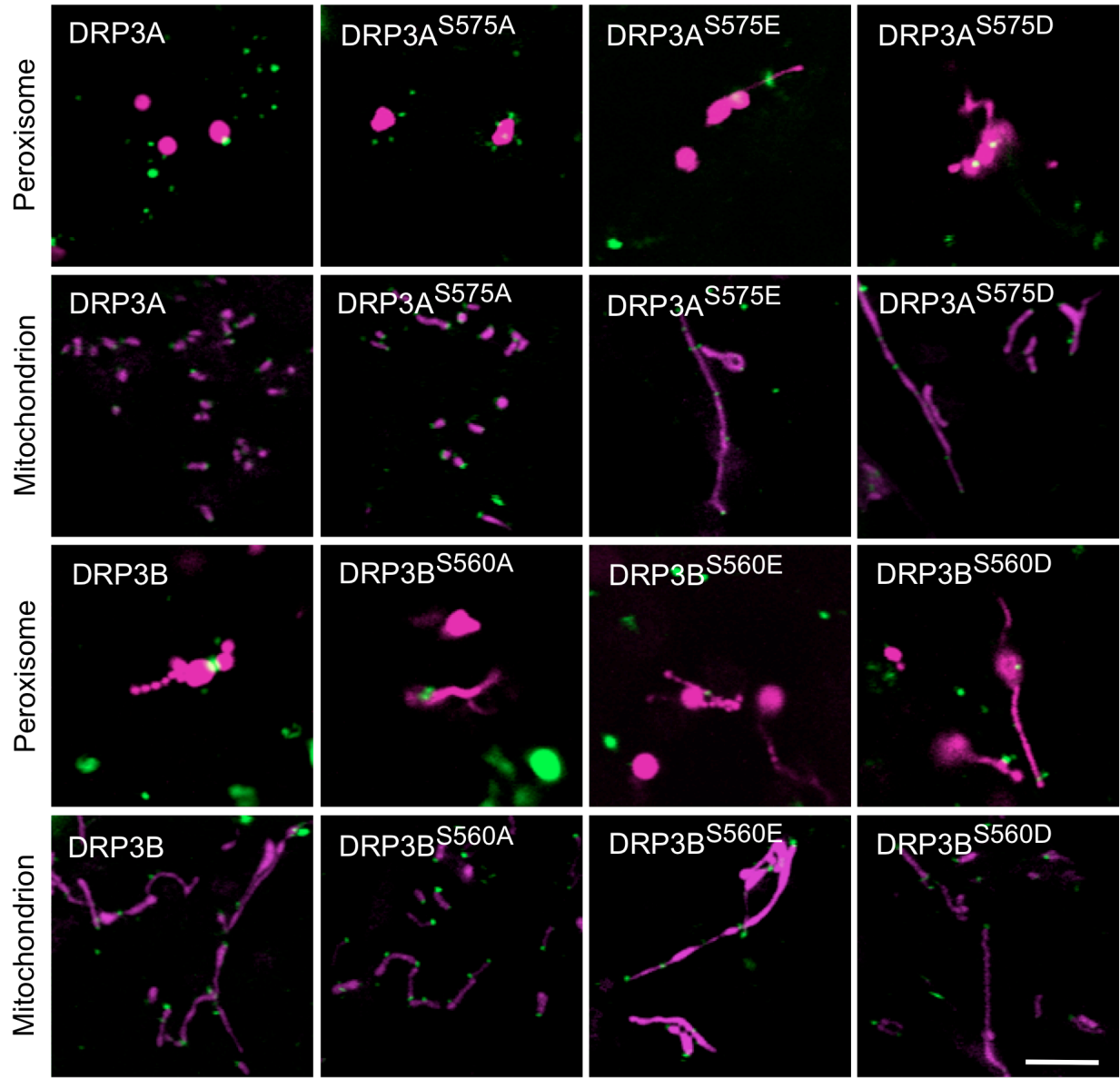


Figure 4.5

Figure 4.5 (cont'd)

Figure 4.5. Peroxisomal and mitochondrial targeting of YFP-DRP3 variants.

Epidermal cells from two-week-old seedlings of *Arabidopsis* expressing YFP-DRP3 variants were imaged for their organelle targeting using confocal microscopy. Peroxisomes and mitochondria were labeled with the peroxisomal marker CFP-PTS1 or the mitochondrial marker COX4-CFP, which are shown in magenta, and YFP signals are shown in green. Images were taken at the same magnification; scale bar = 5 μm .

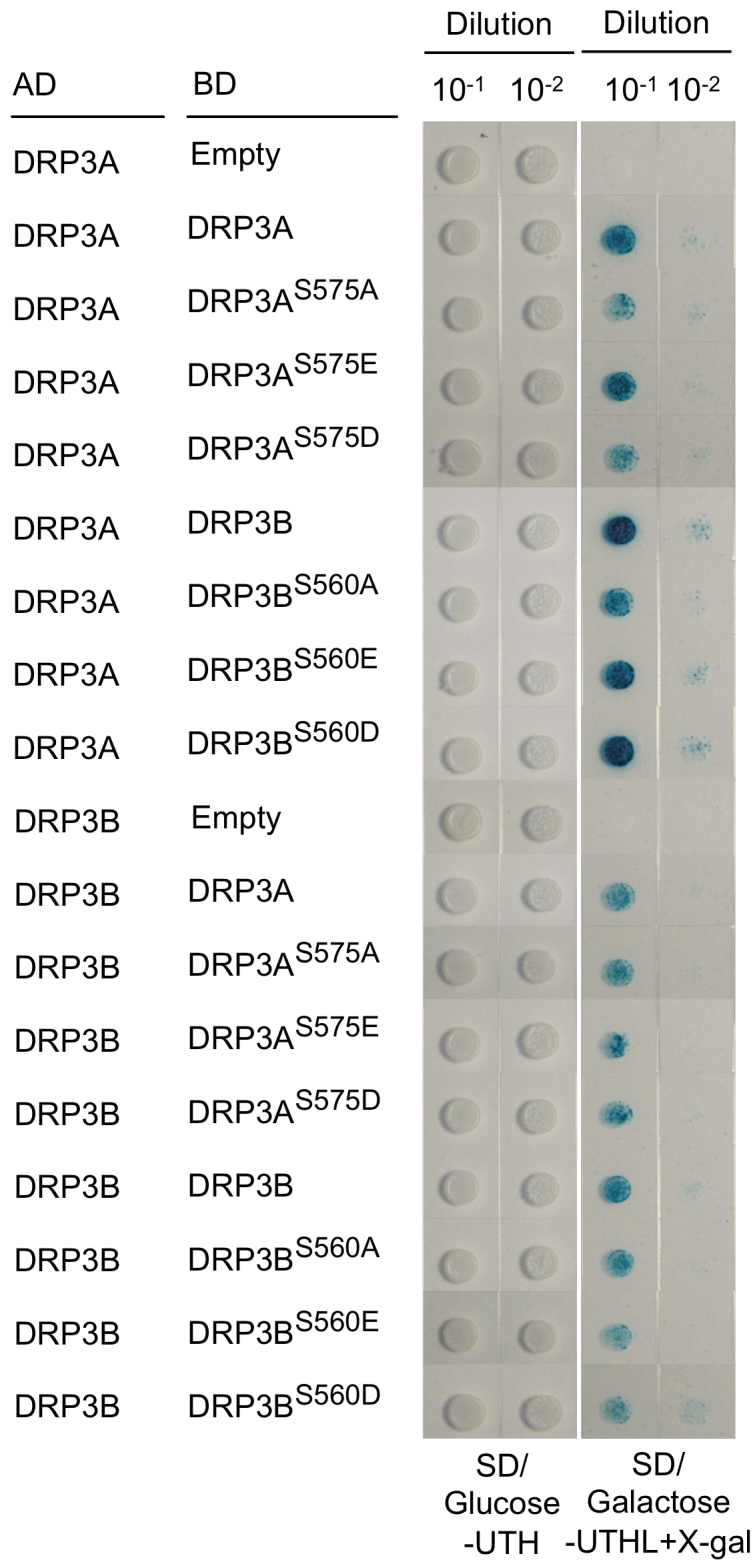


Figure 4.6

Figure 4.6 (cont'd)

Figure 4.6. Yeast two-hybrid analyses for interactions between the wild-type and mutant DRP3A or DRP3B. SD-Glucose (-UTH) screens for transformants and SD-Galactose (-UTHL) with X-gal select for protein-protein interactions. Empty, pGilda-Gw vector only.

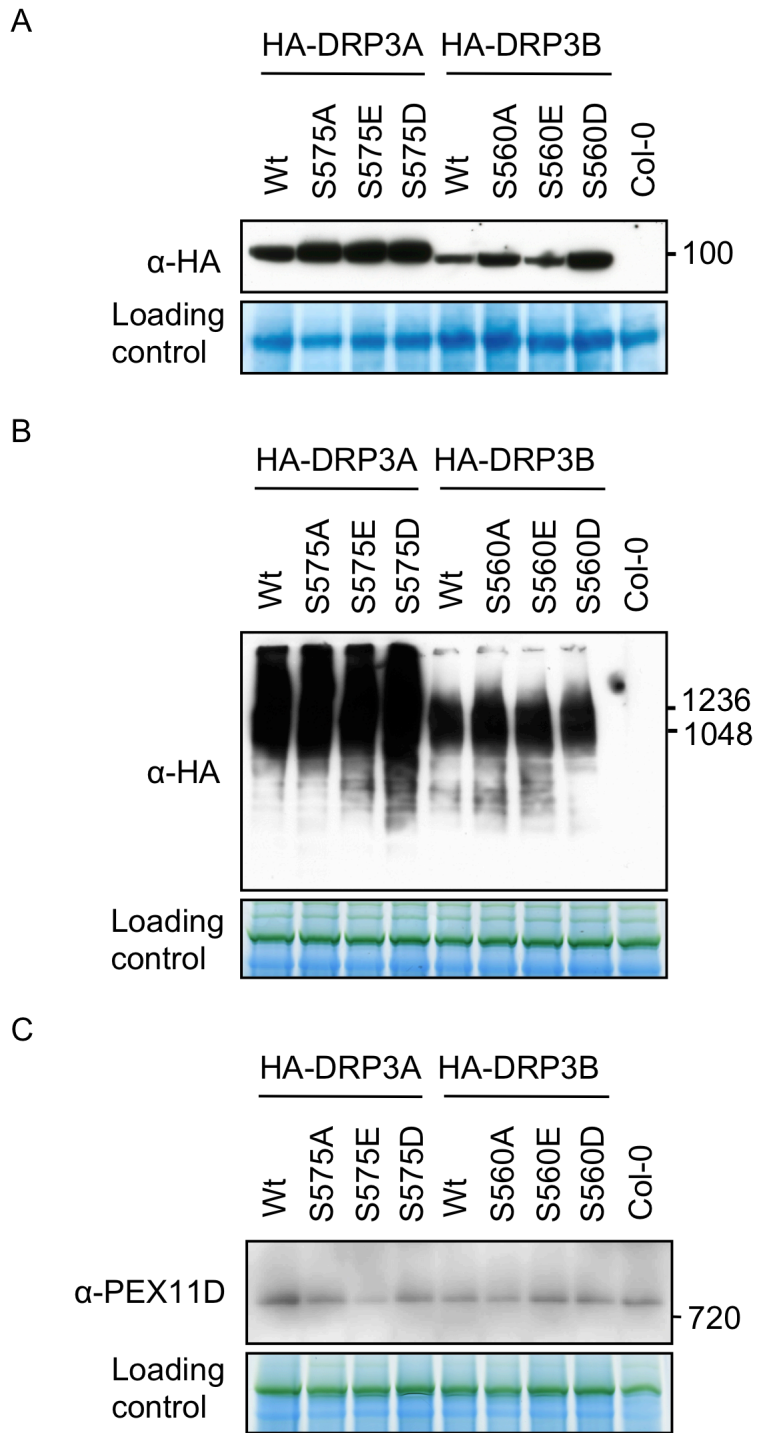


Figure 4.7

Figure 4.7 (cont'd)

Figure 4.7. Immunoblot analysis to detect the formation of the DRP3 protein complex in transgenic plants expressing HA-DRP3.

(A) SDS-PAGE analysis to detect expression of the HA-fusion proteins using the HA antibody. Col-0 was shown as a non-transgenic control plant. The Rubisco large subunit was used as the loading control.

(B) BN-PAGE analysis showing the presence of DRP3A- or DRP3B-containing protein complex in the transgenic plants. HA antibody was used to detect the protein complex.

(C) BN-PAGE analysis showing the presence of PEX11d protein complex in the transgenic plants and wild type Col-0 using α -PEX11d.

The photosystem I and photosystem II (PS1/PS2) core dimer (green band) was used as the loading control in (B) and (C). Numbers indicate the molecular weight in kDa.

Table 4.1. DNA primers used in this study.

Primer	Sequence (5'-3')
YFP:DRP3A-attB1	ggggacaagttgtacaaaaagcaggctcatgactattgaagaagttccg
YFP:DRP3A-attB2	ggggaccactttgtacaagaaagctgggtcttagaatccgtatccatttggtg
YFP:DRP3B-attB1	ggggacaagttgtacaaaaagcaggctcatgtccgtcgacgatctccc
YFP:DRP3B-attB2	ggggaccactttgtacaagaaagctgggtcttacatgaagccgtccgttc
DRP3A-S575A-Fw	gaaatctagagcgtttctcggcagg
DRP3A-S575A-Rev	cctgccgagaaacgctctagatttc
DRP3A-S575E-Fw	gaaatctagagagtttctcggcagg
DRP3A-S575E-Rev	cctgccgagaaactctctagatttc
DRP3A-S575D-Fw	gaaatctagagattttctcggcagg
DRP3A-S575D-Rev	cctgccgagaaaatctctagatttc
DRP3B-S560A-Fw	caaataaaaacccgagcttttctcggccg
DRP3B-S560A-Rev	cggccgagaaaagctcgggtttttatttg
DRP3B-S560E-Fw	caaataaaaacccgagagtttctcggcc
DRP3B-S560E-Rev	ggccgagaaactctcgggtttttatttg
DRP3B-S560D-Fw	caaataaaaacccgagattttctcggcc
DRP3B-S560D-Rev	ggccgagaaaatctcgggtttttatttg

METHODS

Plant material, Growth conditions and Transformation

Arabidopsis thaliana plants were grown as described in Chapter 2. The same floral dip transformation method described in Chapter 2 was used to generate transgenic plants expressing $35S_{pro}:DRP3s$, $35S_{pro}:YFP-DRP3s$, and $35S_{pro}:HA-DRP3s$ in *Arabidopsis* Col-0 or *drp3* mutants expressing the peroxisomal marker and/or the mitochondrial marker. The selected plants were further confirmed for the expression of YFP-fusion proteins using epifluorescence microscopy and the expression of HA-tagged or un-tagged protein using immunoblot analysis as described in Chapter 3.

Gene Cloning and Plasmid Construction

All the constructs were generated using Gateway[®] system according to the manufacturer's instructions (Invitrogen). First, full-length open reading frames of *DRP3A* and *DRP3B* were amplified from cDNA generated from total mRNA of *Arabidopsis* Col-0 seedling using Phusion High-Fidelity DNA polymerase (New England Biolabs). Site-directed mutagenesis of the phosphorylation site was performed as mentioned in Chapter 2. The primers used in this study were listed in Table 4.1. The amplified products were first subjected to BP-recombination with the donor vector (pDonorTM 207) to create an Entry clone. The resulting plasmids were shuttled into different destination for generation of expression clones. The destination vectors include: pEarleyGate100 (CD3-724) for creating $35S_{pro}:DRP3$ clones, pEarleyGate101 (CD3-683) for constructing $35S_{pro}:YFP-DRP3$, pEarleyGate201 (CD3-687) for making $35S_{pro}:HA-$

DRP3 clones, and pGilda-GW or pB42AD-GW (Chapter 2) for generating bait and prey fusion proteins for yeast two-hybrid assays.

Microscopy analyses

All the confocal images were taken by a confocal laser scanning microscope (Zeiss LSM 510 META) as previously described (Reumann et al., 2009).

Immunoblot analysis

Total denatured proteins or total native proteins were separated on SDS-PAGE or BN-PAGE, respectively, and the same immunoblotting approach described in Chapter 3 was adopted to detect the protein expression.

Yeast two-hybrid assay

The Matchmaker two-hybrid system (Clontech) was used to test the homo- and heteromeric interactions between *DRP5B* and *DRP3* as previously described (Chapter 2).

CHAPTER 5

Metabolic Regulation of Peroxisomal and Mitochondrial Morphogenesis in Arabidopsis

ABSTRACT

In eukaryotic cells, ATP is an essential molecule and used as a source of chemical energy for several metabolic processes in membrane-bound organelles. As a major site of ATP regeneration, mitochondrion exports ATP into the cytosol through ADP/ATP carriers such as AAC. In Arabidopsis, although three members of the AAC family (AtAAC1-3) are predicted to be inner mitochondrial membrane proteins, we repeatedly identified AtAAC1 in the peroxisomal proteome of Arabidopsis. Using fluorescent microscopy, AtAAC1-YFP was found on the surface of mitochondria and peroxisomes, suggesting that AtAAC1 is dual targeted to those two organelles. *AtAAC1* is highly expressed in almost all tissue types. The Arabidopsis loss-of-function mutants *aac1-1* and *aac1-2* exhibit several defects in plant growth and development and abnormal peroxisomal as well as mitochondrial morphology. We thus hypothesized that metabolic status within peroxisomes and mitochondria affects the morphogenesis of the organelles. In line with the hypothesis, Arabidopsis mutant lacking the peroxisomal NAD^+ carrier PXN contains giant peroxisomes. Collectively, our data suggest that metabolic homeostasis within organelles is not only critical for plant growth and development but also involved in maintaining morphogenesis of organelles.

INTRODUCTION

In eukaryotic cells, adenine nucleotide (ATP)-dependent biochemical reactions are housed within membrane-bound organelles. Although ATP can be produced in the cytosol and chloroplast in plants, the mitochondrion is the major site to regenerate the ATP (Haferkamp et al., 2011). To maintain the proper function of the biochemical factories within cells, ATP is exported from the generating sites and imported into the consuming sites, including chloroplasts, peroxisomes, endoplasmic reticulum, and Golgi, with the assistance of carrier proteins on membranes (Haferkamp et al., 2011; Traba et al., 2011).

Recent searches for mitochondrial carrier family (MCF) members in various genomes have identified 35, 50, and 58 putative mitochondrial carrier family (MCF) proteins in *Saccharomyces cerevisiae*, human, and *Arabidopsis* respectively (Picault et al., 2004). The 58 members of the *Arabidopsis* MCF include ADP/ATP carriers (AAC), basic amino acid carriers (BAC), carnitine carriers (CAC), dicarboxylate carriers (DIC), dicarboxylate-tricarboxylate carriers (DTC), phosphate carriers, succinate-fumarate carriers, uncoupling proteins (UCP), and unknown transporters (Picault et al., 2004). Although all the carriers are primarily categorized as mitochondrial carriers, many of them have been demonstrated to play roles on the membrane of other organelles, including plastids (Reiser et al., 2004), peroxisomes (Arai et al., 2008; Linka et al., 2008), and endoplasmic reticulum (ER) (Picault et al., 2004).

As the major site of ATP regeneration, mitochondria contain several ADP/ATP transporters (AAC) that function as mitochondrial ATP-ADP exchangers (Klingenberg, 2008; Traba et al., 2011). AAC proteins reside in the inner membrane of mitochondria

and function as ATP/ADP-antiporters, in which ATP and ADP are exchanged in 1:1 stoichiometry (Haferkamp et al., 2002). AAC imports cytosolic ADP into mitochondria and pumps out ATP into the cytosol. The cytosolic ATP is subsequently translocated into different cellular compartments (Klingenberg, 2008). Arabidopsis contains three AAC proteins (AtAAC1-3), sharing more than 70% amino acid sequence identity to one another (Traba et al., 2011). All three AtAACs contain predicted N-terminal mitochondrial targeting sequences, which have been suggested to be important for efficient insertion of the proteins into the inner mitochondrial membrane (Murcha et al., 2005). The ATP/ADP exchange activity of AtAACs has been demonstrated in *E. coli* where these transporters are integrated in the bacterial membrane (Haferkamp et al., 2002). Although AtAACs are suggested to be mitochondrial ADP/ATP antiporters, subcellular localization in vivo and molecular evidence for the importance of these proteins has not yet been reported.

The cytosolic ATPs exported from mitochondria are redistributed into different cellular compartments through an active uptake across the organelle membranes. Recent studies on Arabidopsis and other plants identified several ADP/ATP carriers that serve as importers for ATP on organelles other than mitochondria. In Arabidopsis, two plastidic ADP/ATP transporters (AtNTT1 and AtNTT2) were shown to catalyze the ATP/ADP exchange reaction upon heterologous expression in *E. coli* (Mohlmann et al., 1998; Tjaden et al., 1998). In addition to plastid transporters, an Arabidopsis ER ADP/ATP carrier (ER-ANT1) was recently shown to catalyze the ATP/ADP exchange reaction and import ATP into the ER lumen. Given that several metabolic reactions within the ER require ATP, the absence of the functional ER-ANT1 leads to several

physiological defects in plant growth and development (Leroch et al., 2008).

Peroxisomal adenine nucleotide transporter was first identified from *S. cerevisiae* (Palmieri et al., 2001). The yeast peroxisomal adenine nucleotide transporter ANT1p can actively counterexchange ATP with ADP or AMP upon reconstitution into liposomes. The *ant1p* mutant fails to grow on media that contain medium-chain fatty acids as the sole carbon source, because peroxisomal activity is required to break down these fatty acids (Palmieri et al., 2001). These data suggest that maintaining proper peroxisome functions relies on ATP from the cytosol. Using protein sequence similarity-based blast searches, peroxisomal membrane protein 34 (PMP34) was identified as the human orthologue of Ant1p. Like ANT1p, PMP34 imports cytosolic ATP into peroxisomal matrix across the membrane and was shown to be a functional orthologue of ANT1p (Visser et al., 2002). In Arabidopsis, two ANT1p orthologs were identified through two independent studies, a homology-based search of the Arabidopsis genome (Linka et al., 2008) and a proteomic assay of peroxisomal membrane proteins (Arai et al., 2008). Due to their peroxisomal-specific localization and ability to catalyze the exchange of ATP-ADP in vitro, the proteins were named peroxisomal adenine nucleotide carriers, AtPNC1 and AtPNC2 (Arai et al., 2008; Linka et al., 2008). Suppression of both AtPNC1 and AtPNC2 in Arabidopsis leads to defects in ATP-dependent metabolic reactions within peroxisomes, such as β -oxidation dependent fatty acid degradation during seed germination (Arai et al., 2008; Linka et al., 2008). The findings further support the hypothesis that Arabidopsis peroxisomes lack ATP regeneration systems and rely on cytosolic ATPs (Linka et al., 2008).

In addition to AtPNC1 and AtPNC2, AtPMP38, whose homolog was initially

identified from pumpkin as a peroxisomal ADP/ATP carrier (Fukao et al., 2001), was suggested to be another close homolog of AtPNC in Arabidopsis based on sequence similarity. Peroxisomal localization of AtPMP38 was demonstrated in tobacco epidermal cells, in which the protein is targeted exclusively to peroxisomes. Unlike AtPNC, AtPMP38 fails to catalyze the ATP/AMP exchange (Linka et al., 2008). However, it was recently demonstrated to function as a peroxisomal NAD^+ /AMP antiporter thus re-named peroxisomal NAD^+ carrier, PXN (Bernhardt et al., 2011). An Arabidopsis mutant lacking the functional PXN is delayed in the breakdown of fatty acids during germination but has no obvious defects in plant morphology and peroxisome functions (Bernhardt et al., 2011).

Exporting/importing of ATP and other substrates across different membranes has emerged as a critical role of adenine nucleotide translocators. In addition, some of these transporters also seem to play roles in regulating organelle morphologies and abundance. For example, *Candida boidinii* peroxisomal membrane protein 47 (PMP47) transports small molecules (presumably ATP) into peroxisomes and affects the metabolism of middle-chain fatty acid. Mutants lacking the expression of PMP47 contain fewer peroxisomes in the cell, suggesting that metabolite (e.g., ATP) homeostasis within peroxisomes may affect the division and therefore the number of these organelles (Nakagawa et al., 2000). In Arabidopsis, suppression of the plastidic ATP/ADP transporter AtNTT results in a slow growth phenotype and moreover, structural defects in thylakoid (Reiser et al., 2004). These findings suggest that adenine nucleotide carriers may also play critical roles in maintaining organelle morphology.

Furthermore, recent studies on yeast and plants demonstrated that metabolic

status within peroxisomes regulates the morphogenesis of the organelle. In the yeast *Yarrowia lipolytica*, redistribution of acyl-CoA oxidase, a peroxisomal β -oxidation enzyme, to the peroxisomal membrane triggers interaction between the enzyme and a peroxisomal peripheral membrane protein YIPex16p residing in the matrix side of the membrane. The interaction negates the suppression of YIPex16p on peroxisomal division and allows the mature peroxisomes to undergo fission processes (Guo et al., 2007), suggesting that metabolic status inside peroxisome can activate the peroxisomal division machinery. In line with this finding, several β -oxidation enzyme mutants in *Arabidopsis* exhibit enlarged peroxisomes by as yet unknown mechanism (Baker et al., 2006). The above mentioned evidence from yeast and plants imply that there might be a novel mechanism in controlling the organelle division and morphogenesis, in which metabolic status within the organelle may directly or indirectly control the division and/or morphogenesis of the organelle.

To further study the impact of metabolic status of organelles on their morphogenesis, we characterized two metabolite transporters on peroxisomes and mitochondria in *Arabidopsis*. AtAAC1 was identified from our proteomic analysis of the *Arabidopsis* peroxisomes and later found to be dual targeted to mitochondria and peroxisomes. This protein plays critical roles in plant growth and development as well as the morphogenesis of peroxisomes and mitochondria. Characterization of the peroxisomal NAD^+ carrier mutant *pxn-3* also revealed the involvement of PXN in peroxisome morphogenesis. These results together support our hypothesis that metabolic homeostasis within organelles play important roles in maintaining the morphologies and proper numbers of organelles.

RESULTS AND DISCUSSION

AtAAC1 is a dual-targeted protein of mitochondria and peroxisomes

Three mitochondrial ADP/ATP carriers (AtAAC1-3) have been identified in several Arabidopsis mitochondrial proteomes (Millar and Heazlewood, 2003; Klodmann et al., 2011) and demonstrated their ATP transport activity in *E. coli* (Haferkamp et al., 2002). As carrier proteins, AtAACs contain six putative transmembrane domains (Millar and Heazlewood, 2003). Despite having the mitochondrial targeting signal, AtAAC1 was also identified repeatedly in our proteomic analysis of Arabidopsis peroxisomes (Quan S., unpublished data), suggesting that the protein might also be targeted to peroxisomes. To verify the subcellular localization of AtAAC1, full-length coding sequence of *AtAAC1* was amplified from Arabidopsis Col-0 and yellow fluorescent protein (YFP) was tagged to the N- or C- terminal end of AtAAC1. The fusion proteins were transiently expressed in Tobacco epidermal cells and the YFP signals were observed using epifluorescence microscope. AtAAC1-YFP was observed as punctate spots, whereas YFP-AtAAC1 was found mainly in the cytosol (data not shown). AtAAC1 contains the mitochondrial targeting peptide (Murcha et al., 2005) at its N-terminus, the fusion of YFP at the N-terminal end might disrupt the correct targeting of the fusion protein. To test the mitochondrial and/or peroxisomal association of AtAAC1-YFP in Arabidopsis, the fusion protein was expressed in the marker plants that carry CFP-PTS1 and COX4-CFP. Confocal imaging of AtAAC1-YFP in T₂ plants revealed that the punctate signals are co-localized with the CFP-labeled mitochondria, confirming that AtAAC1 is a mitochondrial protein. Ring-shaped structure of the YFP signals further

suggests that the fusion protein is targeted to the mitochondrial membrane. In addition to mitochondrial localization, we also observed the AtAAC1-YFP signals on the outer surface of peroxisomes (Figure 5.1), suggesting that AAC1 is a dual-targeted protein of peroxisomes and mitochondria.

As AtAAC1 contains the mitochondrial-targeting signal, it is intriguing to observe its localization to peroxisomes. Thus, it would be necessary in the future to study whether peroxisomal targeting of AtAAC1 is achieved through direct targeting of the protein or indirect sorting through intracellular vesicle trafficking from mitochondria to peroxisomes (Neuspiel et al., 2008). AtAAC1 belongs to a small mitochondrial carrier subfamily consisting of three members (AtAAC1-3), which share more than 70% amino acid sequence identities (Arai et al., 2008). Therefore, it would be worthwhile to examine whether AtAAC2 and AtAAC3 are also associated with peroxisomes. All three AtAAC proteins have been demonstrated to be ATP carriers when heterologously expressed in *E. coli* (Haferkamp et al., 2002). However, direct evidence showing the ability in exporting ATP from mitochondria to the cytosol has not been demonstrated. As Arabidopsis peroxisomes lack an ATP regeneration system (Linka et al., 2008), the peroxisomal AtAAC1 might function as an ATP importer, although we cannot rule out the possibility that it functions in exporting extra ATP back to the cytosol. Understanding the topology of AtAAC1 on peroxisomal and mitochondrial membranes will be necessary to confirm the dual-localization of the protein and instrumental to revealing the mechanism for the same protein to exert its transport activity on distinct membranes.

***aac1* mutants contain enlarged peroxisomes and elongated mitochondria**

Given that adenine nucleotide carriers were suggested to play a role in regulating organelle morphogenesis (Nakagawa et al., 2000; Reiser et al., 2004), we sought to examine the peroxisomal and mitochondrial morphologies in *aac1* mutants. To this end, we isolated two independent mutant alleles of *AtAAC1*, *aac1-1* and *aac1-2*, both of which harbor a T-DNA insertion in the first exon (Figure 5.2A). Transcripts for *AtAAC1* cannot be detected in *aac1-1* and *aac1-2*, suggesting that both alleles are null (Figure 5.2B). To observe the organelle morphologies in the mutant, we introduced the peroxisomal marker (YFP-PTS1) or the mitochondrial marker (COX4-YFP) into *aac1* mutants by genetic crosses. Homozygous *aac1* mutants were screened from F₂ populations based on their genotypes, and the organelle morphologies were observed using confocal microscopy. Our results showed that the *aac1* mutants have defects in peroxisomal and mitochondrial morphogenesis and/or division as both mutants exhibit enlarged peroxisomes and incomplete fission of mitochondria (Figure 5.2C and Figure 5.7). The organelle phenotypes suggest that the absence of *AtAAC1* has a direct or indirect impact on peroxisomal and mitochondrial morphogenesis or division.

***AtAAC1* is important for plant growth and development**

The biochemical properties of *AtAAC1* have been previously characterized in *E. coli*. However, the role of *AtAAC1* in plant growth and development hasn't been reported. We thus examined the plant morphology of *aac1* mutants. Both mutants showed pleiotropic effects, including retarded growth, darker green leaves (Figure 5.3), shorter root, and much reduced fertility (data not shown). The pleiotropic phenotype of

the *aac1* mutants suggests that AtAAC2 and AtAAC3 are unable to compensate for the absence of AtAAC1. According to online microarray database (<http://jasp.weigelworld.org>), *AtAAC1* is expressed ubiquitously in all tissue types, whereas *AtAAC2* and *AtAAC3* are expressed at a much lower level than that of *AtAAC1* (Figure 5.4). In line with the microarray data, promoter-glucuronidase (GUS) analyses of *AtAACs* demonstrated that *AtAAC1* and *AtAAC2* are expressed in all tissues, whereas *AtAAC3* is mainly expressed in meristematic tissues, and *AtAAC1* has the highest expression level among the three (Haferkamp, 2007). Together, among members of the AAC family in Arabidopsis, *AtAAC1* seems to have a prominent role in growth and development, *AtAAC2* may play a minor role, and *AtAAC3*'s function may be restricted to meristems.

***aac1* mutants are not strongly compromised in photorespiration**

The pleiotropic phenotype of *aac1* mutants led us to hypothesize that the absence of functional *AtAAC1* may interrupt the regular function and activity of peroxisomes and mitochondria. As photorespiration requires functional peroxisomes, mitochondria, and chloroplasts, we first tested whether the mutants are compromised in photorespiration. It is known that the retarded growth phenotype of photorespiratory mutants can be rescued by growing them in the elevated CO₂ environment; therefore, we grew the mutants in 3,000 ppm of CO₂. As shown in Figure 5.3 (middle panel), the growth phenotype of the known photorespiratory mutant *pex14* was greatly rescued by the elevated CO₂ environment; however, the same condition only slightly compensate for

the growth phenotypes of the *aac1* mutants. In addition, we moved two-week-old seedlings, which were previously grown under ambient air chamber, to low CO₂ conditions (80 ppm) for two weeks to induce photorespiratory-dependent senescence. Wild-type Col-0 and *aac1* mutants showed pale green leaves and stunted growth, whereas *pex14* was killed under the same condition (Figure 5.4, lower panel). Together, our data demonstrated that *aac1* mutants are not strongly compromised in photorespiration. In the future, it would be necessary to determine the photorespiration efficiency using additional approaches, such as measuring maximum quantum yield of photosystem II (Fv/Fm) and quantifying glyoxylate and ammonia (photorespiratory metabolites) in the mutants.

β-oxidation activity of the *aac1* mutants seems unaffected

AtAAC1 is postulated to play a role in importing ATP into peroxisomes, and activation of acyl-CoAs before β-oxidation is an ATP-dependent reaction. We next tested β-oxidation activity in *aac1* mutants. During germination of oilseeds like Arabidopsis, fatty acids are broken down through β-oxidation within peroxisomes (Graham, 2008); therefore, mutant seeds defect in the process fail to germinate or seedlings are unable to establish without exogenous application of soluble carbohydrate, like sucrose (Zolman et al., 2000). In addition, conversion of indole 3-butyric acid (IBA) to indole-3-acetic acid (IAA) takes place solely in peroxisomes via β-oxidation. IAA is a major active form of auxin, which inhibits the growth of Arabidopsis primary root and hypocotyl (Woodward and Bartel, 2005). Hence sucrose dependence and IBA response assays were performed on the *aac1* mutants. Similar to wild-type

Col-0, seed germination and seedling establishment of *aac1* mutants are sucrose independent (Figure 5.5A) and mutants exhibit similar hypocotyl inhibition response to IBA treatment (Figure 5.5B). In contrast, suppression of the peroxisomal ATP transporter *AtPNC1* and *AtPNC2* disrupts the peroxisomal β -oxidation, whereby the knock-down mutant depends upon exogenous application of sucrose for seed germination and becomes insensitive to IBA treatment in root elongation assays (Arai et al., 2008; Linka et al., 2008). Our data show that *aac1* mutants contain functional peroxisomes. Hence, if *AtAAC1* is involved in importing ATP into peroxisomes, it might be playing a minor role. The strong growth phenotypes in the mutants may be due to defect in exporting mitochondrial ATP into the cytosol, thus influencing biochemical reactions in different cellular compartments.

PXN is also involved in peroxisomal morphogenesis

The abnormal peroxisomal and mitochondrial morphologies in the *aac1* mutants suggested a role for organelle metabolism in their morphogenesis. To further test this notion, we also examined the organelle morphologies in the peroxisomal NAD^+ carrier mutant *pxn-3*. Although PXN was initially predicted to be a peroxisomal ADP/ATP carrier, it was recently demonstrated to be a peroxisomal NAD^+ /AMP antiporter. In the mutant, degradation of fatty acid during seedling establishment is delayed, suggesting that PXN plays important roles in NAD^+ -dependent β -oxidation in Arabidopsis (Bernhardt et al., 2011). To this end, we introduced the peroxisomal marker YFP-PTS1 or the mitochondrial marker COX-YFP into *pxn-3* using genetic crosses. Confocal

microscopy revealed that *pxn-3* contains giant peroxisomes, some of which are almost five times bigger than averaged peroxisome in that of the wild type (Figure 5.6 and Figure 5.7). Interestingly, these giant peroxisomes seem to show some characteristics of lipid bodies, such as the perfectly spherical shape and increased translucency (Figure 5.6), prompting us to speculate that there may be high accumulation of fatty acids inside peroxisomes in the *pxn-3* mutant. In agreement with the peroxisome-specific targeting of PXN (Bernhardt et al., 2011), an absence of the functional PXN has no major impact on mitochondrial morphology (Figure 5.6). To verify the peroxisomal and mitochondrial phenotypes of *pxn* mutant, it would be important to examine the organelle morphologies in two additional alleles, *pxn-1* and *pxn-2* (Bernhardt et al., 2011).

In summary, we here show that the Arabidopsis adenine nucleotide carrier AAC1 is sorted to peroxisomal and mitochondrial membrane and involved in the division or morphogenesis of the organelles directly or indirectly. Consistent with this finding, the peroxisomal NAD⁺ carrier PXN is also involved in the morphogenesis of peroxisomes. Based on our data and previously reported organelle morphology in the Arabidopsis peroxisomal β -oxidation enzyme mutants (Baker et al., 2006), we propose that the metabolic homeostasis within peroxisomes and mitochondria may be involved in maintaining the morphogenesis and proliferation of these organelles.

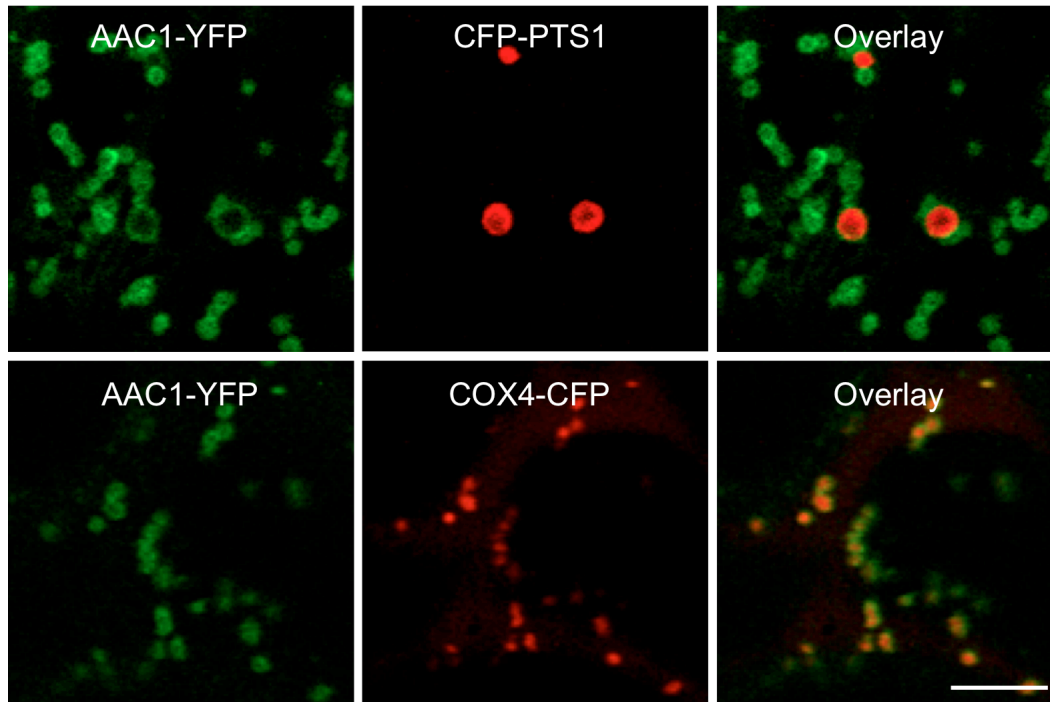
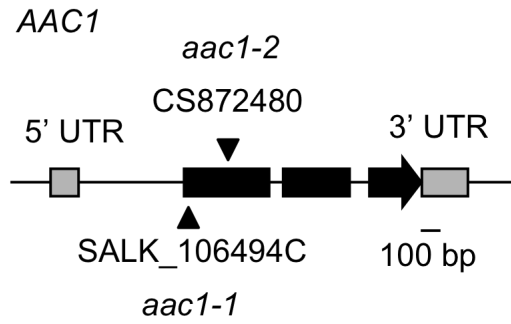


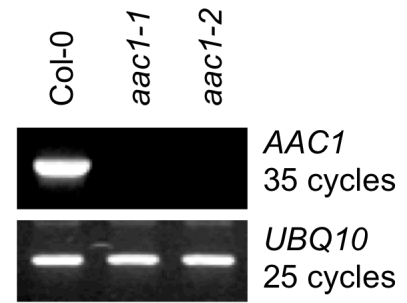
Figure 5.1. Subcellular localization of AAC1-YFP.

AAC1-YFP is shown as green punctuate spots. The peroxisomal marker (CFP-PTS1) and the mitochondrial marker (COX4-CFP) are in red. The merged images show the localization of AAC1-YFP to the surface of peroxisomes and mitochondria. Images were taken at the same magnification; scale, 5 μm .

A



B



C

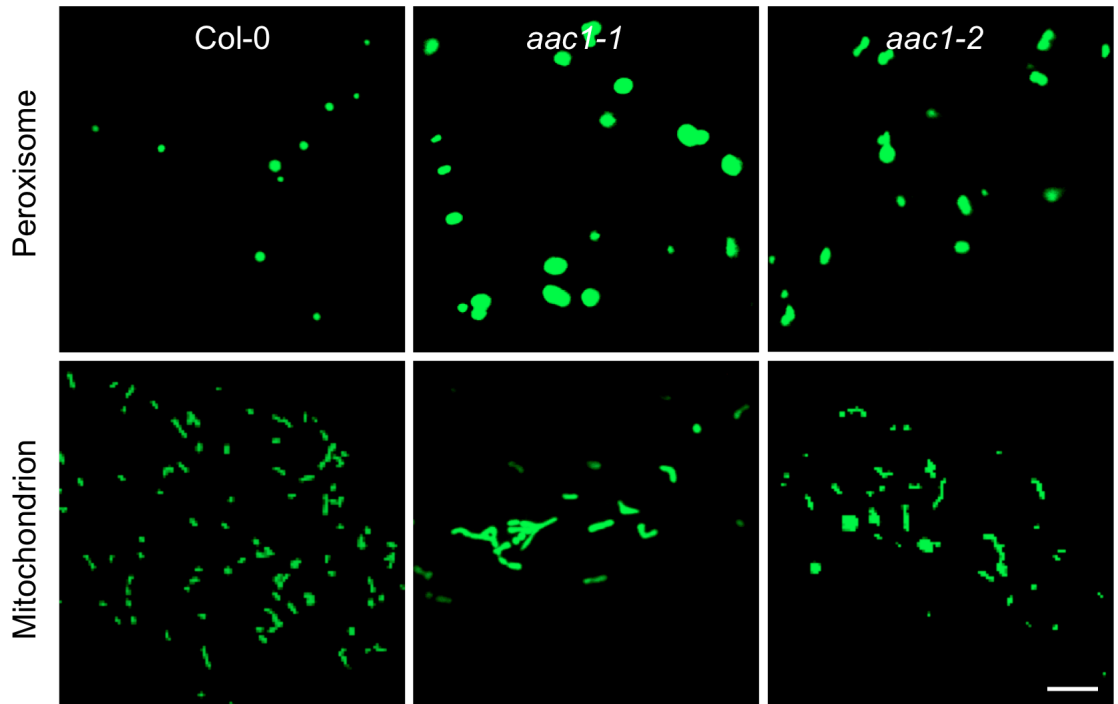


Figure 5.2

Figure 5.2 (cont'd)

Figure 5.2. Peroxisomal and mitochondrial morphology in *aac1* mutants.

(A) Genomic structure of *AtAAC1*. The T-DNA insertion sites in *aac1-1* and *aac1-2* are indicated.

(B) RT-PCR assays showing the presence or absence of full-length *AtAAC1* mRNA in *Arabidopsis* Col-0 or *aac1* mutants. *UBQ10* transcripts served as loading controls.

(C) Confocal images show the organelle morphologies in *aac1* mutants. Peroxisomes were labeled with YFP-PTS1 and mitochondria were marked by COX4-YFP. Images were taken at the same magnification; scale = 10 μm .

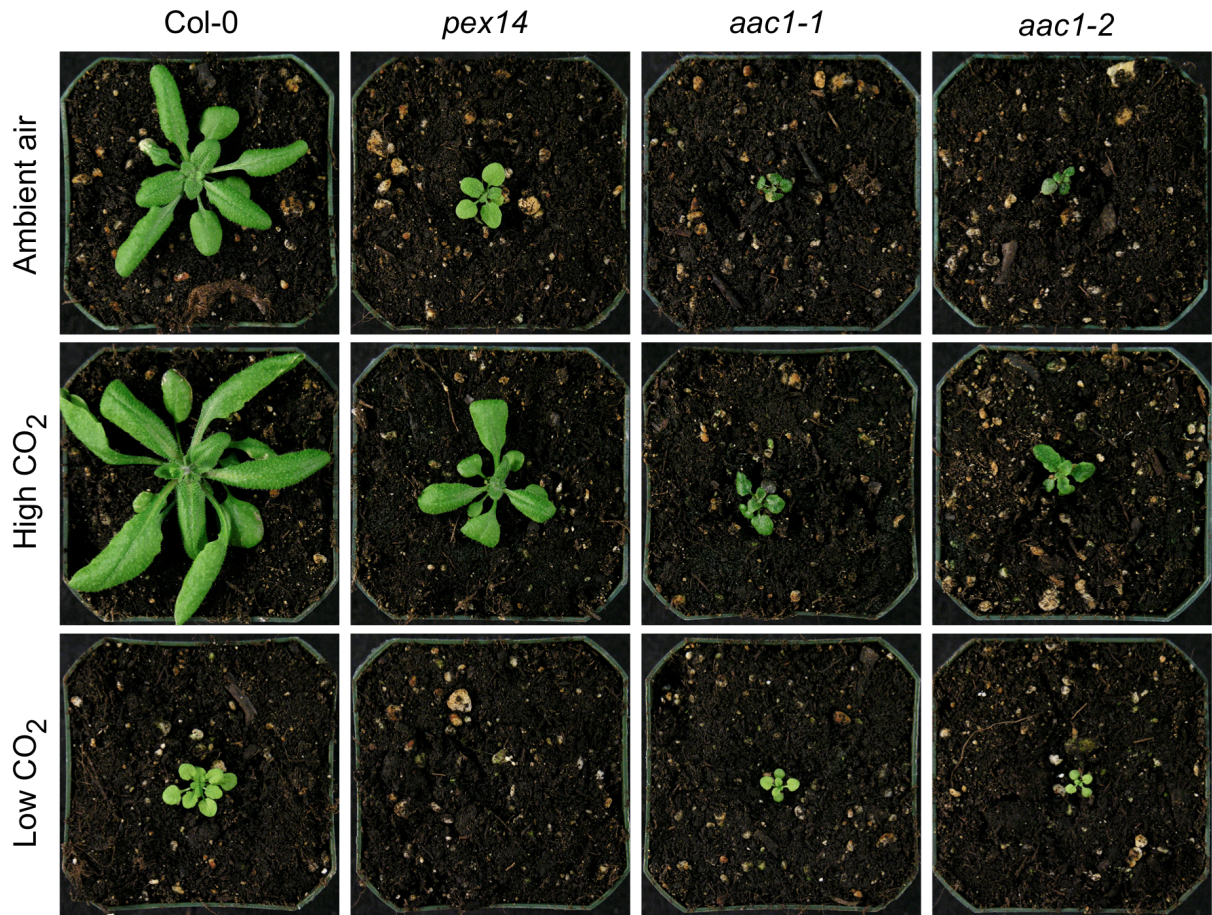


Figure 5.3. Plant morphology of *aac1* mutants.

Four-week-old *Arabidopsis* plants grown under ambient air (top panel), high CO₂ (middle panel), and low CO₂ (bottom panel). Images were taken under the same magnification.

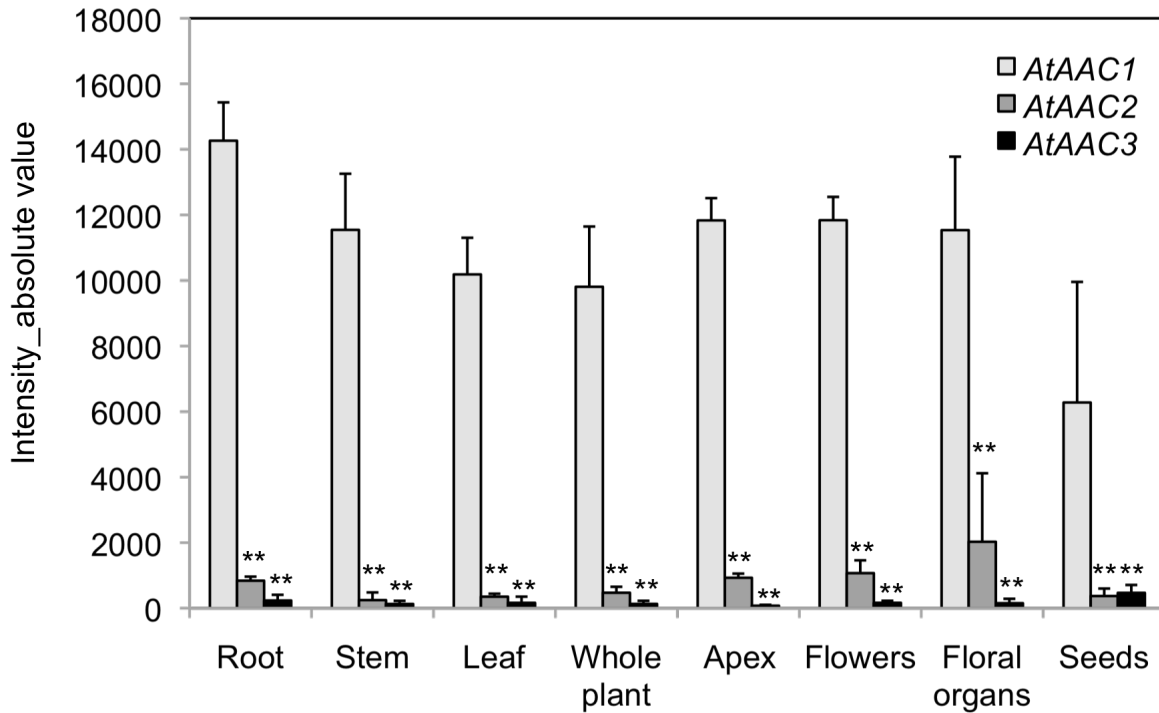
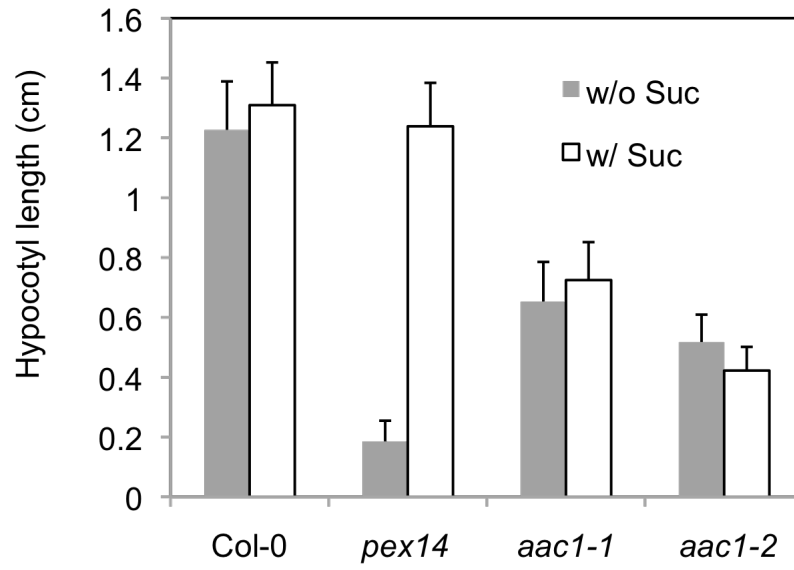


Figure 5.4. Expression level of *AtAACs* in Arabidopsis.

The absolute value of expression of AACs was retrieved from AtGenExpress Visualization Tool. Expression intensity from the same tissue types were averaged and calculated for standard deviation. The p values listed in the figure were calculated from Student's two-tailed t-test against *AtAAC1*. ** P < 0.001.

A



B

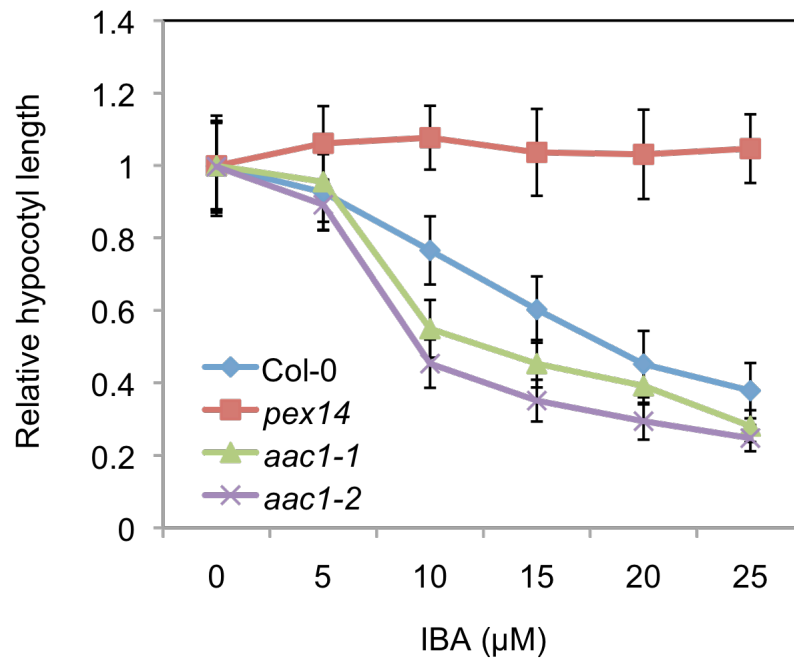


Figure 5.5

Figure 5.5 (cont'd)

Figure 5.5. Assessment of β -oxidation in the *aac1* mutants.

(A) Sucrose dependence assay. Arabidopsis seeds were germinated in the dark for 5 days on 0.5 Linsmaier and Skoog media with (w/) or without (w/o) 1% sucrose.

(B) IBA response assay. Arabidopsis seeds were germinated under dark for 5 days on 0.5 Linsmaier and Skoog media with different concentration of IBA as shown. N = 30.

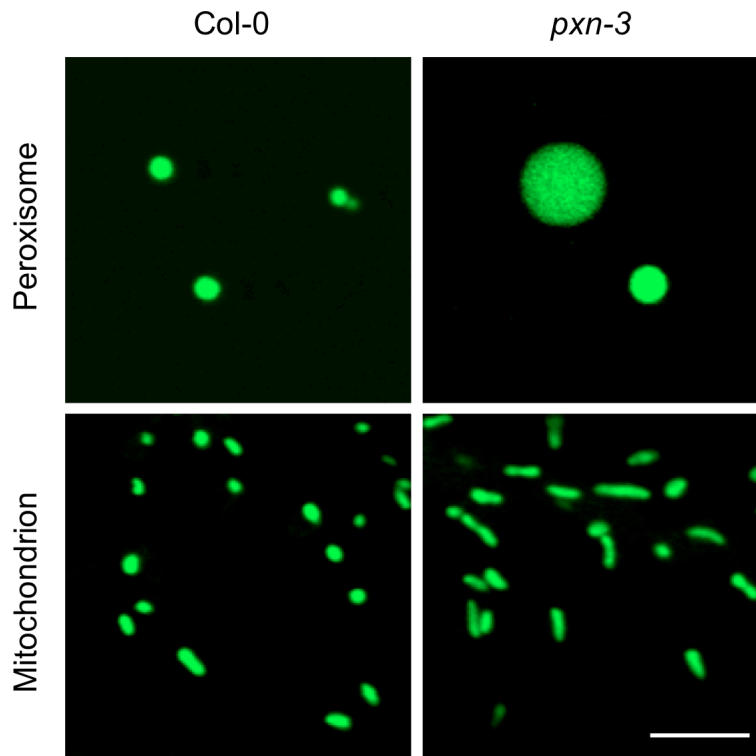


Figure 5.6. Peroxisomal and mitochondrial morphology in *pxn-3*.

Confocal images show the organelle morphologies in *pxn-3*. Peroxisomes were labeled with YFP-PTS1 and mitochondria were marked by COX4-YFP. Images were taken at the same magnification; scale = 5 μm .

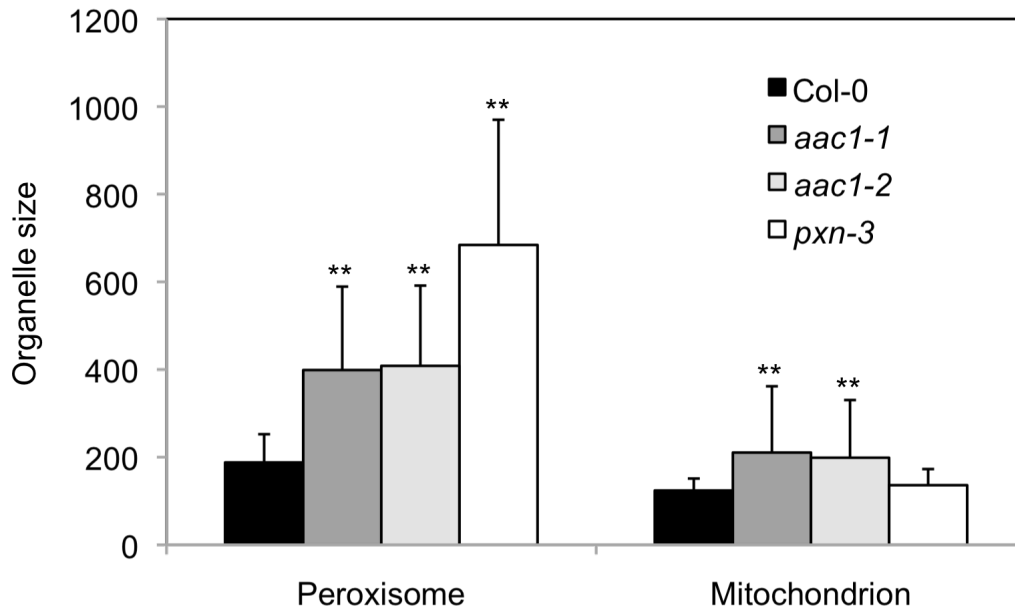


Figure 5.7. Peroxisomal and mitochondrial size in *aac1* and *pxn-3* mutants.

The organelle size was presented as average fluorescent area per organelle. The p values listed in the figure were calculated from Student's two-tailed t-test against Col-0.

** : P < 0.001.

METHODS

Plant Material, Growth Conditions, Transformation and Plant Selection

Arabidopsis thaliana plants were grown at 20°C with 70% humidity, irradiated with 70 to 80 $\mu\text{mol m}^{-2} \text{s}^{-2}$ of white light for 14 h per day. The ambient air chamber has no regulation on the CO₂ content, whereas the high CO₂ chamber is supplied with 3,000 ppm of CO₂ and the low CO₂ chamber is supplied with 80 ppm of CO₂. For the CO₂ treatment, seeds were first germinated on 0.5 Linsmaier and Skoog agar plate containing 1% sucrose for two weeks. The seedlings were then transferred to soil and grown under different CO₂ chambers for another two weeks. To test peroxisomal functions, *Arabidopsis* seeds were surface sterilized and stratified at 4°C for 24 h. The seeds were plated on 0.5 Linsmaier and Skoog agar plate. For sucrose dependence assay, the seeds were grown on the agar plate with or without 1% sucrose. For IBA treatment, the seeds were germinated on the agar plate containing different concentration of IBA (0, 5, 10, 20, or 25 μM) and 1% sucrose. The plates were grown vertically under dark for 5 days and imaged for measuring hypocotyl growth (Strader et al., 2011). All the data points were averaged from at least 30 plants.

T-DNA insertion mutants, *aac1-1* (SALK_106494C) and *aac1-2* (SAIL_247_G08), were obtained from the Arabidopsis Biological Resource Center (ABRC; Columbus, OH, USA). The genotype of the mutants was analyzed by polymerase chain reaction (PCR) of genomic DNA. *aac1-1* was genotyped with the following primers: SALK_106494-LP (5'-TCGTCTCTCTTCTCTGCTTCG-3'), SALK_106494-RP (5'-CCTTG TAGGGTTCAGAAAGCC-3'), and LBb1.3 (5'-

ATTTTGCCGATTTTCGGAAC-3'). *aac1-2* was genotyped with the following primers: CS872480-LP (5'-CTGCTTCTTTTTGTGCGTTTC-3'), CS872480-RP (5'-TTGGCATCATTAGCTAGACGG-3'), and SAIL-LB1 (5'-GCCTTTTCAGAAATGGATAAATAGCCTTGCTTCC-3').

To introduce the organelle markers into the mutant background, the mitochondrial marker plant (COX4-YFP) and the peroxisomal marker plant (YFP-PTS1) were hand-pollinated with the mutant pollens. F₁ population of the outcross progenies was checked for the heterozygosity of the gene using the method described above and screened for the presence of YFP signals using epifluorescence microscope. Next, F₂ population was screened for the homozygous line using the same method described above and the organelle morphologies were observed using confocal microscopy as described below. To test the subcellular localization of AAC1, the AAC1-YFP fusion construct (conferring resistance to basta) was transformed into the peroxisomal marker plant (expressing CFP-PTS1) or the mitochondrial marker plant (expressing COX4-CFP) and the transgenic plants were screened as described in Chapter 2. The transgenic plants were then subjected to confocal imaging to observe the subcellular localization of AAC1-YFP.

Gene Cloning and Plasmid Construction

Full-length coding sequence of AAC1 was amplified from cDNA synthesized from total RNA of wild type (Col-0) seedling using Phusion High-Fidelity DNA polymerase (New England Biolabs). The PCR fragments were cloned into the donor vector (pDonorTM207) and pEarleyGate101 (Earley et al., 2006) destination vectors using a

standard Gateway cloning system to generate YFP-fusion protein (Invitrogen).

RT-PCR Analysis

RNA from leaves of 4-week-old Arabidopsis plants was purified as previously described (Zhang and Hu, 2009). For RT-PCR analysis, 0.5 µg of total RNA was used to make cDNA using high capacity RNA-to-cDNA master mix (Applied Biosystems). PCR amplification was performed as previously described (Zhang and Hu, 2010). Expression level of *AAC1* transcripts was determined by the following primers; AAC1-Fw (5'- ATGGTTGATCAAGTTCAGCAC-3') and AAC1-Rev (TTGGCATCATTAGCTAGACGG) primers. *UBQ10* transcripts were used as an internal control and amplified with the UBQ10-Fw (5'-TCAATTCTCTCTACCGTGATCAAGATG-3') and UBQ10-Rev (5'-GTGTCAGAACTCTCCACCTCAAGAG-3') primers.

Confocal imaging

Confocal images were taken by a confocal laser scanning microscope (Zeiss LSM 510 META). YFP and CFP signals were detected as previously reported (Reumann et al., 2009).

Quantification of Organelles

Peroxisomes and mitochondria were imaged in wild type Col-0, *aac1-1*, *aac1-2*, and *pxn-3* plants expressing the peroxisomal marker (YFP-PTS1) or the mitochondrial marker (COX4-YFP) using confocal laser scanning microscope. Images collected from single focal plane were used to quantify the organelle size using IMAGE J (URL:

<http://rsb.info.nih.gov/ij>) as reported previously (Desai and Hu, 2008). The peroxisomal and mitochondrial sizes were presented as average fluorescent area per organelle. At least 40 or 80 of individual peroxisome or mitochondrion were used to calculate the average respectively. Student's two-tailed t-test was used to examine the statistical significance between wild-type Col-0 and the mutants. Two asterisks were marked if the P value is <0.001.

Accession Numbers

Arabidopsis Genome Initiative locus identifiers for the genes mentioned in this article are as follows: AtAAC1 (At3g08580), AtAAC2 (At5g13490), AtAAC3 (At4g28390), AtPNC1 (At3g05290), AtPNC2 (At5g27520), and AtPXN (At2g39970). Germplasm identification number for *aac1-1* and *aac1-2* alleles used in this works is as follow: *aac1-1* (SALK_106494C) and *aac1-2* (SAIL_247_G08; The Arabidopsis Information Resource stock number CS872480).

ACKNOWLEDGEMENTS

We thank the ABRC (Columbus, OH, USA) for providing the T-DNA insertion mutants (*aac1-1*, *aac1-2*, and *pxn-3*) and Gaëlle Cassin (MSU) for kindly providing homozygous *pxn-3* seeds. We also thank Melinda Frame (Center of Advance Microscopy, MSU) for the help with confocal microscope. This work was supported by grants from the National Science Foundation (MCB 0618335) and the Chemical Sciences, Geosciences and Biosciences Division, Office of Basic Energy Sciences, Office of Science, U.S. Department of Energy (DE-FG02-91ER20021) to J.H.

CHAPTER 6

CONCLUSIONS AND FUTURE PERSPECTIVES

Peroxisomes and mitochondria are eukaryotic organelles playing several conserved as well as plant-specific roles in plants. Elucidating the molecular mechanisms underlying the maintenance of organelle populations within cells is crucial to gaining a complete understanding of the cellular and physiological functions of the organelles. This dissertation aims to dissect the division machinery of peroxisomes and mitochondria in Arabidopsis. When I initiated this work, some evolutionarily conserved division factors of peroxisomes and mitochondria, such as Dynamin-related protein3 (DRP3) and Fission1 (FIS1), had been identified and characterized in Arabidopsis. In addition to the conserved fission factors, several lineage-specific division factors have also begun to emerge in yeasts, animals, and plants.

Novel Peroxisomal And Mitochondrial Division Factors, PMD1 and PMD2

In Chapter 2, I present two novel plant-specific proteins, Peroxisomal And Mitochondrial Division Factor1 (PMD1) and its homologue PMD2. PMD1 is a long coiled-coil protein anchored to the membranes of peroxisomes and mitochondria through its C-terminus. Based on the mutant analyses, PMD1 is suggested to function in the division of peroxisomes and mitochondria. However, PMD1 has no detectable physical interaction with the known division proteins, such as DRP3 and FIS1. I thus hypothesize that PMD1 facilitates peroxisomal and mitochondrial proliferation in a DRP3/FIS1-independent machinery. Using affinity purification, PMD2, a close homolog of PMD1, was identified as a PMD1-interacting protein. PMD2 is sorted only to mitochondria and plays a specific role in mitochondrial morphogenesis. Despite sharing

35% amino acid identity, PMD1 and PMD2 perform non-redundant functions in organelle morphogenesis.

Future directions

Although mutant analyses highly suggest the functional roles of PMD in the division or morphogenesis of peroxisomes and mitochondria, the mode of action for the PMD proteins is yet to be demonstrated. Following are some future directions that can be taken to approach the question.

As the PMD proteins are shown/predicted to be C-TA proteins with the functional domain (coiled-coil domain) facing toward the cytosol, they are ideal candidates for membrane-bound receptors, which recruit the division factor DRP3 or unknown proteins to the division sites. As shown in Chapter 2, PMD1 lacks direct physical interaction with DRP3A/DRP3B and is not critical for sub-organelle targeting of DRP3 to the organelles. However, the peroxisomal and mitochondrial association of DRP3 have not been examined in the *pmd1-1 amiR PMD2* double mutant. To test the peroxisomal and mitochondrial targeting of DRP3 in the double mutant, the FAST technique (Li et al., 2009) described in Chapter 2 can be applied to express the FP-DRP protein.

Since FIS1A and FIS1B are also C-TA proteins and suggested to recruit DRP3 to peroxisomes and mitochondria, it would be interesting to generate a quadruple mutant, in which PMD1, PMD2, FIS1A, and FIS1B, are knocked out. The quadruple mutant can be used to observe the protein targeting of DRP3, the peroxisomal and mitochondrial morphologies, and the effects of these proteins on plant growth and development.

Given the membrane topology of the PMD proteins, the aggregated organelle phenotype in the PMD1 overexpressors, and their ability to form homo- and heterocomplexes, it is tempting to hypothesize that these proteins function as molecular tethers in maintaining a close proximity of peroxisomes and mitochondria. Although there is no discernible difference in the physical distance between peroxisomes and mitochondria in the *pmd* single mutant, double mutant and wild-type Col-0, as observed by confocal microscopy, it is worthwhile to test the hypothesis with alternative approaches. As the *in vivo* interaction between the ER and Golgi bodies has been demonstrated using optical tweezers (Sparkes et al., 2009), it would be interesting to apply the same technique to test the physical association between peroxisomes and mitochondria in wild-type Col-0 and *pmd* mutants that carry both peroxisomal marker CFP-PTS1 and mitochondrial marker COX4-YFP. In addition, it would also be interesting to fuse the functional domain, the N-terminus, of PMD1 with the organelle targeting signal, the C-termini, of the known C-TA proteins, which are sorted to the ER or chloroplast (Abell and Mullen, 2011). If the functional domain of PMD1 acts as a molecular tether, we expect to see aggregation of the targeted organelles when the chimeric protein is expressed. Furthermore, a suppressor screen of *pmd1-1* may reveal the molecular function of PMD1. To this end, EMS mutagenesis of *pmd1-1* expressing the peroxisomal marker YFP-PTS1 has been generated.

DRP5B is Also Involved in the Division of Mitochondria

In Chapter 3, I show that DRP5B mediates the division or morphogenesis of mitochondria without being physically associated with the organelle. Although *drp5B*

mutants resemble the elongated mitochondria phenotype as *drp3* mutants, DRP5B seems to function separately from the DRP3A/DRP3B-dependent machinery. The conclusion is based on the findings that DRP5B does not physically or genetically interact with DRP3 and is not a major component of the DRP3-containing protein complex. I thus hypothesize that DRP5B is indirectly involved in the division or morphogenesis of mitochondria by changing the intracellular architecture of the cells.

Future directions

To test the hypothesis that the enlarged chloroplast phenotype in the *drp5B* mutants indirectly effect the mitochondrial morphology, it would be necessary to examine the mitochondrial morphology in other plastid division mutants such as *arc6* (Robertson et al., 1995; Vitha et al., 2003) and *ftsZ* (Osteryoung et al., 1998; Yoder et al., 2007).

In addition, DRP1C and DRP1E were also shown to regulate the division of mitochondria (Jin et al., 2003). Hence, the relationship between the DRP1s, DRP3s, and DRP5B in maintaining the organelle proliferation and morphogenesis needs to be established. Comprehensive and systematic analyses of organelle morphologies in all the *drp* single and higher order mutants combined with physical interaction analyses between the proteins will provide us with a complete picture of the function of Arabidopsis DRP proteins in organelle fission.

The Function of DRP3A and DRP3B are Controlled by Phosphorylation

In this study, I demonstrate that the function of DRP3 is regulated by protein

phosphorylation at DRP3A^{Ser575} and DRP3B^{Ser560}. Genetic complementation assays showed that phospho-null DRP3A acts like the wild-type protein, whereas phospho-mimic DRP3A causes division defects of peroxisomes and mitochondria when ectopically expressed. In contrast, overexpression of DRP3B causes peroxisomal and mitochondrial division deficiencies in wild type and fails to complement the *drp3B-2* mutant phenotype.

Future directions

The finding here has led to several further questions. First, is the majority of DRP3 phosphorylated in vivo? Although DRP3A and DRP3B were identified as phosphorylated proteins experimentally (Heazlewood et al., 2008), the in vivo or in vitro phosphorylation of DRP3A and DRP3B is yet to be verified. Second, does this phosphorylation affect the GTP-binding or GTPases activity of DRP3A and DRP3B? Third, which kinases or phosphatases function in phosphorylation/dephosphorylation of DRP3A and DRP3B? Lastly, are there any effector proteins like mammalian mitochondrial elongation factor 1 (MIEF1) in regulating the function of DRP3A and DRP3B? MIEF1 is a mitochondrial membrane protein and recruits Drp1 to the mitochondrial membrane, whereby the physical interaction inhibits the function of Drp1 (Palmer et al., 2011a; Zhao et al., 2011). I have generated several valuable materials to approach most of the above-mentioned questions. For example, GST-fusion proteins of all the DRP3 variants have been generated to purify GST-DRP3 recombinant proteins for in vitro phosphorylation and GTPase activity assays. In addition, transgenic plants expressing HA-DRP3 or YFP-DRP3 fusion proteins are available to determine GTP-

binding activity of the DRP3 variants and use affinity purification to identify DRP3-interacting proteins. Furthermore, I have also taken advantage of the publicly available co-expressed gene database of Arabidopsis (ATTED-II: <http://atted.jp/>, and AraNet: <http://www.functionalnet.org/aranet/>) in identifying several putative phosphatases and kinases that are co-expressed with the *DRP3A* gene. Biochemical analyses of the candidate proteins and mutant characterization might uncover kinases, phosphatases or effector proteins that are involved in the regulation of DRP3A and DRP3B functions.

Metabolic Homeostasis in Maintaining Organelle Morphogenesis and Division

In Chapter 5, I show that the ADP/ATP carrier1 protein AAC1 is dually targeted to preoxisomes and mitochondria, and an absence of the functional AAC1 results in enlarged peroxisomes and incomplete fission of mitochondria. Arabidopsis mutant lacking the peroxisomal NAD^+ carrier PXN also has giant peroxisomes without affecting the mitochondrial morphology. I thus propose that metabolic homeostasis within peroxisomes and mitochondria may play a role in maintaining the morphogenesis and proliferation of these organelles.

Future directions

Our experimental evidence strongly suggests that metabolic status within the organelle has a major impact on plant growth and development as well as organelle morphogenesis. In addition to AAC1 and PXN, it is also worthwhile to examine the functional role of PNC1 and PNC2 in peroxisomal morphogenesis, as they have a critical role in importing ATP into peroxisomes (Arai et al., 2008; Linka et al., 2008). It

was previously proposed that metabolic homeostasis, e.g. ADP/ATP and NAD(P)H/NAD(P)⁺, within mitochondria might affect retrograde regulation of gene expression and further influence the morphology of mitochondria (Millar et al., 2008). In this context, the mutants can be used as a valuable tool to approach the question whether metabolic regulation has a direct role in maintaining organelle morphogenesis or whether it indirectly regulates organelle division machineries. In addition, plant peroxisomes are also termed glyoxysomes in germinating seedlings and gerontosomes in senescing tissue, in which slightly different sets of enzymes and different metabolic functions are housed compared with leaf peroxisomes (Kaur et al., 2009). Hence, systemic analyses of peroxisome morphologies in different developmental stages and cell types would provide further evidence to support the hypothesis.

I speculate that the metabolic homeostasis within organelles may affect the organelle division in one or several ways: (1) accumulation of some metabolites may disrupt organelle morphologies and further inhibit the assembly of the division complexes to occur on the organelle, (2) interruption of metabolic homeostasis may block the retrograde signaling in regulating expression of the genes involved in the organelle division, or (3) metabolic status may affect the protein function of the organelle division factors. Although I postulate that the metabolic homeostasis may play roles in regulating organelle division, it is also possible that it affects/regulates organelle fusion. To address some of the above-mentioned questions, examination of the formation of the division complexes in the mutants, comparative transcriptomic, proteomic, and metabolomic analyses between wild type and the mutants, and extensive observation of organelle dynamics in the mutants will uncover the functional

role of metabolic homeostasis in regulating organelle division and morphogenesis.

In summary, results from my thesis work make a significant step forward in our understanding of peroxisomal and mitochondrial division in plants at the molecular level. This includes the discovery of novel organelle division factors PMD1 and PMD2 and the elucidation of the interplay between, and post-translational regulation of, the key organelle division factors, DRPs, in Arabidopsis. These findings will not only contribute to the knowledge of how the dynamics of organelles are controlled in eukaryotic cells, but also provide valuable information to biotechnological efforts for the improvement of crop plants for better quality and yield.

APPENDICES

APPENDIX A

The Arabidopsis peroxisome division mutant *pdd2* is defective in the
DYNAMIN-RELATED PROTEIN3A (DRP3A) gene

This section has been previously published in Plant Signaling & Behavior as an article
addendum.

Kyaw Aung and Jianping Hu (2009)
Plant Signal. & Behav. **4**: 542-544.

Summary

In plants, the division of peroxisomes is mediated by several classes of proteins, including PEROXIN11 (PEX11), FISSION1 (FIS1) and DYNAMIN-RELATED PROTEIN3 (DRP3). DRP3A and DRP3B are two homologous dynamin-related proteins playing overlapping roles in the division of both peroxisomes and mitochondria, with DRP3A performing a stronger function than DRP3B in peroxisomal fission. Here, we report the identification and characterization of the *peroxisome division defective 2* (*pdd2*) mutant, which was later proven to be another *drp3A* allele. The *pdd2* mutant generates a truncated DRP3A protein and exhibits pale green and retarded growth phenotypes. Intriguingly, this mutant displays much stronger peroxisome division deficiency in root cells than in leaf mesophyll cells. Our data suggest that the partial GTPase effector domain retained in *pdd2* may have contributed to the distinct mutant phenotype of this mutant.

In eukaryotic cells, peroxisomes are surrounded by single membranes and house a variety of oxidative metabolic pathways such as lipid metabolism, detoxification and plant photorespiration (Beevers, 1979; Purdue and Lazarow, 2001). To accomplish multiple tasks, the morphology, abundance and positioning of peroxisomes need to be highly regulated. Three families of proteins, whose homologs are present across different kingdoms, have been shown to be involved in peroxisome division in *Arabidopsis*. The PEX11 protein family is composed of five integral membrane proteins with primary roles in peroxisome elongation/tubulation, the initial step in peroxisome division (Lingard and Trelease, 2006; Nito et al., 2007; Orth et al., 2007). Although the exact function of PEX11s has not been demonstrated, these proteins are believed to participate in peroxisome membrane modification (Thoms and Erdmann, 2005; Fagarasanu et al., 2007). The FIS1 family consists of two isoforms, which are C-terminal tail-anchored membrane proteins with rate limiting functions at the fission step (Zhang and Hu, 2009). DRP3A and DRP3B belong to a superfamily of dynamin-related proteins, which are large and self-assembling GTPases involved in the fission and fusion of membranes by acting as mechanochemical enzymes or signaling GTPases (Praefcke and McMahon, 2004). The function of PEX11 seems to be exclusive to peroxisomes, whereas DRP3 and FIS1 are shared by the division machineries of both peroxisomes and mitochondria in *Arabidopsis* (Arimura and Tsutsumi, 2002; Arimura et al., 2004; Logan et al., 2004; Mano et al., 2004; Scott et al., 2006; Fujimoto et al., 2009; Zhang and Hu, 2009). FIS1 proteins are believed to tether DRP proteins to the peroxisomal membrane (Koch et al., 2005; Kobayashi et al., 2007), but direct evidence

has not been obtained from plants. DRP3A and DRP3B share 77% sequence identity at the protein level and are functionally redundant in regulating mitochondrial division; however, DRP3A's role on the peroxisome seems stronger and cannot be substituted by DRP3B in peroxisome division (Mano et al., 2004; Fujimoto et al., 2009; Zhang and Hu, 2009).

In a continuous effort to identify components of the plant peroxisome division apparatus from Arabidopsis, we performed genetic screens in a peroxisomal marker background expressing the YFP (yellow fluorescent protein)-PTS1 (peroxisome targeting signal 1, containing Ser-Lys-Leu) fusion protein. Mutants with defects in the morphology and abundance of fluorescently labeled peroxisomes are characterized. Following our analysis of the *pdd1* mutant, which turned out to be a strong allele of DRP3A (Zhang and Hu, 2009), we characterized the *pdd2* mutant.

In root cells of the *pdd2* mutant, extremely elongated peroxisomes and a beads-on-a-string peroxisomal phenotype are frequently observed (Figure A.1A and B). These peroxisome phenotypes resemble those of *pdd1* and other strong *drp3A* alleles previously reported (Mano et al., 2004; Zhang and Hu, 2009). However, the peroxisome phenotype seems to be less dramatic in leaf mesophyll cells. For instance, in addition to the decreased number of total peroxisomes, peroxisomes in leaf cells are only slightly elongated or exhibit a beads-on-a-string phenotype (Figure A.1C and D). Previously, we reported the phenotypes of three strong *drp3A* alleles, all of which contain a large number of peroxules, long and thin membrane extensions from the peroxisome (Zhang and Hu, 2009), yet such peroxisomal structures are not observed in *pdd2*. On the other hand, *pdd2* has a more severe growth phenotype than most *drp3A* alleles, as it is slow

in growth and has pale green leaves (Figure A.1E). Genetic analysis showed that *pdd2* segregates as a single recessive mutation (data not shown).

The unique combination of peroxisomal and growth phenotypes of *pdd2* prompted us to use map-based cloning to identify the *PDD2* gene, with the hope to discover novel proteins in the peroxisome division machinery. A population of approximately 6,000 F₂ plants (*pdd2* x *Ler*) was generated. After screening 755 F₂ mutants, the *pdd2* mutation was mapped to the region between markers T10C21 and F4B14 on the long arm of chromosome 4 (Figure A.2A). Since this region contains *DRP3A*, we sequenced the entire *DRP3A* gene in *pdd2* and identified a G→A transition at the junction of the 18th exon and intron (Figure A.2A). Further analysis revealed that the point mutation at this junction caused mis-splicing of intron 18, introducing a stop codon in the GTPase effector domain GED near the C terminus (Figure 2B).

DRPs share with the classic dynamins an N-terminal GTPase domain, a middle domain (MD), and a regulatory motif named the GTPase effector domain (GED) (Figure 2B). To date, a total of 26 *drp3A* mutant alleles carrying missense or nonsense mutations along the length of the *DRP3A* gene have been isolated (Mano et al., 2004; Zhang and Hu, 2009). The combined peroxisomal and growth phenotype of *pdd2* and the nature of the mutation in this allele are unique among all the *drp3A* alleles, indicating that the partial GED domain retained in *pdd2* may have created some novel function for this protein. Further analysis of the truncated protein may be necessary to test this prediction.

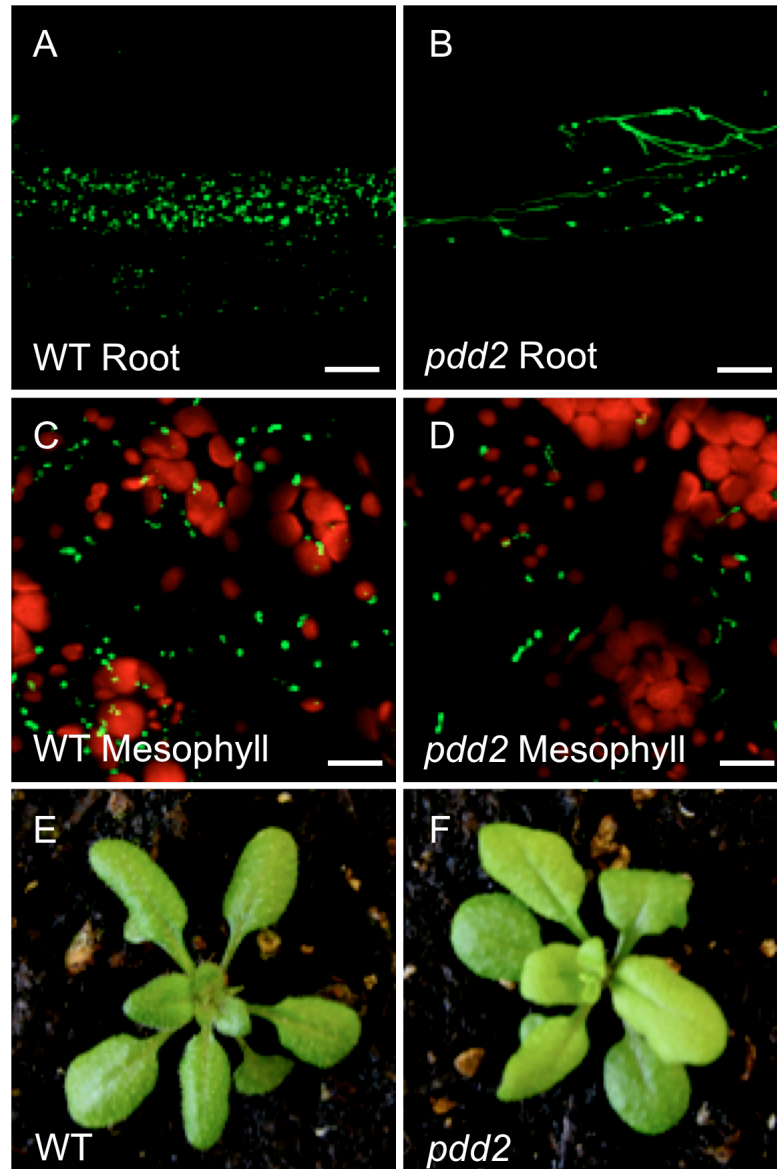


Figure A.1. Phenotypic analyses of *pdd2*.

(A–D) Confocal micrographs of root and mesophyll cells in 3-week-old wild type and *pdd2* mutant plants. Green signals show peroxisomes; red signals show chloroplasts. Images were taken at the same magnification; scale bars = 20 μ m. (E–F) Growth phenotype of 3-week-old mutants.

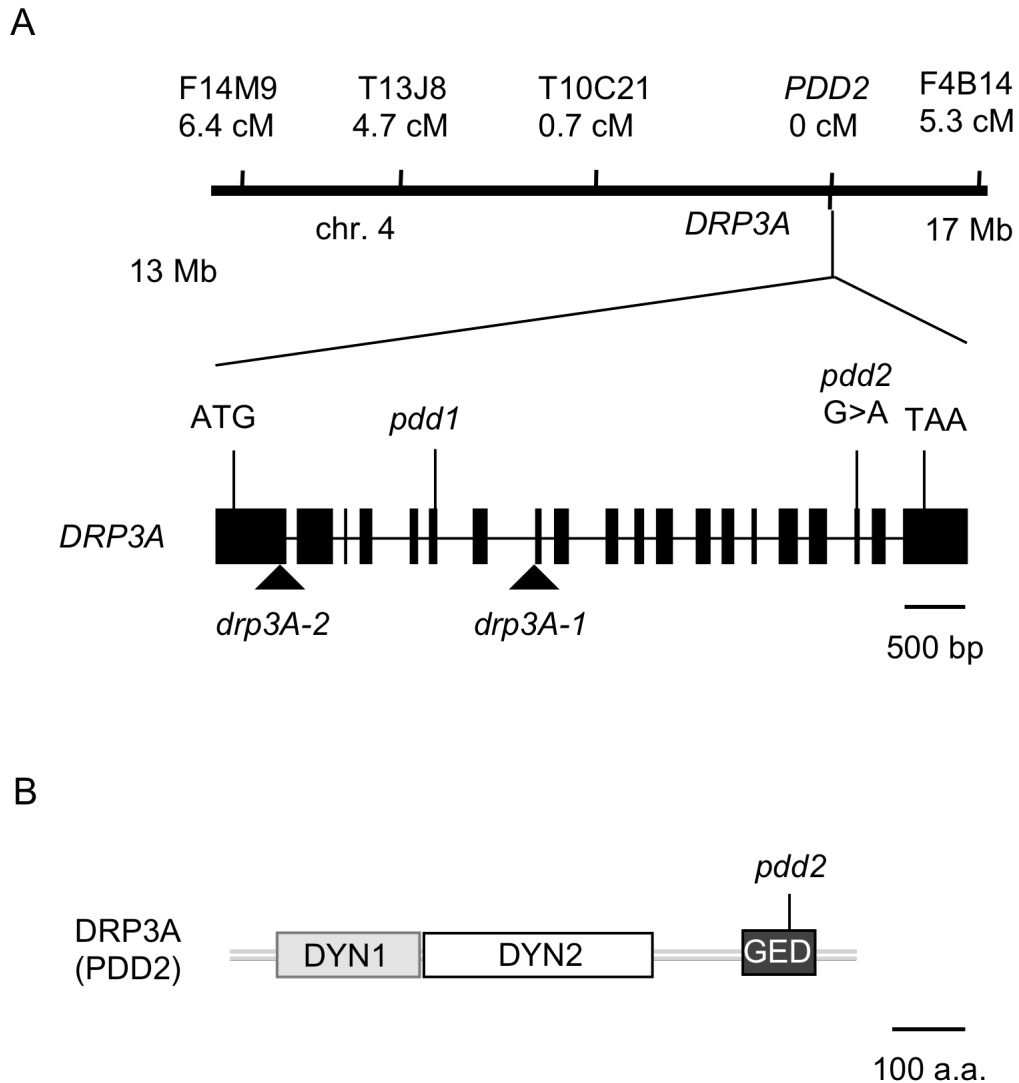


Figure A.2. Identification of the PDD2 gene.

(A) Map-based cloning of the *PDD2* gene. Genetic distance from *PDD2* is shown under each molecular marker. Positions for mutations in previously analyzed *drp3A* alleles and *pdd2* are indicated in the gene schematic. *drp3A-1* and *drp3A-2* are T-DNA insertion mutants, whereas *pdd1* is an EMS mutant containing a premature stop codon in exon 6.

(B) A schematic of the DRP3A (PDD2) protein with functional domains indicated. The *pdd2* allele encodes a truncated protein lacking part of the GED domain.

APPENDIX B

Dissecting the functional domain of PMD1 in peroxisomal and mitochondrial division

Summary

We have recently shown that PEROXISOMAL AND MITOCHONDRIAL DIVISION FACTOR1 (PMD1) is involved in peroxisomal and mitochondrial division and morphogenesis. PMD1 is a coiled-coil (CC) domain-containing C-terminal tail-anchored protein (C-TA), which resides on the surface of peroxisomes and mitochondria. Although no physical interactions between PMD1 and most of the known division factor tested have been detected, we demonstrated that PMD1 can form homodimers; moreover, it can heterodimerize with PMD2 both in vivo and in vitro. Confocal microscopic analysis showed that PMD1 with the second CC domain (CCII) deleted fails to induce peroxisomal and mitochondrial proliferation/aggregation in tobacco epidermal cells transiently overexpressing the proteins, suggesting that CCII is important for its function. In addition, we were able to fine map the functional domain to two sets of heptad repeated domains, CCII-A and CCII-C. In consistent with the finding that CCII is the major functional domain, yeast two-hybrid analysis demonstrated that CCII is also important for self-interaction of PMD1. We concluded that CCII is the functional domain of PMD1 and is required for the self-interaction of PMD1.

PMD1 is a peroxisomal and mitochondrial C-TA protein and suggested to play a role in the division of peroxisomes and mitochondria in *Arabidopsis*. *pmd1* mutants exhibit enlarged peroxisomes and elongated mitochondria, whereas overexpression of the protein leads to overproliferation of the organelles. Similar to the known C-TA protein, the targeting signal of PMD1 is located at its C-terminus, in which the putative TMD and the flanking sequences downstream of TMD (cPMD1) are essential and sufficient. As overexpression of cPMD1 does not cause peroxisomal and mitochondrial proliferation, the N-terminus of PMD1 may contain the functional domain (Aung and Hu, 2011).

PMD1 contains four putative coiled-coil (CC) domains at its N-terminus and is defined as a long coiled-coil protein (Rose et al., 2004). A CC domain is composed of heptad repeats, in which the first and fourth residues of CC are hydrophobic and the fifth and seventh residues are charged or polar (Rose et al., 2004). Coiled coils homo- or heterodimerize by forming intertwined α -helices, which provide a structure domain for protein-protein interaction (Moutevelis and Woolfson, 2009). In addition to CC domains, PMD1 has a single segment of transmembrane domain (TMD). As such, PMD1 is classified as a C-TA protein, in which the functional domain may be located in the cytosolic N-terminus as predicted for most C-TA proteins (Abell and Mullen, 2011). Since PMD1 contains four stretches of CC domains at its N-terminus, we aimed to dissect the functional domain of PMD1 that is required for inducing organelle proliferation and protein-protein interaction.

To this end, we fused a HA-tag to the N-terminal end of truncated or deleted forms of PMD1 (Figure B.1) and transiently overexpressed the HA-fusion proteins in

tobacco epidermal cells along with the peroxisomal marker YFP-PTS1 or the mitochondrial marker COX4-YFP. Confocal imaging of the epidermal cells revealed that, whereas deletions of the extreme N-terminus and CCI ($\text{PMD1}^{\Delta\text{N}}$ and $\text{PMD1}^{\Delta\text{N}\&\text{CCI}}$) had no effect on the induction of organelle proliferation by PMD1, further deletion of CCII ($\text{PMD1}^{\Delta\text{N}\&\text{CCI-II}}$) abolished this phenotype, indicating the importance of CCII in the function of PMD1 (Figure B.2B-2E). Consistent with this data, $\text{PMD1}^{\Delta\text{CCII}}$, in which only CCII was deleted, also failed to promote the proliferation of the organelles, suggesting that CCII is the major functional domain of PMD1 (Figure B.2H).

Since the CCII domain is composed of eight heptad repeats, we removed a heptad sequence at a time within the CCII to generate ΔCCIIA to ΔCCIIH (Figure B.1). When the first (IIA; VDKTAE E) or the third (IIC; LAEIVEK) heptad was removed, PMD1 was unable to induce organelle proliferation/aggregation, whereas deleting the other six heptad repeats in this domain had no effect (Figure 2I-2P). To exclude the possibility that protein expression/stability was the cause for the lack of induction of organelle proliferation, we performed immunoblot analysis of proteins expressed in the tobacco. The result showed that all the tested PMD1 are expressed (Figure B.3). Together these data established the essential role of two of the CC motifs within the second CC domain for the function of PMD1 in inducing organelle proliferation.

Homodimerization of coiled-coil proteins have been shown to be critical for their function (Amery et al., 2001). PMD1 can homodimerize (Chapter 4), thus we were interested in testing whether the CCII domain is also important for self-interaction of PMD1. We used the yeast two-hybrid assay (Matchmaker LexA; Clontech) as described

in Chapter 4 to analyze the interaction between wild-type PMD1 (with TMD deleted) and different deletion variants of PMD1. In consistence with the functional domain analyses, homodimerization was abolished by deletion of CCII. In addition, deletion of CCI also greatly reduced the self-interaction as shown by weak cell growth and light blue colonies on the selection plate (SD/-UTHL) containing β -gal. Together, our data strongly suggested that CCII of PMD1 plays a critical role in the formation of PMD1 homodimers and is important for inducing peroxisomal and mitochondrial proliferation. In addition, CCI is also required for PMD1 homodimerization.

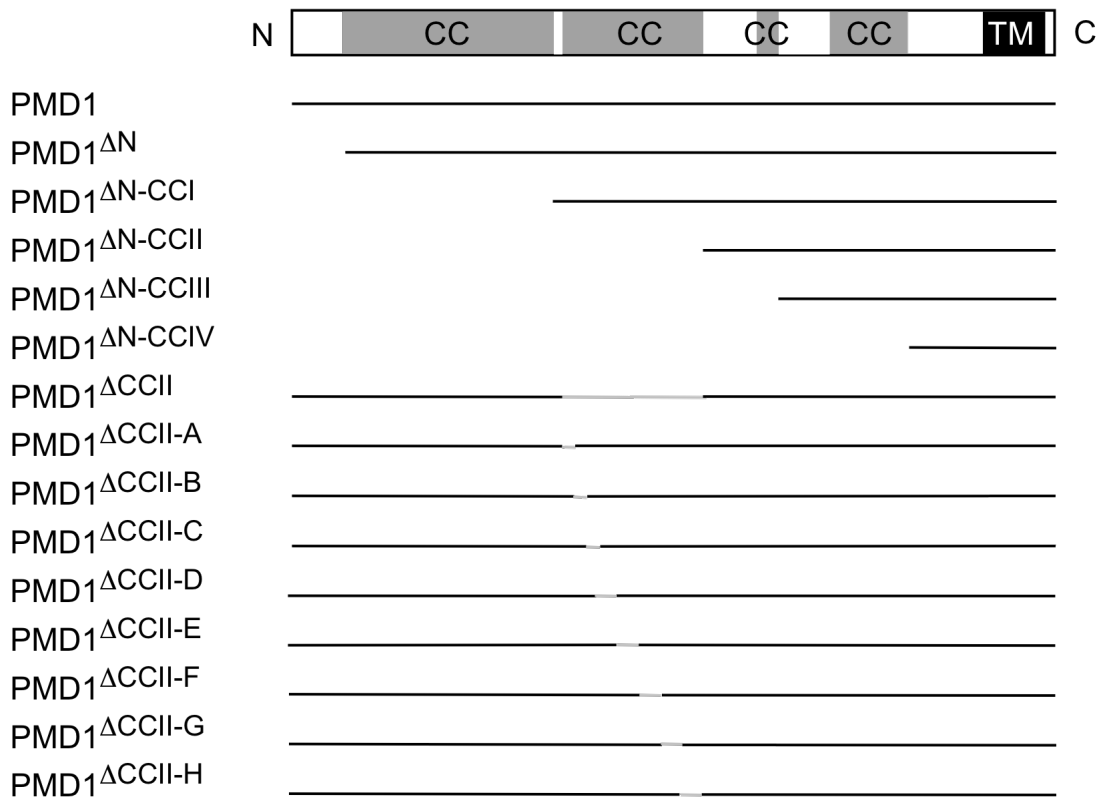


Figure B.1. Schematic drawings of PMD1 variants for mapping the functional domain.

HA-tag was fused to N-terminus (N) of the protein. C, C-terminus. CC, coiled-coil domain. TM, transmembrane domain. Gray lines in between black lines show the region of deleted sequences.

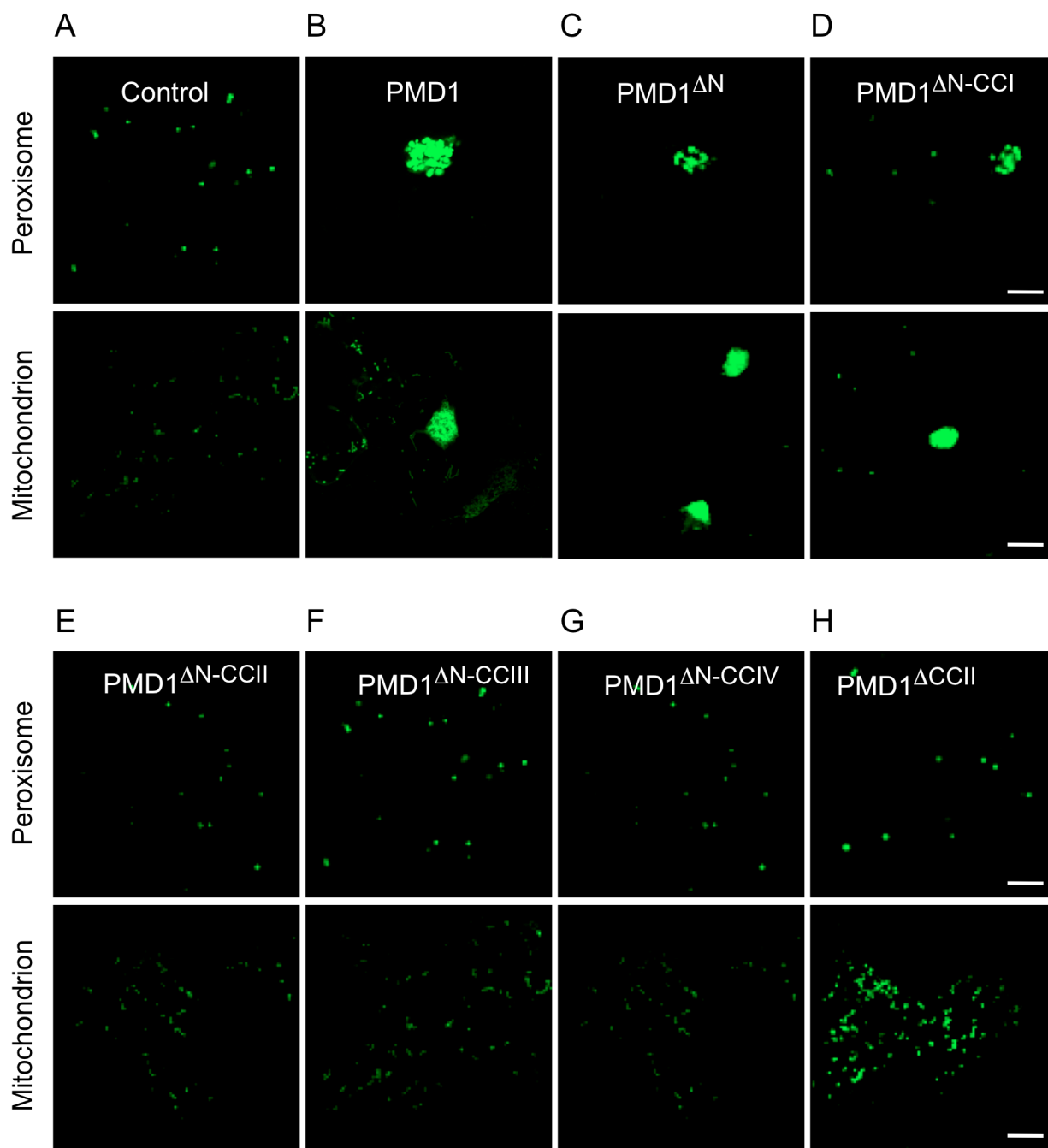


Figure B.2

Figure B.2 (cont'd)

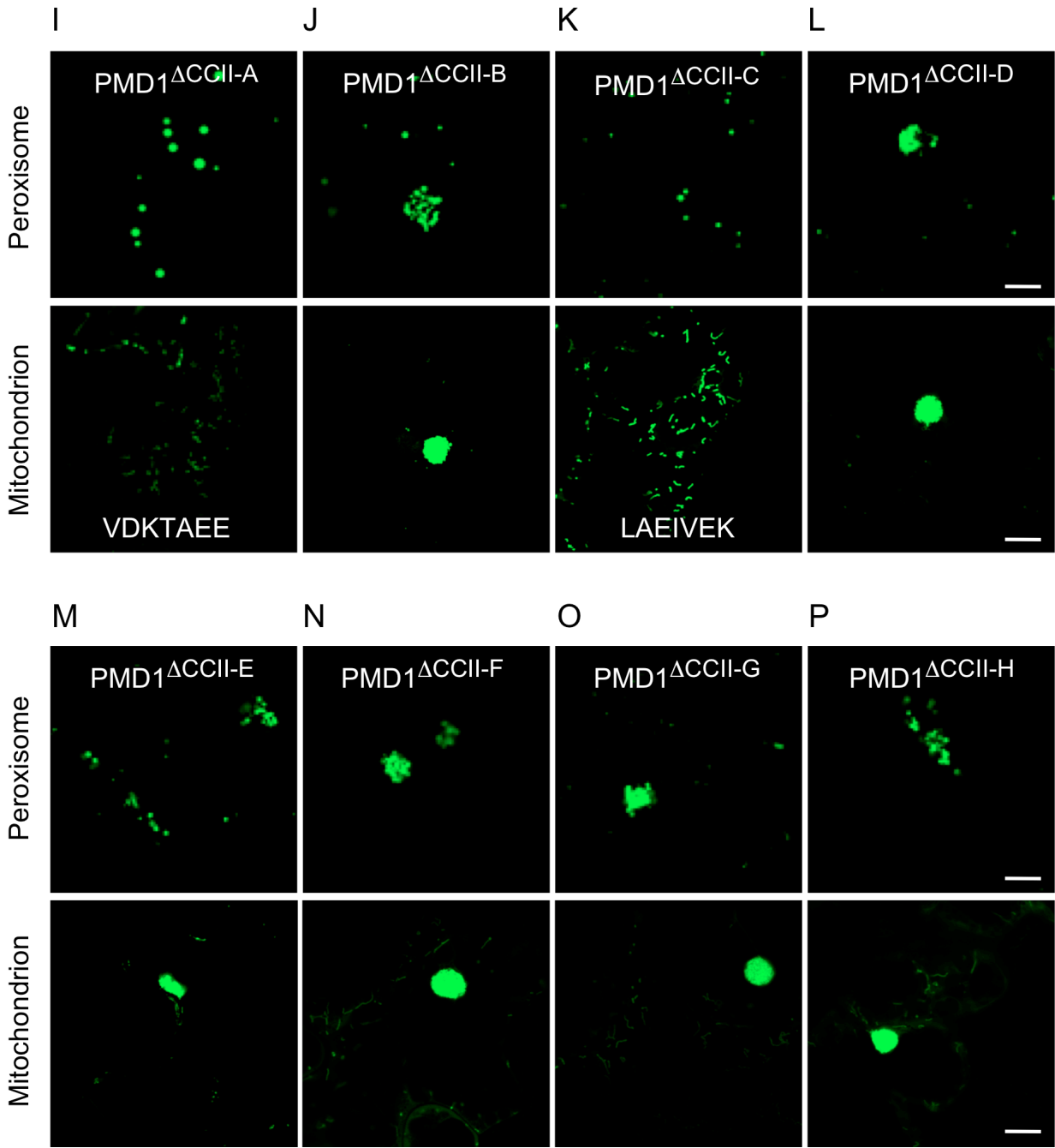


Figure B.2 (cont'd)

Figure B.2. Induction of peroxisomal and mitochondrial proliferation by overexpression of HA-PMD1.

(A) to (P) Confocal images from Tobacco epidermal cells transiently co-expressing HA-PMD1 variants along with the peroxisomal marker YFP-PTS1 (top panel) or the mitochondrial marker COX4-YFP (lower panel). Images were taken at the same magnification; scale bar = 10 μ m.

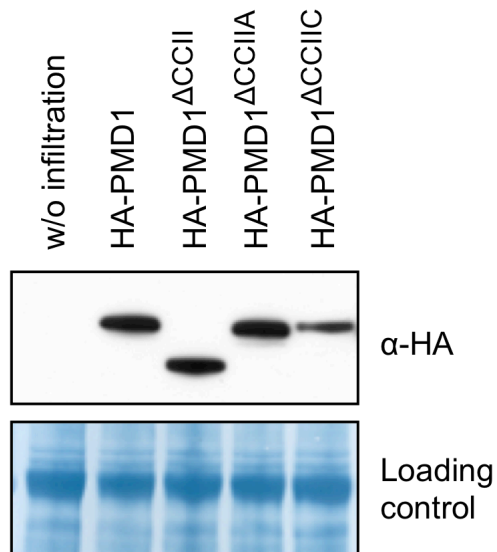


Figure B.3. Expression of the HA-fusion proteins in Tobacco leaves.

Immunoblot analysis using α -HA shows the expression of HA-PMD1 variants in tobacco epidermal cells. Sample without infiltration of Agrobacterium served as a negative control and the Rubisco large subunit was used as a loading control.

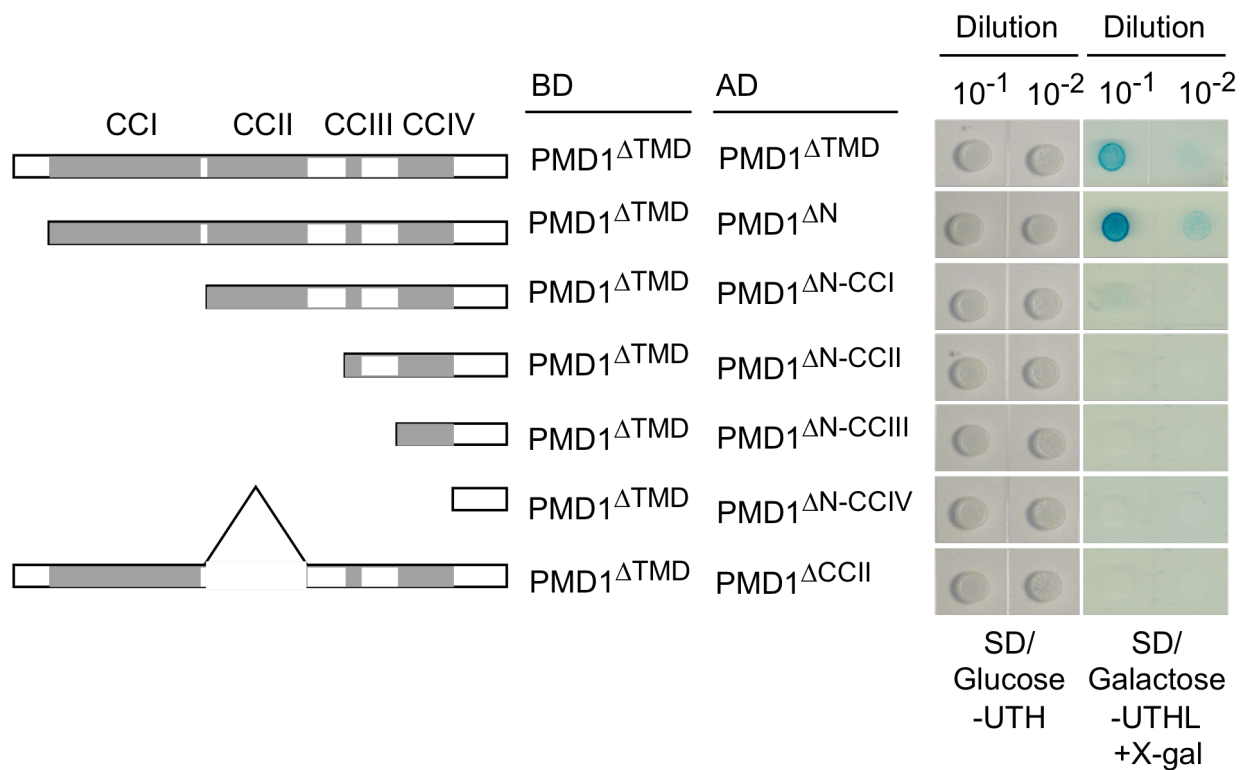


Figure B.4. Mapping the self-interacting domain of PMD1 by yeast two-hybrid analysis. SD/Glucose-UTH selects for transformants and SD/Galactose-UTHL+X-gal selects for interactions.

REFERENCES

REFERENCES

- Arai, Y., Hayashi, M., and Nishimura, M.** (2008). Proteomic Identification and Characterization of a Novel Peroxisomal Adenine Nucleotide Transporter Supplying ATP for Fatty Acid {beta}-Oxidation in Soybean and Arabidopsis. *Plant Cell* **20**, 3227-3240.
- Abell, B.M., and Mullen, R.T.** (2011). Tail-anchored membrane proteins: exploring the complex diversity of tail-anchored-protein targeting in plant cells. *Plant Cell Rep.* **30**, 137-151.
- Amery, L., Sano, H., Mannaerts, G.P., Snider, J., Van Looy, J., Fransen, M., and Van Veldhoven, P.P.** (2001). Identification of PEX5p-related novel peroxisome-targeting signal 1 (PTS1)-binding proteins in mammals. *Biochem. J.* **357**, 635-646.
- Andrade-Navarro, M.A., Sanchez-Pulido, L., and McBride, H.M.** (2009). Mitochondrial vesicles: an ancient process providing new links to peroxisomes. *Curr. Opin. Cell Biol.* **21**, 560-567.
- Anton, M., Passreiter, M., Lay, D., Thai, T.P., Gorgas, K., and Just, W.W.** (2000). ARF- and coatamer-mediated peroxisomal vesiculation. *Cell Biochem. Biophys.* **32**, 27-36.
- Arimura, S., Aida, G.P., Fujimoto, M., Nakazono, M., and Tsutsumi, N.** (2004). Arabidopsis dynamin-like protein 2a (ADL2a), like ADL2b, is involved in plant mitochondrial division. *Plant Cell Physiol.* **45**, 236-242.
- Arimura, S., and Tsutsumi, N.** (2002). A dynamin-like protein (ADL2b), rather than FtsZ, is involved in Arabidopsis mitochondrial division. *Proc. Natl. Acad. Sci. USA* **99**, 5727-5731.
- Arimura, S., Fujimoto, M., Doniwa, Y., Kadoya, N., Nakazono, M., Sakamoto, W., and Tsutsumi, N.** (2008). Arabidopsis ELONGATED MITOCHONDRIA1 is required for localization of DYNAMIN-RELATED PROTEIN3A to mitochondrial fission sites. *Plant Cell* **20**, 1555-1566.
- Aung, K., and Hu, J.** (2009). The Arabidopsis peroxisome division mutant *pdd2* is defective in the *DYNAMIN-RELATED PROTEIN3A (DRP3A)* gene. *Plant Signal. & Behav.* **4**, 542-544.
- Aung, K., and Hu, J.** (2011) The Arabidopsis tail-anchored protein PEROXISOMAL AND MITOCHONDRIAL DIVISION FACTOR 1 is involved in the morphogenesis and proliferation of peroxisomes and mitochondria. *Plant Cell* 10.1105/tpc.111/090142.

- Baker, A., Graham, I.A., Holdsworth, M., Smith, S.M., and Theodoulou, F.L.** (2006). Chewing the fat: beta-oxidation in signalling and development. *Trends Plant Sci.* **11**, 124-132.
- Barnett, P., Tabak, H.F., and Hetteema, E.H.** (2000). Nuclear receptors arose from pre-existing protein modules during evolution. *Trends Biochem. Sci.* **25**, 227-228.
- Bednarek, S.Y., and Backues, S.K.** (2010). Plant dynamin-related protein families DRP1 and DRP2 in plant development. *Biochem. Soc. Trans.* **38**, 797-806.
- Beevers, H.** (1979). Microbodies in higher plants. *Annu. Rev. Plant Physiol.* **30**, 159-193.
- Benard, G., and Karbowski, M.** (2009). Mitochondrial fusion and division: Regulation and role in cell viability. *Semin. Cell Dev. Biol.* **20**, 365-374.
- Bereiter-Hahn, J.** (1990). Behavior of mitochondria in the living cell. *Int. Rev. Cytol.* **122**, 1-63.
- Bernhardt, K., Wilkinson, S., Weber, A.P., and Linka, N.** (2011). A peroxisomal carrier delivers NAD(+) and contributes to optimal fatty acid degradation during storage oil mobilization. *Plant J.* DOI: 10.1111/j.1365-313X.2011.04775.x.
- Bleazard, W., McCaffery, J.M., King, E.J., Bale, S., Mozdy, A., Tieu, Q., Nunnari, J., and Shaw, J.M.** (1999). The dynamin-related GTPase Dnm1 regulates mitochondrial fission in yeast. *Nat. Cell Biol.* **1**, 298-304.
- Borgese, N., Brambillasca, S., and Colombo, S.** (2007). How tails guide tail-anchored proteins to their destinations. *Curr. Biol.* **19**, 368-375.
- Braschi, E., Zunino, R., and McBride, H.M.** (2009). MAPL is a new mitochondrial SUMO E3 ligase that regulates mitochondrial fission. *EMBO Rep.* **10**, 748-754.
- Cereghetti, G.M., Stangherlin, A., de Brito, O.M., Chang, C.R., Blackstone, C., Bernardi, P., and Scorrano, L.** (2008). Dephosphorylation by calcineurin regulates translocation of Drp1 to mitochondria. *Proc. Natl. Acad. Sci. USA* **105**, 15803-15808.
- Chan, D.C.** (2006). Mitochondria: dynamic organelles in disease, aging, and development. *Cell* **125**, 1241-1252.
- Chang, C.R., and Blackstone, C.** (2007). Cyclic AMP-dependent protein kinase phosphorylation of Drp1 regulates its GTPase activity and mitochondrial morphology. *J. Biol. Chem.* **282**, 21583-21587.

- Chang, C.R., and Blackstone, C.** (2010). Dynamic regulation of mitochondrial fission through modification of the dynamin-related protein Drp1. *Ann. N. Y. Acad. Sci.* **1201**, 34-39.
- Chelstowska, A., and Butow, R.A.** (1995). RTG genes in yeast that function in communication between mitochondria and the nucleus are also required for expression of genes encoding peroxisomal proteins. *J. Biol. Chem.* **270**, 18141-18146.
- Cho, D.H., Nakamura, T., Fang, J., Cieplak, P., Godzik, A., Gu, Z., and Lipton, S.A.** (2009). S-nitrosylation of Drp1 mediates beta-amyloid-related mitochondrial fission and neuronal injury. *Science* **324**, 102-105.
- Cline, K., Werner-Washburne, M., Andrews, J., and Keegstra, K.** (1984). Thermolysin is a suitable protease for probing the surface of intact pea chloroplasts. *Plant Physiol.* **75**, 675-678.
- Collings, D.A., Gebbie, L.K., Howles, P.A., Hurley, U.A., Birch, R.J., Cork, A.H., Hocart, C.H., Arioli, T., and Williamson, R.E.** (2008). Arabidopsis dynamin-like protein DRP1A: a null mutant with widespread defects in endocytosis, cellulose synthesis, cytokinesis, and cell expansion. *J. Exp. Bot.* **59**, 361-376.
- Cribbs, J.T., and Strack, S.** (2007). Reversible phosphorylation of Drp1 by cyclic AMP-dependent protein kinase and calcineurin regulates mitochondrial fission and cell death. *EMBO Rep.* **8**, 939-944.
- Cui, J., Liu, J., Li, Y., and Shi, T.** (2011). Integrative identification of Arabidopsis mitochondrial proteome and its function exploitation through protein interaction network. *PLoS One* **6**, e16022.
- de Brito, O.M., and Scorrano, L.** (2008). Mitofusin 2 tethers endoplasmic reticulum to mitochondria. *Nature* **456**, 605-610.
- Delille, H.K., Agricola, B., Guimaraes, S.C., Borta, H., Luers, G.H., Fransen, M., and Schrader, M.** (2010). Pex11beta-mediated growth and division of mammalian peroxisomes follows a maturation pathway. *J Cell Sci.* **123**, 2750-2762.
- Delille, H.K., and Schrader, M.** (2008). Targeting of hFis1 to peroxisomes is mediated by Pex19p. *J. Biol. Chem.* **283**, 31107-31115.
- Desai, M., and Hu, J.** (2008). Light induces peroxisome proliferation in Arabidopsis seedlings through the photoreceptor phytochrome A, the transcription factor HY5 HOMOLOG, and the peroxisomal protein PEROXIN11b. *Plant Physiol.* **146**, 1117-1127.

- Desvergne, B., and Wahli, W.** (1999). Peroxisome proliferator-activated receptors: nuclear control of metabolism. *Endocr. Rev.* **20**, 649-688.
- Dixit, E., Boulant, S., Zhang, Y., Lee, A.S., Odendall, C., Shum, B., Hacoen, N., Chen, Z.J., Whelan, S.P., Fransen, M., Nibert, M.L., Superti-Furga, G., and Kagan, J.C.** (2010). Peroxisomes are signaling platforms for antiviral innate immunity. *Cell* **141**, 668-681.
- Duek, P.D., and Fankhauser, C.** (2005). bHLH class transcription factors take centre stage in phytochrome signalling. *Trends Plant Sci.* **10**, 51-54.
- Duncan, O., Taylor, N.L., Carrie, C., Eubel, H., Kubiszewski-Jakubiak, S., Zhang, B., Narsai, R., Millar, A.H., and Whelan, J.** (2011). Multiple lines of evidence localise signalling, morphology and lipid biosynthesis machinery to the mitochondrial outer membrane of *Arabidopsis thaliana*. *Plant Physiol.* **157**, 1093-1113.
- Earley, K.W., Haag, J.R., Pontes, O., Opper, K., Juehne, T., Song, K., and Pikaard, C.S.** (2006). Gateway-compatible vectors for plant functional genomics and proteomics. *Plant J.* **45**, 616-629.
- Epstein, C.B., Waddle, J.A., Hale, W.t., Dave, V., Thornton, J., Macatee, T.L., Garner, H.R., and Butow, R.A.** (2001). Genome-wide responses to mitochondrial dysfunction. *Mol. Biol. Cell* **12**, 297-308.
- Erdmann, R., and Blobel, G.** (1995). Giant peroxisomes in oleic acid-induced *Saccharomyces cerevisiae* lacking the peroxisomal membrane protein Pmp27p. *J Cell Biol.* **128**, 509-523.
- Faelber, K., Posor, Y., Gao, S., Held, M., Roske, Y., Schulze, D., Haucke, V., Noe, F., and Daumke, O.** (2011). Crystal structure of nucleotide-free dynamin. *Nature* **477**, 556-560.
- Fagarasanu, A., Fagarasanu, M., and Rachubinski, R.A.** (2007). Maintaining peroxisome populations: A story of division and inheritance. *Annu. Rev. Cell Dev. Biol.* **23**, 321-344.
- Fan, J.L., Quan, S., Orth, T., Awai, C., Chory, J., and Hu, J.P.** (2005). The *Arabidopsis* PEX12 gene is required for peroxisome biogenesis and is essential for development. *Plant Physiol.* **139**, 231-239.
- Fidaleo, M.** (2010). Peroxisomes and peroxisomal disorders: The main facts. *Exp. Toxicol. Pathol.* **62**, 615-625.
- Figueroa-Romero, C., Iniguez-Lluhi, J.A., Stadler, J., Chang, C.R., Arnoult, D., Keller, P.J., Hong, Y., Blackstone, C., and Feldman, E.L.** (2009). SUMOylation

of the mitochondrial fission protein Drp1 occurs at multiple nonconsensus sites within the B domain and is linked to its activity cycle. *FASEB J* **23**, 3917-3927.

Ford, M.G., Jenni, S., and Nunnari, J. (2011). The crystal structure of dynamin. *Nature* **477**, 561-566.

Fujimoto, M., Arimura, S., Mano, S., Kondo, M., Saito, C., Ueda, T., Nakazono, M., Nakano, A., Nishimura, M., and Tsutsumi, N. (2009). Arabidopsis dynamin-related proteins DRP3A and DRP3B are functionally redundant in mitochondrial fission, but have distinct roles in peroxisomal fission. *Plant J.* **58**, 388-400.

Fujimoto, M., Arimura, S., Ueda, T., Takanashi, H., Hayashi, Y., Nakano, A., and Tsutsumi, N. (2010). Arabidopsis dynamin-related proteins DRP2B and DRP1A participate together in clathrin-coated vesicle formation during endocytosis. *Proc. Natl. Acad. Sci. USA* **107**, 6094-6099.

Fukao, Y., Hayashi, Y., Mano, S., Hayashi, M., and Nishimura, M. (2001). Developmental analysis of a putative ATP/ADP carrier protein localized on glyoxysomal membranes during the peroxisome transition in pumpkin cotyledons. *Plant Cell Physiol.* **42**, 835-841.

Gabalton, T., Snel, B., van Zimmeren, F., Hemrika, W., Tabak, H., and Huynen, M.A. (2006). Origin and evolution of the peroxisomal proteome. *Biol. Direct* **1**, 8.

Gandre-Babbe, S., and van der Blik, A.M. (2008). The novel tail-anchored membrane protein Mff controls mitochondrial and peroxisomal fission in mammalian cells. *Mol. Biol. Cell* **19**, 2402-2412.

Gao, H., Kadirjan-Kalbach, D., Froehlich, J.E., and Osteryoung, K.W. (2003). ARC5, a cytosolic dynamin-like protein from plants, is part of the chloroplast division machinery. *Proc. Natl. Acad. Sci. USA* **100**, 4328-4333.

Gillingham, A.K., and Munro, S. (2003). Long coiled-coil proteins and membrane traffic. *Biochim. Biophys. Acta* **1641**, 71-85.

Gleason, C., Huang, S., Thatcher, L.F., Foley, R.C., Anderson, C.R., Carroll, A.J., Millar, A.H., and Singh, K.B. (2011). Mitochondrial complex II has a key role in mitochondrial-derived reactive oxygen species influence on plant stress gene regulation and defense. *Proc. Natl. Acad. Sci. USA* **108**, 10768-10773.

Graham, I.A. (2008). Seed storage oil mobilization. *Annu. Rev. Plant Biol.* **59**, 115-142.

Gray, M.W., Burger, G., and Lang, B.F. (1999). Mitochondrial evolution. *Science* **283**, 1476-1481.

- Gray, M.W., Burger, G., and Lang, B.F.** (2001). The origin and early evolution of mitochondria. *Genome Biol.* **2**: 1018.1–1018.5.
- Griffin, E.E., Graumann, J., and Chan, D.C.** (2005). The WD40 protein Caf4p is a component of the mitochondrial fission machinery and recruits Dnm1p to mitochondria. *J. Cell Biol.* **170**, 237-248.
- Guo, T., Gregg, C., Boukh-Viner, T., Kyryakov, P., Goldberg, A., Bourque, S., Banu, F., Haile, S., Milijevic, S., San, K.H., Solomon, J., Wong, V., and Titorenko, V.I.** (2007). A signal from inside the peroxisome initiates its division by promoting the remodeling of the peroxisomal membrane. *J. Cell Biol.* **177**, 289-303.
- Gurvitz, A., and Rottensteiner, H.** (2006). The biochemistry of oleate induction: transcriptional upregulation and peroxisome proliferation. *Biochim. Biophys. Acta* **1763**, 1392-1402.
- Haferkamp, I.** (2007). The diverse members of the mitochondrial carrier family in plants. *FEBS Lett.* **581**, 2375-2379.
- Haferkamp, I., Fernie, A.R., and Neuhaus, H.E.** (2011). Adenine nucleotide transport in plants: much more than a mitochondrial issue. *Trends Plant Sci.* **16**, 507-515.
- Haferkamp, I., Hackstein, J.H., Voncken, F.G., Schmit, G., and Tjaden, J.** (2002). Functional integration of mitochondrial and hydrogenosomal ADP/ATP carriers in the *Escherichia coli* membrane reveals different biochemical characteristics for plants, mammals and anaerobic chytrids. *Eur. J. Biochem.* **269**, 3172-3181.
- Halbach, A., Landgraf, C., Lorenzen, S., Rosenkranz, K., Volkmer-Engert, R., Erdmann, R., and Rottensteiner, H.** (2006). Targeting of the tail-anchored peroxisomal membrane proteins PEX26 and PEX15 occurs through C-terminal PEX19-binding sites. *J. Cell Sci.* **119**, 2508-2517.
- Han, X.J., Lu, Y.F., Li, S.A., Kaitsuka, T., Sato, Y., Tomizawa, K., Nairn, A.C., Takei, K., Matsui, H., and Matsushita, M.** (2008). CaM kinase I alpha-induced phosphorylation of Drp1 regulates mitochondrial morphology. *J. Cell Biol.* **182**, 573-585.
- Harder, Z., Zunino, R., and McBride, H.** (2004). Sumol conjugates and participates in mitochondrial substrates mitochondrial fission. *Current Biol.* **14**, 340-345.
- Heazlewood, J.L., Durek, P., Hummel, J., Selbig, J., Weckwerth, W., Walther, D., and Schulze, W.X.** (2008). PhosPhAt: a database of phosphorylation sites in *Arabidopsis thaliana* and a plant-specific phosphorylation site predictor. *Nucleic Acids Res.* **36**, D1015-1021.

- Hess, D.T., Matsumoto, A., Kim, S.O., Marshall, H.E., and Stamler, J.S.** (2005). Protein S-nitrosylation: purview and parameters. *Nat. Rev. Mol. Cell Biol.* **6**, 150-166.
- Heymann, J.A.W., and Hinshaw, J.E.** (2009). Dynamins at a glance. *J. Cell Sci.* **122**, 3427-3431.
- Hinshaw, J.E.** (2000). Dynamamin and its role in membrane fission. *Annu. Rev. Cell Dev. Biol.* **16**, 483-519.
- Hoepfner, D., van den Berg, M., Philippsen, P., Tabak, H.F., and Hettema, E.H.** (2001). A role for Vps1p, actin, and the Myo2p motor in peroxisome abundance and inheritance in *Saccharomyces cerevisiae*. *J. Cell Biol.* **155**, 979-990.
- Hong, Z., Bednarek, S.Y., Blumwald, E., Hwang, I., Jurgens, G., Menzel, D., Osteryoung, K.W., Raikhel, N.V., Shinozaki, K., Tsutsumi, N., and Verma, D.P.** (2003). A unified nomenclature for Arabidopsis dynamamin-related large GTPases based on homology and possible functions. *Plant Mol. Biol.* **53**, 261-265.
- Hoppins, S., Lackner, L., and Nunnari, J.** (2007). The machines that divide and fuse mitochondria. *Annu. Rev. Biochem.* **76**, 751-780.
- Hu, J.P., Aguirre, M., Peto, C., Alonso, J., Ecker, J., and Chory, J.** (2002). A role for peroxisomes in photomorphogenesis and development of Arabidopsis. *Science* **297**, 405-409.
- Ingerman, E., Perkins, E.M., Marino, M., Mears, J.A., McCaffery, J.M., Hinshaw, J.E., and Nunnari, J.** (2005). Dnm1 forms spirals that are structurally tailored to fit mitochondria. *J. Cell Biol.* **170**, 1021-1027.
- Jacoby, R.P., Taylor, N.L., and Millar, A.H.** (2011). The role of mitochondrial respiration in salinity tolerance. *Trends Plant Sci.* **16**, 614-623.
- James, D.I., Parone, P.A., Mattenberger, Y., and Martinou, J.C.** (2003). hFis1, a novel component of the mammalian mitochondrial fission machinery. *J Biol. Chem.* **278**, 36373-36379.
- Jin, J.B., Bae, H., Kim, S.J., Jin, Y.H., Goh, C.H., Kim, D.H., Lee, Y.J., Tse, Y.C., Jiang, L., and Hwang, I.** (2003). The Arabidopsis dynamamin-like proteins ADL1C and ADL1E play a critical role in mitochondrial morphogenesis. *Plant Cell* **15**, 2357-2369.
- Karbowski, M., Neutzner, A., and Youle, R.J.** (2007). The mitochondrial E3 ubiquitin ligase MARCH5 is required for Drp1 dependent mitochondrial division. *J Cell Biol.* **178**, 71-84.

- Kashatus, D.F., Lim, K.H., Brady, D.C., Pershing, N.L., Cox, A.D., and Counter, C.M.** (2011). RALA and RALBP1 regulate mitochondrial fission at mitosis. *Nat. Cell Biol.* **13**, 1108-1115.
- Kaur, N., and Hu, J.** (2009). Dynamics of peroxisome abundance: a tale of division and proliferation. *Curr. Opin. Plant Biol.* **12**, 781-788.
- Kaur, N., Reumann, S., and Hu, J.** (2009). Peroxisome Biogenesis and Function. *The Arabidopsis Book*. **7**: e0123, doi:10.1199/tab.0123.
- Kerscher, O., Felberbaum, R., and Hochstrasser, M.** (2006). Modification of proteins by ubiquitin and ubiquitin-like proteins. *Annu. Rev. Cell Dev. Biol.* **22**, 159-180.
- Kersten, S., Desvergne, B., and Wahli, W.** (2000). Roles of PPARs in health and disease. *Nature* **405**, 421-424.
- Klingenberg, M.** (2008). The ADP and ATP transport in mitochondria and its carrier. *Biochim. Biophys. Acta* **1778**, 1978-2021.
- Klodmann, J., Senkler, M., Rode, C., and Braun, H.P.** (2011). Defining the protein complex proteome of plant mitochondria. *Plant Physiol.* **157**, 587-598.
- Knoblach, B., and Rachubinski, R.A.** (2010). Phosphorylation-dependent activation of peroxisome proliferator protein PEX11 controls peroxisome abundance. *J Biol. Chem.* **285**, 6670-6680.
- Kobayashi, S., Tanaka, A., and Fujiki, Y.** (2007). Fis1, DLP1, and Pex11p coordinately regulate peroxisome morphogenesis. *Exp. Cell Res.* **313**, 1675-1686.
- Koch, A., Thiemann, M., Grabenbauer, M., Yoon, Y., McNiven, M.A., and Schrader, M.** (2003). Dynamin-like protein 1 is involved in peroxisomal fission. *J. Biol. Chem.* **278**, 8597-8605.
- Koch, A., Yoon, Y., Bonekamp, N.A., McNiven, M.A., and Schrader, M.** (2005). A role for Fis1 in both mitochondrial and peroxisomal fission in mammalian cells. *Mol. Biol. Cell* **16**, 5077-5086.
- Koch, J., Pranjic, K., Huber, A., Ellinger, A., Hartig, A., Kragler, F., and Brocard, C.** (2010). PEX11 family members are membrane elongation factors that coordinate peroxisome proliferation and maintenance. *J. Cell Sci.* **123**, 3389-3400.
- Koirala, S., Bui, H.T., Schubert, H.L., Eckert, D.M., Hill, C.P., Kay, M.S., and Shaw, J.M.** (2010). Molecular architecture of a dynamin adaptor: implications for assembly of mitochondrial fission complexes. *J Cell Biol.* **191**, 1127-1139.

- Konopka, C.A., Backues, S.K., and Bednarek, S.Y.** (2008). Dynamics of Arabidopsis dynamin-related protein 1C and a clathrin light chain at the plasma membrane. *Plant Cell* **20**, 1363-1380.
- Kriechbaumer, V., Shaw, R., Mukherjee, J., Bowsher, C.G., Harrison, A., and Abell, B.M.** (2009). Subcellular distribution of tail-anchored proteins in Arabidopsis. *Traffic* **10**, 1753-1764.
- Kruft, V., Eubel, H., Jansch, L., Werhahn, W., and Braun, H.P.** (2001). Proteomic approach to identify novel mitochondrial proteins in Arabidopsis. *Plant Physiol.* **127**, 1694-1710.
- Kuravi, K., Nagotu, S., Krikken, A.M., Sjollem, K., Deckers, M., Erdmann, R., Veenhuis, M., and van der Klei, I.J.** (2006). Dynamin-related proteins Vps1p and Dnm1p control peroxisome abundance in *Saccharomyces cerevisiae*. *J. Cell Sci.* **119**, 3994-4001.
- Leroch, M., Neuhaus, H.E., Kirchberger, S., Zimmermann, S., Melzer, M., Gerhold, J., and Tjaden, J.** (2008). Identification of a novel adenine nucleotide transporter in the endoplasmic reticulum of Arabidopsis. *Plant Cell* **20**, 438-451.
- Li, J.F., Park, E., von Arnim, A.G., and Nebenfuhr, A.** (2009). The FAST technique: a simplified Agrobacterium-based transformation method for transient gene expression analysis in seedlings of Arabidopsis and other plant species. *Plant Methods* **5**, 6.
- Lingard, M.J., and Trelease, R.N.** (2006). Five Arabidopsis peroxin 11 homologs individually promote peroxisome elongation, duplication or aggregation. *J. of Cell Sci.* **119**, 1961-1972.
- Lingard, M.J., Gidda, S.K., Bingham, S., Rothstein, S.J., Mullen, R.T., and Trelease, R.N.** (2008). Arabidopsis PEROXIN11c-e, FISSION1b, and DYNAMIN-RELATED PROTEIN3A cooperate in cell cycle-associated replication of peroxisomes. *Plant Cell* **20**, 1567-1585.
- Linka, N., Theodoulou, F.L., Haslam, R.P., Linka, M., Napier, J.A., Neuhaus, H.E., and Weber, A.P.** (2008). Peroxisomal ATP import is essential for seedling development in *Arabidopsis thaliana*. *Plant Cell* **20**, 3241-3257.
- Liu, J., and Rost, B.** (2001). Comparing function and structure between entire proteomes. *Protein Sci.* **10**, 1970-1979.
- Logan, D.C., Scott, I., and Tobin, A.K.** (2004). ADL2a, like ADL2b, is involved in the control of higher plant mitochondrial morphology. *J. Exp. Bot.* **55**, 783-785.

- Ma, C., Agrawal, G., and Subramani, S.** (2011). Peroxisome assembly: matrix and membrane protein biogenesis. *J. Cell Biol.* **193**, 7-16.
- Mano, S., Nakamori, C., Kondo, M., Hayashi, M., and Nishimura, M.** (2004). An Arabidopsis dynamin-related protein, DRP3A, controls both peroxisomal and mitochondrial division. *Plant J.* **38**, 487-498.
- Marelli, M., Smith, J.J., Jung, S., Yi, E., Nesvizhskii, A.I., Christmas, R.H., Saleem, R.A., Tam, Y.Y., Fagarasanu, A., Goodlett, D.R., Aebersold, R., Rachubinski, R.A., and Aitchison, J.D.** (2004). Quantitative mass spectrometry reveals a role for the GTPase Rho1p in actin organization on the peroxisome membrane. *J. Cell Biol.* **167**, 1099-1112.
- Marshall, P.A., Krimkevich, Y.I., Lark, R.H., Dyer, J.M., Veenhuis, M., and Goodman, J.M.** (1995). Pmp27 promotes peroxisomal proliferation. *J. Cell Biol.* **129**, 345-355.
- Mears, J.A., Lackner, L.L., Fang, S., Ingerman, E., Nunnari, J., and Hinshaw, J.E.** (2011). Conformational changes in Dnm1 support a contractile mechanism for mitochondrial fission. *Nat. Struct. Mol. Biol.* **18**, 20-26.
- Millar, A.H., and Heazlewood, J.L.** (2003). Genomic and proteomic analysis of mitochondrial carrier proteins in Arabidopsis. *Plant Physiol.* **131**, 443-453.
- Millar, A.H., Small, I.D., Day, D.A., and Whelan, J.** (2008). Mitochondrial Biogenesis and Function in Arabidopsis. In *The Arabidopsis Book*. **7**: e0111, doi/1199/tab.0111.
- Mitsuya, S., El-Shami, M., Sparkes, I.A., Charlton, W.L., Lousa Cde, M., Johnson, B., and Baker, A.** (2010). Salt stress causes peroxisome proliferation, but inducing peroxisome proliferation does not improve NaCl tolerance in Arabidopsis thaliana. *PLoS One* **5**, e9408.
- Miyagishima, S.Y., Froehlich, J.E., and Osteryoung, K.W.** (2006). PDV1 and PDV2 mediate recruitment of the dynamin-related protein ARC5 to the plastid division site. *Plant Cell* **18**, 2517-2530.
- Miyagishima, S.Y., Kuwayama, H., Urushihara, H., and Nakanishi, H.** (2008). Evolutionary linkage between eukaryotic cytokinesis and chloroplast division by dynamin proteins. *Proc. Natl. Acad. Sci. USA* **105**, 15202-15207.
- Miyagishima, S.Y., Nishida, K., and Kuroiwa, T.** (2003). An evolutionary puzzle: chloroplast and mitochondrial division rings. *Trends Plant Sci.* **8**, 432-438.
- Mohlmann, T., Tjaden, J., Schwoppe, C., Winkler, H.H., Kampfenkel, K., and Neuhaus, H.E.** (1998). Occurrence of two plastidic ATP/ADP transporters in

- Arabidopsis thaliana* L.--molecular characterisation and comparative structural analysis of similar ATP/ADP translocators from plastids and *Rickettsia prowazekii*. *Eur. J. Biochem.* **252**, 353-359.
- Motley, A.M., Ward, G.P., and Hetteema, E.H.** (2008). Dnm1p-dependent peroxisome fission requires Caf4p, Mdv1p and Fis1p. *J. Cell Sci.* **121**, 1633-1640.
- Moutevelis, E., and Woolfson, D.N.** (2009). A periodic table of coiled-coil protein structures. *J. Mol. Biol.* **385**, 726-732.
- Mozdy, A.D., McCaffery, J.M., and Shaw, J.M.** (2000). Dnm1p GTPase-mediated mitochondrial fission is a multi-step process requiring the novel integral membrane component Fis1p. *J. Cell Biol.* **151**, 367-380.
- Mullen RT.** 2002. Targeting and import of matrix proteins into peroxisomes. In *Plant peroxisomes: biochemistry, cell biology and biotechnological applications*. Eds. A Baker and IA Graham. Kluwer Academic Publishers. Pp. 339-385.
- Murcha, M.W., Millar, A.H., and Whelan, J.** (2005). The N-terminal cleavable extension of plant carrier proteins is responsible for efficient insertion into the inner mitochondrial membrane. *J. Mol. Biol.* **351**, 16-25.
- Nagotu, S., Krikken, A.M., Otzen, M., Kiel, J.A., Veenhuis, M., and van der Klei, I.J.** (2008). Peroxisome fission in *Hansenula polymorpha* requires Mdv1 and Fis1, two proteins also involved in mitochondrial fission. *Traffic* **9**, 1471-1484.
- Nakagawa, T., Imanaka, T., Morita, M., Ishiguro, K., Yurimoto, H., Yamashita, A., Kato, N., and Sakai, Y.** (2000). Peroxisomal membrane protein Pmp47 is essential in the metabolism of middle-chain fatty acid in yeast peroxisomes and is associated with peroxisome proliferation. *J. Biol. Chem.* **275**, 3455-3461.
- Nakagawa, T., Kurose, T., Hino, T., Tanaka, K., Kawamukai, M., Niwa, Y., Toyooka, K., Matsuoka, K., Jinbo, T., and Kimura, T.** (2007). Development of series of gateway binary vectors, pGWBs, for realizing efficient construction of fusion genes for plant transformation. *J. Biosci. Bioeng.* **104**, 34-41.
- Nakamura, N., Kimura, Y., Tokuda, M., Honda, S., and Hirose, S.** (2006). MARCH-V is a novel mitofusin 2- and Drp1-binding protein able to change mitochondrial morphology. *EMBO Rep.* **7**, 1019-1022.
- Nayidu, N.K., Wang, L., Xie, W., Zhang, C., Fan, C., Lian, X., Zhang, Q., and Xiong, L.** (2008). Comprehensive sequence and expression profile analysis of PEX11 gene family in rice. *Gene* **412**, 59-70.

- Nelson, B.K., Cai, X., and Nebenfuhr, A.** (2007). A multicolored set of in vivo organelle markers for co-localization studies in Arabidopsis and other plants. *Plant J.* **51**, 1126-1136.
- Neuspiel, M., Schauss, A.C., Braschi, E., Zunino, R., Rippstein, P., Rachubinski, R.A., Andrade-Navarro, M.A., and McBride, H.M.** (2008). Cargo-selected transport from the mitochondria to peroxisomes is mediated by vesicular carriers. *Curr. Biol.* **18**, 102-108.
- Nito, K., Kamigaki, A., Kondo, M., Hayashi, M., and Nishimura, M.** (2007). Functional classification of Arabidopsis peroxisome biogenesis factors proposed from analyses of knockdown mutants. *Plant Cell Physiol.* **48**, 763-774.
- Nyathi, Y., and Baker, A.** (2006). Plant peroxisomes as a source of signalling molecules. *Biochim. Biophys. Acta* **1763**, 1478-1495.
- Opaliński, L., Kiel, J.A., Williams, C., Veenhuis, M., and van der Klei, I.J.** (2011). Membrane curvature during peroxisome fission requires Pex11. *EMBO J* **30**, 5-16.
- Orth, T., Reumann, S., Zhang, X., Fan, J., Wenzel, D., Quan, S., and Hu, J.** (2007). The PEROXIN11 protein family controls peroxisome proliferation in Arabidopsis. *Plant Cell* **19**, 333-350.
- Osteryoung, K.W., and Nunnari, J.** (2003). The division of endosymbiotic organelles. *Science* **302**, 1698-1704.
- Osteryoung, K.W., Stokes, K.D., Rutherford, S.M., Percival, A.L., and Lee, W.Y.** (1998). Chloroplast division in higher plants requires members of two functionally divergent gene families with homology to bacterial ftsZ. *Plant Cell* **10**, 1991-2004.
- Otera, H., and Mihara, K.** (2011). Discovery of the membrane receptor for mitochondrial fission GTPase Drp1. *Small Gtpases* **2**, 167-172.
- Otera, H., Wang, C., Cleland, M.M., Setoguchi, K., Yokota, S., Youle, R.J., and Mihara, K.** (2010). Mff is an essential factor for mitochondrial recruitment of Drp1 during mitochondrial fission in mammalian cells. *J. Cell Biol.* **191**, 1141-1158.
- Otsuga, D., Keegan, B.R., Brisch, E., Thatcher, J.W., Hermann, G.J., Bleazard, W., and Shaw, J.M.** (1998). The dynamin-related GTPase, Dnm1p, controls mitochondrial morphology in yeast. *J. Cell Biol.* **143**, 333-349.
- Pagliarini, D.J., Calvo, S.E., Chang, B., Sheth, S.A., Vafai, S.B., Ong, S.E., Walford, G.A., Sugiana, C., Boneh, A., Chen, W.K., Hill, D.E., Vidal, M., Evans, J.G., Thorburn, D.R., Carr, S.A., and Mootha, V.K.** (2008). A mitochondrial protein compendium elucidates complex I disease biology. *Cell* **134**, 112-123.

- Palmer, C.S., Osellame, L.D., Laine, D., Koutsopoulos, O.S., Frazier, A.E., and Ryan, M.T.** (2011a). MiD49 and MiD51, new components of the mitochondrial fission machinery. *EMBO Rep.* **12**, 565-573.
- Palmer, C.S., Osellame, L.D., Stojanovski, D., and Ryan, M.T.** (2011b). The regulation of mitochondrial morphology: Intricate mechanisms and dynamic machinery. *Cell Signal.* **23**, 1534-1545.
- Palmieri, L., Rottensteiner, H., Girzalsky, W., Scarcia, P., Palmieri, F., and Erdmann, R.** (2001). Identification and functional reconstitution of the yeast peroxisomal adenine nucleotide transporter. *EMBO J.* **20**, 5049-5059.
- Passreiter, M., Anton, M., Lay, D., Frank, R., Harter, C., Wieland, F.T., Gorgas, K., and Just, W.W.** (1998). Peroxisome biogenesis: involvement of ARF and coatomer. *J. Cell Biol.* **141**, 373-383.
- Pedrazzini, E.** (2009). Tail-anchored proteins in plants. *J. Plant Biol.* **52**, 1226-1239.
- Penfield, S., Graham, S., and Graham, I.A.** (2005). Storage reserve mobilization in germinating oilseeds: Arabidopsis as a model system. *Biochem. Soc. Trans.* **33**, 380-383.
- Penfield, S., Pinfield-Wells, H.M., and Graham, I.** (2006). Storage reserve mobilisation and seedling establishment in Arabidopsis. *The Arabidopsis Book.* **4**: e0100, doi:10.1199/tab.0100.
- Peterhansel, C., and Maurino, V.G.** (2011). Photorespiration redesigned. *Plant Physiol.* **155**, 49-55.
- Peterhansel, C., Horst, I., Niessen, M., Blume, C., Kebeish, R., Kurkcuoglu, S., and Kreuzaler, F.** (2010). Photorespiration: The Arabidopsis Book. **8**: e0130, doi:10.1199/tab.0130.
- Picault, N., Hodges, M., Palmieri, L., and Palmieri, F.** (2004). The growing family of mitochondrial carriers in Arabidopsis. *Trends Plant Sci.* **9**, 138-146.
- Platta, H.W., and Erdmann, R.** (2007). The peroxisomal protein import machinery. *FEBS Lett.* **581**, 2811-2819.
- Praefcke, G.J., and McMahon, H.T.** (2004). The dynamin superfamily: universal membrane tubulation and fission molecules? *Nat. Rev. Mol. Cell Biol.* **5**, 133-147.
- Purdue, P.E., and Lazarow, P.B.** (2001). Peroxisome biogenesis. *Annu. Rev. Cell Dev. Biol.* **17**, 701-752.

- Qi, Y., and Katagiri, F.** (2009). Purification of low-abundance Arabidopsis plasma-membrane protein complexes and identification of candidate components. *Plant J.* **57**, 932-944.
- Rapaport, D.** (2003). Finding the right organelle. Targeting signals in mitochondrial outer-membrane proteins. *EMBO Rep.* **4**, 948-952.
- Reinders, J., Zahedi, R.P., Pfanner, N., Meisinger, C., and Sickmann, A.** (2006). Toward the complete yeast mitochondrial proteome: multidimensional separation techniques for mitochondrial proteomics. *J. Proteome Res.* **5**, 1543-1554.
- Reiser, J., Linka, N., Lemke, L., Jeblick, W., and Neuhaus, H.E.** (2004). Molecular physiological analysis of the two plastidic ATP/ADP transporters from Arabidopsis. *Plant Physiol.* **136**, 3524-3536.
- Reumann, S., and Weber, A.P.** (2006). Plant peroxisomes respire in the light: some gaps of the photorespiratory C2 cycle have become filled--others remain. *Biochim. Biophys. Acta* **1763**, 1496-1510.
- Reumann, S., Ma, C., Lemke, S., and Babujee, L.** (2004). AraPeroX. A database of putative Arabidopsis proteins from plant peroxisomes. *Plant Physiol.* **136**, 2587-2608.
- Reumann, S., Quan, S., Aung, K., Yang, P.F., Manandhar-Shrestha, K., Holbrook, D., Linka, N., Switzenberg, R., Wilkerson, C.G., Weber, A.P.M., Olsen, L.J., and Hu, J.P.** (2009). In-Depth Proteome Analysis of Arabidopsis Leaf Peroxisomes Combined with in Vivo Subcellular Targeting Verification Indicates Novel Metabolic and Regulatory Functions of Peroxisomes. *Plant Physiol.* **150**, 125-143.
- Robertson, E.J., Pyke, K.A., and Leech, R.M.** (1995). arc6, an extreme chloroplast division mutant of Arabidopsis also alters proplastid proliferation and morphology in shoot and root apices. *J. Cell Sci.* **108**, 2937-2944.
- Rose, A., Manikantan, S., Schraegle, S.J., Maloy, M.A., Stahlberg, E.A., and Meier, I.** (2004). Genome-wide identification of Arabidopsis coiled-coil proteins and establishment of the ARABI-COIL database. *Plant Physiol.* **134**, 927-939.
- Rose, A., Schraegle, S.J., Stahlberg, E.A., and Meier, I.** (2005). Coiled-coil protein composition of 22 proteomes--differences and common themes in subcellular infrastructure and traffic control. *BMC Evol. Biol.* **5**, 66-86.
- Rottensteiner, H., Stein, K., Sonnenhol, E., and Erdmann, R.** (2003). Conserved function of pex11p and the novel pex25p and pex27p in peroxisome biogenesis. *Mol. Biol. Cell* **14**, 4316-4328.

- Sakai, Y., Marshall, P.A., Saiganji, A., Takabe, K., Saiki, H., Kato, N., and Goodman, J.M.** (1995). The *Candida boidinii* peroxisomal membrane protein Pmp30 has a role in peroxisomal proliferation and is functionally homologous to Pmp27 from *Saccharomyces cerevisiae*. *J. Bacteriol* **177**, 6773-6781.
- Schapira, A.H.** (2006). Mitochondrial disease. *Lancet* **368**, 70-82.
- Schliebs, W., Girzalsky, W., and Erdmann, R.** (2010). Peroxisomal protein import and ERAD: variations on a common theme. *Nat. Rev. Mol. Cell Biol.* **11**, 885-890.
- Schluter, A., Fourcade, S., Ripp, R., Mandel, J.L., Poch, O., and Pujol, A.** (2006). The evolutionary origin of peroxisomes: an ER-peroxisome connection. *Mol. Biol. Evol.* **23**, 838-845.
- Schmidt, O., Pfanner, N., and Meisinger, C.** (2010). Mitochondrial protein import: from proteomics to functional mechanisms. *Nat. Rev. Mol. Cell Biol.* **11**, 655-667.
- Schmitz, A.J., Glynn, J.M., Olson, B.J., Stokes, K.D., and Osteryoung, K.W.** (2009). *Arabidopsis* FtsZ2-1 and FtsZ2-2 Are Functionally Redundant, But FtsZ-Based Plastid Division Is Not Essential for Chloroplast Partitioning or Plant Growth and Development. *Mol. Plant* **2**, 1211-1222.
- Schrader, M.** (2006). Shared components of mitochondrial and peroxisomal division. *Biochim. Biophys. Acta* **1763**, 531-541.
- Schrader, M., and Fahimi, H.D.** (2008). The peroxisome: still a mysterious organelle. *Histochem. and Cell Biol.* **129**, 421-440.
- Schrader, M., Reuber, B.E., Morrell, J.C., Jimenez-Sanchez, G., Obie, C., Stroh, T.A., Valle, D., Schroer, T.A., and Gould, S.J.** (1998). Expression of PEX11beta mediates peroxisome proliferation in the absence of extracellular stimuli. *J. Biol. Chem.* **273**, 29607-29614.
- Scott, I., Tobin, A.K., and Logan, D.C.** (2006). BIGYIN, an orthologue of human and yeast FIS1 genes functions in the control of mitochondrial size and number in *Arabidopsis thaliana*. *J. Exp. Bot.* **57**, 1275-1280.
- Seth, R.B., Sun, L., Ea, C.K., and Chen, Z.J.** (2005). Identification and characterization of MAVS, a mitochondrial antiviral signaling protein that activates NF-kappaB and IRF 3. *Cell* **122**, 669-682.
- Shaw, J.M., and Nunnari, J.** (2002). Mitochondrial dynamics and division in budding yeast. *Trends Cell Biol.* **12**, 178-184.

- Sinclair, A.M., Trobacher, C.P., Mathur, N., Greenwood, J.S., and Mathur, J.** (2009). Peroxule extension over ER-defined paths constitutes a rapid subcellular response to hydroxyl stress. *Plant J.* **59**, 231-242.
- Smirnova, E., Griparic, L., Shurland, D.L., and van der Bliek, A.M.** (2001). Dynamin-related protein Drp1 is required for mitochondrial division in mammalian cells. *Mol. Biol. Cell* **12**, 2245-2256.
- Smith, J.J., Marelli, M., Christmas, R.H., Vizeacoumar, F.J., Dilworth, D.J., Ideker, T., Galitski, T., Dimitrov, K., Rachubinski, R.A., and Aitchison, J.D.** (2002). Transcriptome profiling to identify genes involved in peroxisome assembly and function. *J. Cell Biol.* **158**, 259-271.
- Sparkes, I.A., Brandizzi, F., Slocombe, S.P., El-Shami, M., Hawes, C., and Baker, A.** (2003). An Arabidopsis pex10 null mutant is embryo lethal, implicating peroxisomes in an essential role during plant embryogenesis. *Plant Physiol.* **133**, 1809-1819.
- Sparkes, I.A., Ketelaar, T., de Ruijter, N.C., and Hawes, C.** (2009). Grab a Golgi: laser trapping of Golgi bodies reveals in vivo interactions with the endoplasmic reticulum. *Traffic* **10**, 567-571.
- Strader, L.C., Wheeler, D.L., Christensen, S.E., Berens, J.C., Cohen, J.D., Rampey, R.A., and Bartel, B.** (2011). Multiple facets of Arabidopsis seedling development require indole-3-butyric acid-derived auxin. *Plant Cell* **23**, 984-999.
- Suzuki, K., Ehara, T., Osafune, T., Kuroiwa, H., Kawano, S., and Kuroiwa, T.** (1994). Behavior of mitochondria, chloroplasts and their nuclei during the mitotic cycle in the ultramicroalga *Cyanidioschyzon merolae*. *Eur. J. Cell Biol.* **63**, 280-288.
- Taguchi, N., Ishihara, N., Jofuku, A., Oka, T., and Mihara, K.** (2007). Mitotic phosphorylation of dynamin-related GTPase Drp1 participates in mitochondrial fission. *J. Biol. Chem.* **282**, 11521-11529.
- Tam, Y.Y., Torres-Guzman, J.C., Vizeacoumar, F.J., Smith, J.J., Marelli, M., Aitchison, J.D., and Rachubinski, R.A.** (2003). Pex11-related proteins in peroxisome dynamics: a role for the novel peroxin Pex27p in controlling peroxisome size and number in *Saccharomyces cerevisiae*. *Mol. Biol. Cell* **14**, 4089-4102.
- Taylor, N.G.** (2011). A role for Arabidopsis dynamin related proteins DRP2A/B in endocytosis; DRP2 function is essential for plant growth. *Plant Mol. Biol.* **76**, 117-129.
- Thoms, S., and Erdmann, R.** (2005). Dynamin-related proteins and Pex11 proteins in peroxisome division and proliferation. *FEBS J.* **272**, 5169-5181.

- Tieu, Q., and Nunnari, J.** (2000). Mdv1p is a WD repeat protein that interacts with the dynamin-related GTPase, Dnm1p, to trigger mitochondrial division. *J. Cell Biol.* **151**, 353-366.
- Tieu, Q., Okreglak, V., Naylor, K., and Nunnari, J.** (2002). The WD repeat protein, Mdv1p, functions as a molecular adaptor by interacting with Dnm1p and Fis1p during mitochondrial fission. *J. Cell Biol.* **158**, 445-452.
- Titorenko, V.I., and Mullen, R.T.** (2006). Peroxisome biogenesis: the peroxisomal endomembrane system and the role of the ER. *J. Cell Biol.* **174**, 11-17.
- Tjaden, J., Schwoppe, C., Mohlmann, T., Quick, P.W., and Neuhaus, H.E.** (1998). Expression of a plastidic ATP/ADP transporter gene in *Escherichia coli* leads to a functional adenine nucleotide transport system in the bacterial cytoplasmic membrane. *J. Biol. Chem.* **273**, 9630-9636.
- Traba, J., Satrustegui, J., and Del Arco, A.** (2011). Adenine nucleotide transporters in organelles: novel genes and functions. *Cell Mol. Life Sci.* **68**: 1183-1206.
- Tranel, P.J., Froehlich, J., Goyal, A., and Keegstra, K.** (1995). A component of the chloroplastic protein import apparatus is targeted to the outer envelope membrane via a novel pathway. *EMBO J.* **14**, 2436-2446.
- Unsel, M., Marienfeld, J.R., Brandt, P., and Brennicke, A.** (1997). The mitochondrial genome of *Arabidopsis thaliana* contains 57 genes in 366,924 nucleotides. *Nat. Genet.* **15**, 57-61.
- van der Klei, I.J., and Veenhuis, M.** (2006). Yeast and filamentous fungi as model organisms in microbody research. *Biochim. Biophys. Acta* **1763**, 1364-1373.
- Visser, W.F., van Roermund, C.W., Waterham, H.R., and Wanders, R.** (2002). Identification of human PMP34 as a peroxisomal ATP transporter. *Biochem. Biophys. Res. Commun.* **299**, 494-497.
- Vitha, S., Froehlich, J.E., Koksharova, O., Pyke, K.A., van Erp, H., and Osteryoung, K.W.** (2003). ARC6 is a J-domain plastid division protein and an evolutionary descendant of the cyanobacterial cell division protein Ftn2. *Plant Cell* **15**, 1918-1933.
- Voncken, F., van Hellemond, J.J., Pfisterer, I., Maier, A., Hillmer, S., and Clayton, C.** (2003). Depletion of GIM5 causes cellular fragility, a decreased glycosome number, and reduced levels of ether-linked phospholipids in trypanosomes. *J. Biol. Chem.* **278**, 35299-35310.

- Wanders, R.J., and Waterham, H.R.** (2006). Biochemistry of mammalian peroxisomes revisited. *Annu. Rev. Biochem.* **75**, 295-332.
- Wang, G., Moniri, N.H., Ozawa, K., Stamler, J.S., and Daaka, Y.** (2006). Nitric oxide regulates endocytosis by S-nitrosylation of dynamin. *Proc. Natl. Acad. Sci. USA* **103**, 1295-1300.
- Werhahn, W., and Braun, H.P.** (2002). Biochemical dissection of the mitochondrial proteome from *Arabidopsis thaliana* by three-dimensional gel electrophoresis. *Electrophoresis* **23**, 640-646.
- Woodward, A.W., and Bartel, B.** (2005). Auxin: regulation, action, and interaction. *Ann. Bot.* **95**, 707-735.
- Yan, M.D., Rayapuram, N., and Subramani, S.** (2005). The control of peroxisome number and size during division and proliferation. *Curr. Opin. Cell Biol.* **17**, 376-383.
- Yang, Y., Glynn, J.M., Olson, B.J., Schmitz, A.J., and Osteryoung, K.W.** (2008). Plastid division: across time and space. *Curr. Opin. Plant Biol.* **11**, 577-584.
- Yoder, D.W., Kadirjan-Kalbach, D., Olson, B.J., Miyagishima, S.Y., Deblasio, S.L., Hangarter, R.P., and Osteryoung, K.W.** (2007). Effects of mutations in *Arabidopsis* FtsZ1 on plastid division, FtsZ ring formation and positioning, and FtsZ filament morphology in vivo. *Plant Cell Physiol.* **48**, 775-791.
- Yonashiro, R., Ishido, S., Kyo, S., Fukuda, T., Goto, E., Matsuki, Y., Ohmura-Hoshino, M., Sada, K., Hotta, H., Yamamura, H., Inatome, R., and Yanagi, S.** (2006). A novel mitochondrial ubiquitin ligase plays a critical role in mitochondrial dynamics. *EMBO J.* **25**, 3618-3626.
- Yoon, Y., Krueger, E.W., Oswald, B.J., and McNiven, M.A.** (2003). The mitochondrial protein hFis1 regulates mitochondrial fission in mammalian cells through an interaction with the dynamin-like protein DLP1. *Mol. Cell Biol.* **23**, 5409-5420.
- Zhang, X., and Hu, J.** (2008). FISSION1A and FISSION1B proteins mediate the fission of peroxisomes and mitochondria in *Arabidopsis*. *Mol. Plant* **1**, 1036-1047.
- Zhang, X., and Hu, J.** (2009). Two small protein families, DYNAMIN-RELATED PROTEIN3 and FISSION1, are required for peroxisome fission in *Arabidopsis*. *Plant J.* **57**, 146-159.
- Zhang, X., and Hu, J.** (2010). The *Arabidopsis* chloroplast division protein DYNAMIN-RELATED PROTEIN5B also mediates peroxisome division. *Plant Cell* **22**, 431-442.

Zhao, J., Liu, T., Jin, S., Wang, X., Qu, M., Uhlen, P., Tomilin, N., Shupliakov, O., Lendahl, U., and Nister, M. (2011). Human MIEF1 recruits Drp1 to mitochondrial outer membranes and promotes mitochondrial fusion rather than fission. *EMBO J.* **30**, 2762-2778.

Zolman, B.K., Yoder, A., and Bartel, B. (2000). Genetic analysis of indole-3-butyric acid responses in *Arabidopsis thaliana* reveals four mutant classes. *Genetics* **156**, 1323-1337.

Zunino, R., Schauss, A., Rippstein, P., Andrade-Navarro, M., and McBride, H.M. (2007). The SUMO protease SENP5 is required to maintain mitochondrial morphology and function. *J. Cell Sci.* **120**, 1178-1188.